# Applied Optics

October
1963

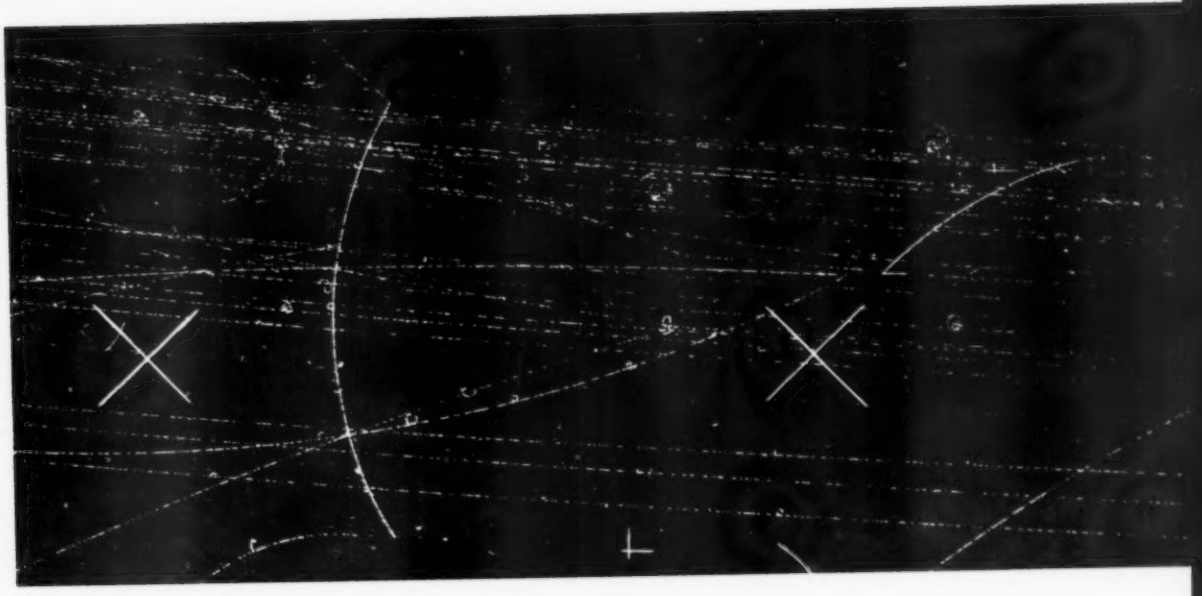

**BUBBLE CHAMBER OPTICS**

Effective Jan. 1, 1965, All back issues and single copies are sold at $3.00 per copy.

*The Barnes*

# PEAC™ PHOTOELECTRIC AUTOCOLLIMATOR

*for ultra-precise, automatic monitoring of angular position*

- Resolution better than 0.1 second of arc
- Repeatability better than 0.5 second of arc
- Angular measuring range of 1000 seconds
- Features both direct measurement and closed-loop control operation
- Available for single- or dual-axis operation
- Built-in visual alignment feature

CALL OR WRITE FOR BULLETIN 23-100

Barnes Engineering Company

Defense and Space Division

30 Commerce Road Stamford, Connecticut
Telephone: (203) 348-5381 TWX: (203) 327-0840

# Applied Optics

VOLUME 2
NUMBER 10
OCTOBER
1963

A monthly publication of the
Optical Society of America

**John N. Howard,** Editor

**Seymour Rosin,** Feature Editor

**Patricia R. Wakeling,** Managing Editor

**COVER:** A new technique for automatic measurement of bubble chamber photographs uses a mechanical flying spot to measure precise coordinates of all the bubbles in the picture. (Hough-Powell Digitizer, see paper by R. B. Palmer, page 1025). The coordinates are transferred to the memory of a large digital computer where a computer program selects from all of the coordinates those belonging to a nuclear event of interest. The upper cover picture is a print of the original bubble chamber negative. The lower is a composite of 16 photographs of a cathode ray tube on which the computer has replotted the coordinates measured by the flying spot digitizer, the plotting being done in small areas to overcome the limited resolution of the CRT. The black bands in several areas are introduced in making the composite. The event of interest here is the first example of the production of the cascade and newly discovered anticascade particles for which both strange particles are observed to decay in the chamber (courtesy Brookhaven and Yale bubble chamber groups). The entire scanning operation takes only a few seconds to complete. Cover supplied by Paul V. C. Hough, Brookhaven National Laboratory.

Published monthly by the Optical Society of America, Inc., in cooperation with the American Institute of Physics, at 20th and Northampton Streets, Easton, Pa. Editorial and advertising offices: 1155 16th St. N.W., Washington, D.C. 20036. 202-Di7-4131 Supported in part by a grant from the National Science Foundation. Subscription rates: $6.00 to OSA members, $8.00 other AIP Societies' members, nonmembers and libraries: $10.00 per year. Single copies $2.00. Second class postage paid at Easton, Pa. ©Copyright 1963 by the Optical Society of America.

981 **Bubble Chamber Optics**—W. T. Welford

997 **The Trigger Circuit for the 80-in. Bubble Chamber Light Source**—S. S. Yamamoto and W. P. Sims

999 **Optical and Mechanical Properties of Bubble Chamber Windows**—F. O. Reitmayer and E. W. Deeg

1003 **Illumination of the 80-in. Bubble Chamber**—Seymour Rosin

1013 **Electronic Flash Illumination of a Large Wilson Cloud Chamber**—Harold E. Edgerton

1017 **The Illumination of the CERN 2-Meter Hydrogen Bubble Chamber**—F. Früngel, H. Köhler, and H. P. Reinhard

1025 **A Flying Spot Film Measuring Machine Employing Crossed Glass Fibers**—R. B. Palmer

1037 **Bubble Chamber Windows**—W. T. Welford

1043 **Photorefractometer II. Measurement of *N* and *K***—N. S. Kapany and D. A. Pontarelli

1049 **Double Monochromator Systems**—Robert L. Christensen and Robert J. Potter

1055 **The Evaporation Rate of Filament Material From Alternating Current Heated Filaments**—A. D. Wilson

1061 **Interferometric Measurement of Vibration Amplitudes**—Glenn E. Bowie

1069 **Optics in the German Democratic Republic**—Paul Görlich

1075 **Optical Physics Research in a Small Liberal Arts College**—J. H. Taylor

1081 **A New Family of Flat-Field Cameras**—Rubin Gelles

## DEPARTMENTS

1085 **Letters to the Editor**

**Illumination of the Slit Source of the Hough-Powell Digitizer**—Seymour Rosin

**Note on Hole Burning Model of Oscillation for Ruby Lasers**—A. J. DeMaria

1036 **From The Editor**

1042 **Meeting Reports**

1060 **Books**

1088 **Optical Activities in Industry**

# WHAT WILL YOU SEE IN BOOTH 37?

*Optical Society of America.... Instrument Show*

**1. Semi-Elements' NEW MKIB GAS LASER**
**Precision Made . . . COMPLETE $750!**

*Wavelength*—Visible and Infrared—6328Å 11,523Å 33,912Å

*Power*—1 to 2 Milliwatt Output

*Adjustability*—Resonator over 2 cm in length
Reflector Angle to 0.1 arc second resolution

*Exciter*—New simplified controls
Plasma Tube warranted for 300 continuous hours
(will usually run 500 continuous hours)
High precision End Windows and Reflecting Mirrors

**2. Optical Crystals for DOUBLE HARMONIC Wave Generation**

**3. GAMMA RAY and NEUTRON SPECTROMETRY SINGLE CRYSTAL PLATES**

Aluminum
Bismuth
Cadmium
Germanium
Gold
Silicon
Thallium
Zinc

**4. SEVAC* Grade Optical Coating Chemicals for Vacuum Deposition**

- All Volatile Impurities Removed
- All −10 Mesh Fineness

**5. SINGLE CRYSTALS**—A wide variety of Single Crystals From the World's Largest Supply. Over 100 Crystals—From A to Z Aluminum to Zirconium Oxide

*Write or Call for Complete Literature*

Semi-elements, inc.
Saxonburg Boulevard, Saxonburg, Pa.
Phone: 412-352-1548

*Trademark

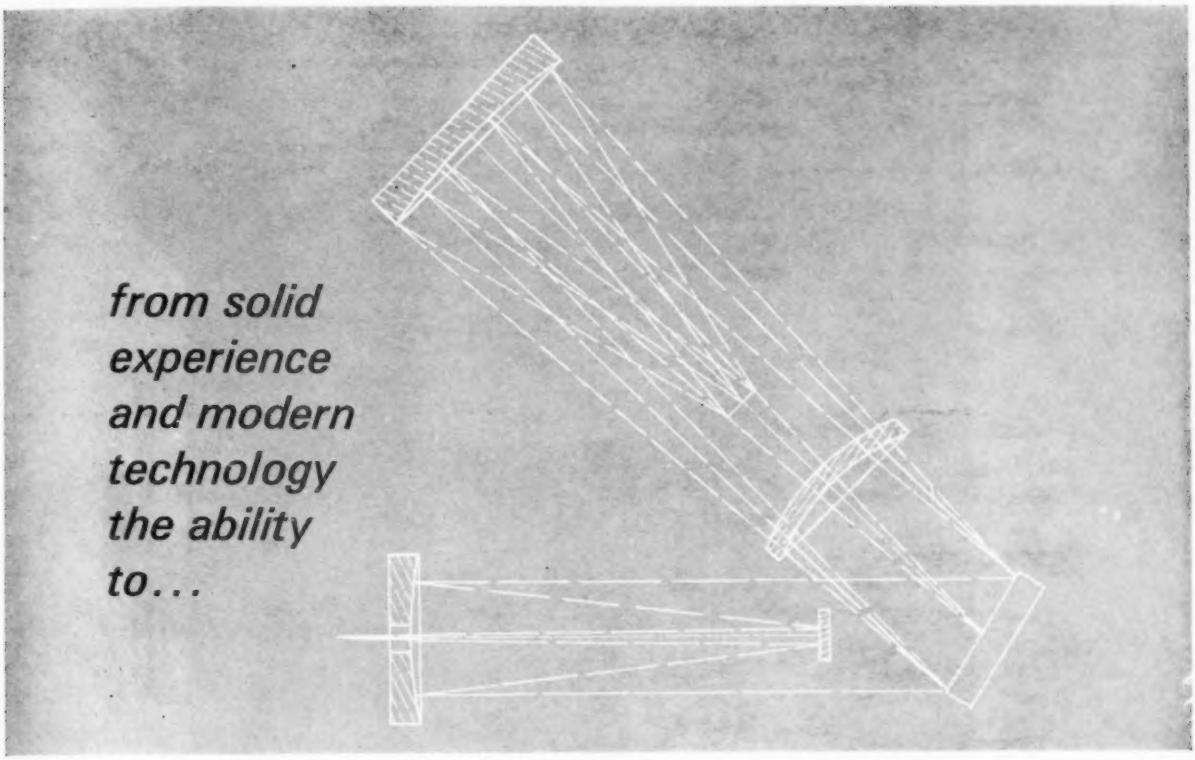


# SOLVE YOUR OPTICS PROBLEMS

Modern electronic computer techniques have made it possible to simulate an optical system in every detail. Multiple ray traces produce a spot diagram from which energy distribution for a spot anywhere in the image surface may be derived. Bolometric energy distribution over a wave length region of interest can be calculated and the contribution due to a particular aberration identified. All this (and a great deal more) is accomplished with our IBM 1620, with amazing rapidity and accuracy.

We, also, are currently engaged with several other firms in a co-operative endeavor to develop a program for the 7090 which will automatically optimize the optical parameters for over-all system performance. The first stages of the program have been tested successfully and completion is scheduled for the near future.

Sounds marvelous? It is – but – machines have no imagination, no experience in "working" glass, no knowledge of what makes a practical optical system. Such things are for men.

In the hands of a man with skill and imagination even a desk calculator produced results, slowly to be sure, by modern standards, and with greater approximation. Today's powerful mathematical machines have multiplied his efforts a thousand fold and made possible a degree of accuracy and sophistication unforeseen a few years back.

The attributes peculiar to the man, imagination, skill, experience are now more necessary and valuable than ever.

Perhaps you have need for the talents of our optical design and engineering staff. We will be happy to tackle your systems or instrumentation problem . . . U-V, I-R, or anywhere between.

We can do the whole job from design to a complete prototype instrument, if you like.

**The experience, imagination, skill, and talents of our staff are at your service at all times. For consultation or quotation, write, wire or telephone: DIRECTOR OF RESEARCH . . .**

**FERSON OPTICS, INC.**
P. O. BOX 398 / OCEAN SPRINGS, MISSISSIPPI
TELEPHONE 875-5422 (Area Code 601)

OPTIC SYSTEMS FOR AMERICA'S FUTURE

# new dual-axis autocollimator

**Kollmorgen Model K222 combines 0.1 second of arc sensitivity ... ease of use ... freedom from eye strain.**

**Demonstrably superior!** No other manual autocollimator on the market today ... imported or domestic ... offers you so many operating advantages.

**Simultaneous measurement of vertical and horizontal angles** eliminates errors or delays inherent in 90° rotation of instrument or eyepiece. Both measurements in the same plane ... no parallax! Each axis has its independent micrometer ... no compromise with accuracy.

**Largest objective lens aperture** (1.8 in.) available on an NAS barrel and full correction of lens for spherical and chromatic aberration permit accurate measurements over a field of view of 26 minutes of arc. Maximum working distance is 150 feet.

**Illuminated fine adjustment scale** utilizes eyepiece readout to eliminate constant refocusing of the viewing eye and resultant eye fatigue. This illumination also permits instrument use in total darkness. Since readouts are located outside the instrument's field of view, micrometer adjustments are always 'honest' ... not influenced by any observer's natural tendency to resolve fractional splits in his favor. Micrometer scale divisions are seconds and tenths of seconds; one minute per revolution.

**A demonstration will convince you** that the Kollmorgen Model K222 Dual-Axis Autocollimator provides the quickest, easiest way to align, square, erect or position structures, machinery and their components to the highest order of accuracy available in a standard commercial instrument.

**Informative 12-page bulletin** contains complete data on Model K222 and other new Kollmorgen optical tooling instruments: Single-Axis Manual and Dual-Axis Automatic Autocollimators, Dual-Axis and Line-of-Sight Alignment Telescopes, Pointing Interferometer and all required accessories. Write for this bulletin today ... 347 King Street, Northampton, Mass.

KOLLMORGEN
CORPORATION
NORTHAMPTON, MASSACHUSETTS

Far-field diffraction pattern produced from laboratory model using coherent light.

# Using coherent light to scale large antenna arrays down to laboratory size

You may find it useful to think of the coherent light output of a continuous wave gas laser as being extremely short radio waves, particularly if you are interested in applying laser technology to various electromagnetic radiation problems. This thinking has suggested, for example, a novel way* to determine antenna directivity patterns based on scale models of antenna arrays.

Where an antenna is hundreds or thousands of wavelengths in diameter, it may be difficult or even impossible to make full-scale measurements of directivity, main-lobe width, side-lobe amplitude, or null spacing. But by using a laser beam to illuminate apertures representing elements in the antenna array being scaled, a far-field diffraction pattern can be generated on the laboratory workbench and directly recorded on photographic film. Such a pattern (as shown above) can be converted to a conventional plot simply by scanning the negative with a densitometer.

As other interesting studies and applications come to light, we will continue to report them to you. Meantime, may we send you a brochure on our new Model 130 "briefcase" laser, and details on other CW gas lasers for advanced laboratory work? Address your inquiry to 1255 Terra Bella Avenue, Mountain View 5, California (or call collect (415) 961-2550).

*Reported in IEEE Transactions, Professional Group on Antennas and Propagation, September 1963, "A New Approach to Antenna Scaling," by Wright H. Huntley, Jr., Stanford Electronics Laboratories, Stanford, California.

Spectra-Physics

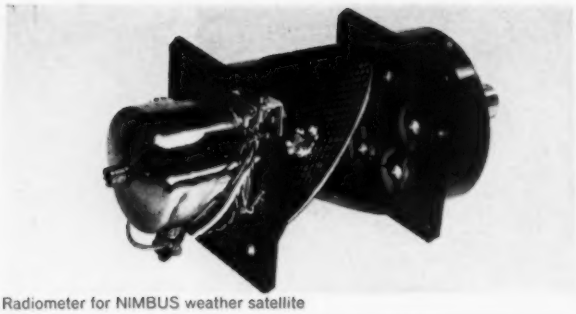

Radiometer for NIMBUS weather satellite

Interceptor IR installation

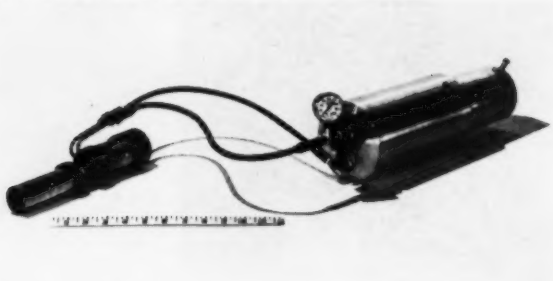

12°K closed-cycle cryostat

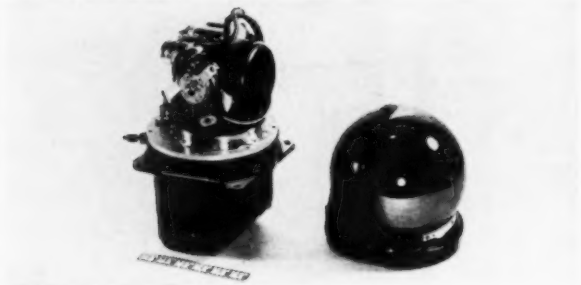

90C IR search/track set

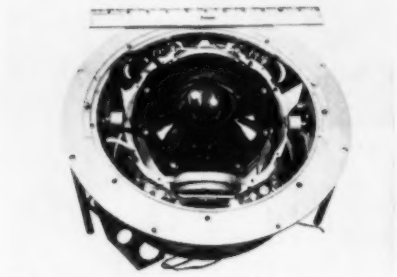

IR multi-channel tracking radiometer

Star tracker for SURVEYOR spacecraft

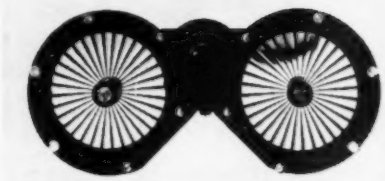

Modulated IR source

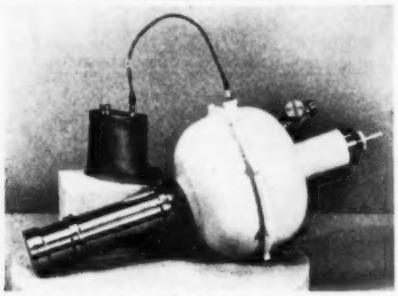

Liquid-helium-cooled IR detector

IR anti-tank missile controller

# Expanding Infrared Programs

## create new career assignments

Rapid growth of HUGHES Infrared activities in the Aerospace Divisions and the Santa Barbara Research Center has created many responsible positions for qualified engineers and scientists in all phases of IR systems development from conception through production engineering.

Immediately available assignments include openings in such diverse technologies as semiconductor physics, optical design, cryogenics, mechanical engineering, precision electro-mechanisms, electronic circuit design, servo systems...and many other areas.

Current HUGHES IR contracts include advanced systems for space exploration, weather reconnaissance, anti-ballistic missile defense, anti-submarine warfare, interceptor weapon guidance & fire control, bomber defense and tactical weapon control.

Professional experience, an accredited degree and U.S. Citizenship required.

*For immediate consideration, please airmail your resume to:*

**MR. ROBERT A. MARTIN**
**Hughes Aerospace Divisions**
**11940 W. Jefferson Blvd.**
**Culver City 33, Calif.**

**HUGHES**

HUGHES AIRCRAFT COMPANY
**AEROSPACE DIVISIONS**
An equal opportunity employer

# HARSHAW POLISHED OPTICS

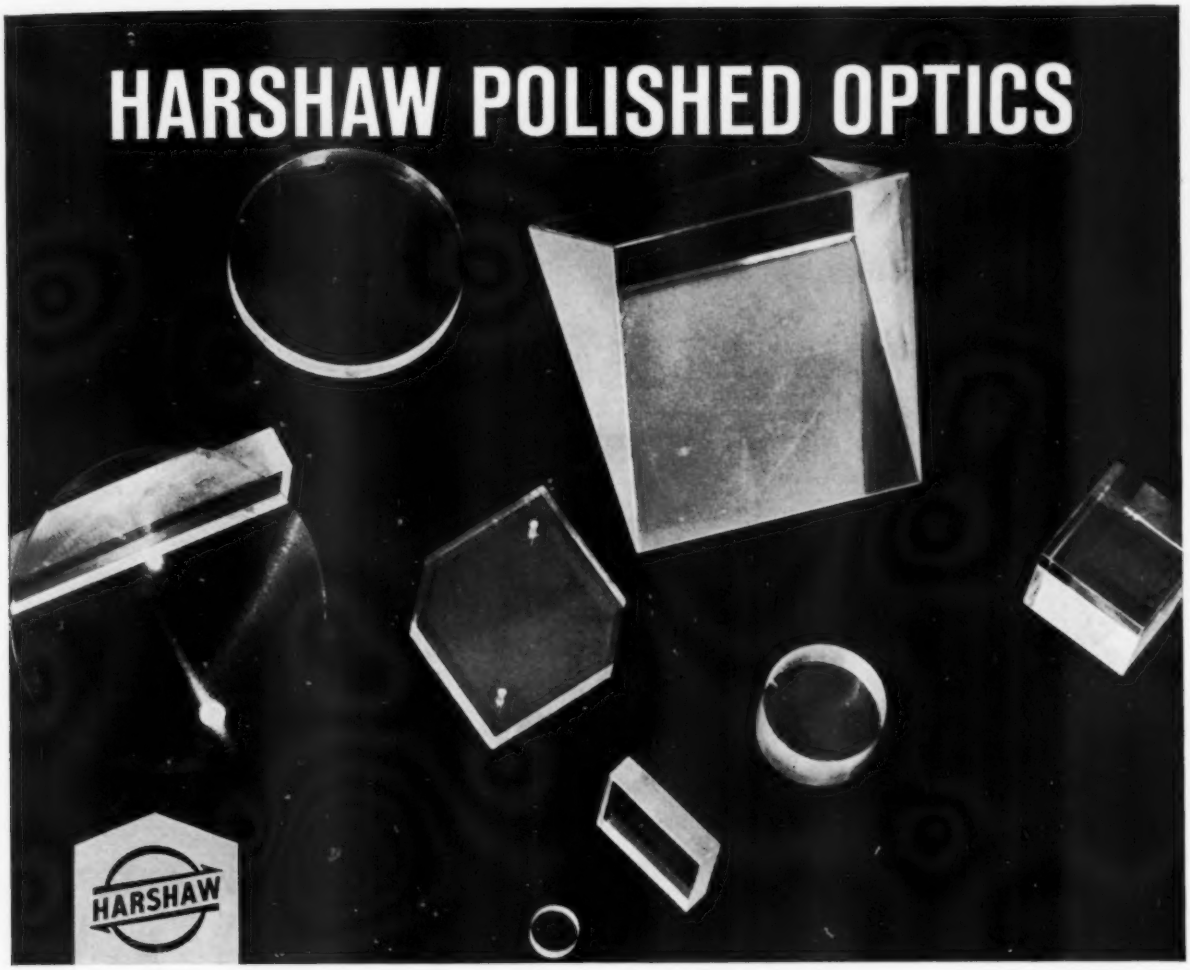


The Harshaw Chemical Company has expanded their services to the Optical Industry by offering polished, tested and guaranteed optics transmitting from 0.1 to 70 microns. This new facility is equipped to produce flats and prisms and lenses as well as specialty items tailor-made to customer specifications. The polishing facility is located in new quarters especially designed to provide the proper air-conditioned, dust-free and controlled humidity environment. Absorption-free optical crystals are available to meet your transmission requirements in the range from the vacuum ultraviolet at 1100 Angstroms to the far infrared at 70 microns.

Materials available include lithium fluoride, calcium fluoride, barium fluoride, sodium fluoride, sodium chloride, potassium chloride, potassium bromide, silver chloride, KRS-5, KRS-6, thallous chloride, thallous bromide, cesium bromide and cesium iodide. Special crystals can be custom grown to customer specifications. Other products include specially oriented crystals, attenuated total reflection components, and X-ray monochrometer plates. For additional information write to the Crystal-Solid State Division, The Harshaw Chemical Company, 1945 East 97th Street, Cleveland, Ohio 44106, phone area code 216, 721-8300.

## CRYSTAL-SOLID STATE
### DIVISION
### THE HARSHAW CHEMICAL COMPANY

**1945 East 97th Street • Cleveland, Ohio 44106**
**Phone Area 216 721-8300**

**Utrecht, Netherlands—Contact Harshaw-Van Der Hoorn N. V.**
**Frankfurt, W. Germany—Contact Harshaw Chemie GmbH**

Please send me your booklet "Harshaw Polished Optics," and specific information about_____

_____

Name_____

Company_____

Address_____

City_____ Zone_____ State_____

★ VISIT OUR BOOTHS AT: 1. 2nd National Applied Spectroscopy Meeting, San Diego, Oct. 14-18
2. Optical Society of America, Chicago, Oct. 22-25

# TINSLEY CAPABILITIES

50-Inch Precision Optical Window

## BUBBLE CHAMBER OPTICS

Proven experience in the fabrication of ultra high precision bubble chamber optical systems, including aspherics, for leading research laboratories.

## LENS MANUFACTURE

All types of refraction systems-fabricators of the world's largest astronomical apochromatic telescope.

## MASSIVE OPTICS

Schlieren systems—telescopes. Special equipment for generating and polishing high precision optical flats and mirrors up to 10 feet diameters.

## DESIGN CAPABILITIES

Optical engineering staff experienced in all fields of optics with IBM 1620 computer design capability.

## TEST FACILITIES

Air conditioned and constant temperature area. Approved quality control department with specially designed test equipment.

**For optical engineering consultation or quotations: telephone (415) 843-6836 or TWX (415) 891-9316**

# TINSLEY LABORATORIES, INC.

**2448 Sixth Street, Berkeley, California 94710**

# surveillance

As space programs extend farther into space, the requirements of visual and graphic acquisition and display systems begin to exceed the existing state of the photographic art. By anticipating future needs through several active R & D programs, Itek is establishing a fundamental role in the aerospace field.

The acceleration of these programs, and increased contractual responsibilities in related areas, have created many key assignments.

One opportunity of more-than-usual significance exists for an **Optical Engineer** with experience in aerial reconnaissance equipment, including the design of complete systems, their evaluation and their performance specifications. Qualified candidates will design and direct calibration controls, recommend lens system liaison with lens manufacturers, establish and monitor total quality controls and act as technical supervisor of a highly-specialized expanding group.

*Several other assignments exist in the following areas of*

## OPTICS

LENS SYSTEMS DESIGN ■ PHOTO-OPTICAL INSTRUMENTATION ■ OPTICAL FABRICATION DEVELOPMENT ■ ASTRONOMICAL SYSTEMS ■ OPTICAL SUB-SYSTEMS TESTING ■ PROJECT-LEVEL HIGH PRECISION OPTICS AND ELECTRO-OPTICS ■ PHOTO-GRAPHIC RESEARCH ■

To gain more complete information concerning the rewarding personal and professional potential of these positions, address your resume to:

Mr. Richard W. Finnegan, Personnel Manager

Itek

**Itek Corporation**

10 MAGUIRE ROAD, LEXINGTON 73, MASSACHUSETTS

Modulating the laser light beam is a key to using the vast data-transmission capability of lasers.

IBM scientists achieved a significant advance when they created the injection laser. With other types of lasers, it is necessary to modulate the output light beam itself. This is relatively inefficient. In contrast, since the injection laser is stimulated by electrical energy, it can be modulated simply by varying the stimulating current. Six months after IBM announced the first injection laser—made of gallium arsenide—engineers were able to demonstrate the first successful transmission of voice signals over an injection laser beam. In addition, IBM scientists have pursued the exploitation of new materials for injection lasers and recently fabricated an indium phosphide device.

The injection laser is excited by passing a current above a certain threshold through a p-n junction. Electrons produce photons by falling from the conduction band to the valence band and stimulate regenerative oscillations between sharply cleaved ends of the crystal in the region adjacent to the junction. The reinforced oscillations emerge from a 0.01 square millimeter cross-sectional face as an infrared beam having a spectral width of less than 0.5 Angstrom and an angle of spread of 2.5 degrees. Modulation of the output light can be accomplished by varying the current across the junction.

If you are interested in making contributions in lasers or other areas in which IBM scientists and engineers look for answers to basic questions, write: Mgr. of Employment, IBM Corp., Dept. 619K, 590 Madison Ave., N. Y. 22, N. Y. IBM is an Equal Opportunity Employer.

## IBM asks basic questions in lasers

### How can we modulate light?

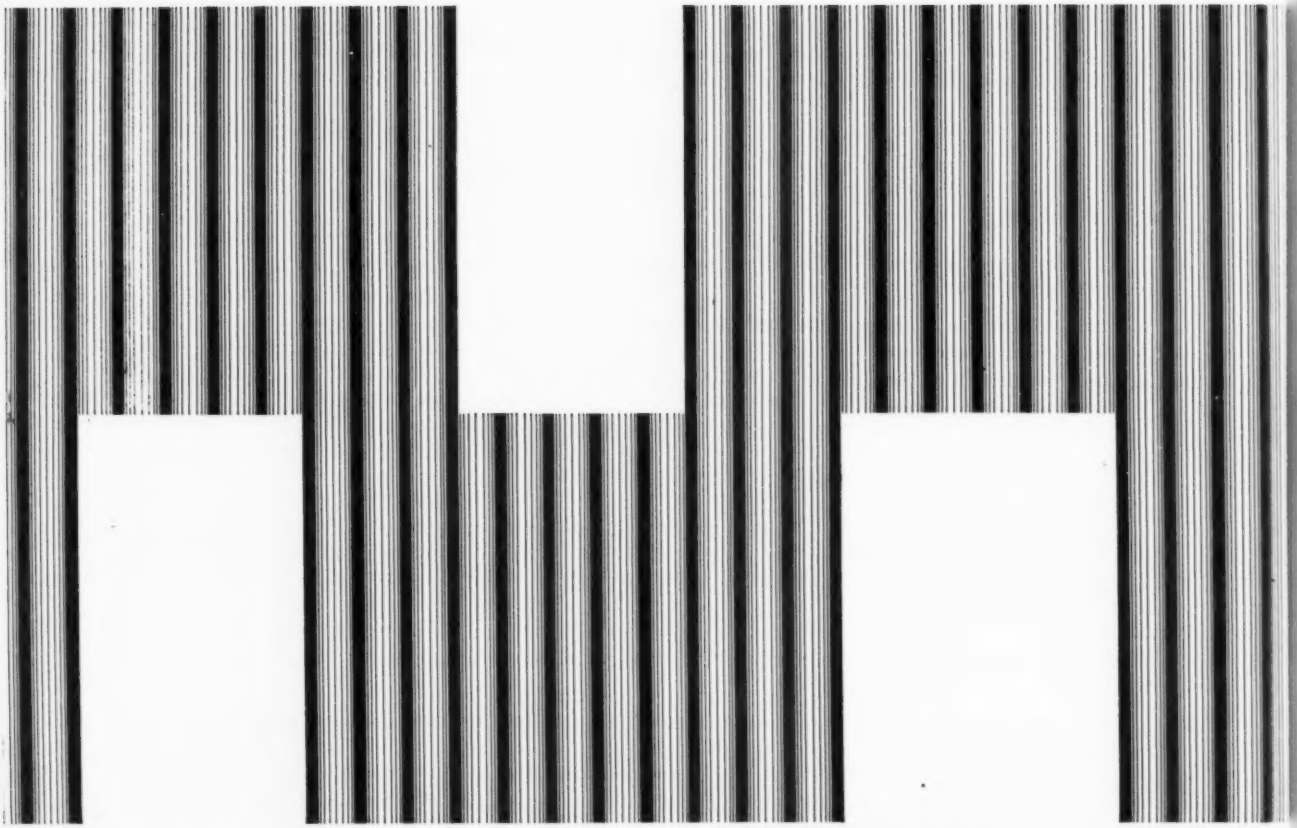

# LOCATE LINES TO 1μ OVER 200 mm WITH THIS HI-PRECISION MICROPHOTOMETER

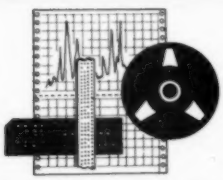

WIDE SELECTION OF READOUT DEVICES AVAILABLE

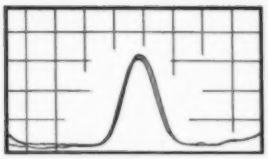

TRACE TAKEN FROM OPTIONAL PHOTOELECTRIC SETTING DEVICE

## Sensitive Model 23-500 Microphotometer measures densities over a 0 to 3.5 range.

**RESOLUTION** . . . two lines, 5μ apart, can be resolved at a transmission level of 50%, at 10x magnification.

**SLITS** . . . width continuously adjustable 0-100μ; length in .1, .2, .5, 1.0, 1.5, 2.0 and 2.5 mm steps. Circular apertures optional.

**ROTARY PLATEHOLDER** . . . can be adjusted through ±90° with vernier to 0.1°. Vernier cross motion to 200 mm.

**FILM, PLATE VERSATILITY** . . . takes films and plates up to 5" x 10". Plates to 8" x 10" optional.

**DIGITAL READOUT** . . . can be supplied with automatic punched card, paper or magnetic tape readout for three or more parameters to meet critical requirements.

**PHOTOELECTRIC SETTING** . . . can be provided for quick, manual setting and reading to better than 1μ between two points.

Ask for Catalog 23-500.

Jarrell—Ash

Dedicated to excellence in the research, development and manufacture of precision analytical instrumentation.

For further information . . . clip the coupon, attach to your company letterhead and mail.

**JARRELL-ASH COMPANY**
**26 Farwell Street, Newtonville 60, Mass.**

Name _____

R. M.

# MASSIVE PRECISION ACRYLIC LENSES AND OPTICAL COMPONENTS NOW AVAILABLE IN SIZES UP TO SIXTY INCHES!

If you use lenses or optical components, you may be interested to learn that facilities are now available for precision finishing of massive optical grade acrylic lenses and other optical components in sizes up to sixty inches. The new acrylics offer: relatively low cost; light weight (45% that of glass); reduced mounting costs, high resistance to chipping and breakage; ease of machining; and higher light transmission.

Some typical acrylic components are shown above, including a massive fifty-six inch optically ground and polished acrylic lens (center). Facilities are available for the production of spark chamber frames, retrodirectors for bubble chamber optics, prismatic lenses for neutrino chamber optics, and other precision components . . . . all in low-cost, light-weight acrylics.

What are your requirements? Perhaps we can help. Use the coupon below to order your free copy of Bulletin 101 today, or let us quote you. Simply return the coupon with a drawing or sketch and specifications.

**CLIP AND MAIL THIS COUPON TODAY!**

**APPLIED PRODUCTS DIVISION**
**Fostoria Corporation**
**Warrington Industrial Park**
**Warrington, Pennsylvania**
**Area Code 215 — Diamond 3-6000**

**APPLIED PRODUCTS DIVISION, Fostoria Corporation**
Dept. A-1, Warrington, Pennsylvania

- ☐ Send free brochure on low-cost, light-weight acrylic lenses and optical components.
- ☐ Quote per enclosed drawing (or sketch) and specifications.
- ☐ Have optical engineer call.

NAME .....

TITLE .....

COMPANY .....

ADDRESS .....

CITY ..... ZONE ..... STATE .....

# Bubble Chamber Optics

W. T. Welford

Developments in optics and optical systems for use with bubble chambers and in measuring bubble chamber film are reviewed.

## I. Introduction: Bubble Chamber Operation

Optics enter at two distinct points in the chain of operations comprising bubble chamber physics. Tracks of bubbles are formed along the paths of ionizing particles in the bubble chamber. The first application of optics is in photographing these from two or more viewpoints, to record the three-dimensional arrangements of the tracks involved in an interaction or *event*. Next the tracks have to be measured in order to obtain parameters of this three-dimensional arrangement which can be used to elucidate the nature of the event, and optics is used in the measurement process. There is also an intermediate stage, *scanning*, in which the photographs are projected and inspected visually for interesting events, but little sophisticated optics is involved here. The whole process is indicated diagrammatically in Fig. 1, which includes also the computer stage; here the measurements are reduced and their fit to different events is tested.

Two points which are relevant to the optical problems are: (a) *the precision of measurement involved*. This depends somewhat on the type of experiment and on the particular bubble chamber, but it may be physically significant to measure coordinates on tracks in the chamber to a precision of $\pm 20\ \mu$ in some cases; and (b) *the number of events*. Bubble chambers have recycling times of a few seconds (compared with many minutes for cloud chambers) and they may run continuously for many days; it turns out to be desirable to measure large numbers of events in a single experiment in order to have good statistics, so that all operations, photography, processing, scanning, and measurement, must be on a mass-production basis in order to keep up with the demands of the physicists for data. This incidentally raises major problems at the computer stage and this is relevant to advanced techniques which we shall mention, in which it is proposed to couple measuring machines and computers directly.

This survey will be in two main sections, covering optics of bubble chambers and the measuring process, respectively. In the first section we deal with light scattering by bubbles, illuminating systems, photography and focal depth problems, fiduciary marks, and choice of film. In the second section we discuss the scanning process, conventional measuring machines of the coordinate table type, photoelectric detection systems and automatic track following, and flying spot measuring machines.

This article is necessarily somewhat different from the more usual survey or review article: it is less specialized, in that we have thought it desirable to include descriptions of things which are familiar to the nuclear physicist but not so to the applied optician, and also it suffers from a shortage of references; this is because many of the interesting instrumental developments in this field are never formally published in a scientific journal. Sometimes they are described only in privately circulated reports but these cannot be cited as formal references. We have tried as far as possible to mention names of originators but sometimes we have not felt sure of a source, so we apologize in advance for any cases where we have failed to give due acknowledgment and credit.

## II. Bubble Chambers

The bubble chamber is now ten years old, having been invented by D. A. Glaser in 1953, so that it is unnecessary to recapitulate its principles. Several good general surveys of bubble chamber technology are available.[1–3] The main optical problems arise in obtaining bright enough images of the bubbles. The refractive index of the liquid is in many cases very close to unity, so that very little light is scattered by the bubble. Table I lists the main liquids of interest with their refractive indices and some other properties of significance for the optical arrangements. These fall

The author is with the Physics Department, Imperial College, London, England.

Received 2 April 1963.

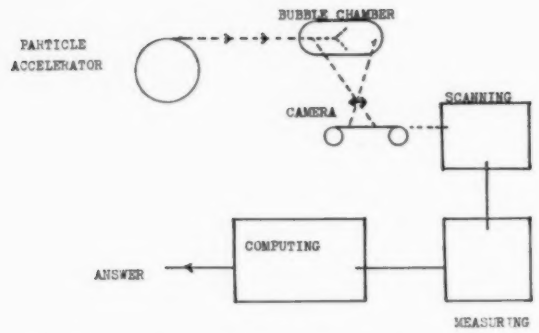


Fig. 1. Block diagram of bubble chamber operations.

naturally into two groups: the light liquids hydrogen, deuterium, and helium, which are used at low temperatures; and the heavy liquids propane, xenon, and the freons, which are used at higher temperatures. The light liquids present the more interesting optical problems because their refractive indices are so low; a survey was given by Welford.[4] With the heavy liquids less sophisticated optics are usually used.

## A. Light Scattering by Bubbles

Very little exact data about bubble diameters are available but it seems to be generally agreed that operating conditions are such that the bubbles are greater than 100 $\mu$ in diameter. It is then permissible to calculate the scattering properties on the basis of geometrical optics except for light scattered closer than, say, 1° to the direction of the incident light.[5] Davis[6] and others[7] described the method of calculation; for the present purposes only approximate values are needed and not many rays need be traced. The results may be expressed in the following form: let $E$ be the incident illumination (flux per unit area) on a bubble of radius $\gamma$ and let $E_s$ be the scattered illumination at a (large) distance $R$ from the bubble in a direction at an angle $\alpha$ to the direction of $E$; then we put

$$E_s = G(\alpha)\left(\frac{r}{R}\right)^2 E, \tag{1}$$

where $G(\alpha)$ is the geometrical scattering function. Figure 2 shows values of $G(\alpha)$ for the light liquids, and the rays used in computing $G$.

For values of $\alpha$ less than about 1° and for bubble sizes of order 100 $\mu$ it is necessary to use the Fraunhofer diffraction approximation.[5] This can be shown to give in place of Eq. (1),

$$E_s = \frac{\pi\gamma^{22}}{\lambda^2}\left[\frac{2J_1\left(\frac{2\pi}{\lambda}r\alpha\right)}{\frac{2\pi}{\lambda}r\alpha}\right]^2\left(\frac{r}{R}\right)^2 E. \tag{2}$$

The first factor on the right-hand side takes the place of $G(\alpha)$ in Eq. (1); the ratio $(r^2/\lambda^2)$ gives very large values, of order $10^4$, for 100-$\mu$ bubbles, so that the scattering does increase steeply at small values of $\alpha$, as suggested in Fig. 2.

It can be seen that the scattered light drops very rapidly as $\alpha$ increases, so that small angle scattering has to be used in order to show up the bubbles in sufficient contrast. To do this one can either use bright field illumination and rely on enough light being scattered out of the illuminating beam to make the bubbles appear dark, or dark-field illumination, when the bubbles scatter light out of the illuminating beam into the camera lenses. In practice dark-field illumination is almost invariably used because the bubbles are too small to be photographed as circular objects, i.e., they appear as diffraction patterns; thus the amount of light subtracted by a bubble from the background in bright field would be very small and the contrast would be poor.[8] However, heavy liquid chambers have been operated in bright-field illumination at MIT and a 76-cm hydrogen chamber has been used in bright field by a Columbia University group. The contrast of the tracks is very low but the negatives are apparently measurable.

The general arrangement of a bubble chamber would then be as in Fig. 3, which shows schematically an illuminating system with a camera lens set to one side of the main beam of light. We may note incidentally that the chamber would be surrounded by pressure and heat shields, and a large magnet; this leaves very little space for optics, even arranged as in this diagram.

## B. Choice of Scattering Angle

The choice of the angle $\alpha$ depends on several counteracting considerations. First, an order of magnitude calculation[8] of the light power needed shows that with available xenon flashtubes as sources it is hardly practicable to go beyond about 15° for hydrogen and less than that for helium. For heavy liquids, on the

**Table I. Liquids Used in Bubble Chambers**

| Liquid | Refractive index | Operating temperature (°K) | Operating pressure (atm, abs.) | Volume expansion (approx. %) |
|---|---|---|---|---|
| Hydrogen | 1.1 | 27 | 6.8 | 2 |
| Deuterium | 1.1 | 34 | 8.8 | 2 |
| Helium | 1.025 | 3.5 | 1.0 | 1 |
| Propane | 1.25 | 330 | 20 | 3 |
| Freons[a] | | | | |
| Xenon | 1.2 | 250 | 3 | 3 |

[a] Freons are halogenated hydrocarbons such as $CF_3Br$ and $C_2ClF_5$. Their refractive indices do not seem to have been measured but from properties of similar compounds one might guess them to be in the region of 1.5. Freons are used in bubble chambers as mixtures, sometimes also mixed with propane. The operating conditions are similar to those for propane.

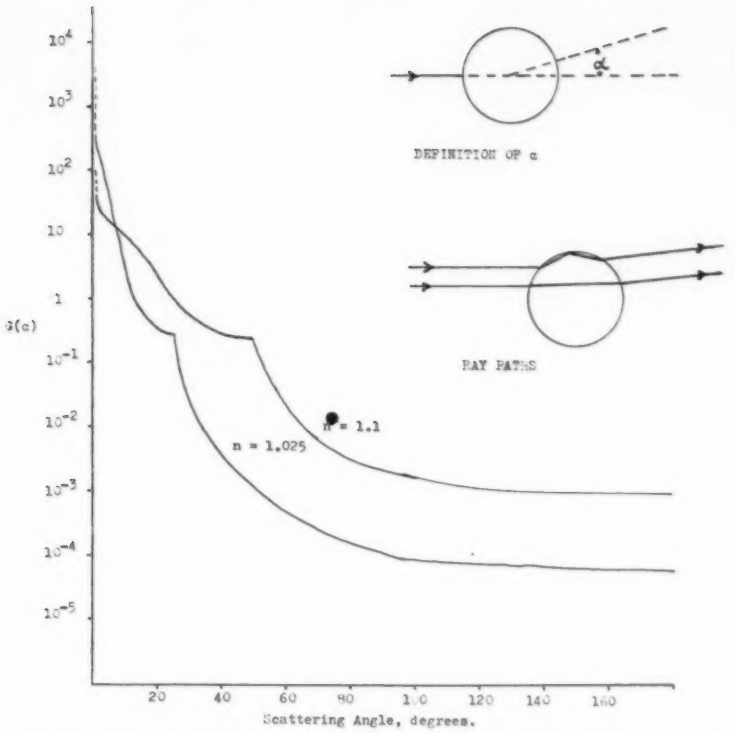


Fig. 2. Geometrical scattering functions for bubbles in liquids of refractive index 1.1 ($H_2$, $D_2$) and 1.025 (He).

other hand, the scattering function does not fall off rapidly and it is possible to use a scattering angle of 90°, which gives a very convenient geometry. The magnitude of the scattering function $G(\alpha)$ is a measure of the contrast of the bubble images against the nominally dark field, which is, of course, not perfectly dark because of parasitic images, scattered light off optical and nonoptical surfaces and, in light liquid chambers, air and pump oil vapors condensed on to optical surfaces, so that a small scattering angle gives good contrast in the bubble images. A lower limit to $\alpha$ is set in practice by irreducible aberrations or manufacturing errors in the condensing system; this limit seems generally to be about 2°, although in one case[9] a value as small as 0.6° was used in a helium chamber, where $G(\alpha)$ falls off very rapidly.

With the usual arrangement of three or four cameras photographing the chamber from one end, as in Fig. 3, it turns out that the volume of liquid seen by two or more cameras decreases as the scattering angle decreases, particularly if each camera has its own light source, as is necessary for small scattering angles. The proportions of chamber volume seen by different cameras and combinations of cameras depend in a complicated way on the scattering angle, the method of illumination and the stereo angles, i.e., the angles subtended at the chamber by joining two cameras. This question of usable volume needs careful consideration in the early stages of laying out the optical design.

Yet another consideration is that of uniformity of illumination of the bubbles in different parts of a large chamber; the actual value of $\alpha$ and also the solid angle subtended by a camera lens aperture vary throughout the chamber, and these, together with the form of the scattering function $G(\alpha)$, determine the variation of the total flux in a bubble image.[4]

## C. Illuminating Systems

Illuminating systems for bubble chambers fall into three classes: (a) "through-illumination", as in Fig. 3, where the light goes through the chamber and a small scattering angle is used; (b) "90° illumination", where the chamber is illuminated at right angles to the camera axes and $\alpha \simeq 90°$; (c) "retrodirective illumina-

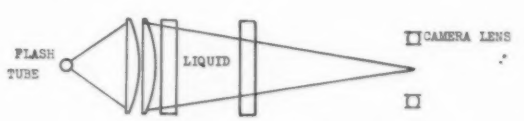


Fig. 3. Dark-field illumination system; the flashtube source is focused centrally between the three camera lenses.

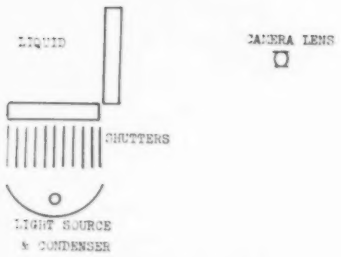


Fig. 4. A 90° illumination system.

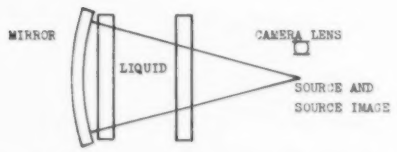


Fig. 5. Principle of retrodirective illumination.

tion", where the light sources and the cameras are both on the same side of the chamber but, again, the scattering angle is small. The case of 90° illumination does not need much consideration since no very sophisticated optics are involved; a simple system of slats or venetian blinds is enough to prevent direct light from reaching the cameras, as in Fig. 4, and such a system is often used in the larger heavy liquid chambers.[10–12] However, through-illumination with small scattering angle has also been used in many heavy liquid chambers, possibly because of the better contrast obtainable.

The retrodirective system is basically as in Fig. 5. The light source is imaged back on itself by the concave mirror and the bubbles are seen in dark ground by light scattered into the camera lenses. This simple version has the serious disadvantage that reflected images of the bubbles are also seen in the mirror and these are sufficiently nearly in focus to be a source of confusion in the measuring process. This was pointed out by Belonogov *et al.*,[7] who described such a system. Many ingenious devices have been proposed to eliminate the reflected images and we describe some of these in Sec. II.C,2 below.

There are two schools of thought which favor strongly the through and retrodirective systems, respectively, and before describing the systems in detail we summarize the general arguments for and against these systems in Table II. There are, of course, arguments which depend on details of each system, and we indicate these in Secs. II.C,1 and II.C,2 at the appropriate points.

**Table II. Pros and Cons of Through- and Retrodirective-Illumination Systems**

| Property | Through-illumination | Retrodirective-illumination |
|---|---|---|
| Parasitic images | Good, since two reflections are needed to form an image which can be photographed | Poor; only one reflection needed to form an image |
| Stray light from nonoptical surfaces | Good, since conventional glare stops can be used | Poor, since nonoptical surfaces are seen from the side from which the light is incident |
| Convenience of cryostats and magnets | Poor, since an optical path right through the system is needed | Good, since one side can be filled with a magnet pole, giving greater field |
| Safety | Poor, since many windows increase risks in the event of an explosion | Good; fewer windows give protection in case of explosion |
| Cost | Expensive; two windows and large condenser optics needed | Cheaper, since only one window is needed if the retrodirective optics are immersed in the liquid |

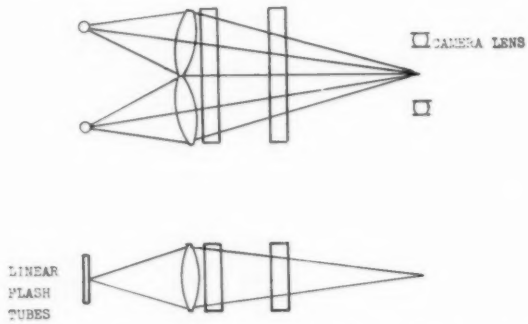


Fig. 6. Optical system of the 81-cm hydrogen chamber of the École Polytechnique.

### 1. *Through-Illumination Systems*

In the simplest form, as described, e.g., by Colley *et al.*,[13] a single source is focused by a condenser so that its image falls centrally between three cameras arranged in a triangle, as in Fig. 3. In a variant of this,[14] two complete systems of this kind are arranged to view a hydrogen chamber in two directions at right-angles, thus giving a 90° stereo angle; such a system is not practicable for chambers with heavy magnets.

For accurate work with particles of high energy (in the $10^9$ eV region) large chambers are needed and the apertures tend to be roughly rectangular with aspect ratio 2:1 or 3:1. In such cases it is natural to split the condenser aperture into two or three sections. Thus the French 81-cm hydrogen chamber[15] has a two-section condenser with linear vertical flashtubes, as in Fig. 6.

A further step in complication is to have three source images, one near each camera, to give a small scattering

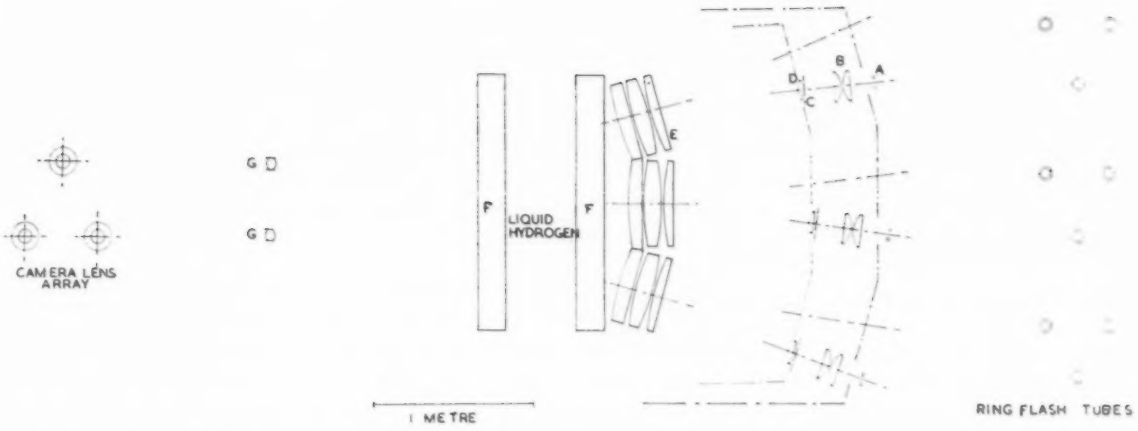


Fig. 7. Optical system of the British National Hydrogen Bubble Chamber, A. flashtube; B. precondenser; C. annular stop; D. field lens; E. main condenser; F. chamber windows; G. camera lenses. The ring flashtubes are imaged at the annular stops by the precondensers.

angle and consequently increased contrast of the bubble images; with $m$ sections to the condenser and $n$ camera lenses this clearly involves $mn$ sources. This system is used in the British National Hydrogen Bubble Chamber[16,17] where the sources are ring-shaped flashtubes which are imaged round the camera lens apertures in order to get as much light at the small scattering angle (2°) as possible. The BNHBC has a clear window aperture 150 cm by 50 cm with semicircular ends; the condenser system is in three sections, each consisting of three components, as in Fig. 7.

In the system shown in Fig. 7 it is required to form reasonably good off-axis images of the light sources and it is, therefore, necessary to consider the aberration correction of the condensers. Those used in the BNHBC are corrected for coma by choice of bending and for spherical aberration by aspherizing the last surface. It is obviously impossible to correct for astigmatism or chromatic aberration in such a system, which is effectively "thin" (the total center thickness of each section is actually 25 cm) and which contains no negative elements, so that these aberrations set the lower limit of 2° for the scattering angle. The effect of chromatic aberration is incidentally reduced by using light of a relatively narrow wavelength range, as explained in Sec. II.C,3 below. It can be seen from Fig. 7 that the actual ring flashtubes are outside the outer vacuum tank, but these are imaged by pre-condenser systems on to annular diaphragms at the inner vacuum tank. This inner tank, called the hydrogen shield, is maintained at the temperature of the liquid in the chamber in order to minimize heat radiation to the chamber, so it is important to keep any windows in it as small as possible. This is the reason for re-imaging the sources, a technique in general use with large chambers.

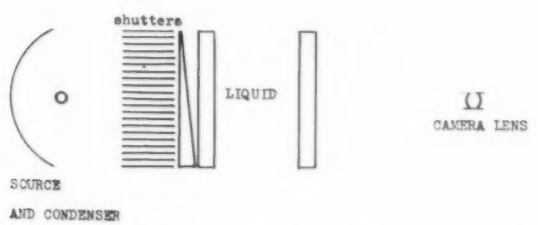


Fig. 8. Thorough-illumination system with shutters and prism for directing the illuminating beam away from the camera lens.

In order to reduce the luminance of ghost images the condenser optics and windows are usually antireflection coated (see Sec. II.C,3); a simpler approach is to use a diffusing screen in front of the light source with patch stops which are imaged on the camera lenses[9,18,25]; this provides a broad source of low luminance and thus the luminance of the ghost images is decreased. This method involves some loss of light because of the diffusing screen, but, more serious, the points of the screen at some distance from the patch stops illuminate the bubbles at effectively large scattering angles and because of the rapid fall-off of the scattering function they do not contribute very much to the total flux in the bubble image. This is most marked in the case of helium, where the scattering function falls off most rapidly.

It is possible to eliminate condensers completely and use instead a shutter system as in Fig. 8; this was done by Bertanza *et al.*[19] for a heavy liquid chamber, but it is probable that the stray-light background from the shutters would be too large for a light liquid chamber.

A compromise system has been described[20] in which linear light sources are used with cylindrical condensers and shutters to prevent light spread in the plane con-

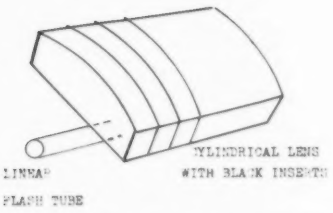


Fig. 9. Cylindrical condenser incorporating shutters for use with linear flashtube in through-illumination.

taining the axes of the cylinders, as in Fig. 9. A simpler version of this is under construction at Saclay, France, in which the shutters are omitted and the light sources are behind diffusing strips with linear patch stops. All of these systems are relatively inexpensive and simple, but all give a heavy background compared to the conventional condenser system.

*2. Retrodirective Illumination Systems*

The prototype retrodirective system as in Fig. 5 has already been described. Gorbunkov[21] has proposed to diminish the brightness of the reflected bubble images by using a thick back-surface concentric concave mirror; this has the effect of spreading the light from the reflected images away from the camera lenses. It is doubtful whether such a system is economically practicable for large chambers.

Shutters in front of the mirror in the form of a solid ensemble of strips of black glass and transparent glass have been proposed by R. B. Palmer of Brookhaven (Fig. 10). He has also suggested a solid mirror composed of transparent glass fibers normal to the mirror surface and fused together in a black glass matrix (private communication).

Most retrodirective systems involve replacing the large concave mirror by an array of smaller elements which reflect the main illuminating beam but scatter or absorb the light scattered by the bubbles toward the mirror. Of these the best known is the celebrated coat-hanger system of the Berkeley 72-in. hydrogen chamber.[1] Figure 11 shows a general view of the optics of this chamber. The coat-hangers are curved solid plastic cylindrical lenses with reflecting strips along their bottom surfaces. These reflecting strips are so positioned that the direct illuminating beam reaches them and is reflected back on its own path, but light scattered by a bubble misses them and is absorbed by blackened surfaces. Thus the bubbles are seen only by light scattered from the returning beam. The coat-hangers are made of "Homolite", a plastic which is said to take a good polish, and the blackened surface is "Luxorb", a material with the same refractive index as Homolite. However, the background from this system is inevitably larger than that from a through-illumination system.

Other variations such as corner cube reflectors have been suggested but not tried. Similarly, a suggestion to use a single large concave mirror with a wavy surface with controlled maximum slope variations[1,2,4] does not seem to have been tried.

Courant[22] showed how the effect of reflections from the window surfaces in retrodirective systems could be minimized by suitably placed patch stops in the pre-condensers which were imaged into the camera lens apertures.

*3. Antireflection Coating of Illumination Optics*

Retrodirective systems rely chiefly on careful off-axis placing of the light sources to eliminate reflected images (see Fig. 11) but in through-illumination systems it is essential to have efficient coating.

Two-layer coatings consisting of bismuth oxide and magnesium fluoride on glass can now be made to give substantially zero (<0.1%) reflectance at the design wavelength[4] and recent trials of the BNHBC (Fig. 7) have confirmed the absence of ghost images even at considerable overexposure. To make the best use of the coatings it is advisable to use a narrow wavelength range (ca. 500 Å) centered on the design wavelength, but in these trials the whole of the visible spectrum from about 4500 Å on was used with panchromatic film. It has also appeared that no very elaborate light-trapping is needed to dispose of the light from the source images which falls on the inside of the hydrogen shield near the camera lens ports. No image is seen reflected in the chamber windows if these parts are simply painted matte black.

*4. Light Sources*

The individual bubbles formed along a track grow rapidly and they also move because of turbulence in the liquid due to thermal gradients and to movements initiated by the expansion. It is thus desirable to have a short exposure time, ideally about 100 μsec. An order-of-magnitude calculation of the required exposure suggests that the flashtubes should dissipate between 10 and 100 J per flash for the geometry of large chambers and this is confirmed in practice. Xenon flashtubes with these properties and with a good working life, about

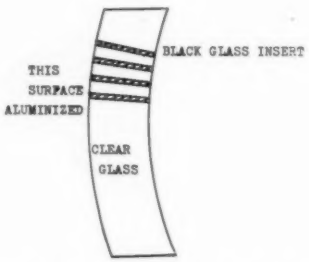


Fig. 10. Retrodirective system with black glass shutters cemented into the mirror.

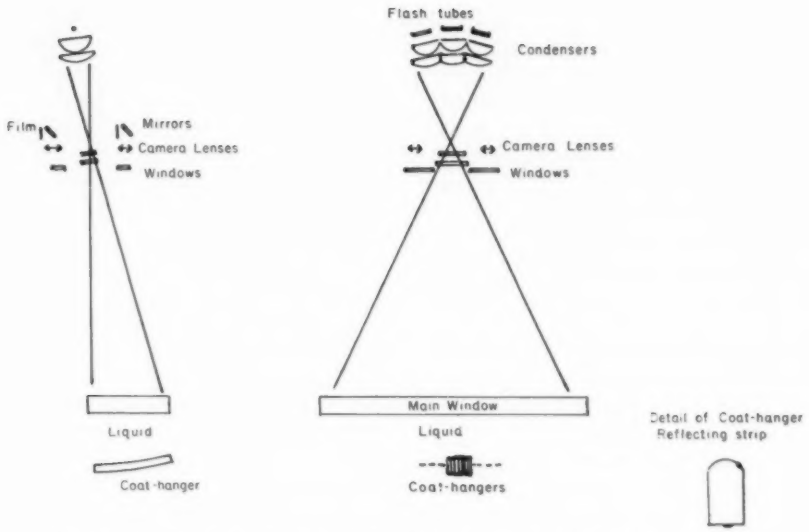


Fig. 11. Optics of the Berkeley 183-cm chamber, with detail of a coat-hanger.

$10^5$ flashes, can now be made. The BNHBC gave good track photographs with 100 J dissipated in each flash-tube; these were ring sources supplied by Physikalische Technische Werkstätten (Wiesbaden, W. Germany), and they have given over $10^5$ flashes at a repetition rate of 30 per minute in trials. One such tube on test at the time of writing has given over 170,000 flashes with no loss in output and no visible damage to the tube.

*5. Windows*

The main windows of large chambers present considerable problems in glass manufacture and working. They may be about 15 cm thick for clear apertures of order 1 m in hydrogen chambers in order to withstand stresses due to the pressure in the chamber and about 25 cm thick for heavy liquid chambers. These dimensions are obtained by taking the generally accepted figure of 1000 lb/in.$^2$ (or say 100 kg/cm$^2$) as the safe tensile stress in glass. This applies to annealed glass, not tempered or toughened; the toughening process is undesirable for precision windows since it may introduce refractive index gradients by undoing the effects of the heat-soaking process which constitutes fine annealing.

Borosilicate crown is almost invariably used since it is the most easily obtained variety in large clean castings. Almost all large bubble chamber windows seem to have been made by Jenaer Glaswerk Schott u. Gen., Mainz, W. Germany. This firm has so far used its BK7 type of glass, but lately has recommended a newly developed glass type, K50, as being easier to produce free from striae and other defects. This glass has $n_d = 1.5226$ and $V = 60.2$.

Usually the expansion in a bubble chamber which produces the effective superheat condition takes place through a manifold of pipes leading to a side wall of the chamber body. A recent project (private communication from D. Norgren) for a 63-cm hydrogen bubble chamber involves expansion by moving one window; this window is on the illumination side in a through-illumination system and it is also a condenser lens. Interesting problems of clamping and stressing would arise here.

## D. Photography

Under the heading of photography we consider problems raised by the large focal depth needed, about 50 cm for large chambers, the choice of camera lenses, the choice of film, and the mechanical design of the cameras. We note also that it is common practice to have a Land Polaroid camera available for test exposures.

*1. Focal Depth*

Depth of focus has been discussed on the basis of geometrical optics[1] or diffraction theory[4,8]; it is also necessary to take account of the properties of the photographic emulsion in such discussions. It turns out that most large chambers operate with camera lenses under very similar conditions, namely a demagnification from the mean plane of the chamber of about 16 times and an aperture ratio of between $f/20$ and $f/25$. This would appear to be because emulsion effects tend to smudge out the nice differences in focal depth predicted by different criteria.

It should also be noted that the focal depth requirement depends very much on the kind of measurement to be made on the film. If only angles and curvatures of tracks are to be determined, then it is not important to distinguish individual bubble images and quite a lot

of image degradation due to defocusing and other effects can be tolerated. This is because the measuring machines can set on the center of a track to a precision which is perhaps a tenth or less of the track half-width. Broader tracks are, however, undesirable when tracks crossing or meeting very obliquely are to be measured. If, in addition, the lengths of gaps between groups of bubbles in a track are to be measured, an operation which is now becoming more in demand, then it is clearly desirable to have very good definition in the bubble images and the focal depth tolerance must be tightened.

It has been proposed[23] to obtain increased focal depth by using a lens of variable power to take two or more exposures in rapid succession on the same film, in photographing cloud chambers; it is unlikely that this process could be made fast enough for bubble chamber photography. Another suggestion[24] is to use a lens of larger aperture (for increased resolution) with an annular stop to increase focal depth.

Aleksandrov *et al.*[26] have pointed out that a bubble acts as a lens of negative power and so forms a virtual image of the light source at a considerable distance behind its center. Thus if the illumination is not symmetrical with respect to the camera lens there will be a slight lateral displacement of bubble images.

### 2. *Choice of Camera Lenses*

The requirements for the camera lens are rather specialized. It is desirable to have as large a stereo angle as possible in order to gain accuracy in determination of depth, and this involves wide-field lenses. The demands on field coverage would be reduced if it were permissible to toe-in the lenses so that their axes all converged to the center of the chamber; but the computer experts concerned with the reconstruction calculations are unanimous in insisting that this would cause serious computing difficulties, so the lens axes must be parallel. Toeing-in would also, of course, require increased focal depth.

It is the general practice to use a wide-field lens (Berkeley and others, Schneider Super-Angulon; British, Ross Aerial Survey Wide-Angle) to cover a field of only about $\pm 30°$ from the axis, on the principle that such lenses vignette and lose speed because of the $\cos^4$ law at their full field of about $\pm 45°$; but their performance is good to a moderate field angle when heavily stopped down.

It is desirable to have fairly good distortion correction so that slightly curved tracks appear curved in the right sense no matter where they may be in the field; however, it is pointless to push this to extremes because even if the whole system, including windows, were corrected for distortion at, say, the mid-plane of the chamber, there would be some distortion at other levels due to the change in depth of liquid between the object and the lens. Furthermore, all lenses as manufactured have nonsymmetric distortions due to errors of edging and centering which amount to a few microns of random distortion at the image plane. Thus a distortion calibration must be used in the computing process.

Apart from distortion and some transverse color it is reasonable to expect that such a stopped-down lens should have almost Rayleigh limit correction over the required field in order to get the best out of the emulsion. Tests on Ross Wide Angle Aerial Survey lenses (unpublished work by K. H. Carnell) have shown that their properties are improved almost to this point by placing between the lens and the image plane a 15-mm thick plate of borosilicate crown glass. This corrects most of the residual coma, astigmatism, and transverse color over the restricted field and wavelength range used.

There appears to be no ideal lens design available if we bring in other considerations. These are that the entrance pupil should be right in the front of the lens, so as to make the vacuum tank windows as small as possible in order to minimize radiation heat input to the chamber, that the color correction should be over the blue and violet region, and that the stop should be roughly telecentric, so that the principal rays in image space meet the film plane nearly normally. This last requirement is necessary in order to relax the tolerances on film flatness, which are extremely tight near the edge of the frame; thus for $\pm 20\ \mu$ precision in the chamber and demagnification $\times 20$ the film must be flat to $\pm 2\ \mu$ at the edge of a 30° semifield.

The present writer is now in the final stages of designing an optical system to fulfill these requirements. It is as shown in Fig. 12; component C is heavily aspherized on the last surface, and the bending and aspherizing are chosen so as to correct distortion and astigmatism simultaneously; it is easily shown that this is possible in Seidel approximation for any stop position. Component B is concentric with the stop and it serves to flatten the field; it also contains some zero-power cemented surfaces to correct transverse color. Component A, at the stop, is of zero power and it corrects residual coma, spherical aberration, and longitudinal color. It seems probable that this design can be corrected as far as 30° from the axis, if not more.

### 3. *Choice of Film*

Most chambers use 35-mm film although a few use 46-mm (e.g., the Berkeley 72-in. chamber) and some are planned to use 70-mm film. Usually unperforated film is used, mainly for economy, since 32 to 33 mm of film width is then available, instead of only 24 mm with perforated film. With large chambers the demagnification required with 35-mm unperforated film is such that some precision in the positions of individual bubble images is lost through film grain and for purposes of

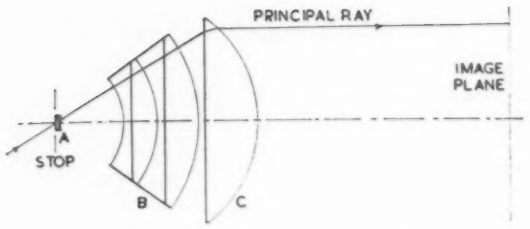


Fig. 12. Telecentric lens system.

gap measurement (see Sec. III.F) a wider film would probably be justified. This is not a decision to be taken lightly because the major part of the material cost of running a bubble chamber is the cost of the film. An advantage of unperforated film is that it can be sucked flat against a backing plate in the camera. As mentioned above, the flatness tolerance is very tight and the usual technique of pressing the film flat against a front glass, as used in aerial cameras, would probably not be good enough. In any case, it is undesirable to allow the emulsion to be pressed into contact with any surface because of the risk of scratching and marking. In this respect bubble chamber negatives are more vulnerable than aerial photographs because they consist of large areas of undeveloped emulsion with just a few black lines and blobs, so that blemishes are more distracting in the measuring process.

Typical films used are Kodak Linagraph Shellburst (Berkeley), Kodak Plus-X and Adox KB17 (CERN), Ilford 5G91 (Birmingham and Liverpool). In a recent survey of film properties[8] the line-spread functions and speeds for line images were compared for several films. It was found that a finer grain film of moderate speed for extended images may be just as fast for line or point images as a film which is fast and coarse grained. Two experimental emulsions, produced by Kodak and Ilford, were found to have more suitable properties for bubble chamber work than standard emulsions; these two were, in addition, not color-sensitized, a useful property when working with roughly monochromatic blue light.

Tests on film distortion were also reported[8]; with reasonable processing conditions the random emulsion movements were found to have a standard deviation of order $\pm 1\ \mu$. There are, of course, much larger linear changes with temperature and humidity, but these can be scaled out in the measuring process.

### *4. Camera Design*

In view of the high over-all precision of measurement aimed at ($\pm 20\ \mu$ in the chamber), it is usual to build a complete camera array comprising the three (or four) lenses and film gates mounted rigidly on one plate. This system can then be surveyed as a whole to determine its distortion characteristics, including any asymmetrical distortions in the lenses.

In general the cameras have to work in a high magnetic field, the fringe field of the main chamber magnet, which is of order 1000 G. Thus electric motors and solenoids must be heavily shielded or else arranged at some distance from the cameras with long drive shafts. Alternatively, it is possible to use an entirely pneumatic drive system. The magnetic field is very inhomogeneous, so that strong forces would be exerted on any ferromagnetic material. Thus it is usual to make the whole camera assembly of nonmagnetic materials.

The Berkeley 72-in. camera system takes one continuous reel of 46-mm film on which all three views are photographed, spaced apart, and interlaced along the film; the measuring and scanning equipment (see Sec. III) must be adapted to this special situation. Most other camera arrays use separate film reels for each view; usually 120-m lengths of film are used, occasionally 300-m lengths. The maximum repetition rate required corresponds to that of the particle accelerator with which the chamber is to be used and is unlikely to be faster than 30 per minute; thus there is plenty of time for winding on the film between exposures.

It is necessary to photograph alongside each frame a *data-board* on which various numerical data such as frame number, reel number, time, and magnet current are displayed. This is done by means of auxiliary periscopic systems which form an image of the data-board adjacent to the image of the bubble chamber.

### *5. Fiduciary Marks*

It is necessary to have in each frame certain fiduciary marks which are used as reference points in relating measurements on the three views of each event. These take the form of crosses or similar marks on the inner surfaces of the chamber windows and also, in some cases, on the film suction plate. Figure 13 shows the system used by the Imperial College group for engraving window fiduciaries. The marks are formed from minute indentations which scatter light isotropically, so that the brightness of the image of the mark is independent of its direction in the plane of the window. Since the inner surfaces of the windows are in com-

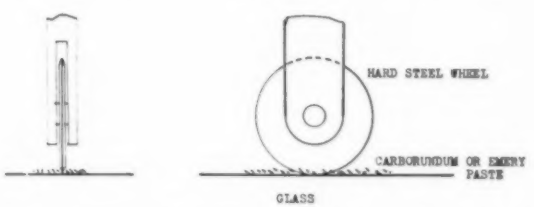


Fig. 13. Engraving fiduciaries on a window; the window and wheel are moved relative to each other in a jig-borer; the wheel rolls in a paste of emery and lubricating grease (system developed by N. Gortmans, A. Thetford, and R. Wilkins).

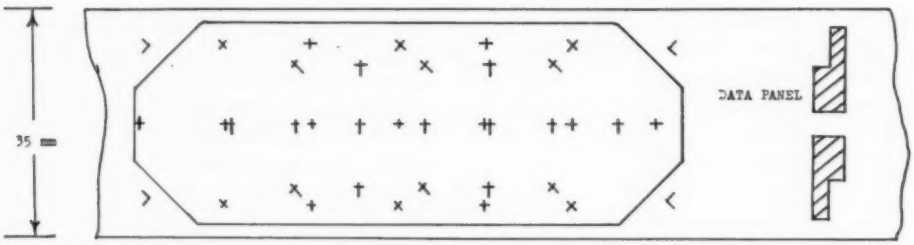


Fig. 14. The fiduciary system as it will appear on the film of the BNHBC. The crosses with equal arms are on the camera side window, those with unequal arms are on the light side window. The octagonal frame is the camera-based fiduciary. The "V" marks at either end are to facilitate the use of a flying spot digitizer.

pressive stress there is no danger of cracks developing from these marks. A method of contact-printing the camera fiduciaries through the film base and the suction plate has been described.[4]

This system of chamber and camera fiduciaries permits a high degree of over-determination in the computation of coordinates of tracks. Figure 14 shows how the two sets of fiduciaries will appear on a frame of the BNHBC.

## III. Bubble Chamber Film Measurement

The well-established measurement procedure, which has been in use for some years now in many laboratories concerned with the analysis of bubble chamber film, resolves itself into three sections: (a) scanning, where the films are inspected to note the events to be measured, if any, on each frame; (b) measurement, where some kind of coordinate measurement machine is used to determine coordinates of sets of points on each track of an event in two or three views; and (c) computing, where the data are reduced and fitted to different possible types of event. General surveys have been given by Goldschmidt-Clermont[27] and by Nikitin[28]; see also many papers in ref. 29.

Some work has been done with stereo comparators of the kind used in aerial survey work (30, p. 4 of ref. 29); these comparators make use of a human observer's stereo perception for depth measurement. It is doubtful whether such systems are suitable for the large output of film measurements needed in bubble chamber work. An additional complication is that the stereo measurements cannot be made in a medium of the same refractive index as that in which the tracks were formed.

More advanced film measurement techniques involve flying spot devices; these are at present being developed but they are not yet in routine use. For these and similar methods it is necessary to have some rough knowledge of the positions of tracks to be measured and this is obtained from *rough digitizers*, i.e., approximate coordinate measuring devices attached to a scanning table.

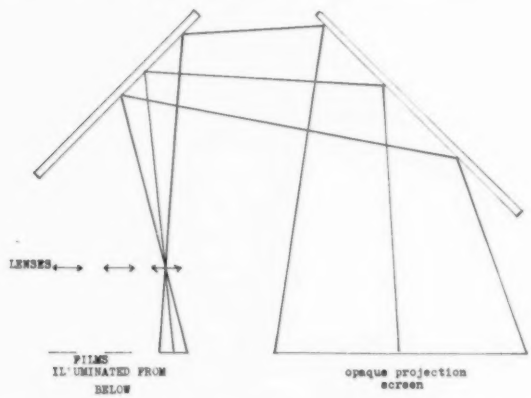


Fig. 15. Optical layout of a three-channel scanning desk. The projection lenses are separately movable in the horizontal plane for stereo coincidence.

### A. Scanning Tables and Rough Digitizers

Scanning tables for bubble chamber work are arranged as multiple projectors through which three or four film spools can be run. The negatives are projected on to a horizontal opaque white screen at about 10× magnification. Figure 15 shows the optical layout of such a scanning table in use at Imperial College. The main points about scanning tables are that fast film transport must be available, since normally only a few seconds may be needed to decide that a given frame contains nothing of interest. It must be possible to project two views of a frame simultaneously so as to enable a scanner to decide whether a track is running upwards or downwards by stereo coincidence. It also should be possible to run the whole picture toward one end of the projection screen to enable the scanner to get a close view of the opposite end of the frame. Usually, the projection lenses are individually movable to obtain stereo coincidence, and the whole lens assembly moves in the direction of the length of the film for shifting the picture bodily.

A large scanning projector being designed at CERN (private communication from G. Chanel, J. Guillaume, and D. Wiskott) will have four projection channels, to take 35 mm or 50 mm film from the 2-m bubble chamber being constructed at CERN. In the ENEDEP

scanning table (made by S.O.M., Paris) the projection table can be tilted so as to enable the operator to sight along tracks and detect slight changes in direction at an interaction or slight positive or negative curvatures. This instrument has also a simple $x$-$y$ coordinate digitizer operating directly on the projection screen with 50-$\mu$ digits. The Image Plane Digitizer (Itek Corporation, Lexington, Mass.) is an attachment for such projectors which measures in 100 $\mu$ digits. An attachment to scanning tables made at CERN uses tape pulled from rotary digitizers to give a bipolar digitizing system (Fig. 16). Other rough digitizers were described by Frisch and Oxley,[32] by Frisch,[33] and by Brunhart *et al.*[34]; the latter used a polarization method for measuring depth stereoscopically.

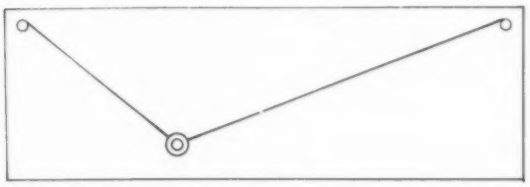

Fig. 16. Bipolar rough digitizer (CERN). The position of a point in the projected image is determined by the lengths of tape unwound.

## B. Conventional Measuring Machines

The type of coordinate measuring machine of which many are now in use measures $x$-$y$ coordinates of selected points on bubble chamber tracks, digitizes the measurements, and punches the results on computer tape. Also included on the tape are coordinates of the fiduciary marks and a large amount of bookkeeping information, e.g., number of frame, number of track in an event, number of view, whether the coordinates refer to a track or a fiduciary and so forth, so that the tape can be sent straight to a computer. In a more elaborate form the machine can be made to follow along a track automatically and punch coordinates on command while moving.

Measuring machines of this kind receive from the scanning process the film together with a sketch of the events to be measured, or possibly an enlargement with penciled instructions, made by using the scanning table as a conventional enlarger.

The Berkeley "Franckenstein" series of measuring machines[1,29] were the first of this type. Figure 17 shows the optical system of the MP II, designed by J. Franck. The film moves on an $x$-$y$ coordinate stage, and the measuring optics are fixed. A general view of the whole frame is seen on the low-magnification screen and the low-power lens moves in such a way as to keep the image stationary as the stage moves. At the same time a high-magnification view of the part of the frame to be measured is seen, and settings can be made either

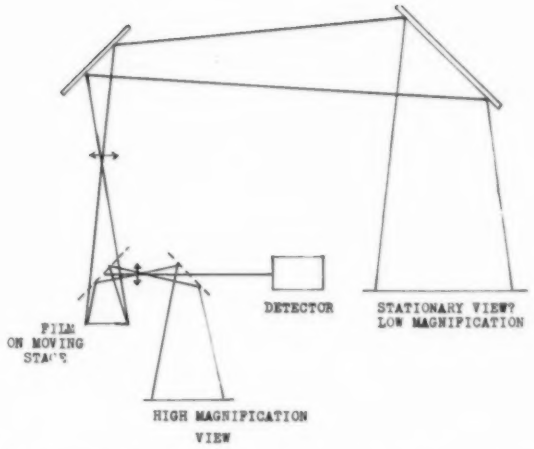


Fig. 17. Optical system of the Franckenstein MP II measuring machine.

visually or photoelectrically by means of an oscilloscope display. We discuss in Sec. III.C the details of the photoelectric detector systems used in this and other machines. In the MP II the detector is used to provide error signals for auto-following along tracks. The digitization of the coordinates was done by means of lead screws and rotary encoders in earlier models and later by moiré fringe digitizers.[35]

In the IEP series of measuring engines made at CERN[27,30] the opposite approach of keeping the film stationary and moving the projection lens is used. This simplifies the mechanical work, since the coordinate stage has only to carry a lens instead of three films and associated film transport gear. On the other hand the condensing is more difficult to arrange and the coordinates given by the digitizers have to be suitably scaled to allow for the lens movement. The optical system comprises a condenser, projection lens, and beam-splitter. The transmitted beam from the beam-splitter goes to a photoelectric detector and the reflected beam to a projection screen. There is no stationary picture of the whole frame but the picture moves past a stationary projected mark representing the measured point.

In the Imperial College measuring machine the film moves on a carriage parallel to its length for the $x$-coordinate and the projection lenses move transversely for the $y$-coordinate. This compromise system has the advantage that the inherent instabilities in a double or piggy-back coordinate stage are avoided. There are three film channels and three separate optical systems and photoelectric detectors. Figure 18 shows the optical layout of one channel. A stationary view of the whole frame is projected in tungsten light by the 9× lens, which moves in the $x$-direction so as to compensate film movement. The measuring channel is served by a high-pressure mercury lamp (shared by all three

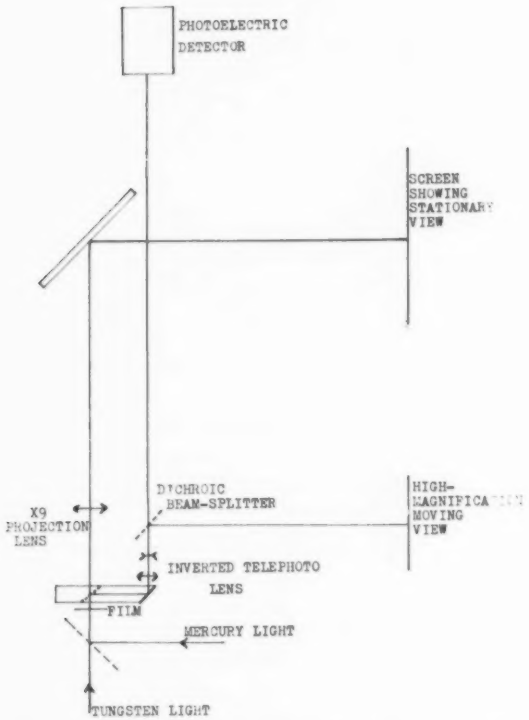


Fig. 18. Optical system (one channel only) of Imperial College measuring machine.

channels). The beam-splitting patch takes off a small beam containing the area of the picture near the measured point and this is projected at 30× onto the photoelectric detector by means of the inverted telephoto projection lens. This beam is also split by the dichroic beam-splitter, which is a thin-film system; the transmitted part, which goes to the detector, contains the mercury blue and violet lines, and the reflected part, containing the mercury green and yellow lines, is used to provide a 30× display of the part of the film being measured. The screen on which this display appears has marked on it a cross representing the measured point which can be rotated to line up with the direction of the track. Thus both visual and photoelectric settings can be made and, as in the Berkeley machines, an error signal for auto-following can be obtained from the detector. The $x$ and $y$ movements are on crossed roller-bearing slides and they are actuated by oil hydraulic rams controlled by electromagnetic valves; moiré fringe digitizers are used. The mechanical design of this machine was done by Beds and Herts Drawing Services, Ltd., of Luton, the mechanical parts were manufactured by Sogenique Service, Ltd., Newport Pagnell, and the digitizers, rams, and hydraulic controls were designed and made by Ferranti Ltd., Edinburgh.

A similar machine built at Imperial College is less elaborate; there is only one detector, no high-magnification screen, and no auto-following.

Crussard[36] described a type of measuring machine used at Saclay which is yet another variant (Fig. 19). The film is on a moving stage with moiré fringe digitizers. In a machine described by Cullwick and Goldsack[37] the film is mounted above a projection lens on a digitized coordinate stage; the enlarged image appears on a horizontal opaque screen with a small hole at the center below which is the photoelectric detector.

Commercially available machines include the Enetra 112 (S.O.M., Paris), which has a projection lens on a coordinate stage and stationary film, and the Precision Film Reader P-2 (Itek, Lexington, Mass.), in which the film is on the coordinate stage.

The chief optical points of difference between these various systems are in the photodetectors, as discussed below. Opinion seems to be divided about the relative precision of measurement obtainable from lead screws with rotary encoders, the commoner method of digitizing, and from moiré fringes. Lead screws suffer from wear, backlash, and pitch errors, particularly if used to give the high accelerations of comparatively large masses needed for auto-following; on the other hand, digitizing with rotary encoders is relatively simple and, within one turn, it is absolute, in the sense that counts cannot be lost. Moiré fringe measurement has no backlash or wear, and the pitch errors are averaged over thousands of grating rulings. Also if hydraulic rams are used as in the Imperial College machine the acceleration can be very high. However, the counting of digits depends on dead reckoning, so that digits can be lost or gained, and this makes the electronic part of the digitizers elaborate and expensive.

## C. Photoelectric Detectors

The essential element in a photoelectric detector for bubble chamber tracks is a slit backed by a photomultiplier; the image of a bubble track is projected on to the plane of the slit, and the coordinate stage is moved until the image lies over the slit. In practice the image is scanned repeatedly over the slit. The signal displayed on an oscilloscope would then appear

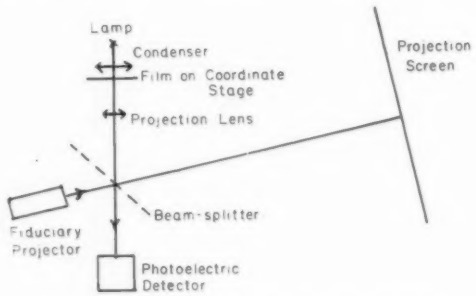


Fig. 19. Measuring machine as used at Saclay.

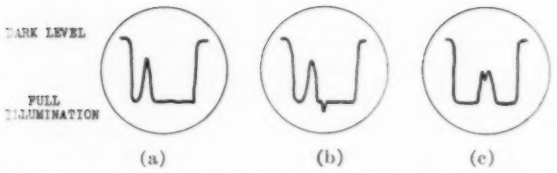


Fig. 20. Oscilloscope signals from a photoelectric track detector: (a) track pulse; (b) track pulse with fiduciary; (c) track pulse correctly set on fiduciary.

as in Fig. 20 (a). Clearly there is also needed an extra pulse to indicate the center of the gate, as in Fig. 20 (b); this is called the fiduciary pulse. The correct setting is then when the track signal is centered on the fiduciary, as in Fig. 20 (c). It is also necessary to rotate the slit in its own plane to line it up with the direction of the track. We describe mechanisms for carrying out these operations below.

In one detector system a rotating disk with radial slits (Fig. 21) is used to provide the slit scan (Berkeley, S.O.M.). The directions of the track and the slit are made to coincide by interposing a Dove prism or similar image rotating device in the beam. The fiduciary pulse is obtained from an auxiliary lamp and photocell system working in conjunction with the same slitted disk.

In the second principal system the scanning is done by means of a square (or octagonal) glass block rotating about an axis parallel to the slit direction (CERN IEP machines, Itek, Imperial College, etc.). The fiduciary signal can be obtained by auto-collimation off reflecting patches on the block faces or by electrical contacts. The image rotation can be achieved by means of a Dove prism as before but in some arrangements the whole assembly of slit and rotating block is mounted to rotate about an axis along the light path. The Itek instrument does not use a fiduciary pulse; instead, the track image is split and reversed by a Porro prism system and the oscilloscope displays two track traces which are mirror images; these coincide at the correct setting.

D. Rahm at Brookhaven National Laboratory has used a vibrating slit to scan across the track. Centering is achieved by coincidence of the signals from the two directions of movement of the slit. In this system the complete assembly of vibrating slit and photomultiplier rotates to follow the track direction.

Kaftanov *et al.*[38] used an image-orthicon as the photodetector in an auto-following system. Yet another form of detector[39] uses a wider slit, effectively a rectangle, which is divided into four quarters; there is a different photopultiplier behind each quarter and these are used to derive error signals for position and angle of the track image. The instrument described in this reference uses moiré fringe digitizers and is claimed to auto-follow to within 2 to 4 $\mu$ at a speed (at the film plane) of 3 mm/sec. The auto-following system on the Itek machine is claimed to be accurate to $\pm 6\ \mu$ on good tracks at 1 mm/sec.

## D. Other Measuring Systems

Here we describe miscellaneous systems which cannot be grouped with the high-speed methods of Sec. III.E,5.

The so-called Baby IEP described by Y. Goldschmidt-Clermont[27] (see also ref. 30, p. 25) is a projector which digitizes angles of tracks and is thus suitable for rapid measurements on tracks formed in a chamber without a magnetic field.

An instrument described by I. A. Pless (ref. 30, p. 21) digitizes coordinates of a projected image by moving a marker attached to $x$-$y$ coordinate movements at the image plane; the digitization is done by timing acoustic pulses down wires and is claimed to be accurate to 75 $\mu$, so that this device is rather in the nature of a "rough digitizer" as in Sec. III.A.

A. J. Oxley (ref. 32, p. 9) described a measuring projector in which the film is moved in two directions by means of a pantograph; the high-magnification movement of the pantograph is digitized photoelectrically by movement over a checkerboard pattern transparency.

A system for measuring curvature of slightly curved tracks in cloud chamber photographs was described by Blackett[40] in 1937, in which the prismatic spectrum line curvature was used to compensate the track image curvature. A development of this in which prisms of variable angle are used is at present under construction at Imperial College (S. J. Goldsack). This system has the attractive feature that a visual judgment can be made of the straightness of a compensated track image over a long length, thus averaging irregularities due to scattering and turbulence in the liquid. This instrument will digitize curvatures and also angles between tracks radiating from a vertex.

## E. Advanced Measurement Systems

In this section we note some proposals for measuring film which are at the development stage at the time of writing but which show promise of being able to cope

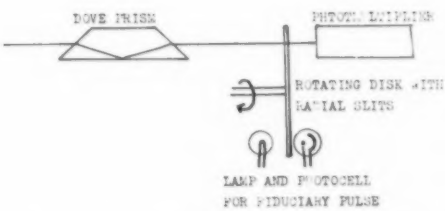


Fig. 21. Rotating slit detector head. The track-image falls on the plane of the disk.

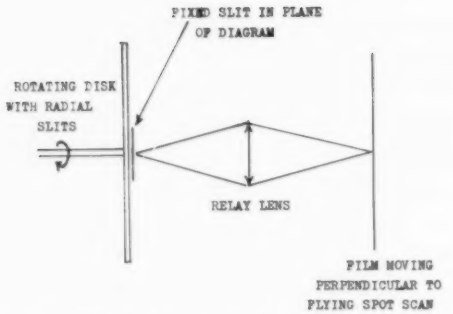


Fig. 22. Principle of optico-mechanical flying spot generator as used in the HPD.

with the vast output of bubble chamber pictures mentioned at the beginning of this article.

A large class of events can usefully be measured as from an origin or vertex which is the intersection of several curved tracks, and *spiral scanners* have been proposed for such events. In the system of McCormick, described by H. Bradner (ref. 30, p. 23), an enlarged view of the event is projected on to a rotating disk with about ten short radial slits arranged in a spiral; the vertex of the event is set at the center of the disk. The light transmitted by each slit goes to a different photomultiplier and by digitizing the times at which signals are received the angles and curvatures of all tracks radiating from the vertex can be computed. A similar device was proposed by G. Brautti (ref. 33, p. 53) and later developments of McCormick's device were described by L. Alvarez (ref. 33, p. 43).

The SMP-1 (scanning and measuring projector) was outlined by J. N. Snyder (ref. 33, p. 45) and has also been described in unpublished memoranda by L. Alvarez. It consists of a projection scanning table in which the screen contains a movable photoelectric detector which can digitize the coordinates of a section of track anywhere within its working field of view (about a 1-cm diam circle). Thus up to this point the SMP-1 appears as operating in much the same way as a conventional measuring machine of the type described in Sec. III.B, except that the track does not have to be brought exactly to the center of the field of the detector. It is, however, planned to operate the SMP-1 with the digitized output connected on-line to a fast computer, e.g., an IBM 7090, which would calculate the parameters of the event as the digitizings came through. In case of inconsistent, inadequate, or missing data, the computer would be programmed to type an appropriate inquiry on to a typewriter at the operator's desk, and the latter would have to complete the measurements in the way requested before passing on to the next event. Snyder suggests that about ten SMP-1 machines could be coupled with one 7090 in such a system of operator interrogation.

A system dubbed "machine tool control" is being developed at Imperial College by A. R. Edmonds and S. J. Goldsack to speed up the operation of conventional measuring machines. In this system rough digitizings obtained at the scanning stage will be used in a computer to prepare an instruction tape for a measuring machine of the auto-following kind. This tape is similar to those used in computer control of machine tools and it will be used through the $x$-$y$ digitizers of the measuring machine to drive the coordinate stage to points *near* tracks. The auto-following system will then pick up the track and follow along it, making accurate digitizations. In this way the machine will be guided automatically through the whole measurement procedure, including measurement of fiduciaries.

The most advanced system so far proposed is the flying spot digitizer (FSD). Such a machine requires some preliminary information about the location of tracks of interest which is obtained from rough digitizings at the scanning stage, as described above. It then scans the bubble chamber negative in a rectangular raster and prints out coordinates of points on tracks within the areas indicated by the rough digitizing. These areas, called *roads*, may typically be strips about 0.2 mm wide on the film containing wanted tracks. Several FSD's on lines proposed by Hough and Powell[41] are at advanced stages of construction; in their system, called the HPD (Hough-Powell device) the scan lines of the raster are obtained as the intersection of slits in a rotating disk with a stationary slit (Fig. 22). The scan line is imaged by a relay lens across the film and it is made to traverse the frame by moving the film parallel to its length. The light is collected by a suitable condenser system behind the film. Among several refinements suggested by R. B. Palmer we may mention the use of glass fibers about 1 mm in diameter in the slits; these produce an astigmatic spot because of the necessary separation of the moving and fixed slits, and this spot is made stigmatic by means of cylindrical optics further on in the path. The rotating slits may be slightly curved to give a scan which is linear with angle

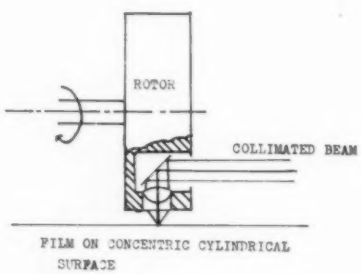


Fig. 23. Edmonds system for generating a flying spot with microscope objectives used on axis.

of rotation of the disk; also an extra set of optics is introduced to produce the so-called *orthogonal scan*, in which the scan lines are parallel to the length of the film, so as to facilitate the measurement of tracks running nearly at right-angles to the film length.

One of the important parameters in an FSD system is its speed of operation. This may be limited finally by photon noise in the signal if a bandwidth of order $10^7$ cps is required, so very high-pressure mercury lamps are used as sources of maximum luminance. The Hough-Powell type of FSD may then be limited because of the spot size which can be produced by the relay lens. Alternative proposals have been made by A. R. Edmonds (ref. 33, p. 83) to use moving microscope objectives working always on axis to provide a very well-corrected spot image at large numerical aperture. In Edmonds' system (Fig. 23) the $x$-scan (along the film direction) could be produced by moving either the film or the rotor with its microscope objectives; an essential feature is that the $x$-scan would not necessarily be linear but would be varied on command from a computer linked to the device, so that detailed studies of doubtful regions of a picture could be made.

In a system under development at MIT by I. A. Pless a precision cathode ray tube with a very small spot (diameter $\backsim 20\ \mu$) is used to provide the raster, and its position is checked by scanning it over auxiliary gratings. This system will have an important advantage in flexibility, since, in principle, the spot can be guided to elucidate the details of complex patterns.

## F. Gap Measurement

The size distribution of gaps between clumps of bubbles in a track provides information about the intensity of ionization due to the particle which made the track. Gap measurements have so far been made laboriously on conventional measuring machines or on measuring microscopes. Clearly an FSD (Sec. III. E) would give information about gap sizes if the line scan interval were close enough but this would not be the case when scanning as normally envisaged. Special devices are under construction at CERN (Cooper) and at Imperial College (I. Butterworth). The CERN system will involve a television pick-up tube which receives an enlarged image of a section of track and analyzes it. The Imperial College device will resemble a conventional measuring machine but the detector head, of the rotating block type, will be modified to generate a very short flying spot scan across the track, and it will auto-follow along the track at a constant speed, so that the time between bubble image intersections is a measure of gap length.

The writer is grateful to all who have helped in preparing this survey by discussions and advice, particularly to C. C. Butler and A. R. Edmonds.

## References


1. H. Bradner, Ann. Rev. Nucl. Sci. **10,** 109 (1960).
2. N. C. Barford, Progr. Cryog. **2,** 89 (1960).
3. D. A. Glaser, in *Handbuch der Physik*, S. Flügge, ed. (Springer, Berlin, 1958), Vol. 45, pp. 314–341.
4. W. T Welford, *Optical Instruments and Techniques* (Chapman and Hall, London, 1962), pp. 173–192.
5. H. C. van de Hulst, *Light Scattering by Small Particles* (Wiley, New York, 1957).
6. G. E. Davis, J. Opt. Soc. Am. **45,** 572 (1955).
7. A. V. Belonogov, A. G. Zel'dovich, V. Z. Kolganov, L. G. Landsberg, A. V. Lebedev, S. Ya. Nikitin, V. T. Smoliankin, and A. P. Sokolov, Instr. exptl. tech. No. 1, 39 (Jan.-Feb. 1958).
8. W. T. Welford, J. Phot. Sci. **10,** 243 (1962).
9. E. di Capua, U. Dore, G. C. Gialanella, P. Guidoni, I. Laakso, and G. C. Moneti, Nuclear Inst. Methods **15,** 273 (1962).
10. M. Bloch, A. Lagarrigue, P. Rancon, and A. Rousset, Rev. Sci. Instr. **32,** 1032 (1961).
11. Wang Kang-ch-ang, M. I. Solov'ev, and Yu. N. Shkobin, Instr. exptl tech. No. 1, 43 (Jan.-Feb. 1959).
12. M. A. Alston, B. Collinge, W. H. Evans, R. W. Newport, and P. R. Williams, Phil. Mag. **2,** 820 (1957).
13. D. C. Colley, J. B. Kinson, and L. Riddiford, Nucl. Instr. Methods **4,** 26 (1959).
14. E. R. Flynn and P. J. Bendt, Rev. Sci. Instr. **33,** 223 (1962).
15. J. Badier, L'Onde Électrique **41,** 1025 (1961).
16. C. C. Butler, New Scientist **7,** 22 (1960).
17. L. Riddiford, H. B. van der Raay, N. C. Barford, C. C. Butler, D. McMullan, A. Thetford, D. B. Thomas, W. T. Welford, A. Amery, W. H. Evans, M. J. Moore, P. Polak, H. W. B. Skinner, P. R. Williams, D. Shaw, A. G. Ashburn, and M. C. Snowden, *International Conference on High Energy Accelerators and Instrumentation* (CERN, Geneva 1959), pp. 445–453.
18. E. V. Kuznetzov and I. Ya. Timoshin, Instr. exptl. tech. No. 4, 550 (July-Aug. 1959).
19. L. Bertanza, P. Franzini, I. Manelli, and G. V. Silvestrini, Nucl. Instr. Methods **9,** 354 (1960).
20. A. M. Rezikayan and K. G. Mnatsakayan, Instr. exptl. tech. No. 6, 975 (Nov.-Dec. 1960).
21. V. M. Gorbunkov, Instr. exptl. tech. No. 6, 41 (Nov.-Dec. 1962).
22. H. Courant, *International Conference on High Energy Accelerators and Instrumentation* (CERN, Geneva, 1959), pp 465–466.
23. F. de S. Barros, D. M. Binnie, and B. D. Hyams, J. Sci. Inst. **35,** 129 (1958).
24. W. T. Welford, J. Opt. Soc. Am. **50,** 749 (1960).
25. H. M. Block, W. M. Fairbank, E. M. Harth, T. Kikuchi, C. Metzer, and J. Leitner, *International Conference on High Energy Accelerators and Instrumentation* (CERN, Geneva, 1959), pp. 461–465.
26. Yu. A. Aleksandrov, V. M. Gorbunkov N. B. Delone, and V. M. Likhochev, Instr. exptl. tech. No. 1, 127 (Jan.-Feb. 1960) and pp. 977 (1960).
27. Y. Goldschmidt-Clermont, *International Conference on High Energy Accelerators and Instrumentation* (CERN, Geneva, 1959) pp. 523–532
28. S. Ya. Nikitin, Instr. exptl. tech. No. 2, 19 (March-Apr. 1961).
29. J. D. Gow and A. H Rosenfeld, *International Conference on High Energy Accelerators and Instrumentation* (CERN, Geneva, 1959), pp. 435–439.

30. *International Meeting on Instruments for the Evaluation of Photographs* (CERN, Geneva, 1958). This reference contains short descriptions of many different instruments.
31. A. I. Filippov, M. M. Kulyakin, Yu. A. Shcherbakov, R. M. Sulyaev, and A. T. Vasilenko, *International Conference on High Energy Accelerators and Instrumentation* (CERN, Geneva, 1959), pp. 545–550.
32. O. R. Frisch and A. J. Oxley, Nucl. Instr. Methods **9**, 92 (1960).
33. Informal Meeting on *Track Data Processing*, M. Benot and B. Elliot, eds. (CERN, Geneva, 1962).
34. G. Brunhart, C. D. Gall, C. Vittitre, K. Schneider, and V. P. Kenney, Nucl. Instr. Methods **14**, 38 (1961).
35. J. Guild, *Diffraction Gratings as Measuring Scales* (Oxford Univ. Press, New York, 1960).
36. J. Crussard, L'Onde Électrique **61**, 1042 (1961).
37. B. B. Cullwick and S. J. Goldsack, Nucl. Instr. Methods **13**, 118 (1961).
38. V. S. Kaftanov, J. C. Lichtenbaum, B. N. Moisseev, S. Ya. Nikitin, and O. P. Fedotov, *International Conference on High Energy Accelerators and Instrumentation* (CERN, Geneva, 1959), pp. 550–554.
39. E. M. Andrejev, P. Hirsch, G. M. Kachkov, S. M. Korochenko, V. M. Lachinov, A. G. Morozov, K. G. Nekrasov, R. Pose, M. I. Popov, V. V. Smirnov, N. S. Tolstoi, and I. A. Zarubin, Nucl. Instr. Methods **11**, 297 (1961).
40. P. M. S. Blackett, Proc. Roy. Soc. (London) **A159**, 1 (1937).
41. P. V. C. Hough and B. W. Powell, Nuovo Cimento **18**, 1184 (1960).

# Meetings Calendar

**October**

— Internatl. Conf. on the Science of Photography, Turin, Italy
— 4th Internatl. Color Conf., Budapest *M. K. Egyesület, Szabadság-tér 17, Budapest 5, Hungary*
— IAU, 23rd Exec. Comm. Mtg., Erevan, Armenia, U.S.S.R. *D. H. Sadler, c/o Royal Greenwich Observatory, Herstmonceux Castle, Hailsham, Sussex, England*
— IUPAP, 11th Gen. Assembly, Warsaw, Poland
1–6 Internatl. Soc. of Photogrammetry, Commissions 1–4 Mtg., Milan *A. L. Nowicki, c/o Army Map Service, 6009 Mass. Ave. N.W., Wash., D.C.*
3–4 Conf. on The Physics of Glass, Lathom, Lancs. *Adm. Asst., Inst. of Phys. & Phys. Soc., 47 Belgrave Sq., London S.W. 1, England*
13–18 SMPTE, 94th Semiann. Conv., Boston, Mass. *SMPTE, 55 W. 42 St., New York 36, N.Y.*
14–18 Soc. for Appl. Spectroscopy, El Cortez Hotel, San Diego *E. P. Wadsworth, Jr., Chemistry, San Diego State Col., San Diego 15, Calif.*
16–18 Am. Vacuum Soc., Boston *AVS, P.O. Box 1282, Boston, Mass.*
17–19 SPSE Color Photographic Systems Symp., Marriott Motel, Washington, D.C. *SPSE, P.O. Box 1609, Wash., D.C.*
21–23 11th Detroit Anachem Conf., Wayne State U., *C. M. Gambrill, Ethyl Corp., 1600 W. Eight Mile Rd., Detroit 20, Mich.*
23–25 **Optical Society of America Annual Meeting, Sherman House, Chicago** *M. E. Warga, OSA, 1155 16th St. N.W., Wash. 6, D.C.*
28–Nov. 1 Internatl. Symp. on Plasma Phenomena and Measurements, San Diego *AFOSR, Attn: Lt. Col. C. D. Colchagoff, SRE, Wash. 25, D.C.*
29–Nov. 1 Internatl. Symp. on Plasma Phenomena & Measurement, San Diego *Secy., IEEE, Box A, Lenox Hill Station, New York 21, N.Y.*

**November**

7–9 Acoustical Soc. of Am., Ann Arbor *G. Peterson, U. of Mich., Ann Arbor, Mich.*
12–14 AFIPS, Fall Joint Computer Conf., Los Angeles, Calif. *P. Huggins, AFIPS, P.O. Box 55, Malibu, Calif.*
12–15 Magnetism and Magnetic Materials Conf., Atlantic City, N.J. *J. D. Blades, Burroughs Corp. Res. Center, Paoli, Pa.*
13–15 5th Ann. Eastern Analytical Symp., Statler Hilton Hotel, NYC *R. F. O'Connell, Sperry Rand Research Center, Sudbury, Mass.*
20 OSA Chicago Sect. *C. R. Lambrecht, 7729 N. Ashland Ave., Chicago, 31, Ill.*

**December**

26–31 AAAS, 130th Ann Mtg., Cleveland, Ohio *AAAS, 1515 Mass. Ave. N.W., Wash. 5, D.C.*

**1964**

— Colloquium on Magnetism, Nottingham, England *IUPAP, Institut d'Optique, 3 boul. Pasteur, Paris 15e, France*

**Spring**

Colloq. on Development of Optical Masers, Switzerland *W. D. Wright, Tech. Opt. Sect., Imperial Col., London S.W. 7, England*

**January**

19–24 ACS Natl. Mtg., Denver, Colo. *ACS, 1155 16th St. N.W., Wash. 6, D.C.*
29–31 Am. Meteorological Soc., Ann. Mtg., Los Angeles *AMS, 45 Beacon St., Boston 8, Mass.*

**March**

2–6 15th Pittsburgh Conf. on Analytical Chem. and Appl. Spectroscopy, Pittsburgh, Pa.
4–6 Thermal Radiation of Solids Symp., Sheraton-Palace Hotel, San Francisco *W. D. Harris, Eng. & Sci. Ext., U. of Calif., Berkeley 4, Calif.*
15–21 Am. Soc. of Photogrammetry, Am. Cong. on Surveying and Mapping, Washington, D.C.

**April**

— Internatl. Measurements and Instruments Conf., 3rd, Stockholm *G. Ljungberg, Royal Swedish Acad. of Engin. Science, Box 5073, Stockholm, Sweden*
1–3 **Optical Society of America Spring Meeting, Sheraton-Park Hotel, Washington, D.C.** *M. E. Warga, OSA, 1155 16th St. N.W., Wash. 6, D.C.*
5–10 ACS Natl. Mtg., Phila., Pa. *ACS, 1155 16th St. N.W., Wash. 6, D.C.*
5–10 Asia-Pacific Acad. of Ophthalmology, 2nd Cong., Melbourne *R. N. Mellor, 82 Collins St., Melbourne, C1, Australia*
12–17 SMPTE, 95th Semiann. Conv., Los Angeles, Calif. *SMPTE, 55 W. 42 St., New York 36, N.Y.*
28–May 2 SPSE Internl. Conf. of Photographic Science and Engineering, American Hotel, N.Y.C.

**May**

— Soc. of Technical Writers and Publishers, 11th Ann. Conv., San Diego, Calif.
4–5 Inter-Soc. Color Council, Statler-Hilton Hotel, NYC *R. M. Evans, Eastman Kodak Co., Rochester 4, N.Y.*
5–9 15th Natl. Science Fair-Internatl., Baltimore, Md. *Science Service, 1719 N St. N.W., Wash. 6, D.C.*
2nd week French Soc. of Ophthalmology, 71st Cong., Paris *M.-A. Dollfus, Soc. Française d'Ophtalmologie, 27, rue du Faubourg-St.-Jacques, Paris 16, France*

# The Trigger Circuit for the 80-In. Bubble Chamber Light Source

S. S. Yamamoto and W. P. Sims

A circuit was designed to trigger a high-power flashtube at one per second repetition rate. It also increased the life of the tube by a factor of ~100 from its rated life.

The 80-in. hydrogen bubble chamber currently in construction at Brookhaven National Laboratory is designed to operate at a repetition rate as fast as one per second. This means that the flashtubes which illuminate the bubble chamber must be triggered at this rate, and must have a long life to avoid frequent changing of the tubes.

The flashtube selected for the 80-in. bubble chamber is a modified FX-1, manufactured by Edgerton, Germeshausen & Grier, Inc., of Boston. It consists of a quartz tubing of 4-mm i.d. with a wall thickness of 1 mm. It has an arc length of 46-cm, and is filled with xenon to a pressure of 20 cm Hg. It is rated to operate at 6 kV with a capacitor of 30 $\mu$F. Its expected life is about 100,000 flashes triggered once every 10 sec at half the maximum rated input power.

A sample of this modified FX-1 tube was tested at a 1-sec repetition rate using a conventional circuit shown in Fig. 1. Under this arrangement the tube flashed about 2000 times, and then it went into a continuous discharge. This seemed due to an excessive heating of the electrodes caused by a rapid repetition rate, even though the tube was cooled by two muffin fans rated at 3400 liters/sec.

About the time of this test we learned from S. R. Borenstein of Imperial College, London, that he had been using a circuit which increased the life of a flashtube by a factor of ten.[1] The main feature of this circuit is shown in Fig. 2. The resistor in parallel to the flashtube keeps the electrodes at the same high voltage in order to avoid a spontaneous discharge. The spark gap, when triggered, will drop the potential of the cathode to ground. Because of the high resistivity of the parallel resistor, the current through this chain is negligible. The same source which triggers the spark gap also triggers the flashtube at the same time, thereby causing a discharge. The trigger rate used by Borenstein was once every 3 sec, and his flashtube was operated with a 25-$\mu$F capacitor charged to $3 \sim 3.5$ kV.

We modified the spark-gap circuit by replacing the spark gap by an ignitron. The main reason for this modification is due to the fact that a high current and high repetition rate spark gap is very difficult to construct, and that it may not have a long lifetime. A complete circuit diagram including a trigger circuit is shown in Fig. 3.

Using the circuit mentioned above we performed three life tests on the modified FX-1 flashtube. The trigger rate was one per second, and the tube was loaded at 6 kV with 30 $\mu$F. The flashtube was cooled by two fans directed at the electrodes. The number of triggers was recorded by a mechanical counter. The flashtube was viewed by a 1P39 photocell tube behind the crossed polaroid sheets. The output from the photocell was fed to another mechanical counter to count the number of flashes. It was also fed into a

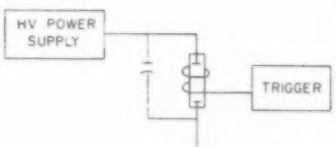


Fig. 1. Block diagram of a conventional trigger circuit.

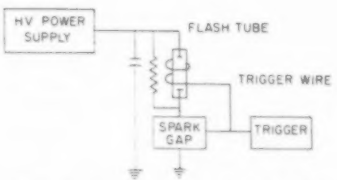


Fig. 2. Block diagram of Borenstein's trigger circuit.

The authors are with Brookhaven National Laboratory, Upton, New York.

Work performed under the auspices of the United States Atomic Energy Commission.

Received 29 March 1963.

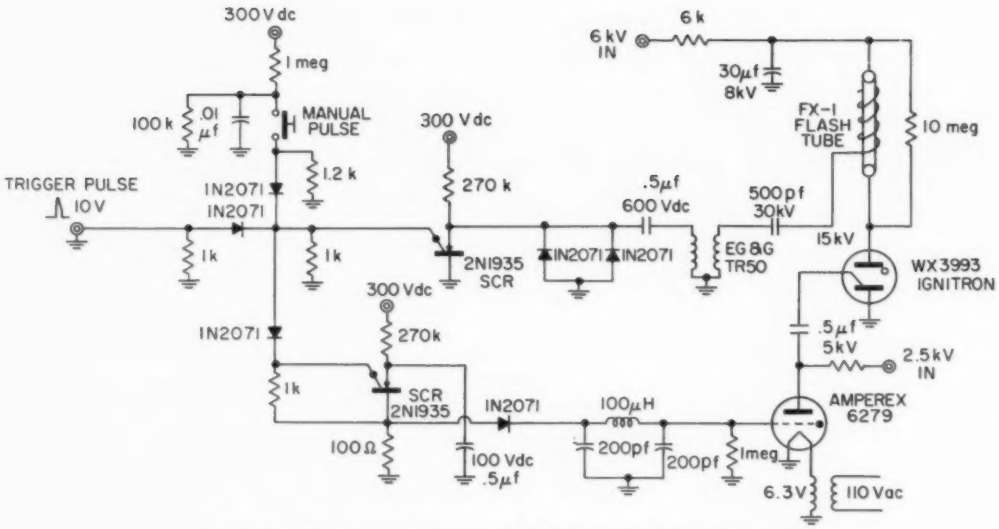


Fig. 3. Complete circuit used for the 80-in. bubble chamber.

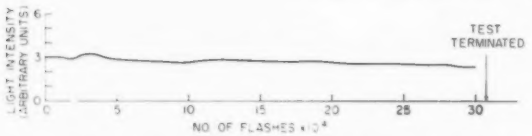


Fig. 4. Light intensity vs number of flashes.

scope to observe the light intensity. The photocell was adjusted in such a way that the pulse height observed in the scope was linearly proportional to the flashtube light intensity. The result of one of the tests is shown in Fig. 4. In this graph the light output is plotted against the number of flashes. The flashtube began to misfire at about 300,000 flashes in this test. The light intensity remained nearly constant to 15% throughout. In two other tests each of the tubes flashed over 500,000 flashes without a serious loss of the light intensity, and was still flashing when the tests were terminated.

These results may be compared with our previous result of 2000 flashes when a conventional circuit was employed. Therefore, we conclude that the new circuit enables a rapid triggering of high-power flashtubes, and it increases their useful life.

## Reference

1. S. R. Borenstein (private communication).

University of Michigan physicists are building the world's biggest "heavy liquid" bubble chamber—it will be surrounded by a 300-ton magnet—for study of invisible atomic particles by bubbles particles leave in speeding through freon or propane. Standing by optical model of chamber, looking at one of lights which will illuminate bubbles for photographs, are, left to right: Byron P. Roe, Daniel Sinclair, and John Vander Velde. AEC is sponsoring this $550,000 project.

# Optical and Mechanical Properties of Bubble Chamber Windows

F. O. Reitmayer and E. W. Deeg

In producing large glass blanks for bubble chamber windows and other applications, the thickness and, therefore, size and weight can be materially reduced by increasing the strength characteristics through tempering. The resulting adverse optical effects are discussed, and quantitative measurements of these are given to ascertain whether or not they are tolerable.

## I. Introduction

Optical developments in the field of astrophysics have made it necessary to produce large disks of different glasses of excellent optical quality. A similar problem had to be solved in order to allow the construction of large bubble chambers and Wilson chambers.[1,2]

It is known that bubble chambers, for example, filled with propane are operated at relatively high pressures (approx. 30 kg/cm²). The chambers of the type mentioned are operated at approximately room temperature. Hydrogen chambers work at very low temperatures. Bubble chamber windows have to meet the requirements determined by these conditions. From the optical and engineering standpoint the thickness of the bubble-chamber windows should be as small as possible.

In order to meet all of the requirements, special melting procedures had to be developed. Furthermore, it turned out that a reduction in thickness of the window is possible if the glass blank is quenched in a very careful and defined manner. By this process permanent stresses are produced in the glass. This causes an increase in mechanical durability. On the other hand, the optical properties of a piece of glass are also influenced by a quenching process. How the optical properties are changed by the quenching process is shown in this paper.

## II. Tempered Glass

Glasses can be considered as highly disordered solids. Since the kind and the degree of the disorder depends on the thermal history of the sample, all glass properties are also determined by the thermal history.[3] How greatly the properties of a glass can be changed by a rapid quenching process is shown e.g. by the difference of the properties of glass fibers and well-annealed glass.[4–7] The most characteristic property of a glass is that it does not show a sharp melting point as crystals do. Owing to the random distribution of the ions in a glass its softening takes place within a certain temperature interval, called the transformation range (Fig. 1).

If, for example, a plane-parallel sheet of glass is quenched from a temperature above the transformation range to room temperature, equally from both sides, a parabolic stress distribution through the sheet can be measured at room temperature (Fig. 2). During the quenching operation the stress distribution in the plate changes with time.

Glass fractures practically only from tensile stresses. This is due to the fact that the extremely high intrinsic strength of a glass of more than 70,000 kg/cm², is lowered by surface flaws. For an adequate safety factor, the working stress for annealed, not very carefully treated, glass may be approximately 70 kg/cm². The fact that the actual strength of a piece of glass is determined by the surface properties explains also that the strength of a glass cannot be considered as a material constant. It depends on the handling of the material, the size of the sample used for testing purposes, and the clamping conditions.

There are different possibilities for reducing the weakening influence of the surface flaws on the intrinsic strength of a glass. One is to put the glass surface under compression. If a load is applied to the piece of glass in question, this compression has to be cancelled before the tension caused by the applied load becomes active. It can be seen from Fig. 2 that quenching of a sheet of glass produces a compression zone in the glass surface. As a result the over-all mechanical durability of quenched glass is higher than that of an annealed sample: The glass is toughened, or "tempered".

Usually the compression zone is considered to be a

The authors are with Jenaer Glaswerk Schott & Gen., Laboratorium, Mainz, Germany.

Received 18 April 1963.

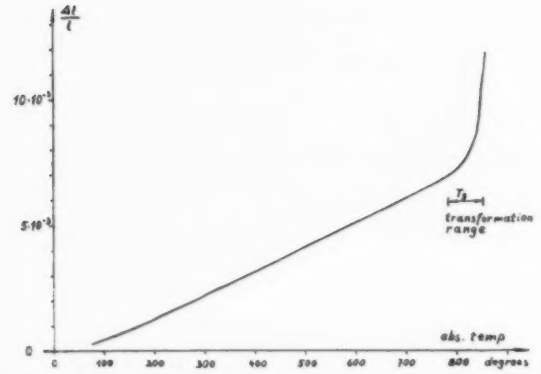


Fig. 1. Thermal expansion of the optical glass BK 7 vs temperature. The symbol $T_g$ indicates the transformation range of the glass.

skin which covers the sample. Therefore, it would seem to be impossible to grind or polish a tempered piece of glass. From theoretical considerations this was reckoned to be incorrect and it has now been shown by tests on very carefully quenched plates of glass that it is possible to grind and polish tempered glass pieces. Figure 2 shows the birefringence measured on one of the plates mentioned after different grinding processes. It can be seen that, after the surface layer was removed, the over-all stress distribution in the disk was changed. The existence of a compression "skin" could not be verified. Meanwhile, experience showed also that large disks of tempered optical glass can be ground and polished if the handling is done carefully. Of course, it is necessary that the quenching operation be done in a specific way in relation to the shape of the piece. However, even if a properly tempered piece of glass is ground and polished, deep and sharp cracks in the glass surface or cutting of the material must be avoided. Such artificially produced flaws may cause an explosion of the glass. Figure 2 shows also that the compression of the glass surface and, therefore, the over-all strength of the whole sample is reduced by the grinding process; therefore, it is advisable not to remove too much of the glass.

## III. Light Propagation Through Tempered Glass Sheets

As mentioned above, the glass properties depend on the thermal history of the piece considered. Caused by the quenching process the thermal history of the surface parts of the glass is, in general, different from the thermal history of the core. Even if there were no permanent stresses in the quenched piece of glass, the refractive index would be different in the inner and outer parts. Since the resultant change of refractive index is caused by a superposition of different influences, they should be considered in detail.

Local changes in refractive index depend on the following factors: (a) homogeneity of the melt; (b) changes of glass structure during annealing; (c) permanent stresses in the glass.

It is possible by using special melting procedures to hold local differences in refractive index of optical glasses resulting from factor (a) extremely low, if striae are neglected.

Special annealing procedures allow, furthermore, the reduction of differences in refractive index even in large

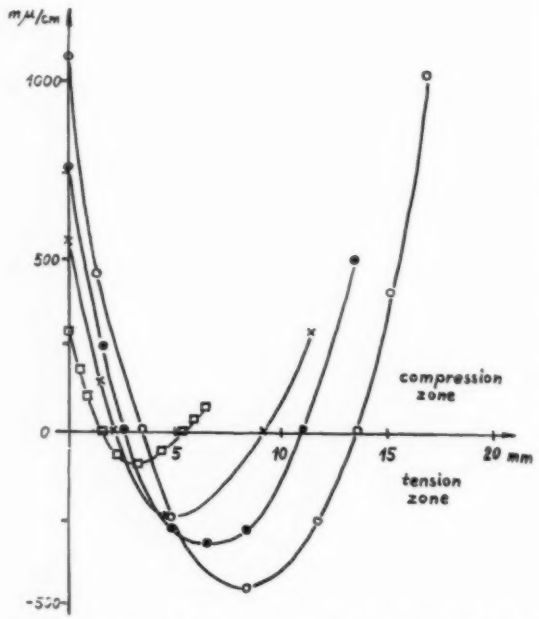


Fig. 2. Distribution of birefringence in a tempered BK 7 disk. Its thickness was reduced by careful grinding and polishing from one side. Thickness of the plate: ○ 17.0 mm, ● 13.4 mm, × 11.5 mm, □ 7 mm.

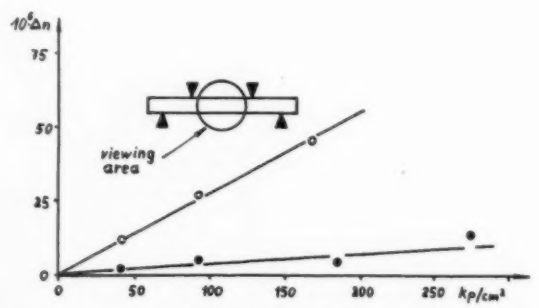


Fig. 3. Change in refractive index of BK 7 glass as a function of the applied stress. The sketch in the diagram shows the experimental arrangement which was used for loading the specimen in the light path of a Twyman interferometer. ● is the light vector vibrating parallel to the direction of principal stress. ○ is the light vector vibrating perpendicular to the direction of principal stress.

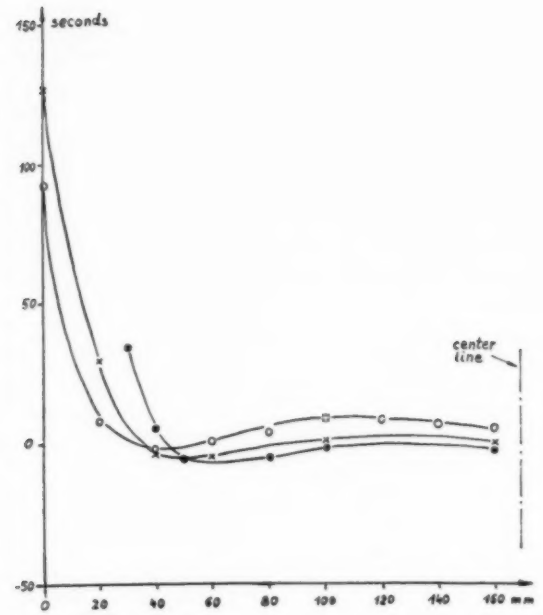


Fig. 4. Average deviation of a parallel light beam after passing through a tempered bubble-chamber window plotted against the distance from the edge of the window. ● is the angle of incidence 30° towards the edge; ×, the angle of incidence 0°; and ○, the angle of incidence 30° toward the center of the window. Dimensions of the window: length 85.5 cm, width 33 cm, thickness 5.6 cm. For circular windows the minimum deviation is in the center.

pieces of optical glass to $\pm 5 \times 10^{-6}$ by special annealing.

Local changes in refractive index caused by factor (e) are, in well-annealed glasses, usually in the order of $\pm 5 \times 10^{-6}$ or $\pm 1 \times 10^{-5}$. Tempered glasses, however, show because of their permanent stresses much higher differences in refractive index.

In order to show the influence of mechanical load on the refractive index of a homogeneous glass, the light propagation through a bent bar was studied by interferometric means.[8] Bending of the glass sample was produced by a four-point loading device. Results of measurements of change in refractive index for light vibrating parallel and perpendicular to the direction of the applied stress are shown in Fig. 3. Details of the experiments and the evaluation of the measurements may be taken from Schuster and Reitmayer.[8] Figure 3 demonstrates that the light propagation through an isotropic material which is exposed to mechanical load will be influenced by two different factors: a change in total refractive index caused by the applied stress, and a birefringence caused by the nonisotropic distribution of the load.

These results applied to the problem of propagation of unpolarized light through a tempered window indicate that there must be a deviation as well as a splitting of a beam of such light passing through the window. Figure 4 shows the deviation of a parallel beam of light passing a highly tempered bubble-chamber window at various distances from the edge and under different angles of incidence. It can be seen that the main portion of the window is tempered in a manner which does not influence the light propagation very much.

The stress distribution in a tempered window is known to be three dimensional. Furthermore, the stresses vary from point to point. Therefore, it is advisable to characterize the tempered window optically by effective differences in refractive index $\Delta n'$. These $\Delta n'$ values are different from the actual differences $\Delta n$. In the center of a window the influences of compression and tension compensate each other almost completely.

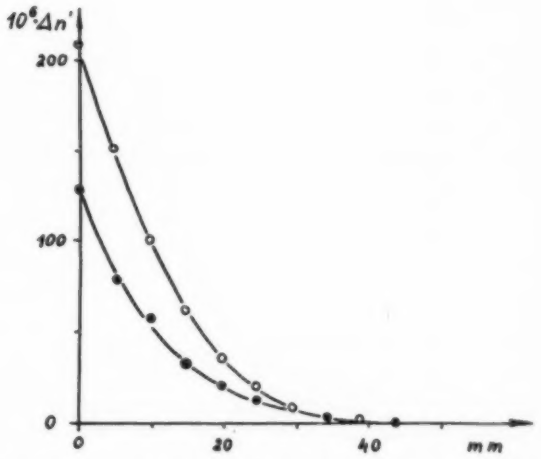


Fig. 5. Effective change of refractive index of a tempered bubble chamber window plotted against the distance from the edge. ○ light vector vibrating perpendicular to the edge; ● light vector vibrating parallel to the edge. Dimensions of the window as in Fig. 4.

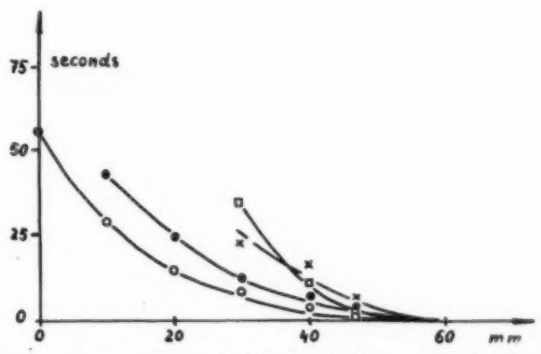


Fig. 6. Beam splitting of a light beam after passing through a tempered window (dimensions as in Fig. 4) vs distance from the edge. Angle of incidence: ○ 0°, ● 10°, × 30°, □ 45°. All angles toward the center of the window.

In order to measure the $\Delta n'$ values, an interferometer should be used. In the case of a tempered window with a degree of prestressing of 800 to 1200 kg/cm², the effective values given in Fig. 5 have been determined. Without considering the possibility of compensating the influences of compression and tension, one should expect an actual difference in refractive index $\Delta n_{max}$ of approximately $200 \times 10^{-6}$. The effective values $n'$ are much smaller (Fig. 5).

The above-mentioned splitting of a light beam after traversing a tempered bubble chamber window causes double images of the bubbles. Measurements of the beam splitting on a tempered window are shown in Fig. 6. This limits the degree of tempering which can be applied in order to retain high optical quality in the windows.

## Conclusion

Large bubble chamber windows can be tempered. However, the tempering process influences the optical properties of the window. The competition between the requirements arising from mechanical engineering problems and optical problems during planning a bubble chamber should, therefore, lead to a compromise. A high degree of tempering increases the safety factor of the window. On the other hand, the optical quality is reduced considerably. In order to reach optimum quality of a bubble chamber window from the optical as well as the mechanical standpoint, the influences mentioned above should be considered very carefully. This is of special importance if the light has to pass through a thick window. From the optical point of view sometimes it may be preferred to apply only a moderate degree of tempering, especially for thick windows.

## References


1. E. Deeg and F. Reitmayer, Physik. Verhandl. **12,** 192 (1961).
2. F. Reitmayer, "Contribution to the problem of the mechanical and optical properties of a bubble chamber window" Paper given on the occasion of a bubble chamber glass window discussion at Brookhaven National Laboratory, Upton, New York, 4 Aug. 1960.
3. E. Deeg, *Physikalische Schriften*. Heft 10, Physik von Heute Folge 3 (Physik-Verlag, Mosbach, 1963).
4. O. L. Anderson, J. Appl. Phys. **29,** 9 (1958).
5. S. Bateson, J. Soc. Glass Technol. **37,** 302 (1953).
6. E. Deeg and A. Dietzel, Glastech. Ber. **28,** 221 (1955).
7. G. Slayter, Bull. Am. Ceram. Soc. **31,** 276 (1952).
8. E. Schuster and F. Reitmayer, Glastech. Ber. **34,** 130 (1961).


## Information for Contributors

**Scope:** Papers are welcomed in the broad areas of applied optics, in disciplines related to optics and employing optical techniques. Papers should be sent to *The Editor, APPLIED OPTICS, 1155 Sixteenth St. N.W., Washington 6, D.C.* Manuscripts may be submitted in English, French, German, or Russian, and the presentation should be as succinct as comprehension will permit. In general, the metric system of units is preferred. One original and one carbon copy of the manuscript, with two sets of all illustrations, must be sent in. Manuscripts should be typed double or triple spaced on one side of 22 × 28 cm (8½ × 11 in.) paper, leaving a 3.8 cm (1½ in.) margin all around. Equations must be typed not hand written wherever possible. Papers on the more fundamental aspects of experimental and theoretical optics should be sent to *The Editor, JOURNAL OF THE OPTICAL SOCIETY OF AMERICA, National Bureau of Standards, Washington 25, D.C.*

An **abstract,** adequate as an index and a summary, of not more than 100 words should appear at the beginning of the paper after the *title, author's name, affiliation, and address.* In the case of papers in a non-English language, they must be accompanied by an abstract in English as well as an abstract in the language of the paper. It should be borne in mind that this abstract may be used in toto by the abstracting journals, therefore it should be self-contained.

**Figures** suitable for printer's use should be sent. Bear in mind that illustrations will normally be reduced to column width (8.4 cm—3⅜ in.—20 picas). *Halftones:* two sets of glossy prints are needed, which should be mailed flat, with any proportion or framing indicated on a working copy. *Line drawings* should be suitable for reproduction and be not larger than 22 × 28 cm (8½ × 11 in.). *Captions* should be listed on a separate sheet in addition to each caption appearing on each illustration.

**Tables** should be typed on separate sheets and the data therein be intelligible, by title, without reference to the text. Tables should include a minimum of vertical ruling.

**References** must be typed on a separate sheet, be numbered consecutively in the order of their appearance in the text, and follow this form:

1. F. C. Brown, Phys. Rev. **12,** 345 (1821).
2. J. Culpeper, *Space Optics* (Georgetown Institute of Technology Press, Washington, D.C., 1861), pp. 12, 345.

A list of abbreviations for the names of journals is published in *Chem. Abstr. List of Periodicals 1961.* To make for uniformity of presentation generally, the American Institute of Physics *Style Manual,* second edition, should be used. In general, *APPLIED OPTICS* differs from the *Style Manual* only inasmuch as footnotes appear at the bottom of the page of text, while references are listed numerically at the end of the paper.

There will be no **page charge** for publishing in *APPLIED OPTICS* for the time being.

**Letters to the Editor** should follow the above suggestions, but no abstract is required.

# Illumination of 80-in. Bubble Chamber

Seymour Rosin

It is possible to design a cylindrical condensing system whose geometry allows light to be collected along the length of narrow tubular sources and to pass through a restricted port area. The quantity of light collected is many times that possible to obtain with axially symmetric lenses. This system has been applied to the illumination of the Brookhaven 80-in. bubble chamber. The optical arrangement is described. Other unique features include the use of plano reflectors to extend optically the flashtube and condenser lengths and the provision of a spot plate to eliminate surface reflections from the chamber window

Before discussing the problems associated with the illumination of the chamber, a short description of the entire system is indicated.

The phenomena to be photographed are viewed through the chamber window whose free aperture dimensions are 193 cm wide by 63.5 cm high. The thickness of the window is 16.5 cm and the over-all depth of the chamber, including window is 91.5 cm. The chamber tapers back, as shown, so that at the rear the dimensions are 233 × 84 cm. The arrangement is shown in Fig. 1.

Particles from the Brookhaven 33 BeV Alternating Gradient Synchrotron (AGS)[1-3] are introduced into the chamber from the side in a direction parallel to the long dimension of the window. A momentary reduction in pressure above the hydrogen is created producing bubbles along the particle trajectories. After a short interval during which the bubbles grow to a size approximately equal to the diffraction limit of the photographic lenses recording the event, the chamber is flash-illuminated and the pictures recorded on film.

The type of illumination specified is of the retrodirective dark-field type. The illumination diverges from a port of limited area some 182 cm from the chamber window and proceeds through it to the rear of the chamber. If a spherical mirror lined the rear of the chamber of radius equal to the apparent distance between it and the port, the rays would be sent back upon themselves and re-enter the port from which they emerged. Four cameras simultaneously photograph the chamber at each flash. These are situated in a square array 63.5 cm on a side symmetrically disposed about the port and facing the chamber. If the rays on their return paths are undeviated they cannot enter the cameras. However, if perchance they strike something such as a bubble they can be diverted into the cameras and be recorded. Thus the tracks show up as bright streaks on a black background. It is obvious that the amount of light used in recording the tracks is extremely small compared with that emerging from the port, and great quantities of light must emerge from the port in order to obtain sufficient film exposure.

The word picture drawn above is somewhat simplified. It is clear that scattering from the bubbles could take place on the forward path of the rays, strike the spherical mirror, and be reflected back into the cameras. These would show up as duplicate tracks in the image of the chamber in the spherical mirror, leading to confusion in the interpretation of the event. It is thus necessary to suppress the photographic recording of scattering on the forward path of the rays. Therefore, the mirror is replaced by some other form of retrodirective device, one which retains the property of returning light in the same direction from which it came but does not have image-forming properties. Several such have been proposed and that chosen is known by the term "coat-hanger assembly".[4] Nothing more will be said here concerning the nature of this device, except that it is quite effective in suppressing the unwanted track images.

All of the factors associated with the geometrical arrangement above, together with data available from xenon flashtube characteristics and experience derived from the 20-in. chamber at Brookhaven and the 72-in. chamber at Berkeley were analyzed[5,6] in detail, including estimates for optical

The author is a consultant for the Brookhaven National Laboratory, Upton, New York.

The work described in this paper was performed under the auspices of the United States Atomic Energy Commission.

Received 20 March 1963.

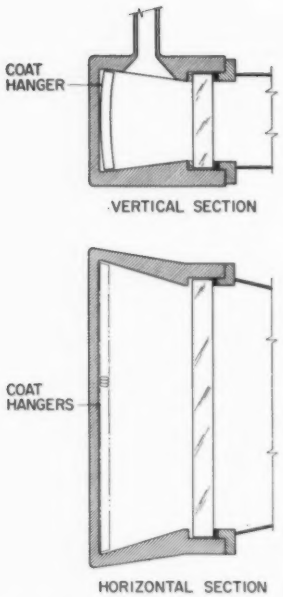


Fig. 1. Cross-sectional view of chamber.

transmission and film sensitivity. The final estimate for the requirements for desired levels of illumination was given by Anderson[6], and his calculations set the desired illumination port area at 145 cm² of effective xenon source image. Furthermore, upon laying out the geometrical arrangement with care it was determined that the beam spread required from the port to the chamber amounted to a numerical aperture of 0.167 in the vertical direction and to 0.42 in the horizontal (19° 15′ × 50°).

Thus, to recapitulate the requirements, it was necessary to provide at the port an illuminating area of 145 cm² and brightness essentially equal to the source and to provide the beam with angular spreads of N.A. = 0.167 vertically and N.A. = 0.42 horizontally. All this operating from a source whose diameter is a mere 4 mm!

Let us assume for the moment that we set as the upper limit of practicability the provision of a condenser system which is able to collect a numerical aperture of 0.75 from the source, corresponding to a semi-angle of about 48.6°. To increase the numerical aperture above this figure can obviously be done only at great effort and for relatively small gain. If such a system works at 4.5 × magnification, it will deliver a numerical aperture of 0.167, just sufficient to cover the small dimension of the chamber, but far from sufficient to cover the large dimension. For the latter purpose three such systems would be needed, each covering approximately one-third of the chamber horizontally.

It is indeed just this threefold system that is in use at Berkeley to illuminate the 72-in. chamber. According to Anderson,[6] the effective illuminating port area in the Berkeley system is 18.5 cm².

It is a reasonable assumption that the threefold Berkeley arrangement squeezes the utmost that can be expected out of conventional optical condensing systems, and that to obtain the manyfold-larger desired port area and corresponding illumination increase for the Brookhaven chamber, which at the same time has sufficient beam spread, requires an entirely new approach.

Conventional condensing systems use axially symmetric optical components to form a magnified image of the source somewhere else in the optical train which is coherent. This, however, is not a necessary requirement. Suppose for the moment that we have succeeded in our task of providing 145 cm² of port area acting as an effective xenon source to illuminate the chamber. Each and every point of this area must send rays of illumination to all points in the chamber. The requirement for the condenser system is that each and every one of these rays must have the original luminous source as origin, and, if this condition is fulfilled, it does not matter in the least whether or not a coherent image of the source is produced.

The arguments given above indicate implicitly that, when only a limited length of tube can be used, the luminous flux is insufficient. But xenon flashtubes while limited in diameter to 4 mm are not so limited as to length, and if the condensing system were designed so as to take full advantage of the length, much more luminous flux could be made available.

The procedure adopted is given schematically in Fig. 2. In (a) we see a cross section through the vertical. The source S delivers a beam of high numerical aperture to the cylindrical lens L. The image of S is formed at the port P and is shown magnified into S′, from which the beam spreads out vertically to illuminate the chamber C. The magnification chosen is such as to deliver the finally required vertical

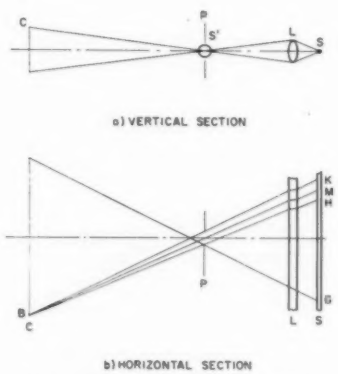


Fig. 2. Schematic representation of theory of cylindrical system

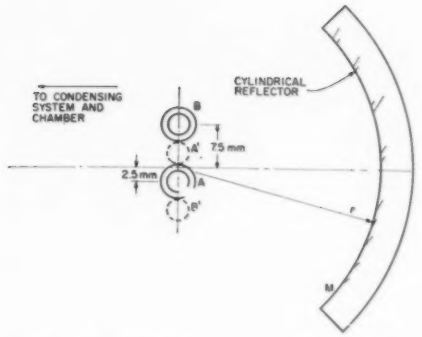


Fig. 3. Cylindrical source assembly schematic.

beam spread. However, in (b) lens L has no power, and an image of S is not formed at P. In this schematic representation, the source length required to illuminate the full chamber width is *GK*, and rays delivered to point B of the chamber may arise anywhere between H and K. A similar length of tube will serve to illuminate any other point of the chamber.

Let us examine for the moment the effect of adding spherical power to the system at the port P. Referring first to the vertical (a), it is to be noted that no effect will occur in the vertical meridian. However, in the horizontal (b), the effect of spherical power at P will be to alter the interval KH about the point M. If the power be gradually increased from zero, the points K and H will approach M, becoming coincident when the points M and B are conjugate. For this condition the required length of source will be a minimum. For still greater power, point H will move to the outside of M, and the required length will again increase.

It is to be noted that the system in no instance forms a coherent image of the source. Even in the case where M and B are conjugate, any point corresponding to B receives rays from all points of the source at M transverse to the source length, so that irregularities in the source in this direction are smoothed out. However, if the source should have irregularities along its length, the conjugate position will show bars of illumination variation in the chamber. In the present application, as will be seen later, spherical power has been added to the system at P substantially greater than that required for the conjugate condition, and is used for other purposes. For this reason, local irregularities in the source do not show up in the chamber.

The fact that we have chosen to use a cylindrical system affords favorable geometrical circumstances for source increase through duplication. In spherical condensing systems, there often is provided behind the source a spherical mirror which either images the source back upon itself or alongside itself so that the effective area is increased. Theoretically, this increase can be as high as 2 ×, but in practice is usually considerably below this. There is no prospect of increasing source area through the provision of additional sources because of the mechanical interference of such sources with each other or with the spherical mirror and condensing system.

The cylindrical system affords freedom from this limitation. The modified FX-1 flashtube[7] to be used has an internal diameter of 4 mm, and the brightness is fairly uniform across this cross section.[8] The walls are 1 mm in thickness. Two such tubes are used in conjunction with a cylindrical reflector in an arrangement illustrated in Fig. 3.

The two xenon flashtubes are shown at A and B with their outer walls separated by 4 mm. A cylindrical reflector at M is so situated that tube A has its center 2.5 mm below the mirror axis and tube B 7.5 mm above the axis. Under these circumstances the effective inner 4 mm of tube A is imaged by M at A′ which is mutually tangent to both tubes as shown, and the effective inner 4 mm of tube B is imaged at B′ tangent to tube A. The result is a source area which is physically 19 mm high, of which 16 mm is effective. The radius of M is relatively unimportant, except that it be large compared to 19 mm to minimize aberrations. The central axis of M should of course be in the plane of the tubes. The dimension of M in the plane of the figure should be somewhat larger than that needed to cover the source numerical aperture required (0.75), and it should be roughly as long as the tubes. A photograph of the actual apparatus is shown in Fig. 4. Means are provided for quick insertion of a new source system including tubes and mirror in case of tube failure. Figure 5 is an exposure of a flash taken directly from the source system (attenuation needed required the use of two sets of crossed polarizing plates). In this picture the four component sources (two real and two imaged as explained) are readily apparent.

We turn now to a consideration of the design of the cylindrical condenser system itself. As stated before, we will collect a wedge of rays whose numerical aperture is 0.75 and transfer this into another at the port of N.A. = 0.167, with therefore a magnification of 4.5 ×. It is implicit in our discussion that since we have expressed our beam spreads in terms of numerical aperture that we intend, in addition to correction for spherical aberration, to effect a high degree of agreement with the sine condition in our design. It is well known that, for infinite magnification, fulfillment of the sine condition is needed to ensure even illumination in the exit bundle. In a recent paper,[9] Wallin ascribes to some unpublished notes of R. K. Luneberg the criterion for uniform illumination of an axially symmetric system, the equation

$$\sin u = m \tan u',$$

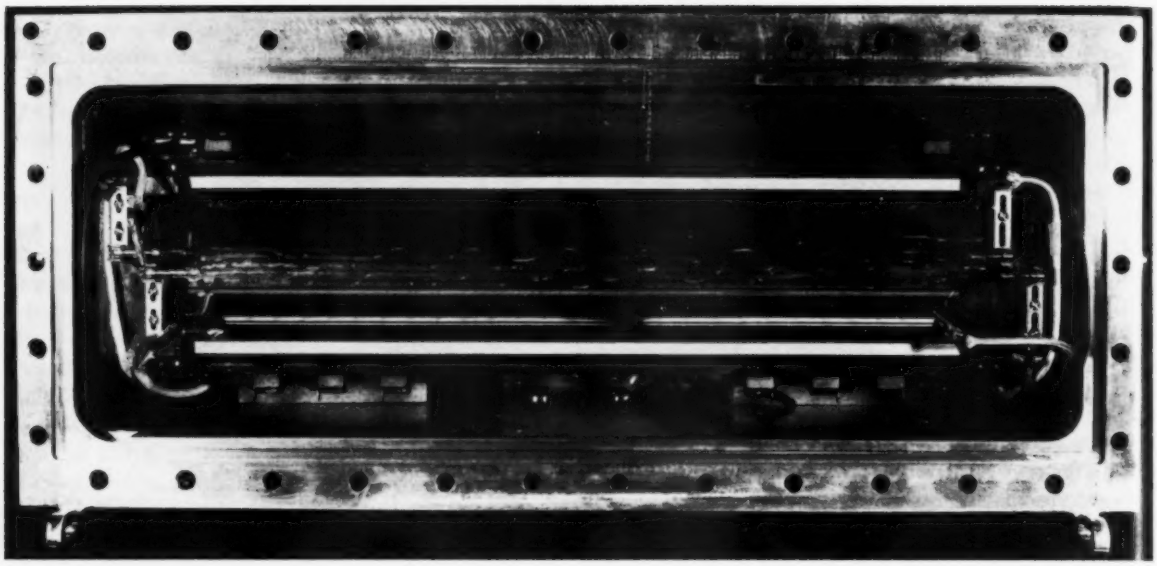

Fig. 4. Photograph of source assembly.

where $u$ is the entrance angle (at the source), $u'$ the exit angle (at the port), and $m$ is the magnification. Since this presupposes a planar source (which ours is not), a plane surface to be illuminated (which ours is not, since the retrodirectors are curved) and a spherical system (which ours is decidedly not), this expression will not strictly hold. It is to be noted that in any case the Luneberg criterion is equal to the sine condition for large $m$. The development of an exact criterion for even illumination of our system poses a difficult problem in analysis, particularly in view of the curved image line resulting from a point object, to be discussed later. The development of such a theory would be interesting and perhaps should be done, but it is quite certain that, whatever criterion results, it cannot be much different from that given by satisfaction of the sine condition. Thus the optical design problems associated with our system take on some of the same characteristics as those of designing a microscope objective.

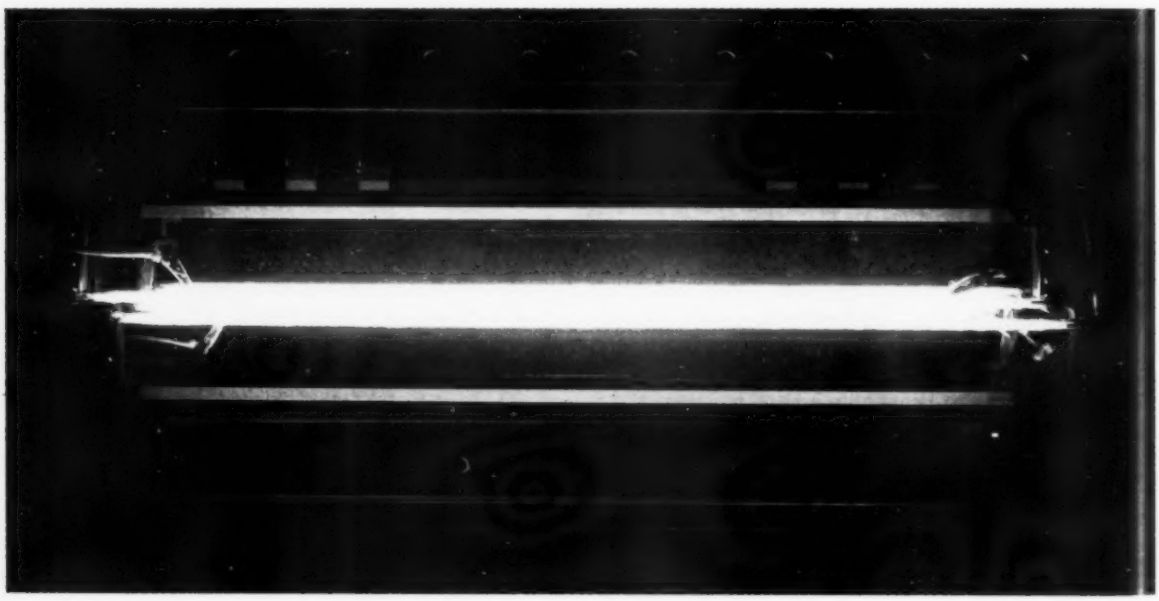

Fig. 5. Exposure of actuated source assembly.

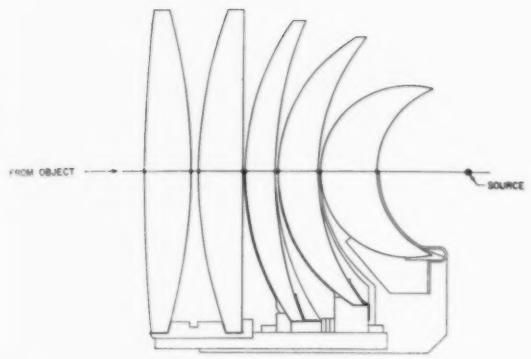


Fig. 6. Cylindrical lens system cross section (source and image reversed).

**Table I. Optical Data Cylindrical Lens System**

| Criteria | | |
|---|---|---|
| E.F.L. | 70.00 | Lens purpose condensing |
| Image distance | 39.00 | Lens type cylindrical |
| N.A. | 0.750 | Object distance (−379.5) |
| Stop height | 140 | Object size 85.6 |
| Magnification | 0.2193 | Instrument 80-in. bubble chamber |
| Image size | 19 | Dimensions in mm |

| Radius of curvature | Separation | Height | $N_F$ | Material |
|---|---|---|---|---|
| 734.7 | | | | |
| | 20.0 | 140 | 1.57952 | LBC2 |
| −258.4 | | | | |
| | 3.0 | | | |
| 205.3 | | | | |
| | 20.0 | 140 | 1.57952 | LBC2 |
| ∞ | | | | |
| | 1.0 | | | |
| 115.14 | | | | |
| | 13.0 | 130 | 1.57952 | LBC2 |
| 175.03 | | | | |
| | 1.0 | | | |
| 67.467 | | | | |
| | 17.0 | 116 | 1.57952 | LBC2 |
| 93.180 | | | | |
| | 1.0 | | | |
| 37.423 | | | | |
| | 24.0 | 74.846 | 1.46318 | Quartz |
| 39.000 | | | | |
| Length of cylinders 406.4 | | | | |

Figure 6 and Table I give the resultant design. The first three lenses nearest the source are aplanatic, that is, the entering surfaces are normal to the axial bundle while the exit surface is aplanatic. The lens nearest the source is made of fused quartz because of the heat. Thus each of these lenses reduces the numerical aperture by a factor equal to its index of refraction, until it is small enough to be turned into a convergent bundle with the required 0.167 N.A. The radius of the innermost surface is 39 mm, while the next surface actually extends more than 180°. While no attempt is made to correct for chromatic aberration, the scale is small enough so that it is unimportant for our purposes.

At this point it seems appropriate to consider a serious aberration of this system which has no counterpart in spherical or axially symmetric systems. In a vertical meridian a point object at the source is imaged at the port. Ordinary Gaussian calculations are sufficient to determine the position and the magnification of a small object at the source. However, in actuality, a point source is not imaged as a point but as a line. If this line were straight and normal to the axis at the port with constant N.A., no difficulty would result. But this is very far from the case. This line is very strongly curved concavely to the lenses as illustrated in Fig. 7, and this curvature is accompanied by a severe reduction in magnification and corresponding increase in numerical aperture at its outer portions which would lead to an intolerable reduction in illumination at the horizontal ends of the chamber if left uncorrected. However, it will be shown that provision of spherical power at the port serves to correct this defect so that the final over-all illumination at the chamber is remarkably uniform. The writer has not explicitly met up with this aberration in his experience, nor does he recall it from the literature. It is hoped that some reader will be able to point out such a reference, or, failing this, to suggest an appropriate name for it.

In order to assess the magnitude of this effect, consider a ray originating at the source and lying in the plane containing the cylindrical axes of all of the lenses. This ray, assumed incident at an angle different from zero, can be traced through the cylinders as if they were a series of parallel plates. Consider the Coddington equations, namely,

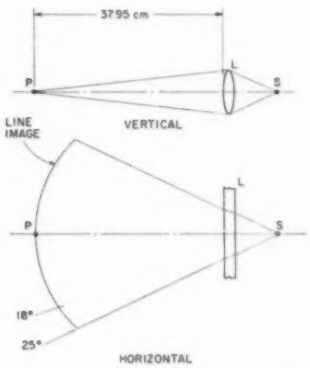


Fig. 7. Image of point by cylindrical system.

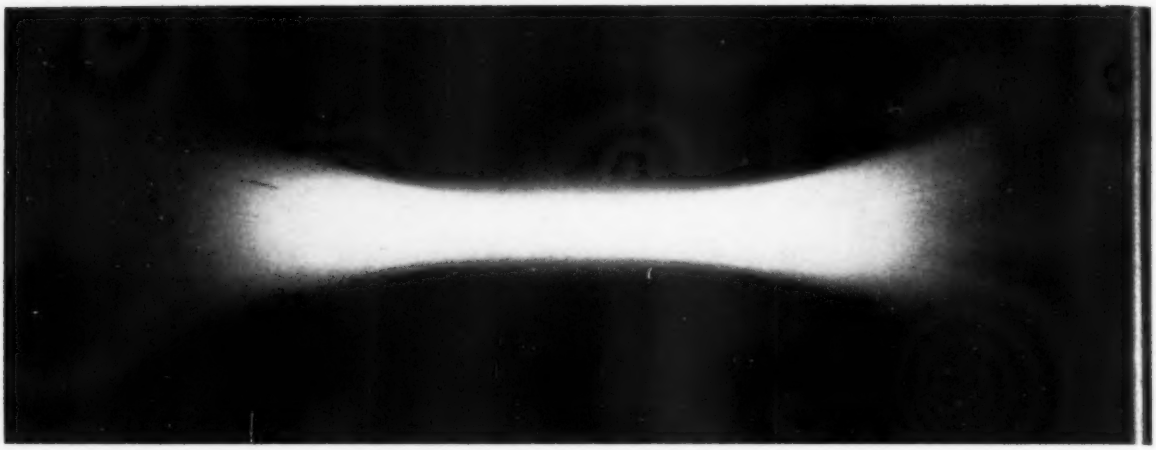

Fig. 8. Illumination pattern of a point source by cylindrical lenses only.

$$N' \cos^2 I'/t' = N \cos^2 I/t + (N' \cos I' - N \cos I)/r_t$$

and

$$N'/s' = N/s + (N' \cos I' - N \cos I)/r_s.$$

In these equations $r_t = \infty$ and $r_s$ is the stated radius of curvature of the surface in Table I. We are not concerned with the first of these equations in our system but only with the second, since we are interested only in the magnification of a small element of the source normal to the plane containing all of the cylindrical axes. In this calculation $s_1$ is the oblique distance of the first surface from the source along the ray. The magnification at each surface is given by $y'/y = Ns'/N's$. The position of the point along the curved image line is determined by the final $s'$, and the magnification by the product of the magnifications at each surface. Experimental verification of these calculations was afforded by setting up a high-intensity point source in the proper position. The curved image line was readily discerned on a screen placed not quite parallel to the cylindrical axes, and the locations of each point on the curved line corresponded with the calculations as closely as could be measured. A screen placed normal to the exit beam well beyond the line demonstrated a strong pincushion effect as illustrated in Fig. 8. The smallest vertical section at the center corresponds to the vertical N.A. = 0.167 as desired, but the much larger sections at the ends reflect the effect of the greater N.A. associated with the outer parts of the curved line, resulting in corresponding reduced illumination. This latter would have amounted to a factor of approximately 2 at the ends of the chamber if left uncorrected.

The nature of the effect and the means for its correction are shown in Fig. 9 which is schematic in nature, showing the xenon source, the cylindrical system, and the port. The chief ray to the center of the chamber originates at $S_1$ and passes through $S_1'$ at the port. The chief ray to the end of the chamber originates at $S_2$. Other rays from $S_2$ normal to the plane cross the plane of the paper at $S_2'$ because of the curved line aberration described above. A small element of the source at $S_1$ normal to the paper is imaged at designed magnification at $S_1'$ while a small element at $S_2$ is imaged at a much lower magnification at $S_2'$. Now if spherical power is added at the port, no effect is produced on the position of $S_1'$, and $S_{1F}$, its image in the lens, is shown coincident with it. However, the off-axis image $S_2'$ occurs before the port, and the effect of the spherical power at the port is to displace it still further away to $S_{2F}$. However, at the same time it will be magnified, reducing the numerical aperture and restoring the illumination at the chamber ends. The results are shown in two graphs, Figs. 10 and 11. Figure 10 shows the positions of the images above referred to, the upper curve referring to the image position $S_2'$ after the cylindrical system, and the lower

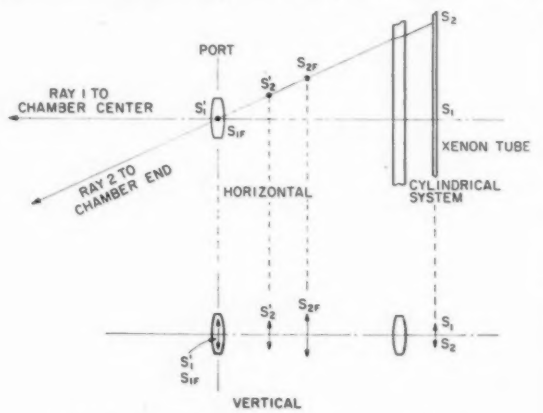


Fig. 9. Correction effect of lens power at port. Position of image measured along ray.

to that after passing through the spherical power introduced at the port, the latter designated by the term "aspheric lens" for reasons to be apparent later. Figure 11 gives the same data for the magnification. The results show an actual increase in source magnification with field angle, but since the source image is physically further away from the chamber as given in the preceding graph, the illumination is no greater. But neither is it less, except for a normal $\cos^3\theta$ fall off.

There is one minor difficulty with this arrangement, and a means for ameliorating it. The vertical port dimension is only moderately larger than the images $S_{1F}$ or $S_{2F}$. Since there is a substantial displacement between the port and $S_{2F}$, vignetting of $S_{2F}$ by the port will result in reduced illumination in the corners of the chamber. If we were to reduce the distance between $S_{2F}$ and the port, this vignetting will be lowered. This can be done at the expense of separating $S_{1F}$ from the port by moving the xenon source closer to the cylindrical system. This situation is illustrated in Fig. 12. This procedure will introduce more magnification of the source for both $S_1'$ and $S_2'$, which are

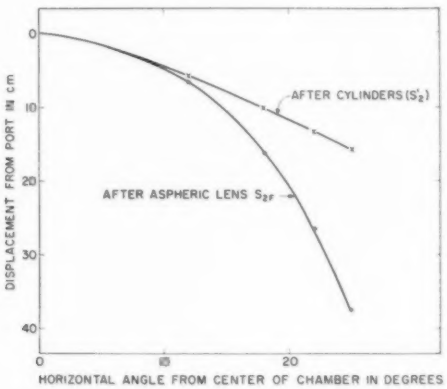


Fig. 10. Position of image measured along ray.

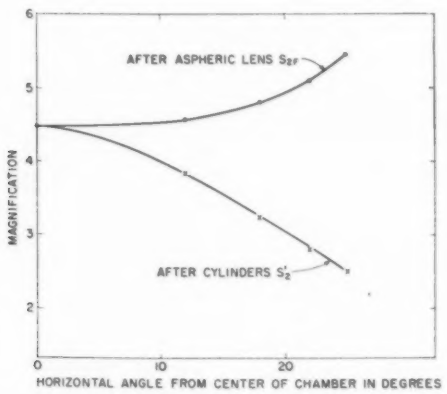


Fig. 11. Magnification of image.

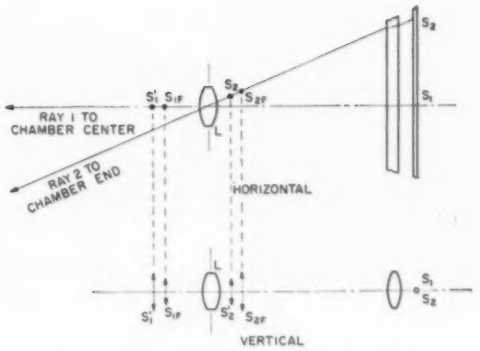


Fig. 12. Effect of displacing source forward.

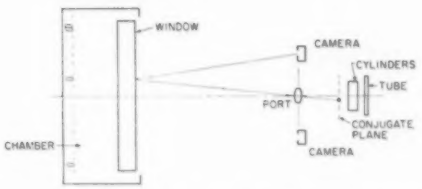


Fig. 13. Schematic of optical system illustrating spot system.

both shown larger than before. However, spherical lens L will tend to operate upon $S_1'$ to pull it back and reduce the magnification, while the magnifying effect on $S_2'$ is smaller than before because it is closer to L. The effect of L in this regard is to act as an optical balance wheel or governor of the system. Of course, if this procedure is carried too far, while it would be possible to eliminate vignetting at the chamber ends, one could introduce it at the center. Practically speaking, it is advisable to make the position of the source adjustable so as to bring it empirically to the most favorable distance.

We turn now to a discussion of a major disability of all dark-field retrodirective systems and means for its elimination. Referring now to Fig. 13 we see a schematic of the system as we have built it up so far. A tremendous amount of light leaves the port toward the chamber and is returned by the retrodirectors. However, a portion of this light is reflected from each of the two surfaces of the window, and these reflections may be seen directly by the cameras. The camera apertures approximate a point (they are only about 6 mm in diameter). The net result of this is that each photograph is completely fogged over an area whose linear dimensions in relation to the chamber picture are approximately half those of the port. While this area is small related to the entire picture, it is large enough to be quite objectionable. One solution of this problem is to set the large window at an angle so that the reflected rays are thrown out of the field of view of the cameras. This has obvious geometrical

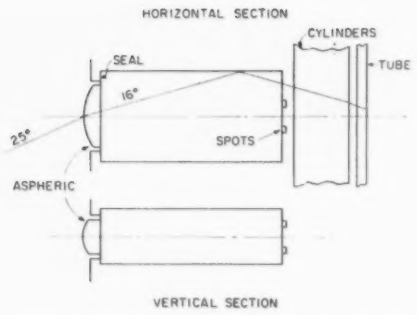


Fig. 14. Arrangement of aspheric, glass block, and spots.

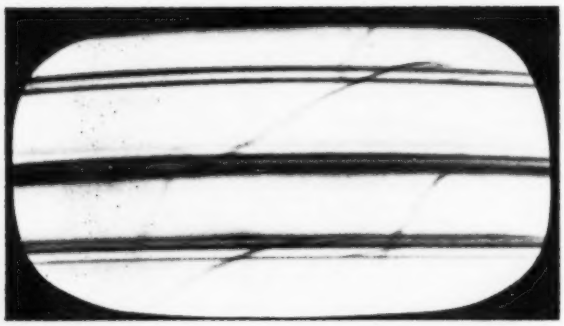

Fig. 15. Photograph of port from chamber upon actuation of flash.

have seen, spherical power exists at this position. Consequently there must exist a plane conjugate to the camera apertures on the illumination side of the port, as shown in Fig. 13. Ideally the four camera apertures would image as four tiny dots in this conjugate plane. If now we set up a plate of glass at this position and opaque the area corresponding to the dots, no light will proceed from the illumination system and be reflected by the window into the cameras.

The system described above is complicated somewhat, so that the dots are more than infinitesimally small. Firstly, two systems are involved, corresponding to each of the two window surfaces so that the opaque areas must be large enough to cover dots in two slightly separated conjugate planes. Secondly, the images are far from Gaussian and subject, because of their off-axis position, to aberration, particularly astigmatism. Since the port lens turns out to have a high relative aperture, aberration spread is large. Spherical aberration for this reflected system is taken care of by making the port lens strongly aspheric, but astigmatism cannot be controlled because the pupil of this system is at the lens, and the astigmatism is determined, as is well known, by the power of the lens alone. The most favorable position for the spot plate is to place it in the sagittal focus, and the spots themselves are roughly lines pointing generally toward the axis.

It was decided to make the port lens from a single

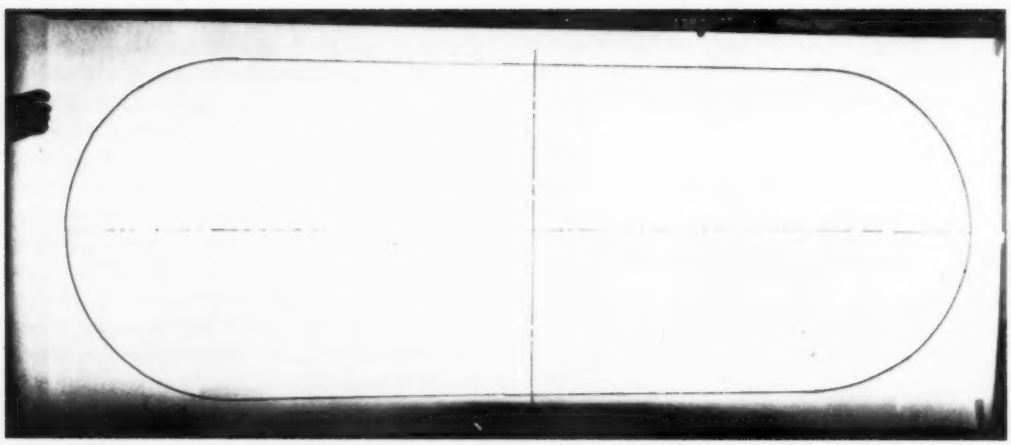

Fig. 16. Illumination of screen placed at chamber position.

disadvantages. It had been decided at Brookhaven to keep the window perpendicular to the axis, although the angled window arrangement is employed at Berkeley.

Consider the system in reverse. Rays from the camera apertures strike the window and are reflected from either surface back through the port. As we

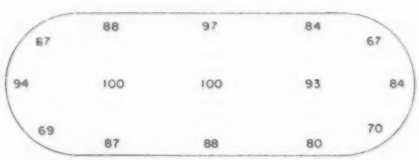


Fig. 17. Relative intensities at various points of chamber.

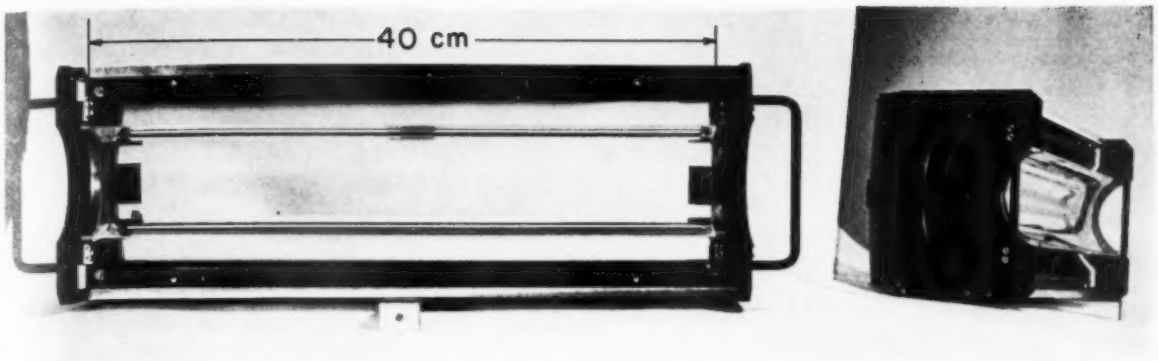


Fig. 18. Photograph of cylindrical lens system.

aspheric surface in front, to make its rear surface plano, to join, by cementing, the rear face of this lens to a large glass block, on the rear face of which the spots are located. In this way the number of air glass surfaces is reduced and the contrast in the images of the spots maintained high. Another advantage of this arrangement arises from the fact that the sides of the block can be optically polished, and use made of the internal reflection at these sides for the high angular rays (see Fig. 14) thus reducing substantially the required length of the cylindrical lenses and the xenon tubes.

Returning now to the spots themselves, certain other properties are required. Since the system is such that a large amount of light flux is redirected back into the port, there is a danger that this light can illuminate the spot area from behind and again be reflected forward whence it will re-emerge from the port and be reflected back by the window precisely into the camera apertures which are conjugate to the spots. To eliminate this, the spots are made of wafers of highly absorbing dark glass of index of refraction equal to that of the block, and cemented thereto by cement of the same index so as to eliminate the possibility of Fresnel reflection at the joint. The outside of the wafer is coated with an opaque layer of protected aluminum, preventing direct light from passing through the wafer. The dimensions of the wafer are determined finally by a mockup of the camera-window-port-block system and observing the image of the camera aperture, illuminated from behind, as seen by a microscope at the end of the glass block. Every vestige of light should be eliminated by the wafer. Whether or not the spot system will be completely successful is not known at the time of this writing, but a system mockup is encouraging.

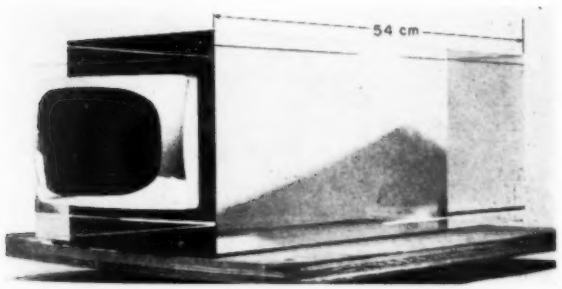


Fig. 19. Photograph of aspheric lens and glass block.

The system has not yet been installed, but careful mockups have been made. Figure 15 is a photograph of the port area (front of the aspheric lens) when the source was actuated, showing the image of the source as produced by the optical system. Two pairs of crossed polaroids again attenuated the light. It may be compared with Fig. 5. The corresponding four components are easily discernible and the vertical magnification quite apparent. Faint images of the fine wires wrapped around the flashtubes can still be discerned.

The system was turned toward a screen upon which was traced the chamber outline. Figure 16 shows a flash of the screen. Flash photometric measurements were taken at various positions on the screen, and the relative intensities at different points are shown in Fig. 17. The uniformity is quite good for a system of this angular size and seems to reflect little more than the natural $\cos^3\theta$ falloff.*

The apparent area of the source presented to the chamber at the port is approximately 8 cm vertically $\times$ 18 cm horizontally. Preliminary estimates of the actual intensity at the chamber distance indicate it to be as expected from this area, allowing for reasonable transmission and other losses.

Figure 18 shows a photograph of the cylindrical lens system, and Fig. 19 that of the aspheric lens and glass

* The photometer was turned toward the port in making the measurement, eliminating one cosine of the usual $\cos^4\theta$. This was thought more realistic for the measurement of spherical bubbles.

**Table II. List of Important Optical and Mechanical Data**

| | |
|---|---|
| Optical distance—from field lens to inside of window | 190.5 cm |
| Window-free aperture, inside | 193 cm × 63.5 cm |
| Angles from field lens | 25° × 9° 38′ |
| Numerical aperture | 0.42 × 0.167 |
| Numerical aperture at source | 0.75 |
| Magnification condenser system | 4.56 × |
| Source height | 1.9 cm |
| Image of source height | 8.6 cm |
| Image of source length | 18 cm (arbitrary) |
| Effective image of source area | 146 cm² |
| Field lens-free aperture | 19.7 cm × 10.8 cm (corners rounded) |
| Field lens to retrodirector | 257 cm (air) |
| Camera lens to field lens (reflected by surface half-way between 2 window surfaces) | 380 cm |
| Field lens to spot plate | 37.5 cm (air) |
| Sagittal field curvature displacement (at height 3.12 cm) | 0.175 cm |
| Clearance last condenser to spot plate | 0.62 cm |
| Equation of aspheric surface (approximate) $x = 2.804 \times 10^{-2} y^2 + 1.043 \times 10^{-5} y^4$ (cm) | |
| Sagitta at corner of aspheric ($y$ = 11.2 cm) | 3.10 cm |
| Length of glass block (BK7) | 56.8 cm |
| Magnification of camera apertures at spot plate | 0.0982 × |
| 63.5 cm square → 6.23 cm square on spot plate | |
| Size retrodirector | 234 cm × 83.8 cm |

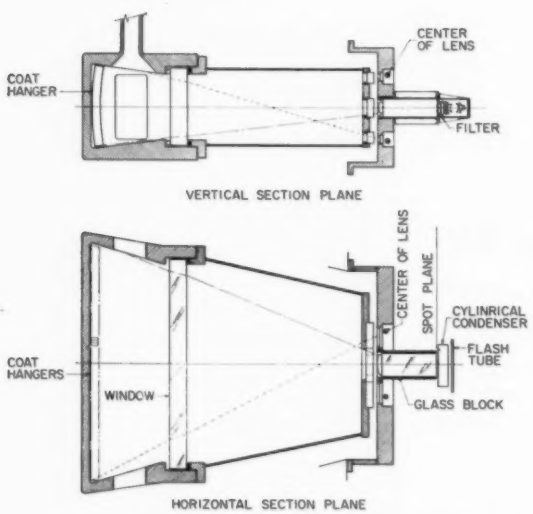


Fig. 20. Over-all sketch of entire system.

block. Table II is a set of values giving pertinent dimensions and optical data. Figure 20 is an over-all sketch of the entire system.

It is obvious that a project of this magnitude and importance required the contributions of several individuals and contractors. For the sake of space many of the detailed points have either not been discussed or only lightly touched upon in this article.

R. Ronald Rau (BNL) is responsible for the over-all performance and thus guided the project, making all of the hard decisions required. S. S. Yamamoto (BNL) made important measurements on the lateral and transverse source brilliance, and on tube lifetime. Irving Winters (BNL) solved many important problems relating to the mechanical assembly. Robert H. Palmer (BNL) worked closely with the writer throughout the project in consideration of basic factors of design and execution. In particular, Palmer is responsible for the concept of the glass block with its attached aspheric, while the writer's chief contribution is the concept and design of the cylindrical system.

As to contractors, Edgerton, Germeshausen & Grier, Inc., supplied the tubes of their FX-1 type but modified into a length over three times the normal 15 cm. Schott and Gen., Mainz, supplied the raw glass for the large glass block to a tight bubble specification, required for reasons not discussed. The J. W. Fecker Division of American Optical Company, Pittsburgh, supplied the cylindrical lenses, which, because of their size and general requirements are unique in the optical art. The large glass block and the aspheric lens were fashioned to tight specifications by Photronics Corporation, Flushing, N.Y.

The illumination arrangement as described in this article will no doubt be installed and used to illuminate the 80-in. chamber for the investigation of nuclear phenomena between the time of writing (January 1963) and that of publication (October 1963). It is hoped that a further account of its performance will be made available later.

## References


1. J. P. Blewett, Rept. Progr. Phys. **19,** 37 (1956).
2. G. K. Green and E. D. Courant, *Handbuch der Physik* S. Flügge, ed. (Springer-Verlag, Berlin, 1959), Vol. 44, p. 218.
3. J. P. Blewett and M. S. Livingston, *Particle Accelerators* (McGraw-Hill, New York, 1962).
4. H. L. Kraybill, Brookhaven National Laboratory Internal Report No. E-41. (unpublished).
5. H. L. Kraybill, Brookhaven National Laboratory Internal Report No. E-59 (unpublished).
6. F. Anderson, Brookhaven National Laboratory Internal Report No. E-67 (unpublished).
7. Edgerton, Germeshausen and Grier, Inc., Data Sheet 1000.
8. Independently confirmed by S. S. Yamamoto (BNL).
9. W. Wallin. J. Soc. Motion Picture Television Engrs. **17,** 76 (1962).

# Electronic Flash Illumination of a Large Wilson Cloud Chamber

Harold E. Edgerton

Electronic flash tubes may be used to illuminate cloud chambers in order to freeze particles in motion and obtain sharp, clear photographs without blurring the image. Introductory theory of flash tubes is given, and the illumination of a 120 × 150 × 60 cm cloud by four 132-cm (54-in.) flash tubes is described. A total energy of 58,800 W-sec is used.

## Introduction

Wilson,[1] in his efforts to photograph tracks in his first cloud chamber, used a capacitor discharge into a mercury lamp since he realized that a short flash of intense light was necessary to freeze the motion of the small water droplets that form the tracks. Many experimenters[2–4] have followed this lead of Wilson, with the trend toward xenon-filled flash lamps, instead of the original high-pressure mercury-vapor lamp.

The present paper presents data on several flash lamps and indicates how the design of special flash lamps can be made by extrapolation of known data from the efficiency and flash duration of existing xenon flash lamps.

## Theory of Flash Tubes

Several items are always of interest to the user of a flash tube. First, the flash duration is of primary importance, as in bullet or bird flight photography, in order to "freeze" motion and to obtain sharp, clear photographs without blurring the image. Second, the total quantity of light may be of importance for large-scale projects; for example, night aerial photography or the large Wilson cloud chamber described in this paper.

The "duration" of a flash can be defined as the time between the $^1/_3$ peak light instants. The actual flash duration is a curve of light output showing the buildup, the peak, the ripples if any, and the decay as shown in Fig. 1. The "$^1/_3$ peak" duration has been found to be a convenient value to measure on the face of a cathode-ray oscilloscope that displays the light vs time curve.[5] A duration of less than 0.005 sec is required for most cloud chambers to stop effectively the motion of the droplets.

The "resistance" $R$ of a flash lamp is, like duration, a quantity which must be defined. Let tube "resistance" be given as the ratio of the initial voltage of the capacitor to the peak current in the flash lamp. For this experiment, the series resistance and inductance of the circuit should have negligible voltage drop.

If the flash lamp did act as a constant resistor and the light output was proportional to the power, then the time constant of the *power* transient would be $T = RC/2$ sec, where $C$ = capacitance in F, $R$ = resistance in Ω, and $T$ = time in sec.

This time constant, $T$, is equal roughly to the "duration" mentioned above, especially for a flash lamp that is loaded heavily as described in the following.

Experimental data are given in Table I for three flash lamps of different dimensions so that the resistance $R$ can be found for tubes of other dimensions. Figure 2 shows how tube "resistance" $R$ varies with capacity. Notice that the resistance tends to become constant for large values of capacitance; that is, above a given energy value. The xenon gas pressure of these three lamps was about $^1/_4$ of an atmosphere.

As rough criteria for cloud-chamber flash lamp resistance calculation: if the energy per cm³ is greater than about 10 or 20 W-sec per cm³, the tube resistance is

$$R = p\,\frac{\text{length}}{\text{area}} = p\,\frac{L}{\frac{\pi d^2}{4}}\ \Omega,$$

and the flash duration is

$$T = \frac{RC}{2}\ \text{sec},$$

where $d$ = i.d. (inside diameter) in cm and $L$ = arc length in cm.

The author is with the Massachusetts Institute of Technology, Cambridge, Massachusetts.

Received 10 December 1962.

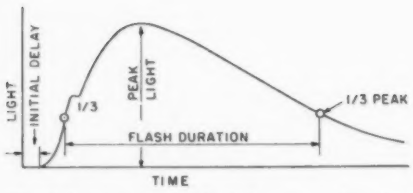


Fig. 1. The light output of a flash lamp as a function of time.

**Table I. Resistivity of Three Flash Lamps[a]**

| Tube type | Inside diameter (cm) | $L$ (length) (cm) | $R$ (resistance) (Ω) | $p$ (resistivity) (Ω-cm) | W-sec (cm³) |
|---|---|---|---|---|---|
| EG & G FX-1 | 0.4 | 15.2 | 2 | 0.015 | 21 |
| Tube A | 0.4 | 61 | 8 | 0.0165 | 10.5 |
| Tube B | 0.7 | 55 | 2.3 | 0.0162 | 21 |

[a] Resistivity, $p$, in Ω-cm and energy per cm³ at the resistance break point as marked on Fig. 2 with a square point.

## Efficacy

The output[6] of the FX-1 flash tube, as measured by a phototube with an S-4 surface is about 4.8 horizontal cp/W with 100 μF at 2000 V (200 W-sec). A curve of the efficacy of the FX-1 tube as given by the manufacturer is shown in Fig. 3. Note that a tube of this dimension and loading seems to show a flat peak of efficacy around the rated values of voltage and capacity.

A tube of twice the length and of the same diameter of the FX-1 would be operating at the same energy and gradient conditions per unit volume if operated at 4000 V and with a capacitor of 50 instead of 100 μF. Notice that the duration of the new double length tube is exactly the same as the single length tube. However, the total light will be double that of the FX-1 since the energy input is double. The energy per unit volume is the same as before and so the efficiency of producing light is the same for both cases. Likewise, the voltage per unit length is the same for both lamps.

Several experimental attempts to check this efficiency prediction were made. The data were always suspected to be in error because of the conditions of measurement, as caused by the geometry and by reflections.

## Large Cloud Chamber Illumination System

The flash lamp for a large cloud chamber[7] at M.I.T.'s Nuclear Science Department has a length of 54 in. (132 cm) with an i.d. of 4 mm. Some tubes were also made with an i.d. of 7 mm. Figure 4 shows a general view of the cloud chamber.

The calculated resistances of these two lamps are 5.5 and 16.9 Ω and the flash durations with 600 μF are 0.005 and 0.00165 sec.

The tubes were flashed from a 600-μF capacitor charged to 7000 volts. The energy per flash was therefore 14,700 W-sec. A total of four lamps was used on the cloud chamber with a total of 58,800 W-sec.

Parabolic reflectors, of aluminum reflector sheets, were formed to concentrate the light into the cloud chamber. Two lamps in reflectors were used on each side at right angles to the camera axes.

Photographs were made with two cameras at $f/22$ on Eastman Linagraph Ortho 70-mm film. The active volume of the chamber is 120 × 150 cm with a depth of about 60 cm.

This large cloud chamber, after being used for several years on Mt. Evans, Colorado, and Brookhaven National Laboratory (1954–1956), is now at work on Mt. Chacaltaya, Bolivia, on the Bolivian Air Shower Joint Effort (BASJE). Those cooperating on the project are the Universidad Mayor de San Andreas, the University of Tokyo, the University of Michigan, and the Massachusetts Institute of Technology.

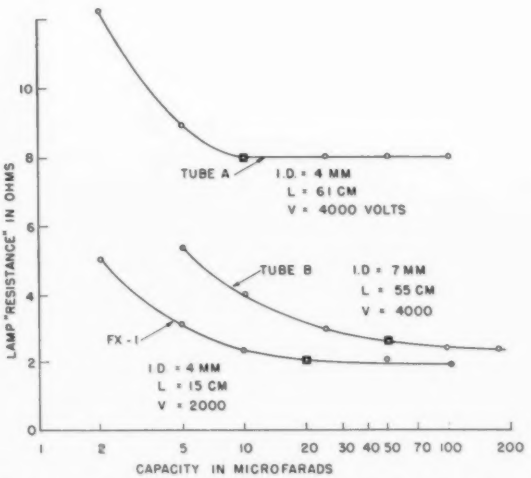


Fig. 2. Flash lamp "resistance" as a function of voltage and capacitance for three sample flash lamps.

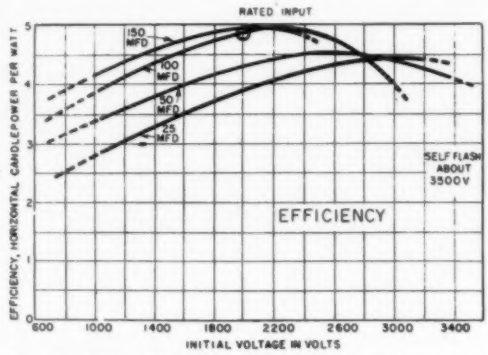


Fig. 3. Efficiency of the FX-1 flash lamp as a function of capacity and voltage.

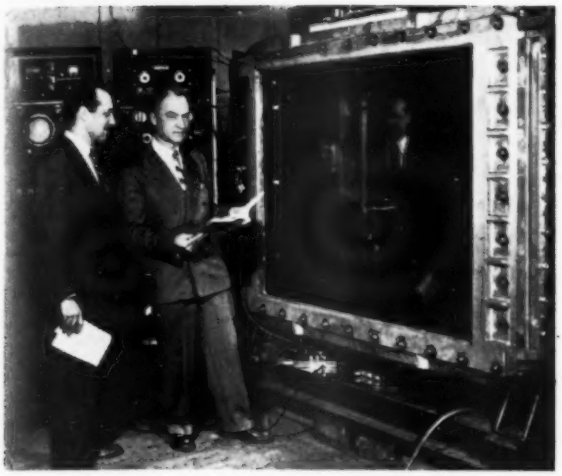

Fig. 4. Herbert S. Bridge (left) and Bruno Rossi of M.I.T. with the 1.2 × 1.5 m cloud chamber whose illumination system is described in this article. Dr. Bridge was in charge of the design of the cloud chamber.

The design of large xenon flash lamps for high power use has recently been treated by Edgerton *et al.*[8,9]

## References


1. C. T. R. Wilson, Proc. Roy. Soc. (London) **A85,** 285 (1911).
2. M. LaPorte, *Les Lampes à Eclairs, Lumière Blanche et Leurs Applications* (Gauthier-Villars, Paris, France, 1949), p. 6.
3. N. Warmholtz and A. M. C. Helmer, Philips Tech. Rev. **10,** 178 (1948).
4. M. A. Cerineo and A. B. Milojevic, Bull. Inst. Nucl. Sci. Boris Kidrich Lab. Phys., Belgrade No. 36, 47 (Aug. 1953).
5. H. Edgerton and R. Shaffner, Electronics **34,** 56 (1961).
6. H. Edgerton, R. Bonazoli, and J. Lamb, J. Soc. Motion Picture Television Engrs. **63,** 15 (1954).
7. H. Bridge, *Annual Progress Reports*, M.I.T. Laboratory for Nuclear Science, Cambridge, Mass., 1953–1954.
8. H. Edgerton, J. Goncz, and P. Jameson, "Xenon Flash Lamp Limits of Operation", presented at the *VI International Congress on High-Speed Photography*, The Hague, Netherlands, 17–22 September 1962. To be published in 1963 by H. D. Tjeenk Willink & Zn., Haarlem, Netherlands.
9. H. Edgerton, "Xenon Flash Lamp Design", Presented at the *2nd International Conference on Quantum Electronics*, Berkeley, California, March 23–25, 1961.


## Brookhaven

Physicist readies a piece of plastic which will be bombarded by billion-volt protons in the Cosmotron at Brookhaven National Laboratory, Upton, New York. When the rectangular slab is moved tightly against the rectangular groove, air is pumped out of the small chamber. An operator in the control room (not shown) can then set automatic equipment which, after the Cosmotron is started up, will push the target into the path of the protons as they circulate in the vacuum chamber (left). Fragments of the nuclei of target atoms which then fly out are trapped in research equipment (not shown) in studies of the structures and properties of the atomic nucleus.

# Papers to appear in subsequent issues

We have had almost 500 papers submitted for publication during the past two years, and we have already built up a backlog which is as embarrassing for a new publication as it is a demonstration of the need for this journal. We have done, and are doing, our best to publish papers as quickly as we can by bringing out bigger issues than had originally been intended last year, by **becoming a monthly in 1963** and by occasionally dropping some of the "filler" departments. The Editors wish to express their sincere appreciation to all contributors who have thus demonstrated their faith in **Applied Optics.**

Refractive Gradient Effects in Proposed Liquid Lasers—*Winston and Gudmundsen*

Infrared Transmission through Fogged Salt Windows—*Morrow and Turk*

A Simple Grating Calibrator for the Visible and Vacuum Ultraviolet—*Hammer, Arakawa, and Birkhoff*

The Use of Polarized Infrared Radiation in Magneto-optical Studies of Semiconductors—*Palik*

An Optical Null Double-Beam Double-Pass IR Spectrophotometer—*Minami*

A Photomultiplier Circuit for Precision Spectrophotometry—*Budde*

Large-Scale Photoelectric Planimeter for Leaves—*Carman*

A New Method for High-Speed Motion Picture Photography of Transparent Drops—*Pfeiffer*

Photometric Accuracy of Infrared Spectrophotometers—*Stewart*

Study of the Fabrication of Aspherical Surfaces—*Sakurai and Shishido*

Transmission of Isotropic Radiation Across an Interface Between Two Dielectrics—*Stern*

Isosceles Total Internal Reflectors as Optical Elements—*Rothstein*

Test of Theoretical Absorption Band Model Approximations—*Burch and Williams*

Optics in Norway—*Hisdal and Omholt*

Use of an Analog Computer in Side-on Arc Spectroscopy—*Shumaker and Yokley*

Attenuation by Ozone and the Earth's Albedo in the Middle Ultraviolet—*Green*

Experiments with the Optical Excitation of Mercury Vapor for the Production of Isolated Fluorescence—*Zito and Schraeder*

Observations of Near Infrared Radiation from the Solar Atmosphere—*Taylor and MacQueen*

Irradiance on a Flat Object Underwater—*Tyler and Shaules*

Kirchhoff Diffraction Pattern Calculations—*Moore*

Interference Filter Spectrometer for Low Intensity Extended Sources—*Carter, MacRae, Nelson, Birkhoff, and Arakawa*

A Universal Spectrophotometer—*Kaye*

The Stressed-Plate Shutter: A New Moderate-Speed Electro-Optical Light Modulator—*Hauser, Smith, and Marlowe*

Measurement of Energy Flux Density Distribution in the Focus of an Arc Image Furnace—*Beyer, McCulley, and Evans*

Irradiance Linearity Corrections for Multiplier Phototubes—*Baker and Wyatt*

Optics in Australia—*Steel*

Slit-Induced Errors in Pressure-Broadened Line Measurements—*Dalton*

Variation of Lead Sulfide Response with Incident Angle and Orientation in Detector Plane—*Groner and Stoliar*

A Continuously Variable Optical Beam Splitter and Intensity Controller—*Harrick*

Dispersion in the Vicinity of an Optical Resonance—*Fork and Bradley*

Design for a Wide-Angle, Linear-Output, Horizon-Sensor Optical System—*Palser*

A Redetermination of Some Optical Properties of Calcium Fluoride—*Malitson*

Test Methods in Spectrophotometry: Stray Light Determination—*Poulson*

The Scattering of Infrared Radiation from Clouds—*Bauer*

Temperature Measurements with an Optical Pyrometer under Adverse Conditions—*Paul*

An Absolute Reflectometer for Use at Low Temperatures—*Hartman and Logothetis*

Field Photometer with Nine-Element Filter Wheel—*Frentress, Young, and Edwards*

On the Astrophysical Work of W. W. Coblentz—*Strong*

Jet-Controlled Arc II: Excitation of Third Spectra—*Moore, Thygesen, Derwin, and Eward*

Optical Properties of "Liumogen": A Phosphor for Wavelength Conversion—*Kristianpoller and Dutton*

Exfocal Pumping of Optical Masers in Elliptical Mirrors—*Roess*

Optical Harmonic Generation in Two Ferroelectric Crystals—*Smith*

Spectroscopy Applied to Hypersonic Atmospheric Penetration—*Planet*

A New Grazing Incidence Spectrometric Mounting—*Landon*

Coblentz's Contribution to Infrared Spectroscopy—*Jones*

Spectral Emittance of Refractory Materials—*Blau and Jasperse*

The Influence of W. W. Coblentz on Radiometry—*J. A. Anderson*

The Infrared Transmittance of Carbon Dioxide—*Stull, Wyatt, and Plass*

An Automatic Calibrating Apparatus for Standard Scales by Counting Interference Fringes—*Doi, Shimizu, Tsuboi, and Kouno*

Data Processing System for the Automatic Transformation of Observed Plasma Intensities into Their Radial Distribution—*Paquette and Wiese*

Characterization of Bolometric Detectors—*Hoffman*

Push-Pull Optical Modulators and Demodulators—*Sterzer*

Errors in IR Absorption Measurements Due to Wall Adsorption of Water Vapor—*Howard*

6-m Focal Length Ebert-Type IR Spectrograph. Part I—Details of the Spectrographs—*Rao and Nielsen*

6-m Focal Length Ebert-Type IR Spectrograph. Part II—Precision of Measurements—*Rao and Fraley*

Spectral Variation of Blackbody Variation—*Dreyfus*

Interferometric Measurement of Wavelengths of IR Atomic Emission Lines in the Extraphotographic Region—*Humphreys*

The Effect of Extraneous Radiation on Photometric Accuracy of IR Spectrophotometers—*Stewart*

The Modulation Transfer Paradox—*Hempenius*

The Use of IR Spectra of Chars in Coal Structure Research—*Friedel*

On the Correction of Phase Errors in Interferograms—*Mertz*

Spectroradiometry by Means of Modified Spectrophotometers—*Hammond*

Quantitative IR Spectroradiometry of Liquid Propellant Flames—*Tourin*

Microdensitometer Modification for Continuously Scanning Angularly Oriented Spectral Lines—*Wiebe*

# he Illumination of the CERN 2-Meter ydrogen Bubble Chamber

Früngel, H. Köhler, and H. P. Reinhard

A general description of the optics of the CERN 2-m hydrogen bubble chamber is given. The chamber is illuminated by three demountable flashtubes with the help of a condensing lens system. The requirements for the light sources and the properties of the prototype are discussed, which combine high intensity (up to 2500 J) with short flash duration (200 μsec), small size of the emitting plasma (15-mm diam) and long life (more than 40,000 discharges at 1000 J). The condenser consists of three units, each with two plano-convex lenses, one of them having an aspherical surface. Theoretical values of the residual aberrations as well as experimental results are given. A short description of the windows and the problem of their antireflection coating is added.

## Introduction

A 2-m hydrogen bubble chamber is now being built at CERN. For the optics a straight-through dark-field illumination system with point sources and a condensing lens system has been chosen by Peyrou and Bridge.[1] This system has many advantages:

(1) The illumination of the chamber is uniform and gives bubble pictures of almost equal brightness, for all possible positions of a track in the chamber and all positions of the cameras on a fixed circle.

(2) The images of the "point sources" are confined to a narrow circular region and this allows free choice for the position of the cameras. The system adopted uses either three cameras on the corners of an equilateral triangle or four cameras on the corners of a square. Consequently, the camera windows of the vacuum tank are made sufficiently large. Two additional windows serve for direct viewing, polaroid photographs, closed-circuit television, or an immediate access camera system.

(3) Since all the light flux in the chamber is well centered to a narrow image of the light sources, it is easy to put plates or absorbers into the liquid without disturbing the illumination. The only effect will be a slight restriction of the field of view of the cameras. In this case four cameras are especially useful.

(4) Finally, the straight-through illumination with a condensing lens system gives good contrast and a clean dark field. This is particularly important for automatic scanning and measuring devices.

Although the illumination system as a whole is rather conventional and found in many bubble chambers, some details are new and will be discussed in detail especially the light sources and the big condensers.

F. Früngel is with Hamburg-Rissen, Sülldorfer Landstrasse 400, Germany, H. Köhler is with Carl Zeiss, 7082 Oberkochen, Germany, and H. P. Reinhard is with CERN, Geneva.

Received 6 March 1963.

## General Description of the Illumination System

Figure 1 shows a schematic view of the bubble chamber optics (not to scale). In order to avoid excessively large glass lenses, the chamber has been divided into three parts, each of them being illuminated by its own system of light source and condensers. They are essentially the same and consist of a flashtube with an elliptic mirror, an intermediate collecting system, and the main condenser. The collecting system consisting of two lenses is placed at the second focus of the mirror. Lens 2 images the light distribution in the second focus (about 60-mm diam) via the main condenser into the chamber, whereas lens 1 is placed into the second focus and images the mirror itself into lens 2 which in turn is imaged by the main condenser into the camera plane. The cameras are placed on a circle of 60-cm diam around this image (about 15-cm diam). The average scattering angle is thus 7° which is a good compromise between intensity and sufficient stereo angle. These three illumination systems illuminate a cone-shaped useful volume of about 500 liters.

The elliptic mirror has a slightly rough surface in order to bring as much light as possible rather uniformly distributed into the second focus. Measurements show that about 30 % of the total light output is

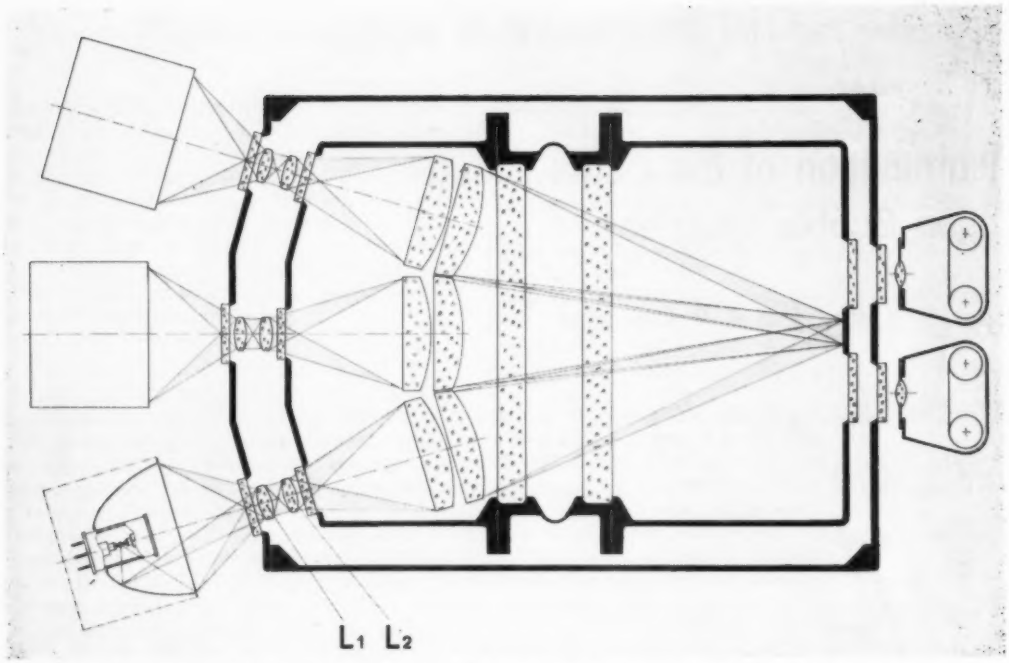


Fig. 1. Schematic view of the optical system of the CERN 2-m hydrogen bubble chamber (not to scale).

collected within a region of 60-mm diam, the intensity variations being less than 1:2.

The spark plasma itself is about 15-mm diam. Small displacements which occur statistically or are due to the stray field of the bubble chamber magnet do not affect the light intensity in the second focus.

## Requirements for the Light Sources

The total light required to illuminate the chamber has been determined in a semiempirical way. The geometry of the chamber is known as well as the scattering of light by small bubbles.[2,3] Other factors can only be estimated, such as the bubble diameter and the film response. It was, therefore, easier to extrapolate the data for the 2-m chamber by comparing it with the 30-cm chamber at CERN[1] which has a similar illumination system and gives excellent pictures. One assumes that the above-mentioned unknown factors are the same in both cases and calculates the light flux in the 2-m chamber which is necessary for pictures of the same density and contrast on the film as those of the 30-cm chamber.

This flux depends on the aperture of the camera lenses, which is fixed by the condition that the diameter of the bubble image be as small as possible. This is the case when the diameter of the circle of confusion due to the depth of the chamber is the same as the diffraction disk with blue light, the cameras being focused on a plane near the central plane of the bubble chamber. In practice the stop will be opened a little more since the effective diameter of the bubble image is smaller than calculated, the film not reproducing the outer parts of the image which have rather low intensity. The diameter of the geometric image of the bubbles is small compared to the diffraction disk and can be neglected in this approximation.

A simple equation can now be derived which gives the density of light flux in the 2-m chamber ($I_{200}$) as a function of the flux in the 30-cm chamber ($I_{30}$), the demagnification factors ($m_{200}$ and $m_{30}$), the depths of the chambers ($d_{200}$ and $d_{30}$), and factors describing the distribution of the scattered light [$G(\theta_{200})$ and $G(\theta_{30})$].

$$I_{200} = I_{30}\left(\frac{m_{200}}{m_{30}}\right)^2 \cdot \left(\frac{d_{200}}{d_{30}}\right)^2 \cdot \frac{G(\theta_{30})}{G(\theta_{200})}.$$

With $m_{200} = 1:13.5$ (for the central plane of the chamber), $d_{200} = 50$ cm, and $\theta_{200} = \theta_{30} = 7°$, we get $I_{200} = 7 \cdot I_{30}$ for the flux densities.

For the total fluxes in the chambers we get a factor 87, which reduces to one-third for each light source of the 2-m chamber, that is 29. Comparing the useful solid angles for both types of light sources we get a factor of 2 for the total light output of each flash. On the other hand we have to add a narrow filter in the case of the 2-m chamber in order to make full use of the antireflection coating. Thus we arrive at the conclusion that the total light output of each light source of the 2-m chamber must be a factor of 16 higher

than that of the 30-cm chamber which uses the General Electric flash FT 230 at 120 J in a circuit with low losses.

If one assumes that the efficiency of a bigger flash will not change drastically with increasing power, the electric power put into the big flash has to be about 2000 J. The repetition rate is 3 sec. Also faster triggering up to 1 sec is foreseen, the power being reduced correspondingly.

A factor greater than 16 would allow a slower film with finer grain or a shorter flash delay which reduces the danger of distortions due to turbulence in the liquid.

Other important requirements for the flashes are: (a) flash duration must be short compared with the time delay between the moment when the particles pass through the bubble chamber and the moment of photographing them. This requires a flash not exceeding 200 μsec. A longer tail is without effect for the photography and can be neglected, provided that it contains less than 20 % of the total light flux, (b) small dimensions of the light emitting plasma ("point sources"), (c) long lifetime of each lamp and simple maintenance. Conventional sealed-off flashtubes hardly fulfill these requirements. There are tubes in the 2000-J range available, but their duration is as long as 1–2 msec, their average life less than 10,000 discharges and their dimensions rather big. The total length of the arc always exceeds 20 cm. In the most favorable cases this is wound to a helix of about 5-cm over-all dimensions. It was, therefore, decided to develop a demountable flashtube, which was built in 1950 for high-speed photography purposes.[4]

## Description of the Light Sources

A cylinder of hard glass is closed with two flanges and sealed by means of O-rings (see Fig. 2). Both flanges hold the interchangeable and adjustable electrodes. The cylinder is filled with argon or krypton of some atmospheres overpressure. It is continously connected to a gas reservoir in order to keep the pressure constant even in the case of small leaks. The whole spark unit is mounted in an elliptic mirror, the center of the spark being at its focus. The condenser bank is placed close to the spark gap, thereby setting the inductance of the circuit to the preset value of 1 μH. This value represents the desirable optimum, because a lower inductance, though permitting shorter flash duration, would cause excessive electrode sputtering, thereby impairing the useful operating period of the flashlamp and necessitating too frequent cleaning of the spark chamber, whereas the selected value of 1 μH is the correct setting for obtaining the effective photographic exposure time of 100–200 μsec. The spark unit and the mirror, together with the auxiliary circuits, are housed in a compact box which can be adjusted as a whole by means of its supporting frame.

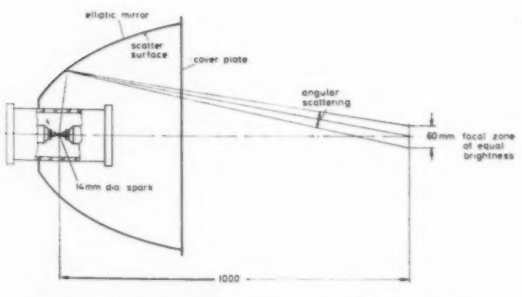


Fig. 2. View of the flashtube and the elliptic mirror.

The box is closed with a Plexiglas cover and cooled by a continuous flow of nitrogen which also maintains a slight overpressure in it in order to reduce possible hazards of hydrogen leaking into the box.

The spark unit must be replaceable quickly during operation of the bubble chamber for the following reasons: The sputtering of the electrodes gives a deposit on the glass cylinder which reduces the light output partly by absorption and more seriously by scattering of the light which, therefore, misses the aperture in the second focus. As soon as a light monitor indicates a certain lowest level of the light flux into the chamber the spark unit must be replaced by a clean one. Since it is kept in the mirror by plug-in sockets it can be taken out quickly. No readjustment is necessary because the mirror always stays in its place. The interruption of the run is thus very short. After cleaning the glass cylinder and readjustment of the electrode distance the spark unit is again ready for use.

The time after which it has to be replaced by a clean one is mainly a function of the electrode material and the triggering mode. The electrodes are made of special sintered tungsten with about 15 % thorium. The thorium content should be as high as possible, but more than 15 % is difficult to achieve because the electrodes become too brittle.

In the first version of the lamps the triggering was effected by means of a third electrode. This has disadvantages because it requires careful adjustments in order to prevent the main discharge from hitting the triggering electrode and destroying it. Therefore, the useful life of a spark unit (i.e., the time until the light in the second focus is reduced to 60 %) was sometimes as short as 2000 discharges. An important improvement[5] has been achieved with the circuit shown in Fig. 3.

There is no third electrode. The trigger circuit is put in parallel to the main discharge circuit, consisting of the condenser bank and the flashtube. A fast trigger pulse is fed in by the pulse transformer. Its risetime is further shortened by the help of an auxiliary spark gap. The main discharge line is covered with ferrite rings giving a total inductance of 100 μH and thus blocking it against the trigger pulse which has to pass through the spark lamp. The main discharge

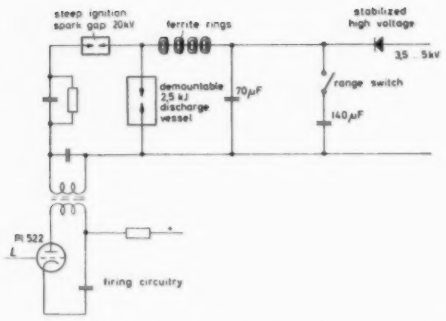


Fig. 3. Triggering circuit.

follows immediately. Its high current saturates the ferrite rings and reduces their inductance to about 1 $\mu$H which keeps the length of the discharge below 200 $\mu$sec. A trigger pulse of 40 kV and with 0.1-$\mu$sec risetime triggers safely and permits use of a rather low voltage for the main discharge. Low voltage at a given electrode distance and gas pressure means high discharge current with correspondingly low content of double ionization processes. This improved the optical efficiency in the visible spectral range of the spark considerably. The factor 16 relative to the light output of the FT 230 could already be reached with a factor of 7 for the electric energy stored in the condenser: that means 870 J compared to 120 J for the FT 230. The details of the prototype for prolonged operation are as follows:

| | | |
|---|---|---|
| condenser battery | = | 140 $\mu$F, |
| energy stored | = | 850 J, |
| voltage | = | 3.5 kV, |
| electrode distance | = | 14 mm, |
| electrode diameter | = | 14 mm, |
| gas pressure (argon) | = | 3–6 atm (increasing pressure increases the efficiency), |
| diameter of the plasma | = | about 15 mm, |
| flash duration | = | 200 $\mu$sec, |
| spark resistance | = | 0.02 $\Omega$ on the average, |
| repetition rate | = | 1–3 sec. |

The lifetime (defined as time for a reduction of the useful light in the second focus to 60 %) is more than 40,000 discharges; the total life of the electrodes is more than $10^5$ discharges. The electrodes are interchangeable.

Though the results with the prototype show that already 900 J give the light output required, the final lamps are built for a maximum power of 2500 J at 3-sec repetition rate, i.e., 800 W of average thermal load of the lamps. This gives sufficient reserve or allows a faster operation up to 1-sec repetition rate at 850 J.

Increasing the gap between the electrodes would further increase the light efficiency of the spark but unfortunately this gain is of no use for the illumination of the bubble chamber. The reason is that the light flux has to be concentrated into a small zone of 60-mm diam near the second focus of the elliptic mirror, only small variations of intensity and uniformity being allowed.

At 35-mm electrode distance the position of the spark varies statistically within a region of about 20-mm diam, thus causing strong fluctuations of the useful light flux. Only by reducing the gap to a distance equal to the electrode diameter (14 mm) the illumination was sufficiently stable and uniform. Figure 4 shows a series of photographs of the spark image in the second focus, taken with a 14-mm electrode distance. The reference circles have diameters of 50, 70, 90, and 110 mm. The distortion is due to an inclination of the photographic camera.

The chamber is illuminated by three synchronously operated lamps. Each of them has its own supply and its own light monitor in order to make sure that the whole bubble chamber is uniformly illuminated. An automatic control of the light output is not foreseen but might be incorporated later.

Besides the important result that these flashes correspond well to the initial requirements they have also economic advantages. The capital investment for three lamps and their accessories and spare units is higher than that required for ordinary sealed-off flashes. On the other hand the running costs are considerably lower since only inexpensive parts such as electrodes, argon, and glass cylinders are consumed. Estimates based on the rather conservative data given in the table show that the higher investment costs will be paid off after $1 \times 10^6$ pictures of the chamber.

## Main Condenser

The main condenser has to image an object of up to 70-mm diam, this being the image of the elliptical mirror produced by the first collector lens into the second one (see Fig. 1). The image quality should be so good that even if there is a short distance between the final image of the light sources and the cameras a perfect dark-field illumination is ensured.

Consequently no stray light caused by geometric-optical aberrations or imperfections of the lenses must reach the camera aperture. This leads to the following basic requirement for the condenser:

The deviation of any beam of the imaging pencil from its ideal path must not exceed 0.5°, or in other words, the lateral aberrations in the image plane should not exceed 26 mm (at an image distance of about 3 m).

This state of correction has to be obtained for a numerical aperture of a single condenser unit amounting to 0.4 (on the side of the object) and for a focal ratio of $f$:0.9, the focal length being 92 cm. This large aperture is due to the requirement that the

bble chamber should be as short as possible and lect as much light flux as possible.

In spite of employing three condenser units the ses are still rather big, the dimensions being 720 × ) mm. It was decided to use the glass BK 7 of aer Glaswerke Schott, Mainz, because this optical glass is melted in large quantities and offered the smallest risk as regards striae and bubbles at the present state of glass melting technique.

Fig. 4. Photographs of the spark image in the second focus.

In order to achieve the desired state of correction it is necessary to use at least one aspherical surface for each condenser unit, provided that the number of individual elements included in each condenser unit is limited to a maximum of three. This is necessary for economic reasons.

In order to keep the linear dimensions of the lenses as small as possible, the aperture diaphragm had to be arranged in the condenser plane. Therefore, there is no way to correct the astigmatism of oblique rays. A reduction of the lateral aberration is possible by using lens shapes which are most favorable with regard to coma. This however would not allow the use of plano-convex elements for the condenser unit, such a construction being desirable for economic reasons. We therefore decided to use plano-convex lenses of approximately equal refractive power and have one external spherical surface aspherized. The aspherizing constants were chosen in such a way that the spherical aberration of the axial pencil is corrected. We then calculated the magnitude of the deviations for the extra-axial pencils. Fortunately, it turned out that for two- and three- element groups the lateral aberration for the extra-axial points caused by astigmatism and coma is within the tolerances indicated above.

It now remained to decide whether a two- or three-element system should be built. The disturbing effect of stray light due to imperfections of the surfaces or multiple reflections as well as economic reasons suggest a two-lens system. The ideal condenser would even consist of one single element. On the other side it has to be considered that the refractive power of the individual elements and consequently their center thickness increases with decreasing number of elements for each condenser unit. Moreover, the thicker the glass body, the larger the difficulties to get sufficient freedom of striae, bubbles, and other defects.

Another important requirement is given by the fact that the condenser together with the glass windows and the chamber body has to be cooled down to about 27°K, the working temperature of the bubble chamber. The big glass pieces must be cooled as uniformly as possible in order to avoid excessive temperature gradients which might crack the glass. This limits the cooling rate to a few degrees centigrade per hour, the total cooling time being several days.

The best compromise between all these considerations is the two-element system, the lenses being about 170 mm thick in the center, which is equal to the thickness of the windows. A cooling rate of about 5°C per hour should be safe for both. The weight of each lens is about 160 kg, that of the complete condenser nearly one ton.

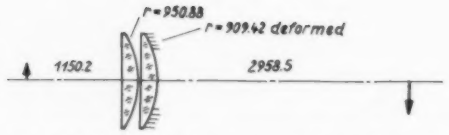


Fig. 5. Details of the two-component condenser units.

The choice of two plano-convex lenses for each condenser unit also simplifies the task of designing a suitable clamping system for the lenses which has to be elastic in order to keep the lenses well in place over the wide temperature range. Aberrations due to displacements of the lenses during the cooling process must not exceed the tolerances given above.

Figure 5 shows the details of the lens system. The meridian curve for the aspherical surface reads as follows:

$$p = (h^2/2r) + c_1(h^2/2r)^2 + c_2(h^2/2r)^3,$$

where $p$ is the sagitta, $h$ the height of incidence, $r$ the vertex radius ($r = 909.42$ mm).

The constants $c_1$ and $c_2$ have the following values:

$$c_1 = +3.99 \times 10^{-4},$$
$$c_2 = -1.64 \times 10^{-7}.$$

Figure 6 gives the aberrations in the image plane for points on the axis and at 81.4 mm off-axis, this being the largest possible distance. The wavelength is 4800 Å. The solid curves show the results of the trigonometric calculation, whereas the dotted curves correspond to a measurement carried out by stopping out individual zones (Hartmann's method). The measurements indicate that although the residual aberrations in the axis exceed the calculated value due to the inaccuracies during the manufacturing process they are well within the tolerance limits of 26 mm.

Figure 7 shows photographs of a star, taken on the axis of each condenser unit and at a distance of 81.4 mm above and below axis. All of them are much smaller than the tolerances. Their irregular shape is due to imperfections at the rectangular corners of the lenses.

Figure 8 shows a first measurement of the light distribution in the image plane, the object being a ground glass disk of 50 × 50 mm. The relative intensity of the image has been measured at different distances from the optical axis. The dotted line at about 60 mm corresponds to the theoretical border of the image.

The cameras of the bubble chamber will be at a distance of 300 mm from the optical axis. These meaurements prove that at this distance the amount of stray light due to the condenser is negligible.

Figure 9 is a photograph of one condenser unit, mounted provisionally for tests. This unit will illuminate the central part of the bubble chamber, whereas the side units have a semicircular shape.

## Windows

The specifications for the glass windows are even more strict than those for the lenses, because they are within the range of camera focus and any defects would show on the pictures. Though their weight is 660 kg (length 218 cm, width 77 cm, thickness 17 cm) they must be as free as possible from bubbles, stones, veins, and scratches. The casting of borosilicate crown glass BK 7 is successfully completed at Jenaer Glaswerke Schott. The number of bubbles is less than 1 per liter, the number of stones and similar defects only three to four per glass block, and only one or two short veins are found near the edges where less than 15 cm extend into the visible region.

The thickness of the window had been determined in such a way that a sufficiently high safety factor is incorporated. Though the bubble chamber pressure is about 6 atm, the window must withstand 60 atm. The thickness of the window could be brought down to 17

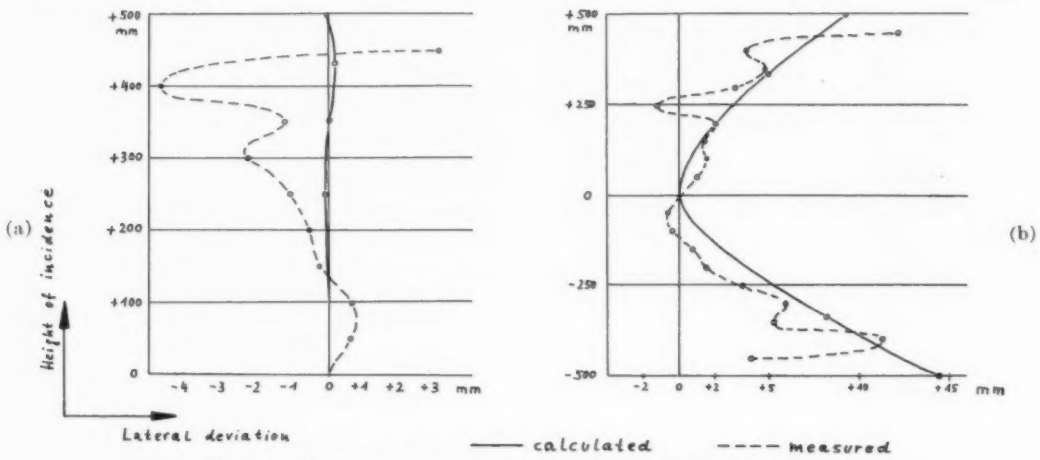


Fig. 6. Aberrations in the image plane for points (a) on the axis and (b) 81.4 mm off-axis.

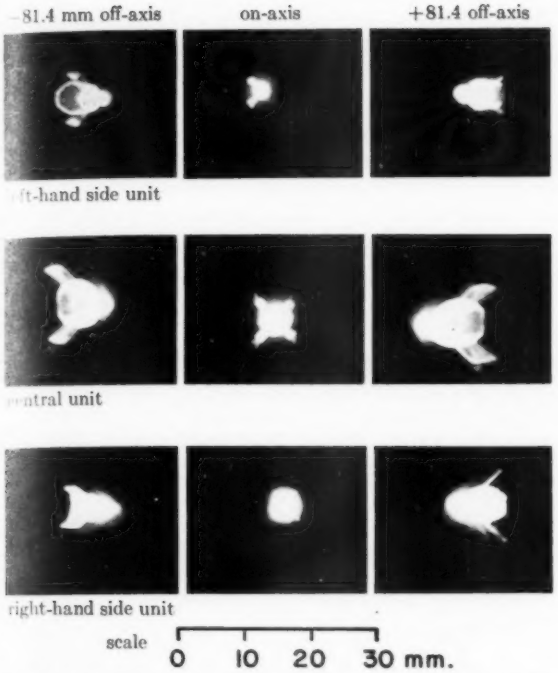


Fig. 7. Photographs of the image of a star, taken on the axis and 81.4 mm off-axis.

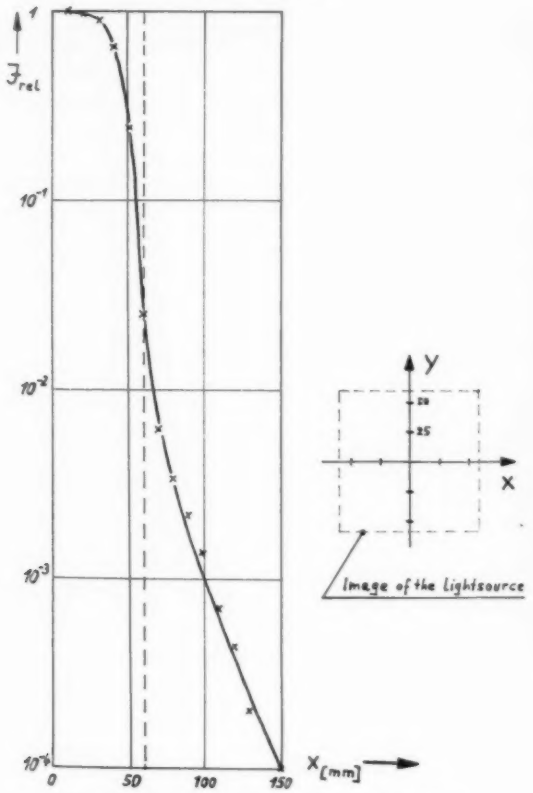


Fig. 8. Light distribution in the image plane.

cm because the maximum tensile strength doubles when going down from room temperature to working temperature and in addition the window as a whole is prestressed. Fully tempered glass should not be used since deviations of light rays and birefringence introduce too many distortions into the pictures of the bubble chamber. More details are given in a paper by Reitmayer and Deeg.[6]

## Coating

The surfaces of the lenses and windows have to be coated with an efficient antireflection coating. Two lenses and two windows with their 8 surfaces produce by double reflection $\binom{8}{2} = 28$ parasitic images. For the whole chamber this gives 84 parasites, most of them not being serious, but some are well in the chamber itself and produce ghosting on the film. They have to be suppressed by an antireflection coating which also reduces over-all losses of the light flux and the corresponding deterioration of the dark field. The combination of a double-layer coating and a narrow filter solves the problem. The main difficulties are due to the size of the windows whereas the coating of the lenses is easier.

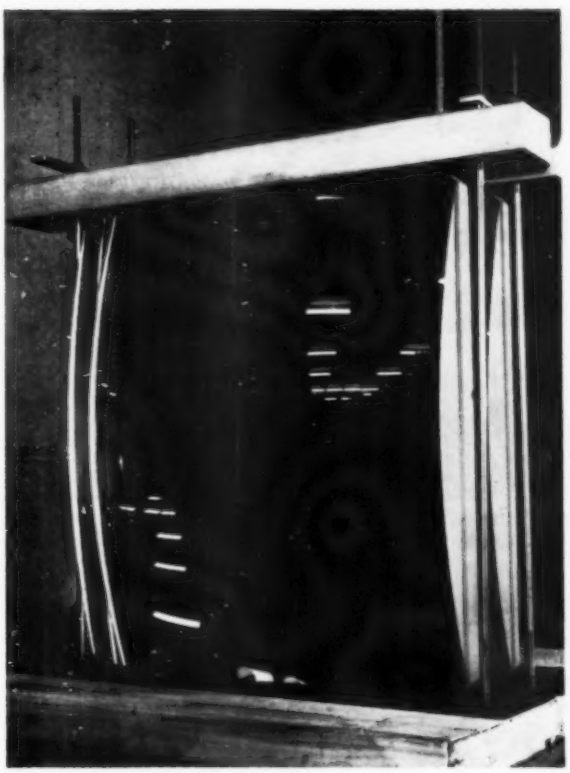

Fig. 9. View of the central condenser unit (mounting system provisional).

The coating must satisfy two requirements: it has to be uniform and hard enough to allow easy cleaning of the glass. Also stability in liquid hydrogen is important.

A procedure developed by Reichelt at Heraeus, Hanau, Germany is used. The window and 16 evaporation sources are fixed in a vacuum tank. Predetermined quantities of tantalum oxide and magnesium fluoride are completely evaporated. Repeated gentle heating and cleaning of the glass by means of an electric discharge give layers of sufficient hardness.

## References


1. C. Peyrou and H. S. Bridge, in *Proceedings of the International Conference on High-Energy Accelerators and Instrumentation*, CERN, Geneva, 1959, p. 454.
2. G. E. Davis, J. Opt. Soc. Am. **45**, 572 (1955).
3. H. C. Van de Hulst, *Light Scattering by Small Particles* (Wiley, New York, 1957).
4. First published and manufactured by F. Früngel, Optik **3**, 128 (1/2) (1948), translated and issued by technical information and library services, Ministry of Supply, T.I.L./T 4666.
5. This technique has been developed by G. Roeder, Impulsphysik Hamburg, and will be published in a separate paper.
6. F. O. Reitmayer and E. W. Deeg, Appl. Opt. **2**, 999 (1963).

S. Rosin, feature editor for this issue (left), R. Palmer *Brookhaven* and W. T. Welford *Imperial College*, all authors of papers in this issue. They are standing beside the Hough-Powell device, and one of the condensers described in the Letter on page 1050 is clearly visible at the middle left.

The 80-in. Bubble Chamber assembly, which is housed in a building contiguous to the north side of the Brookhaven Alternating Gradient Synchrotron magnet ring. Particle beams are guided from the AGS ring into the chamber, and the tracks of the resultant high energy interactions are photographed. At the lower left side of the chamber is the hydraulic ram that serves to move the assembly along its track, as necessitated by the experimental program. Above the ram, on the first platform, is the aperture at which the light source and photographic equipment is installed. On the second platform is the high-vacuum pumping system. The vacuum chamber and coils can be seen in the large rectangular opening on the facing side of the magnet structure. At the far right of the assembly is the cryogenic equipment, and below it the console for the hydraulic system.

**80-in. Bubble Chamber**

# A Flying Spot Film Measuring Machine Employing Crossed Glass Fibers

B. Palmer

Flying spot measuring machines for use on bubble chamber film were first proposed by Hough and Powell in 1960. A new machine nearing completion at Brookhaven National Laboratory employs a fixed and moving fiber to generate a 15-$\mu$ spot that will scan over an area 53 × 160 mm in 10 sec. Centers of marks on the film will be digitized to an accuracy of $\pm 5\mu$ and the coordinates fed on line into a computer for analysis.

## I. Introduction

Since the measuring machine to be described will measure bubble chamber film, it is appropriate first to say what a bubble chamber is and what sort of film it produces. The principle of operation of a bubble chamber was first proposed by Glaser.[1] A liquid is heated under pressure to a temperature above its normal boiling point. A sudden reduction of pressure brings the liquid into a superheated condition. If a charged particle, say a proton, passes rapidly through the liquid in this superheated condition, then the liquid begins to boil along the track of that particle. Stereo photographs are taken about 1 msec after the particle has passed, and the boiling appears then as a row, or track, of tiny bubbles. Figure 1 shows such a photograph where many particles have passed through the chamber and thus many tracks are seen. Each track consists of a row of dots, and each dot is the image of a tiny bubble. The tracks are curved because there is a magnetic field in the chamber which deflects the particles as they move. The higher the momentum of the particles the less they are deflected, and the less the curvature. Measurement of the curvature of a track thus gives a determination of the particle's momentum. The particle's velocity can also, although less accurately, be determined by observing the density (the number of bubbles per cm) of a track. By comparing these two determinations the particle's mass can often be found. In Fig. 1 most of the tracks are seen to pass right through the chamber. These might be tracks of beam protons accelerated by the Synchrocyclotron and deliberately brought into the chamber. In general, such beam tracks are uninteresting unless they represent a proton that interacted with the material of the liquid. In Fig. 1 one such event did occur, and one of the beam tracks is seen to fork into two tracks at different angles. The three tracks of this particular fork might be of a proton that struck a stationary proton of the liquid and bounced off it "like a billiard ball", sending the stationary proton away at a different angle. Many "events" are far more complicated than this but the principles are the same. By measuring the angles, lengths, curvatures, and densities of the tracks information is found on the properties of the particles involved. Note that the many beam tracks which pass right through the picture have no connection with the event and need not be measured.

The accuracy required in the determination of curvatures and angles is equivalent to an accuracy of coordinate determination of about $\pm 5\mu$, and advantages would be gained if the accuracy could be improved to $\pm 1\mu$. This is formidable in itself but made more so by the number of pictures to be measured. The Brookhaven National Laboratory 80-in. liquid hydrogen bubble chamber is expected to produce several million 53 × 160 mm pictures per year. Admittedly, not all of these pictures require measuring. Many pictures have no events in them, only having beam tracks. The pictures are, therefore, first projected one by one onto a table and viewers then pick out those containing events. From among the several million pictures, up to one million events per year might be found, and all these would require measurement to the accuracies mentioned.

It has already been noted that in the pictures containing events there are many beam tracks which can

The author is with Brookhaven National Laboratory, Upton, New York.

The work described in this paper was performed under the auspices of the United States Atomic Energy Commission.

Received 29 March 1963.

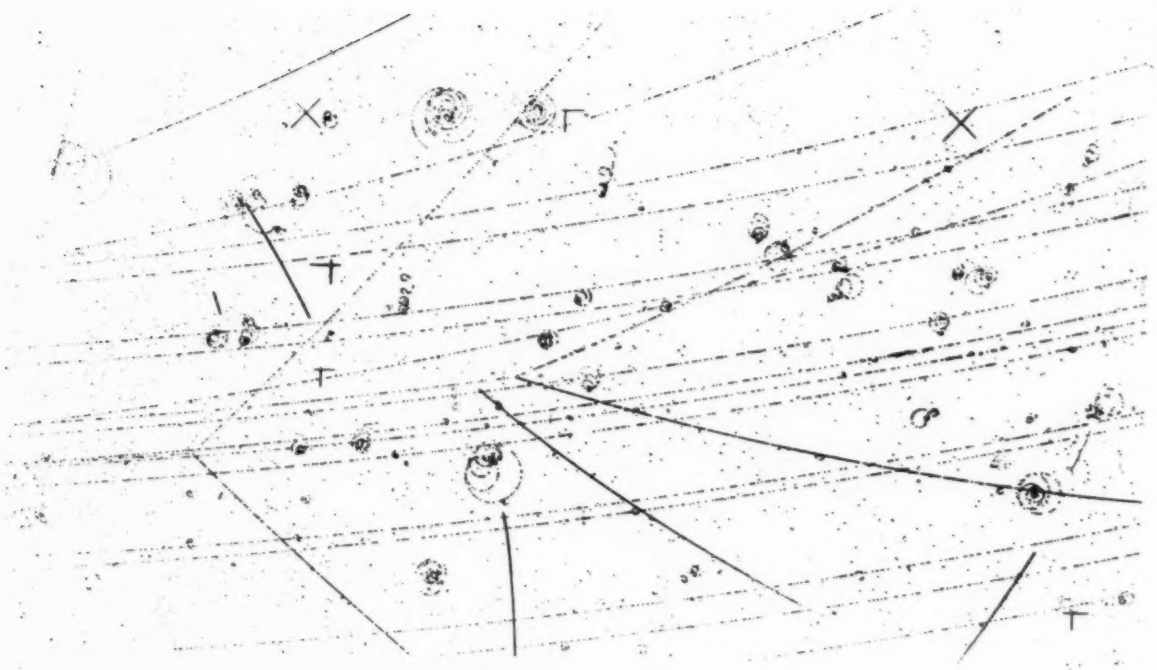

Fig. 1. Tracks in BNL 20-in. liquid hydrogen bubble chamber.

give no information. In fact, useful information is contained only in strips along the tracks of the event. When designing a measuring machine it is tempting to make use of this fact and conceive of some device that drives along the tracks of interest, measuring them as it goes, leaving unmeasured all the unwanted tracks. In the past this approach[2] has usually been followed. The steering of the device along the road is performed by a human operator, and the need for this human operator usually limits the speed of measurement. A typical "Franckenstein" measuring machine, which is of this type, takes about 5 min to measure each picture (15 min to measure a stereo triad).

Hough and Powell in 1960[3] proposed an entirely different scheme. They proposed that a spot of light should be made to scan over the entire film area with a television type raster. Behind the film a photomultiplier would detect whenever the spot passed over a bubble image, and the coordinates of each bubble would then be digitized electronically and sent on line into a large electronic computer. There in the computer the selection would be made between useful information (on the event) and useless information (on beam tracks). The selection could, in principle, be made in two ways:

(a) If programs could be developed, the patterns on the pictures would be "recognized" and only coordinates of interesting patterns, such as the fork in our photograph (Fig. 1), would be passed on to the programs that compute the required data on the event.

(b) Until such programs did exist the computer could select the useful information on the basis of what it had been "told" should be there. When the picture is viewed to determine if an event is present at all, the viewer can also take rough measurements of the event. These rough measurements can be digitized using a simple measuring device lying on the table on which the picture is projected (Fig. 2). The digitized rough coordinates of each event can then be punched onto cards, and these cards could be fed into the computer before the flying spot measuring machine (HPD) measures an event. Then when the measured coordinates start flowing from the measuring machine the computer would "know" approximately where to "look" for the event and could with relative ease find the coordinates of interest.

It may seem at first that this system would be slower than the more conventional type of machine that measures only the parts of the film of interest. It was shown, however, that with reasonably high speed electronics track centers could be located to within a few microns even when the spot of light was traveling 25 $\mu$ every microsecond. At this speed it would be possible to scan the entire 53 × 160 mm picture with 30-$\mu$ spaced scan lines in only 10 sec. It was also shown to be easily possible to feed all the coordinates obtained, and there might be over 100,000 of them, into an IBM 7090 or similar computer within the same 10 sec. This speed was a considerable advance on the 5 min needed by the conventional measur-

ing machines and made practical the measurement of the million pictures per year that are expected to become available.

The first step in demonstrating the practicability of these proposals was taken at the European Organization for Nuclear Research (CERN) with the collaboration of Brookhaven National Laboratory and Lawrence Radiation Laboratory. There, in June 1961, a prototype measuring machine (Hough-Powell Device) was operated and 30,000 coordinates of tracks on a small picture were digitized and fed into an IBM 709 computer.[4] At that time the three laboratories involved in the collaboration all started to build complete systems with the hope of measuring film usefully as soon as possible. At the time of writing all three of these systems are working mechanically and electronically, although program difficulties are still delaying the production use of the machines. At the same time that these Mark I machines were being built, the author started thinking of possible improvements in design that could be incorporated in Mark II machines. It is to one of these Mark II machines that the rest of this paper is devoted. This machine has been designed to measure film from the BNL 80-in. bubble chamber, and at the time of writing the machine is nearing completion, most of the critical parts having been run and tested. To the author's knowledge at least five other machines are to be built which will incorporate most of the basic ideas described here.

## II. The Crossed Fiber Flying Spot Generator

In the previous section we have introduced Hough and Powell's idea of scanning bubble chamber film with a fine raster, but we have said little as to how this raster is to be produced. It will be remembered that measurements are required to an accuracy of a few microns over an area 53 × 160 mm. A raster of this size is, therefore, required, in which the spot's position is always known to a few microns; also since the finest bubbles may be as small as 15-$\mu$ diam the spot should be of this order of size. Although high-resolution cathode ray tubes are rapidly improving, it is fair to say that it is not yet practicable to obtain a 15-$\mu$ spot over 53 × 160 mm. Even when the spot size requirement is relaxed, the problem of knowing the spot position to a few microns is severe, though not insuperable.[5] Hough and Powell in their prototype used a mechanical system in which a spot was moved repetitively across the film while the film was slowly moved at right angles to that line, so generating a raster. The present machine also uses this principle.

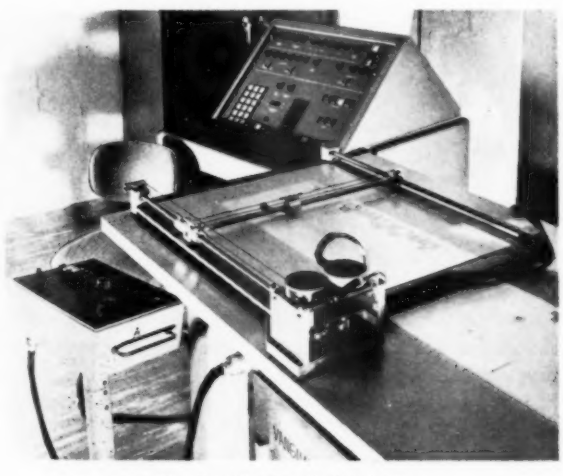

Fig. 2. The rough digitizer.

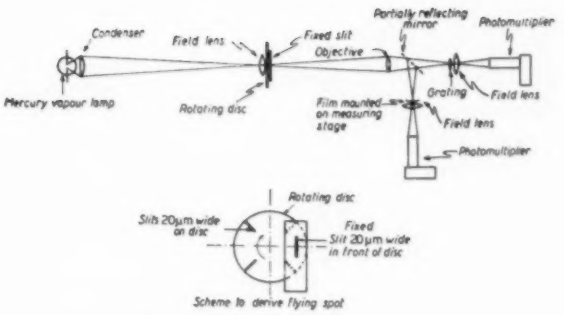


Fig. 3. The original slit system.

In the prototype a rotating disk with radial slits was placed very near to a long straight fixed slit (Fig. 3). Where a radial slit intersected the fixed slit a small "pinhole" was formed. As the disk rotated, so this pinhole moved in a straight line. When illuminated from one side the moving pinhole became a moving spot which was projected down onto the film. In order to know where the spot on the film was at any time, the beam was split and an identical spot projected onto a high-precision grating. Behind both the film and the grating there were photomultipliers, the first of which detected when the spot passes over a bubble image, and the second of which provided a scale against which the position of the spot was determined. It is this crossed slit system that provided the basis for the crossed fiber system to be described.

In either system one of the main requirements is a high flux of light in the spot on the film. In order to observe the track and grating signals from the photomultipliers the bandwidth of the circuits has to be large. At these large bandwidths the noise due to the corpuscular nature of light is far from negligible, and the ratio of signal to this noise can only be reduced by having more light flux. Before considering the crossed fiber system it will be convenient to consider the limitations on the light flux in the slit system. A similar consideration will be given later for the fiber system.

The light flux $F$ in the spot on the film is given by

$$F = A\,\Omega\,B, \tag{1}$$

where $A$ is the geometrical area of the spot on the film (assuming no lens aberration), $\Omega$ is the solid angle subtended by the projection lens stop at the film, and $B$ is the luminance of the source. Area $A$ can obviously not be increased since we require a small spot. $\Omega$ can only be increased if larger aperture lenses with the required resolution can be found. $B$, the luminance of the source, is, of course, limited by the lamps that are available. The Mark I machine at Brookhaven which uses the slit system, employs a Westinghouse BH6 (1 kW) high-pressure mercury capillary arc which has a luminance of 40,000 lumens $mm^{-2}$ $sr^{-1}$, over an area of $20 \times 1$ mm. Higher continuous luminance is, to the author's knowledge, only available from smaller mercury arc lamps. For instance, an Osram HB0 100-W lamp with an arc 0.3 mm in diameter has a luminance of over 160,000 lumens $mm^{-2}$ $sr^{-1}$. It is of interest, therefore, to calculate the minimum size of arc lamp that can be used.

Referring to Fig. 4, letting the scan length on the film be $\eta$, and letting the solid angle subtended by the objective on the film be $\Omega$; it can be seen that the fixed slit length is $\eta/M$ and the arc length $L = \eta/MM_1$, where $M$ and $M_1$ are the magnifications of the objective and condenser, respectively. Similarly, it is seen that the solid angle at the slit is $\Omega M^2$ and the solid angle at the arc lamp is $\Omega_1 = \Omega M^2 M_1^2$. In practice there is a limit to the aperture of condenser that can be used; $\Omega_1$ will thus have some maximum value $\Omega_1$ max:

$$\Omega\,(MM_1)^2 \geq \Omega_1 \text{ max}$$

thus

$$MM_1 \leq \sqrt{\Omega_1 \text{ max}/\Omega}$$

and the length of the arc

$$L = \frac{\eta}{MM_1} \geq \eta \sqrt{\frac{\Omega}{\Omega_1 \text{ max}}}, \tag{2}$$

the arc length is thus limited by the scan length $\eta$, the solid angle subtended by the objective on the film $\Omega$ and the maximum practical condenser aperture.

For a scan length $\eta = 50$ mm, and objective aperture $f/4$ and an $f/2$ condenser we get

$$\Omega = 2.2 \times 10^{-2}$$

$$\Omega_1 \text{ max} = 19.5 \times 10^{-2}$$

$$L = 50 \sqrt{\frac{2.2}{19.5}} = 17 \text{ mm}.$$

The 20-mm BH6 lamp is thus only just adequate, and smaller higher intensity arc lamps cannot be considered.

The fundamental change made to the system just described was to replace the fixed and moving slits by fixed and moving glass fibers, each about 1 mm in diameter. Although this may seem a simple change it does, in fact, generate a moving spot by a fundamentally different process which, as far as the author knows, has not been used before. As in the slit system there is a rotating disk but where there were radial slits there are now radial 1-mm diam glass fibers held in jaws such that light is stopped from passing through the disk anywhere except through the fibers. Near the disk is placed a straight tangential fiber, also with jaws to stop light passing anywhere except through the fiber. The geometry of fixed and moving fibers is exactly the same as that of the slits shown in the lower part of Fig. 3. As in the slit case, a source is placed behind the disk such that, if the disk were removed, the full length of the fixed fiber would be illuminated. Where before the intersection of a radial with the fixed slit defined a pinhole, now the intersection of a radial fiber with the fixed fiber defines an aperture in which there are two crossed glass fibers, each of which acts as a cylindrical lens. Together the two cylindrical lenses act as one spherical lens which forms an image of the source. Since the fibers are small in diameter, their focal length is also small and the image of the source they form becomes a tiny spot of light. As the disk is rotated, so this spot of light moves with the point of intersection of the fixed and moving fibers, and can be focused onto the film in just the same way that the illuminated pinhole was in the slit system.

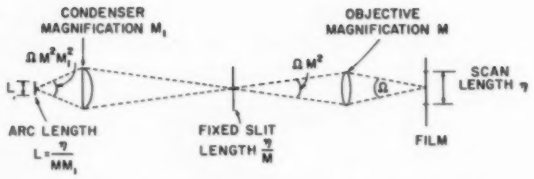


Fig. 4. Calculation of arc length for the original slit system.

Whereas the fixed and moving slits could be brought into nearly the same plane, the fixed and moving fibers, with their finite diameter, cannot possibly be brought into the same plane. The crossed fibers do not, therefore, act like a simple spherical lens. The images of the source produced by each fiber are, in fact, lines just behind each fiber (Fig. 5). These two lines, images together, when viewed from the side opposite the source, form a single astigmatic image of the source. Only if this astigmatic image is projected with a lens to which a weak cylindrical element is added will a single corrected image of the source be formed on the film (Fig. 5). When the disk is rotated it is this tiny image of the source that moves across the film; in contrast to the slit system in which it is an image of a rectangular hole that moves across the film.

The limitations on the light flux in this fiber system may now be considered. As before the flux $F$ in the

spot is given by

$$F = A\,\Omega\,B, \tag{4}$$

and once again the flux can only be increased if a lamp with higher luminance $B$ can be employed. In order to see if a higher luminance lamp can be used, the minimum size of the lamp must be calculated. Consider Fig. 6. As for the slit system if the scan length is $\eta$, the fixed fiber length is $\eta/M$, and the arc length is given by

$$L = \eta/MM_1, \tag{5}$$

where $M$ is the objective magnification and $M_1$ is the condenser magnification. The calculation of the solid angle at the lamp $\Omega_1$ is different from the slit case. For a spot source image on the film of radius $r$ the source image just behind the fibers must be

$$r_1 = r/M,$$

where $M$ is again the objective magnification. The solid angle of light $\Omega_2$ leaving the fibers is then given by

$$\Omega_2 = \frac{\pi r_1^2}{l^2},$$

where $l$ is the conjugate distance from the fiber to the source image. Since this conjugate is very small compared with the long conjugate $l'$, $l$ is approximately equal to the fiber focal length $f$. Thus,

$$\Omega_2 \approx \frac{\pi r_1^2}{f^2} = \frac{\pi r^2}{M^2 f^2},$$

and the solid angle at the source $\Omega_1$ is

$$\Omega_1 = \frac{M_1^2}{M^2}\,\frac{\pi r^2}{f^2}.$$

Setting an upper limit on this condenser aperture, $\Omega_1$ max,

$$M_1 \leq \frac{Mf}{r}\sqrt{\frac{\Omega_1 \max}{\pi}}.$$

Using expression (5) the arc length can be expressed by

$$L \geq \frac{1}{M^2 f}\,\eta r\sqrt{\frac{\pi}{\Omega_1 \max}}. \tag{6}$$

This expression is seen to differ considerably from that derived for the slit system [Eq. (2)]. In the slit system the arc length is a function only of $\Omega$, $\Omega_1$ max, and $\eta$, none of which could be varied to reduce the arc length. In the fiber case [Eq. (6)] the arc length is seen to be

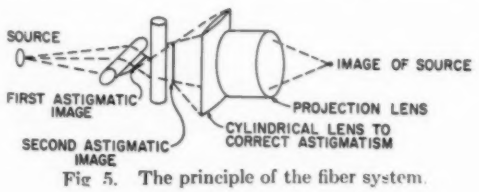


Fig. 5. The principle of the fiber system.

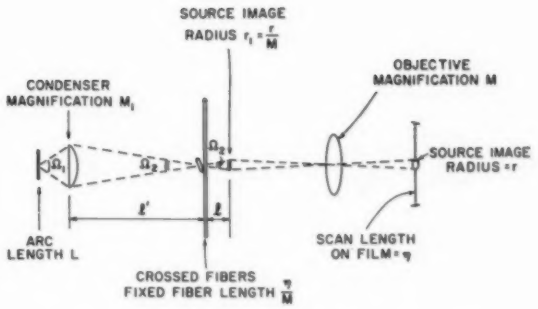


Fig. 6. Calculation of arc length for the fiber system.

a function of both $f$, the focal length of the fibers, and of $M$, the magnification of the objective. With reasonable choices of $f$ and $M$ the value of $L$ could be reduced to as little as 1.5 mm, which is to be compared with 17 mm for the slit case [Eq. (3)]. In fact it was desired to use an 0.3-mm diam source for which the gain due to the use of the fibers was not sufficient, and a "following" illumination was developed. Before describing this system, however, some of the other advantages of the fiber system will be considered:

1. Since the spot on the film is a real image of the source it is clearly easy to vary the size of the spot by placing an iris in front of the source. To change the spot size in the slit system the fixed slit and all the moving slits would have to be changed. In the fiber system it would even be possible to scan with a short line element, or other shape, simply by placing a suitable stop in front of the source.

2. Unlike the case in the slit system, a large cone of light leaves the crossed fibers, and this cone of light is not a function of the illumination system. Objectives of very large aperture could be used without changing the arc lamp, or several objectives may be set up to take light from the fiber at different angles. This was in fact done with two objectives, as will be described in Sec. III. There is, of course, a limit to the useful cone of light due to aberrations in the fibers at the wider apertures involved in large cones. Such aberrations, however, can always be made negligible by reducing the fiber diameters.

3. Because of the astigmation no single point near the fibers is conjugated with the spot image on the film. Thus no single particle of dirt near the fibers can block out the spot. This should result in much greater constancy in the intensity of the flying spot compared with the slit case in which a single piece of dirt in one of the slits can completely cut off the light. There is similarly no problem with ragged edges and nonconstancy of width of a fine slit. It is relatively easy to obtain fibers whose diameters are constant to a fraction of a percent, whereas the problem of making a 20-$\mu$ slit with such constancy of width would be almost

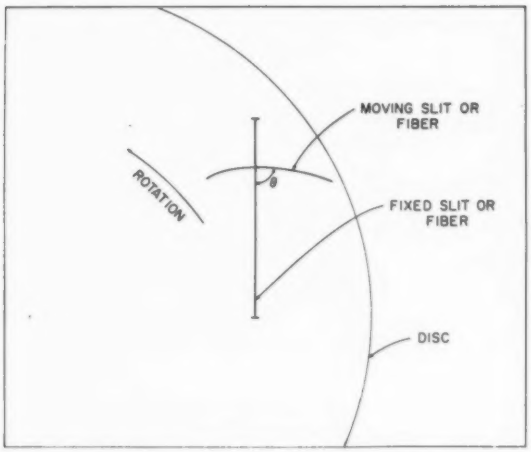


Fig. 7. Involute fiber to give constant spot velocity.

insurmountable. In principle, it is felt that the fiber system could be used in photometric applications where slits are inapplicable.

4. The moving fibers can be curved without affecting their constancy of diameter or focusing properties. Why is it desirable to curve the slits of fibers? If straight radial slits or fibers are used, the spot of light generated does not move with a constant velocity. Although in view of the use of the grating scale, this may not seem of consequence yet, if interpolation is to be done between the lines of the grating scale, fairly constant velocity is desirable. If the slits or fibers are curved into suitable involutes and the fixed fiber is offset (see Fig. 7), then not only is a constant velocity of spot achieved, but it is seen that at the intersection the fixed and moving fibers are always perpendicular—a condition necessary if full correction of the astigmation is required. The fibers can easily be curved by allowing them to sag in an oven into a machined former of the required shape. Any fine irregularities in the former are not imparted to the fiber.

5. It is easy to obtain a very straight fixed fiber, much easier than it is to obtain a very straight slit. When a 1-mm diam hand-drawn fiber is held under a tension of 2 kg it is found to be straight within a fraction of a micron. With time it is expected that the fiber will flow enough that it will become even straighter, although the measurement of the effect will become difficult.

This basic moving spot generator consisting of a disk with radial or curved fibers moving near a fixed fiber held under tension should find application in other fields besides our own. The latter part of this paper will be devoted to other details of the present design which may be of interest but which should not be considered necessary parts of a crossed fiber spot generator.

## III. Details of the Mark II Flying Spot Digitizer

In the last section the principle of a crossed fiber flying spot generator has been described. Details will now be given of one particular measuring machine which uses this idea. At the time of writing some parts of the machine have not been completed, but the flying spot generator itself has been successfully tested.

The specification for the machine has been given in earlier sections of the paper and may be summarized as follows:

| | |
|---|---|
| Spot size | 15 $\mu$ |
| Spot intensity | As high as possible |
| Least count on position of spot | 1.6 $\mu$ |
| Length of scan | 53 mm |
| Speed of scan | Approx. 25 $\mu$/$\mu$sec. |

Perhaps the most critical component in the machine is the objective that projects the generated flying spot onto the film. No suitable commercial objective was found[6] that was capable of producing the required 15-$\mu$ spot over a 53-mm field, and it was necessary to have a special lens designed for the purpose. Consider what magnification should be chosen. For maximum spot intensity the numerical aperture on the exit side of the objective $\Omega$ should be as large as possible. For a given aperture of the objective the larger the demagnification, the larger is this numerical aperture on the exit side, although little is gained by a demagnification

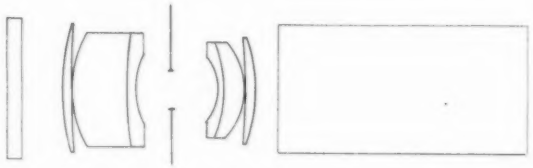

Fig. 8. The objective designed by C. Wynne.

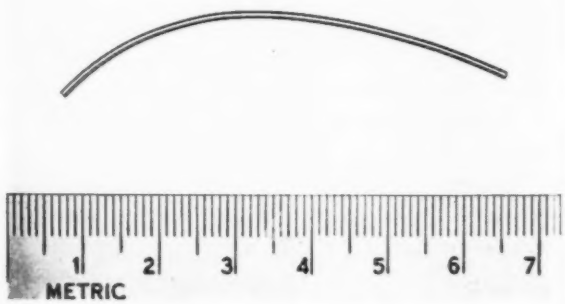


Fig. 9. A curved moving fiber.

greater than 2. The entrance field (length of fixed fiber) was in fact chosen to be 100 mm, giving a demagnification of 1.89. The design of a special lens was undertaken by Wynne of Imperial College, London. After an initial design of a six-element lens using third-order theory, the parameters were optimized using a powerful computer program.[7] The lens has a focal length of 91.5 mm, an aperture of $f/4$, and is corrected for two of the strongest lines of the mercury spectrum: 436 and 546 m$\mu$. The lens was designed for use with 6 mm of glass in the long conjugate and a large block of glass (83.3 mm) in the short conjugate. The original reason for the large block was to increase the physical path length between the lens and film; in fact it also

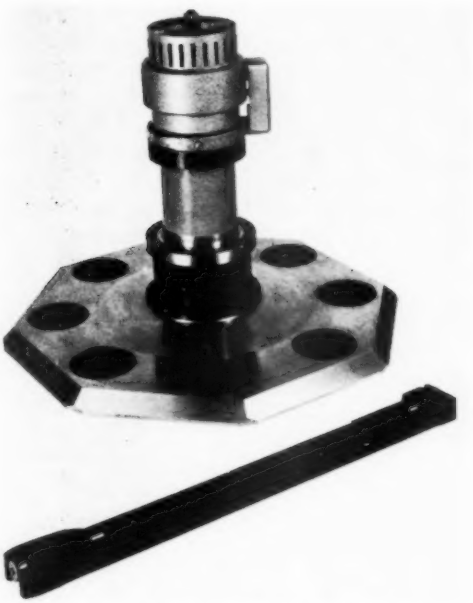

Fig. 10. The disk and fixed fiber mount.

made possible a higher lens performance. A cross section of the lens is shown in Fig. 8. A typical lens gives a modulation of 0.65 of a 40 lines/mm sinusoidal grating over the entire field. This is roughly equivalent to an image less than 8-$\mu$ diameter at half-height. The lens is clearly well capable of providing the 15-$\mu$ spot required.

Consider now the disk and fixed fiber which will generate the flying spot. For a scan length of 53 mm and a demagnification of 1.89 the fixed fiber is 100 mm long. Eight moving fibers were used in the disk in order that the involute curves of the fibers be not too strong. This fixed the diameter of the disk at approximately 40 cm. A spot speed of 25 $\mu$/$\mu$sec required one scan in 2 msec, one revolution of 8 fibers in 16 msec, or approxi-

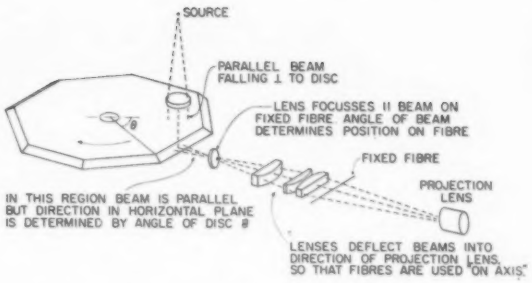
SOURCE
PARALLEL BEAM FALLING ⊥ TO DISC
LENS FOCUSSES II BEAM ON FIXED FIBRE ANGLE OF BEAM DETERMINES POSITION ON FIBRE
FIXED FIBRE
PROJECTION LENS
IN THIS REGION BEAM IS PARALLEL BUT DIRECTION IN HORIZONTAL PLANE IS DETERMINED BY ANGLE OF DISC θ
LENSES DEFLECT BEAMS INTO DIRECTION OF PROJECTION LENS SO THAT FIBRES ARE USED ON AXIS

Fig. 11. The principle of the following illumination.

mately 3600 rpm. 3600* rpm was chosen as being a convenient speed to obtain with a synchronous motor. The moving fibers were mounted near to the lower face of the disk, clamped between two curved jaws. One of the curved moving fibers is shown in Fig. 9. In Fig. 10 is shown the disk, on the upper face of which can be seen the eight plugs in which the moving fibers are mounted. The disk is seen mounted in its bearing with a synchronous motor above.

Also, in Fig. 10, eight 45° mirrored surfaces will be seen around the periphery of the disk. These surfaces form part of the illumination system that will bring light down onto the crossed fibers from above. In a straightforward system the source lamp would be placed above the disk with a condenser immediately in front of it. It will be remembered that one of the advantages given of the crossed-fiber system was that it enabled a smaller, and, in general, brighter, source to be used. In practice, however, the only suitable lamp available with higher luminance than the 20-mm Westinghouse BH6 lamp (40,000 lumens/mm$^2$) is the Osram HBO 100-W (over 160,000 lumens/mm$^2$) mercury arc.† This Osram lamp has an arc only 0.3 mm long, and the crossed fiber system alone did not allow its use. However, the gain of light flux of 4 was considered of sufficient importance to consider some other way to enable the use of the Osram lamp. A system was, therefore, designed that, instead of illuminating the whole fixed fiber at any one time, would illuminate a small region that followed the point of intersection of the fixed and moving fibers. The method is illustrated in Fig. 11. The light from the source is focused into a parallel beam which falls on to 45° mirrored faces on a disk. The angle of the parallel light reflected off the disk moves with the angle of the disk. The parallel light leaving the disk is focused by a fixed lens to a point on the fixed fiber and as the disk rotates so this point moves along the fixed fiber. Field lenses are

* It is also possible to spin the disk at 7200 rpm doubling the rate of measurement.

† Similar lamps are also available from Pek Labs Inc., Palo Alto, California.

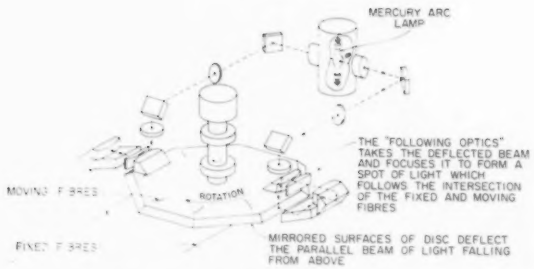
MERCURY ARC LAMP
THE "FOLLOWING OPTICS" TAKES THE DEFLECTED BEAM AND FOCUSES IT TO FORM A SPOT OF LIGHT WHICH FOLLOWS THE INTERSECTION OF THE FIXED AND MOVING FIBRES
MOVING FIBRES
ROTATION
FIXED FIBRES
MIRRORED SURFACES OF DISC DEFLECT THE PARALLEL BEAM OF LIGHT FALLING FROM ABOVE

Fig. 12. The illumination system.

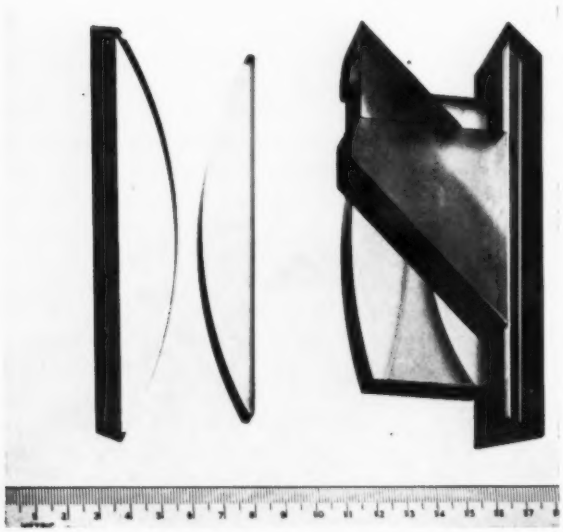

Fig. 13. The following optics.

inserted before the fiber performing two functions. Firstly, they focus the light so that it is heading for the projection lens. In this way the fibers are used "on axis". Secondly, these field lenses are designed to provide a constant velocity of movement of the spot given constant angular velocity of the disk. Since the intersection of the fixed and involute moving fibers also moves with constant velocity it only remains to synchronize the rotation of the mirrored disk with that holding the moving fibers. A simple way of obtaining this synchronization is to make the two disks into one and the same disk. This was, in fact, done and thus it is that these mirror faces were seen on the disk in Fig. 10. After the light is reflected from the 45° mirrored faces it is bent round by reflection in a number of prisms and brought down again onto the disk in the correct position to follow the fiber intersections. Figure 12 shows these prisms together with the arc lamp and condenser system. It is seen here that there are two identical following illumination systems placed on either side of the disk, each taking light from opposite sides of the same arc lamp. The reason for this will be given later. The arc lamp is placed some distance from the disk to keep its heat away. Light is brought through a chain of lenses and finally brought down onto the disk as a parallel beam. After reflection from the mirror faces it enters the complex of prisms and lenses that bring the light round and down onto the fibers. Figure 13 shows the prisms and lenses used in the following illumination. They are seen in this photograph as though viewed from below.

Using the 0.3-mm diam Osram arc and an $f/0.7$ condenser, an area 2 mm in diameter is illuminated around the intersection of the fibers. At the present time this illuminated area follows the intersection of the fibers to within 0.5 mm and provides a spot of light whose intensity remains constant to within ±15%. It is hoped that this will be improved. Some difficulty was experienced using the $f/0.7$ condenser due to aberration introduced by the bulb of the Osram lamp. This aberration turned out to be primarily astigmatism and was corrected by a simple cylindrical element.

Figure 14 shows the disk mounted in its vacuum tank together with the fixed fiber and following optics. Light enters the port holes to the left and right of the synchronous motor. Underneath the tank there are, of course, two more windows through which the flying spot may be viewed.

It is now necessary to explain the reason for there being two complete illumination systems. Consider the sort of picture that is to be measured (Fig. 1). In the main it contains tracks that lie along the longer dimension of the picture. A spot flying across the short dimension of the picture will usually intersect each track at a reasonably large angle so that little difficulty should be experienced in sorting out the information. Occasionally, however, there is in a picture a "steep" track nearly perpendicular to the long dimension and thus nearly parallel with the flying spot. As the spot runs down such a steep track, a confusing signal will be received on the photomultiplier and it will

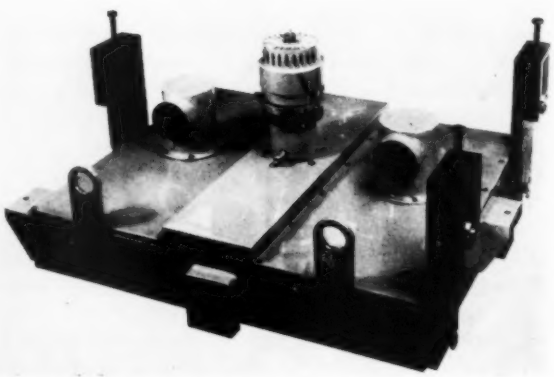

Fig. 14. The vacuum tank containing the disk and following optics.

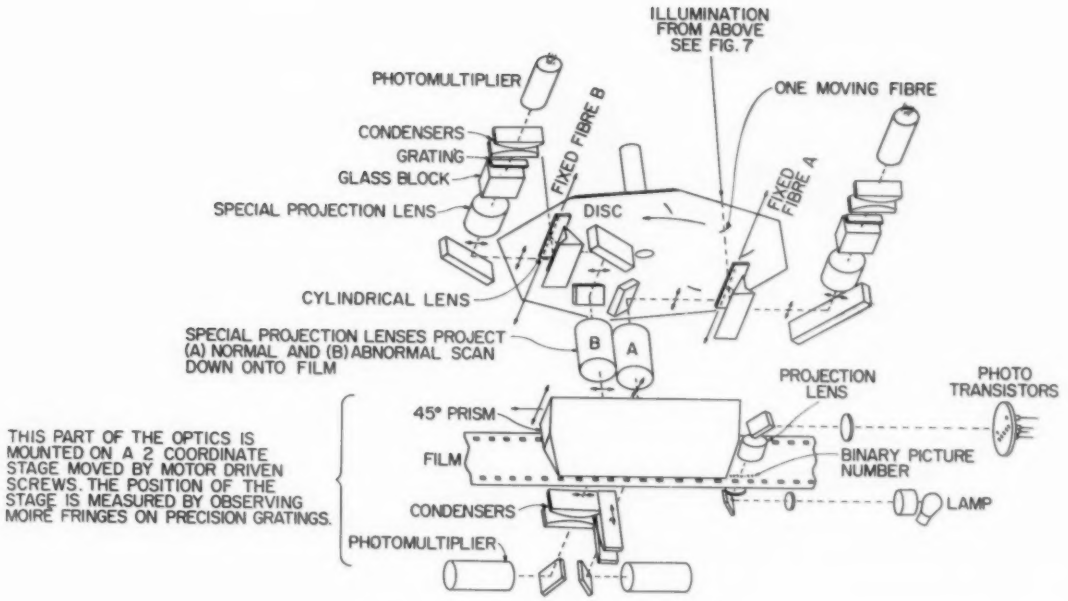


Fig. 15. The optical system below the disk.

be difficult to obtain useful information on the track. For this reason an abnormal mode of operation of the machine is provided. In this abnormal mode a spot is used which flies along the long dimension of the film, while the stage moves the film slowly along its short dimension. In this mode the spot intersects the steep track at a large angle and no trouble is experienced. In practice the normal and abnormal mode flying spots are brought down onto the film at all times and are viewed by two different photomultipliers, the signal from either of which may be used as required. The two illumination systems and spot generators are used to provide these normal and abnormal flying spots. Figure 15 shows how the light from the two parallel flying spot generators is reflected in mirrors and brought down through two objectives to form the two scans on the film. The arrangement is complicated by the film being on edge to ease certain film transport problems. Just before the film is a large prism which reflects the light from above onto the film surface. After the film are field lenses and finally the two photomultipliers.

In the upper part of Fig. 15 are also seen the grating channels where spots identical to those in the normal and abnormal scans are projected onto two precision gratings. From the signals on the photomultipliers placed behind these gratings the positions of the spots on the film are known. In the Mark I machines the identical scan on the grating was obtained by splitting the light beam on its way between the spot generator and the film. When crossed fibers are used it is no longer necessary to split the beam and lose half the light. As was stated above, the cone of light leaving the fibers is large, and more than one objective can be placed in the cone. In the Mark II design two objectives are placed with their axes perpendicular to the fixed fiber (Fig. 16). Each objective projects an identical moving spot onto the film and grating, and no light splitter is used. The two objectives are not,

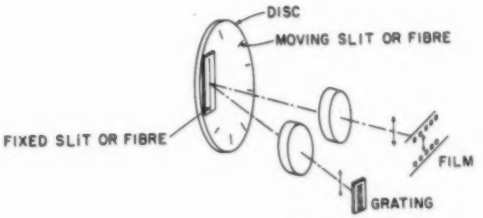


Fig. 16. Elimination of light splitter.

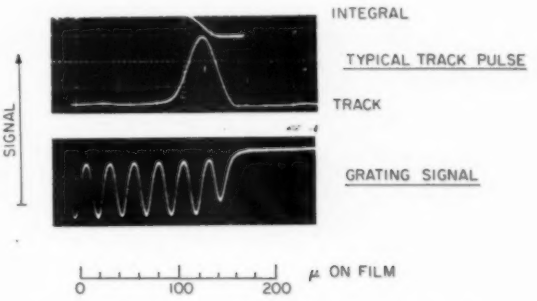


Fig. 17. Track and grating photomultiplier signals.

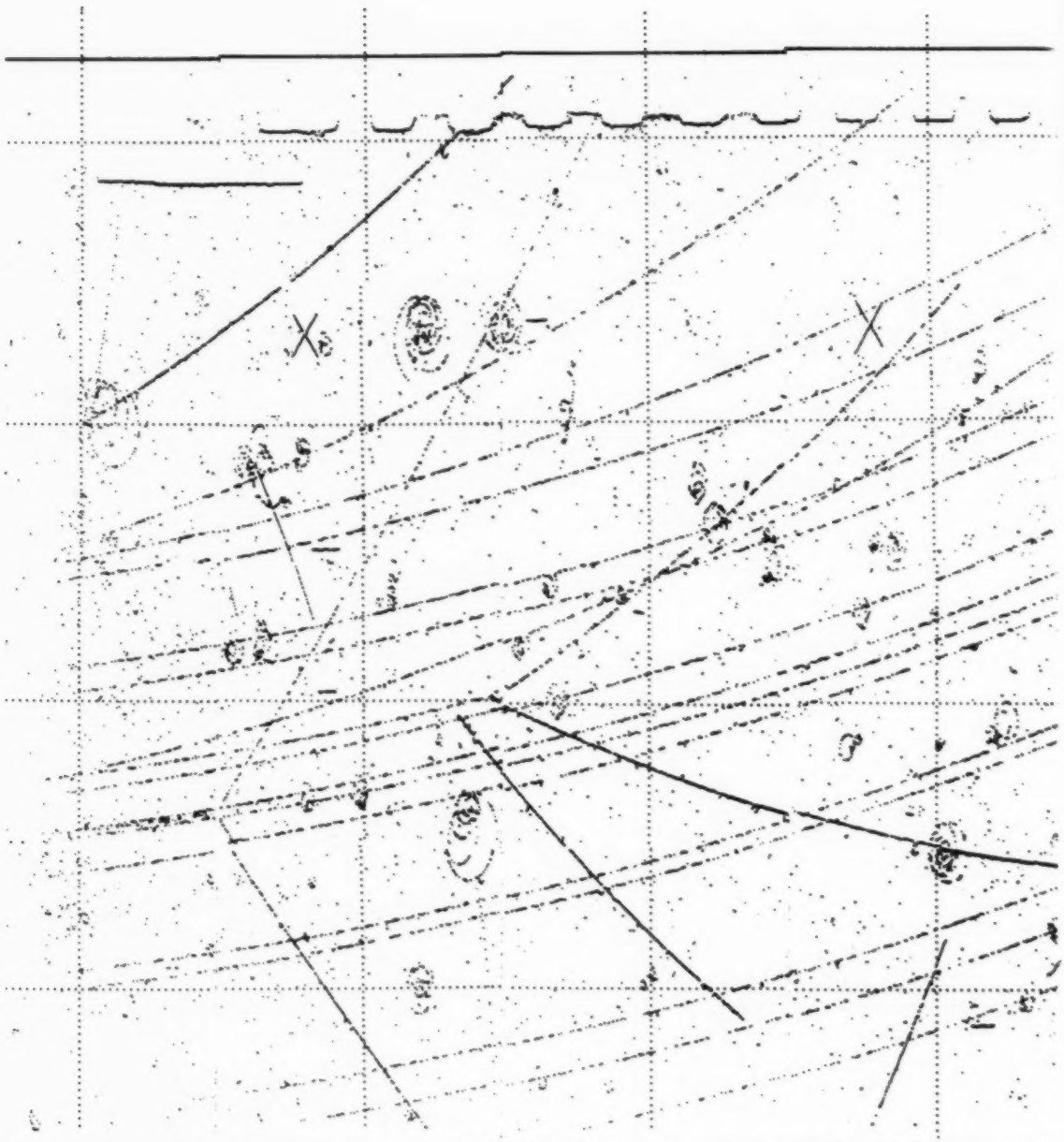

Fig. 18. Plot of all individual measurements made on a 20-in. bubble chamber photograph using the Mark I flying spot measuring machine (HPD).

of course, physically placed one beside the other as in Fig. 16; mirrors are used to place the image positions of the two lenses, one straight in front of the fibers, and the other at 7.5° to one side.

The grating used* has 1000 black lines per inch printed photographically on it. The widths of the black lines and the spaces between them are approximately equal and the edges between them are very sharp. The precision is of the order of 1 $\mu$. A signal seen on a grating photomultiplier is shown in the lower half of Fig. 17 with a track signal above. (These signals were obtained with a mock up of the final system.) The grating signal is used to generate a grating pulse at every cycle, corresponding to every 25.4 $\mu$. In order to obtain the specified least count of 1.6 $\mu$ 15 interpolation pulses are, in effect, inserted between each grating pulse, using a clock.[8] Since the spot speed is certainly constant

* Provided by the National Physical Laboratory, England.

to ±1% the use of a clock introduces negligible error. A track center pulse is obtained using an integration method[8] and is then compared with a count of the interpolated grating pulses. This count is then transmitted to the computer via a buffer memory and represents the coordinate of the bubble along the scan line. The coordinate of the scan line in the orthogonal direction is obtained by reading the position of the stage using moiré fringes. This coordinate is only transmitted to the computer every scan line.

In the course of scanning an entire picture about 10,000 coordinates of bubbles may be transmitted to the computer. As a demonstration all these coordinates may be plotted on a cathode ray tube and the resultant "picture" of the original photograph viewed. Since the Mark II machine is not yet running, it is not possible to show such a picture. It may still be of interest, however, to include a photograph of the plotted

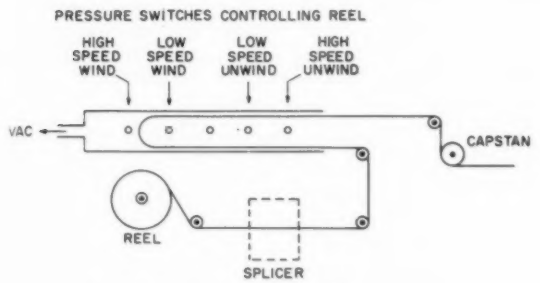


Fig. 19. One-half of the film transport.

points measured with the Mark I flying spot digitizer (HPD). Figure 18 shows this plot and it will be seen to be of the same photograph shown in Fig. 1. With care it will be found that even the specks of dust are faithfully digitized, fed to the computer, and plotted on the cathode ray tube in their correct positions.

One last feature of the final machine needs to be mentioned. It will only take 10 sec to measure one bubble chamber picture, but this speed is of no use unless the time to wind the film into place and stop it is short compared with the 10 sec. In order to ensure that this is the case, an automatic picture number readout and a fast film transport are used. A digital representation of the picture number, such as that seen at the top of Fig. 1, is projected from the film onto a pattern of phototransistors which read the number serially as the film moves. The projection system used will have been noticed in Fig. 15. The film transport* will move film at 6 m/sec and stop it in 20 cm. Since it is not possible to stop the 1000-ft reels of film fast enough to allow such a rapid deceleration, loops of film are formed between the drive capstans and the reels. These loops

* Based on a design by the Bureau of Census, Washington, D.C.

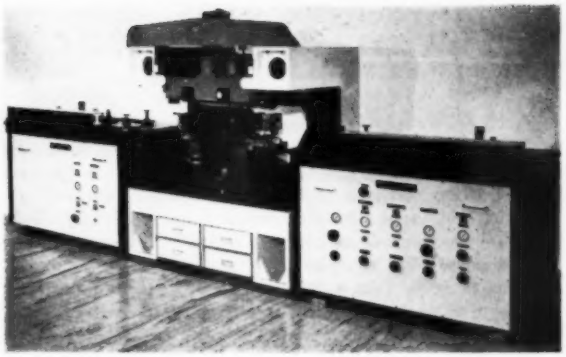

Fig. 20. The complete flying spot measuring machine.

are held in vacuum boxes and the length of film in the boxes is used to servo-drive the reels. One-half of this system (similar to an IBM tape transport) is illustrated in Fig. 19. The splicer is inserted to avoid having to rethread film through the machine every time a new reel is put on.

Figure 20 shows the complete machine which stands 1.5 m high 5.2 m long. On either end are the film transport tables, while in the center can be seen the stage, over which the disk box is held by a heavy cantilevered support.

It should be stressed in closing that a project of this magnitude involves the participation of many people. The original ideas for this flying spot digitizer are due to Paul Hough and Brian Powell in CERN, Geneva. The design and construction of the Mark II has involved the work of P. V. C. Hough, J. Rosenblum, C. L. Goodzeit, and S. C. Mo, while the computer programs are being written by a collaboration involving CERN; Lawrence Radiation Laboratory, California; and Brookhaven. The author's contribution is the concept of the crossed fiber spot generator.

## References

1. D. A. Glaser, Phys. Rev. **87**, 665 (1952).
2. Y. Goldschmidt-Clermont, *International Conference on High-Energy Accelerators* (CERN, Geneva, 1959).
3. P. V. C. Hough and B. W. Powell, Nuovo Cimento **18** 1184 (1960).
4. M. Benot *et al.*, *An Analysis of Results From The Prototype HPD* (CERN Yellow Report 61-31, Geneva, 1961).
5. T. Lingjaerde, *PEPR Precision Encoding Servo System* (M.I.T. PEPR Engineering Report No. 2, Cambridge, Mass., 1963).
6. R. B. Palmer, *Lenses for Flying Spot Measuring Devices* (CERN Internal Report DD/IEP/61/33, Geneva, 1961).
7. C. G. Wynne, Proc. Phys. Soc. (London) **74**, 316 (1959).
8. T. Lingjaerde, *The HPD Logic* (CERN Yellow Report 62-10, Geneva, 1962).

# From the Editor

Twice a year, at the meetings of the Optical Society of America, we gather together for lunch and two or three hours of discussion the Feature Editors, Reporters, Patents Panelists, and columnists of *Applied Optics* to discuss our progress and problems. One item on each agenda is the selection of feature topics for future issues. We have also extended standing invitations to all of you to write your suggestions to us. However, we must confess that we were a little surprised when we received a letter from Seymour Rosin suggesting that we feature Bubble Chamber Optics. Your Editor, who prior to functioning on this journal had remained immersed in the rather specialized field of the infrared transmission of the atmosphere, was not quite sure what a bubble chamber was, let alone its optics. After a kind friend had brought us up to date on the happenings in nuclear physics over the past ten years or so, we put the suggestion on the agenda of our next meeting. Dr. Rosin attended the meeting, gave us a short description of the various bubble chambers now in operation or construction all over the world, and agreed to serve as Feature Editor. Let that serve as a word of caution to the rest of you; if your suggestion is taken seriously you are very likely to be asked to work. Dr. Rosin went to work with a will, and not only persuaded W. T. Welford to write the major review paper but also enlisted the help of Dr. Welford in stimulating and reading other pertinent papers. When we had first agreed on this topic your Editor had had the secret hope that perhaps such a specialized topic would result in a smaller feature section, leaving a little more room in the journal for the mountain of backlogged contributed papers. But alas this was not to be: we are beginning to suspect that there is no topic so specialized that it could not fill an issue. A few months after we had chosen this topic we attended a lecture on Strange Particles by Edwin McMillan where it became abundantly clear how essential the bubble chamber as an optical tool is to the exploration of this field of physics. (In fact we have a vague private apprehension that perhaps some of the stranger particles are really internal reflections in the apparatus.) We are grateful to Dr. Rosin, Dr. Welford, and all of the others who have contributed to this issue.

Let us turn again to our Complaint Department, which we have been neglecting lately. "I have always been somewhat lukewarm toward the idea of publishing survey papers such as Optics in . . . in this type of a journal. Such articles are certainly devoid of lasting interest, and do nothing to advance the state-of-the-art. A periodical such as *Physics Today*, or something having more the characteristics of a newspaper would seem a more appropriate place for this kind of article." "Can I make a suggestion about your review articles, a suggestion which stems from the one on Optics in Great Britain? Such articles are always better if they are by one person because that person usually makes a great effort to obtain a fair balance. If there is more than one person it is difficult for them to know how to share the remaining topics outside their own work. For example, in this particular case, work on photographic objectives received very little attention nor did fibre optics. I know all three of the authors, and admire them and their work greatly. My criticism is merely concerning their working as a 'troika'." In our third issue last year, which featured "International Optics" we had quite a number of these survey papers. This was intended to give our audience a feeling for the magnitude and diversity of the optical activities in other countries. Many people have said they found these useful, and from time to time we hope to include some additional articles of this sort, particularly for those countries which we missed in that issue. We are not yet persuaded that a single author gives a more uniform coverage of optics than a team. This is because no two people have quite the same concept of what is optics, and particularly applied optics. Most of the single authors of these surveys made a good summary of optics *per se*, but the coverage of such topics as astrophysics, physical meteorology, and atomic and molecular spectroscopy was rather spotty, even though many of our authors and our readers consider themselves as belonging in these fields. One must remember, however, that most of these authors had already submitted their manuscripts before the first issue of our journal appeared, so that our "character" was not yet established.

One or two of you have disapproved of our historical articles, with the same arguments as those above: they do not contribute to the state-of-the-art, they use up space that could be used for contributed papers. It is true that we have a large backlog of papers at the moment, and we are exploring ways to reduce this, but the saving that would have been gained by omitting the two or three historical articles that we have had would be practically imperceptible. An occasional paper of this sort helps maintain our character just as much as do our various departments. While we will cheerfully agree that scientists should face forward most of the time, we need from time to time to have our field put into perspective, and articles of this sort help to do that. Science is much more than the mathematical representation of physical reality; it is another aspect of man groping, and most of us need to be reminded of this.

JOHN N. HOWARD

*photo D. L. MacAdam*

Archie Mahan *Applied Physics Laboratories*, Rudolph Kingslake *Eastman Kodak*, and David Richardson *Bausch & Lomb*

# Bubble Chamber Windows

W. T. Welford

Methods of specification and testing of large windows for bubble chambers are described.

## I. Introduction

Windows for large bubble chambers represent a large capital investment by reason of their size and the amount of work which has to be put into the optical polishing. It is, therefore, desirable to consider carefully the optical specification of such a window to ensure that the result is adequate for the job for which it is intended but that unnecessary expense is not incurred. In this paper we discuss the considerations leading to the specification and methods of testing the windows of the British National Hydrogen Bubble Chamber (BNHBC). We consider in turn the choice of window thickness and type of optical glass, the annealing specification, optical homogeneity, surface flatness, parallelism, and quality of polish.

In drafting such a specification one is hampered in England by the lack of a British Standard specification for optical finishes, such as the German D.I.N. 3140, "Optikteile"; however, even that is not of much use as a guide, partly because it is intended chiefly for use with small instrument optics, and partly because in England it is frequently the case that tolerances for special jobs are settled by friendly discussion on the shop floor on the basis of what looks reasonable. The present author drafted his own "Optical Finish Code" to help in such cases and to simplify the detailing of drawings of optical parts; this is reproduced in this paper (Table II).

## II. Choice of Window Thickness and Glass Type

The working aperture of the BNHBC has the dimensions shown in Fig. 1 in dashed line outline; the solid line represents the actual size of the glass, the extra being to allow clamping. The glass is held by a soft indium gasket on one face and another indium gasket on an inflatable tube of stainless steel[1] on the other face; for the purposes of stress calculations it might be assumed that the edge of the glass is "simply supported," rather than "clamped." The pressure difference between the faces is about 7 atm when the chamber is in operation. It is usually assumed that a tensile stress of about 1000 lb/in.$^2$ may be tolerated in nontempered glass with a small probability (ca. 1 %) of failure (private communication from R. W. Douglas, confirmed by several other sources).

*Machinery's Handbook* (1927 edition) gives for the thickness $t$ of a rectangular plate simply supported at the edges the formula

$$t = 0.75 \left\{ \frac{WLl}{S(L^2 + l^2)} \right\}^{1/2},$$

where $W$ is the total distributed load in pounds, $L$ and $l$ are the dimensions of the rectangle in inches, and $S$ is the permitted stress. S. Timoshenko (*Theory of Plates and Shells*, 1940) gives an approximate formula which for plates of 1:3 aspect ratio is equivalent to

$$t = 0.85 \left( \frac{Wl}{SL} \right)^{1/2}.$$

Taking due account of the variability of these formulas and of the uncertainty about whether the glass is strictly "simply supported," the thickness was finally taken as 16 cm. It is not possible, of course, to determine this very precisely because the intrinsic ultimate strength of glass is much higher, as is confirmed by experiments on fibers and other forms of unworked, fire-polished glass, but failure in worked glass is considered to occur at undetectable flaws. However, it is generally agreed that the strength of glass increases at very low temperatures and also the slight stress remaining after the best annealing is of such a sign as to toughen the glass, so that we have some extra factors in hand. (In fact the windows for the BNHBC were eventually made only 155-mm thick and they have not burst under running conditions.)

The choice of glass type was made after considerable

The author is with the Physics Department, Imperial College, London, S.W. 7, England.

Received 8 April 1963.

discussion with H. Rauch and F. Reitmayer of Jenaer Glaswerk Schott und Genossen, Mainz, West Germany. The only purely optical requirement is that the glass should be transparent to the blue end of the spectrum, so dense flints would not have been suitable. Considerations of homogeneity, freedom from bubbles and stones, chemical stability and frequency of melting pointed to BK7, a borosilicate crown with $n_d = 1.5168$ and $V = 64.2$ as most suitable. This has also the advantage of being one of the cheapest optical glasses. At one stage we considered using a zinc crown, which has a low thermal expansion coefficient, but this compares unfavorably with BK7 in all the respects mentioned above.*

## III. Optical Tolerances

In order to arrive at the rest of the specification we need optical tolerances on the performance of the window. The image-forming pencils collected by the camera lenses are very small in diameter and they have very small convergence angles; the convergence angle is about 0.002 rad and the maximum diameter of a pencil is about 1 mm. Thus the principal effect of errors in the window is a local distortion and we can state a basic tolerance in the form of the maximum deviation permissible for any ray. We take the maximum permissible displacement of a bubble as $\pm 10\,\mu$ in any direction†; then since the chamber is 450-mm deep in the direction of the camera axes the maximum deviation is $\pm 5$ sec of arc, in round numbers.

We use this deviation tolerance to set tolerances for double refraction, inhomogeneity, etc.

## IV. Annealing

The importance of good annealing is twofold: it reduces stress-birefringence and it makes the refractive index uniform throughout the glass by the normalizing effect of heat-soaking at the annealing temperature.

We can obtain one order-of-magnitude estimate of the importance of stress-birefringence by assuming as an approximation that the stress is homogeneous over a reasonable volume of the window, so that the glass behaves as a uniaxial crystal. Let the axis be parallel to the window surfaces, so that in a direction normal to the window surfaces there will be a difference in optical path between the two polarizations corresponding to, say, $\delta n$ in refractive index. Let $t$ be the thickness of the window. Then if the principal ray is incident at an angle $\phi$ (in vacuum) the images formed by the two polarizations will have a lateral displacement of

$$(\delta n/n^2)t\phi.$$

The extreme field angle is about 30° so that the maximum displacement is about $40(\delta n)$ mm, since $t = 160$ mm; putting this equal to 0.01 mm, the displacement tolerance mentioned in Sec. III, we find $\delta n = 0.00025$, corresponding to a stress-birefringence of 2500 m$\mu$/cm. This is an absurdly high figure and would not be approached in any piece of optical glass, however badly annealed.

A second consideration is that of rate of change of birefringence along the window. A rate of change of refractive index $dn/dx$, where $x$ is a coordinate parallel to the window surface, gives a deviation of a normally incident ray of

$$t\left(\frac{dn}{dx}\right).$$

Setting this equal to the deviation tolerance (Sec. III) of $2.5 \times 10^{-5}$ we obtain

$$\frac{dn}{dx} = 1.5 \times 10^{-7}/\text{mm},$$

or, a birefringence change of 15 m$\mu$/cm for each centimeter run along the surface. In fact, stress-birefringence varies three-dimensionally and it is impossible to compute in detail the effect on an image; H. Courtney (private communication) found that an image doubling amounting to about 50 sec of arc occurred at one place in a 16 cm thick partly tempered window when the principal ray was incident at 30°.

A third, quite different approach is to note that, as mentioned at the beginning of this section, the normalizing or heat-soaking process is essential for making the refractive index uniform throughout a glass blank[2,3] and low stress-birefringence is certainly a necessary indication that this process has occurred, although it is perhaps not a sufficient indication. The smallest value of stress-birefringence which it is reasonable to ask for depends on the size of the blank; values ranging from 5–25 m$\mu$/cm have been suggested for fine annealed glass[2,3] and we took 25 m$\mu$/cm.

The tolerance on rate of change of refractive index derived above ($dn/dx \leqslant 1.5 \times 10^{-7}$/mm) also applies, of course, to actual changes in refractive index due to inadequate heat-soaking, irrespective of whether there is birefringence, and thus it is reasonable to take the view that stress-birefringence should be as low as possible to ensure that refractive gradients of this kind are made as small as possible. Thus we arrive at the conclusion that stress-birefringence is not of itself harmful but it should be minimal as an indication of good normalizing.

In fact, it is extremely difficult to detect slow refractive index gradients in a blank in a state of inspection polish; it can only be done by a laborious procedure based on the deviation testing process as described in

* More recently a new glass, K50, with $n_d = 1.5226$, $V = 60.2$, has been recommended by Schott.

† This is probably too tight a tolerance by comparison with particle scattering effects in the liquid but it is better to have the optics appreciably better than is really necessary.

Sec. VIII. In practice we have found that the manufacturers' warranty is reliable, as is confirmed by tests as in Sec. VIII.

Thus the window blank was finally specified to have stress-birefringence not exceeding 25 mμ/cm, the residual stress being smoothly distributed and in such a manner that the outer layers are in compression. Also the annealing was to be such that refractive index gradients would not be large enough to cause ray deviations exceeding 5 sec if the surfaces were polished plane and parallel; this corresponds to a refractive index gradient of $1.5 \times 10^{-7}$ per mm in a direction parallel to the surface, if this gradient is uniform through the 160 mm depth of the window.

## V. Veins and Other Defects in the Casting

As mentioned in Sec. II the choice of BK7 was suggested mainly because it was likely to be easiest to pour with few defects. Table I gives a comparison of some properties of BK7 and K50, the new Schott glass, taken from catalog material. It has been stated by Schott engineers (private communication) that K50 is rather easier to cast without veins than BK7. As far as stones and bubbles are concerned one can clearly only specify the quality offered in catalog data, and it should be said that in this respect the windows made for the BNHBC have been well within the tolerances promised. It is difficult to formulate a tolerance for veins (striae) which will extract the best from the glassmaker but yet will not appear impossible when written down in black and white. In early discussions it was stated that at least one very long, heavy vein, deviating one or two degrees, was inevitable because of the technique of pouring the window but that efforts would be made to make this "pouring vein" come near one edge of the blank, not in the middle. Later on it appeared that the manufacturing technique had been changed and no pouring vein was found in the blanks which were eventually used. Short veins deviating perhaps a few minutes of arc were found but these were nearly all near the edges and were thus outside the area used optically. The veins are detected by shadow-testing the blank after it has received a rough inspection polish and this method can pick up veins deviating 5–10 sec of arc.

**Table I. Properties of Optical Glasses for Windows**

| | BK7 | K50 |
|---|---|---|
| $n_d$ | 1.5168 | 1.5226 |
| $V$ | 64.2 | 60.2 |
| Density | 2.51 | 2.61 |
| Thermal expansion coefficient | $8.2 \times 10^{-6}$ | $7.6 \times 10^{-6}$ |
| Transformation temperature °C | 547 | 560 |
| Young's modulus (kg/cm²) | $8.2 \times 10^5$ | $7.3 \times 10^5$ |
| Bubble cross section (mm² per 100 mm³ of glass) | 0–0.1 | 0–0.029 |
| Transmission at 3650 Å in 25 mm thickness | 0.945 | 0.960 |

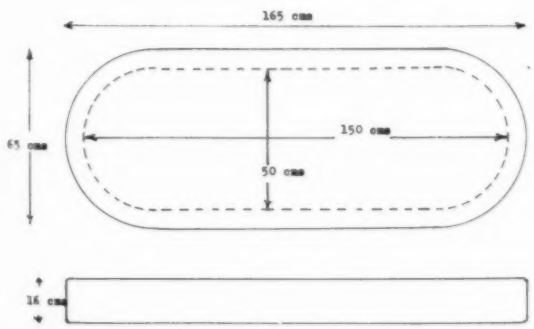


Fig. 1. Window for the British National Hydrogen Bubble Chamber. The broken line indicates the optically used area.

One could say, of course, that an isolated weak vein in a bubble chamber would hardly be a serious matter anyway: it would only affect measurements on a track which it happened to cross very obliquely. However, it is clearly possible to obtain blanks of a size suitable for bubble chamber windows with no veins in the optical region deviating more than 5 or 10 sec; so we originally specified the vein quality in such a way as to allow a pouring vein and a few smaller veins, but in the light of experience we should now be inclined to say, no veins at all with deviation exceeding 5–10 sec, with discretion for the examiner to pass a blank with just a few veins.

A defect which we frequently have found in large blanks consists of a well-defined continuous sheet of small bubbles; it appears to be due to the folding over of masses of semifluid glass in the pouring process.* We have specifically excluded such defects even in the nonoptical region because they might be a source of mechanical weakness in a window under stress.

## VI. Surface Flatness and Parallelism

There are three main considerations which determine tolerances on the surface flatness. These are: First, that both surfaces must be parallel enough to comply with the deviation tolerance of ±5 sec for single transmission; second, any errors of flatness on the surface adjacent to the hydrogen must not introduce a wedge in the hydrogen enough to deviate images of bubbles at the rear windows more than ±10 μ; and third, the over-all flatness must be good enough to permit good sealing on the vacuum gaskets.

The first two tolerances must clearly be expressed as limits on the maximum gradient of the surface with respect to a mean plane. A gradient $\theta$ gives an angular displacement $(n-1)\theta$ and if we put this equal to 5 sec

* In German this is called *schleier* (veil).

we obtain $\pm 5 \times 10^{-5}$ for $\theta$, i.e., a gradient of one test-plate fringe per 5 mm; allowing for the fact that two surfaces are involved we therefore put a surface flatness tolerance of a fringe per 10 mm maximum gradient. It is easily seen that this is an ample allowance for effects of wedge in the liquid due to nonflatness in the glass.

The third consideration, that of the effect of nonflatness on vacuum sealing, is more difficult to deal with. The seals are made with gaskets of indium and little is known about how this material takes up surface errors at low temperatures. In the event an over-all parallel tolerance of $\pm 0.05$ mm was specified together with the surface gradient tolerance above and this has so far sealed successfully.

A fourth consideration is that of the effect of a simple wedge with plane surfaces in the window; to a first approximation this has no effect but in second approximation it causes an error in track curvature because of the prismatic spectrum line curvature effect. The spectrum line curvature is for minimum deviation

$$\frac{2(n^2-1)}{n^2 f}\tan I,$$

where $I$ is the angle of incidence in air and $f$ the focal length of the lens which focuses the spectrum.[4] Thus if $\epsilon$ is the (small) wedge angle we can put

$$\tan I \sim {}^1/_2(n\epsilon);$$

now if the extreme field angle of the camera lens is $\beta$ and the depth of the chamber is $t$ we have for the maximum departure from straightness of a track at the far side of the chamber,

$$\beta^2 \frac{n^2-1}{n}(\epsilon t).$$

Putting $\beta = 0.5$, corresponding to a 30° semifield, we obtain a tolerance on $\epsilon$ of $10^{-4}$ rad, i.e., a parallel tolerance on the whole window of 0.2 mm. This is in fact a cruder tolerance than that proposed for facilitating the vacuum sealing, and this latter is not difficult to achieve in practice.

## VII. Quality of Surface Polish and Edge Finish

The window surfaces are photographed in dark-field illumination and are within the focal range; thus any residual gray from fine grinding will show up as general background illumination and scratches and sleeks will show as bright lines. It is possible in principle to measure the background of light due to incomplete polish by photographing the window, but to do this it is necessary to have a condenser system to go with it and this is not generally available at the time and place of inspection. Also it is impracticable to set quantitative tolerances on scratches and sleeks. We adopted instead a system of visual inspection on the finishing tolerances listed in Table II. In this system, which is largely a codification of present practice for convenience in optical drawings, the glass surfaces are inspected with a hand-magnifier and a hand inspection lamp held at a suitable position. It has always been possible to agree with workshop personnel about the presence or absence of specified faults in surface finish. For a bubble chamber window the code P1, C1, F1/10 would be used.

**Table II. Optical Finishing Codes**

| | |
|---|---|
| Surface figure: | |
| | $F/n$ means surface fits test-plate to $n$ fringes overall. |
| | $F/n/m$ means surface fits test-plate to $n$ fringes per $m$ mm ru in any direction. |
| | $F/\infty$ means condenser quality figure, i.e., no test plate. |
| | The above apply to within 1 mm of edges unless stated otherwise. |
| Surface polish: | |
| P1: | completely polished when viewed a 20× magnificatio under dark ground illumination. |
| P2: | as P1 but with 3× magnification. |
| P3: | occasional spots of gray allowed. |
| P4: | cloth polish or buff. |
| Surface cleanness: | |
| C1: | no sleeks or scratches at 20× magnification. |
| C2: | as C1 but 3× magnification. |
| C3: | a few small sleeks and scratches permitted. |
| Edges: | |
| E1: | no visible chips. |
| E2: | chips not larger than 0.3 mm. |
| E3: | chips not larger than 1 mm. |
| Ch/$n$: | chamber $n$ mm across diagonal. |
| Nonoptical surfaces: | |
| G1: | fine gray finish. |
| G2: | coarse gray or diamond milled. |
| G3: | edges as cut but with sharp corners removed. |
| GE: | gray and etch in hydrofluoric acid to relieve stresses. |

The method of finishing edges denoted by GE in Table II was originated by Jenaer Glaswerk Schott und Gen. The writer is grateful to F. Reitmayer of that firm for drawing attention to it; the edges of the windows are heavily etched to a depth of 0.5–1 mm after rough grinding to shape. This opens out all cracks, and it is claimed that glass so treated is stronger than optically polished glass.

## VIII. Testing Methods

The techniques of shadow testing and stress-birefringence measurement used on the glass blank are standard and need no comment. The principal innovation is in the method of testing for deviation. The window is mounted in a vertical plane on a trolley which can roll on a concrete floor. A plane mirror and an autocollimator are mounted on either side of the window on steady pillars, as in Fig. 2. The window is rolled clear of the optical path and the autocollimator reading noted; then the window is moved across and

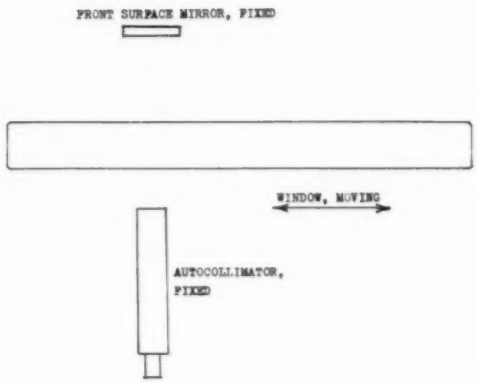


Fig. 2. Method of measuring ray deviation. The window is moved on a trolley between the mirror and the auto collimator.

the two components of deviation measured at different parts of the window. If desired, this process can be repeated at different heights and different angles of incidence. We note also that this method can be extended to differentiate between deviations due to surface gradients and to refractive index gradients; for this purpose it is necessary to measure also the angle between rays reflected from the two surfaces of the window; let the component of this angle in say, the $x$ direction be $\alpha$ and let the component of the deviation measured as above be $\beta$. Then we have

$$\alpha = 2n\epsilon + 2t\frac{dn}{dx},$$

$$\beta = 2(n-1)\epsilon + 2t\frac{dn}{dx},$$

where $\epsilon$ is the wedge angle in the glass and $t$ is the thickness of the glass. Thus $\alpha$ and $dn/dx$ can be found. A Hilger & Watts Microptic autocollimator reading to 1 sec of arc was found suitable for this purpose.

The writer is grateful to D. S. Brown and G. E. Manville of Grubb, Parsons for much useful discussion and for help in realizing the method of deviation testing outlined in Sec. VIII. He has also had much help and useful comment from F. Reitmayer.

## References

1. H. Bradner, Ann. Rev. Nuclear Sci. **10**, 109 (1960).
2. L. C. Martin, *Technical Optics* (Pitman, London, 1948) Vol. I.
3. L. W. Tilton, J. Res. Natl. Bur. Std. **42**, 279 (1949).
4. W. T. Welford, *Geometrical Optics* (North-Holland, Amsterdam, 1962).

Perkin-Elmer

Shown undergoing final inspection following grinding and polishing operations, is one of three of the world's largest optically ground windows ground and polished by Perkin-Elmer for the Brookhaven 80-in. liquid hydrogen bubble chamber. Cast by Schott in Germany of borosilicate crown glass, the window, weighing 680 kg and measuring 205 cm long, 76 cm wide, and 16.5 cm thick, permits photographs to be taken of experiments conducted in the chamber. During operation of the chamber, the window is subjected to temperatures as low as −248°C, and pressures up to 9 kg per square cm. One of the optical specifications of the window, which took approximately 800 h to grind and polish, was a flatness of 2 fringes per 2.5 cm over the entire surface.

Schott

# Meeting Reports

## 18th Symposium on Molecular Structure and Spectroscopy, The Ohio State University, 10–14 June 1963

Reported by John Overend, University of Minnesota.

Over 600 spectroscopists met in Columbus for the eighteenth Symposium on Molecular Structure and Spectroscopy. The arrangements and the program were excellent, and we thank H. H. Nielsen and his colleagues for their efforts in organizing this meeting, covering fourteen invited and 173 contributed papers, the latter presented in four parallel afternoon sessions.

A considerable number of papers were devoted to the discussion of new optical techniques for spectroscopic research. C. H. Townes *MIT* reviewed some recent developments in maser technology, reporting that maser action has now been observed at a very large number of wavelengths from 3125 Å to 28,000 Å. Most of these wavelengths fall in the red and near-infrared regions. He also described experiments with two ruby masers operated in tandem to give high power output in pulses as short as $7 \times 10^{-9}$ sec. Little progress appears to have been made toward the development of continuously tunable masers for use as spectroscopic sources. The use of masers as Raman sources, in both conventional Raman spectroscopy and experiments with stimulated Raman[1] was critically discussed by B. Stoicheff *NRC-Ottawa* in an invited paper, and also by S. P. S. Porto and his co-workers from the Bell Telephone Laboratories. Stoicheff, recalling that two years ago Porto and Wood described the excitation of the Raman spectrum of liquid benzene with about 50 flashes of a ruby maser in a conventional Raman setup, stated that he had succeeded in detecting the Raman line corresponding to $\nu_1$ of $CS_2$ at 655 $cm^{-1}$ with 20 flashes. The Bell group have carried their experiments forward and have built a large ruby maser capable of giving pulses of about 30 with the object of obtaining a Raman spectrum with a single flash. On their first try they succeeded in burning a hole in the Raman tube and carbonizing the benzene! However, they are working to overcome this difficulty by going to lower energy masers in different configurations. They have also used a strained ruby with an absorption line-width of about 3 $cm^{-1}$ to remove the exciting line; this allows them to illuminate in the direction of observation. They also reported that the Raman intensities appear somewhat irregular and suggest that there is a stimulated Raman effect. Stoicheff, in his paper, touched on the stimulated Raman effect and reported some recent results of Terhune in which he established that, in diatomic molecules, the line occurring with about twice the shift of the fundamental definitely results from double excitation and is not attributable to the overtone. There were two other interesting papers on the use of the infrared maser as a tool for attacking the spectroscopic problems associated with finite slit-widths: H. W. Morgan *ORNL* spoke on the use of a gas maser to measure spectrometer slit-functions, and F. P. Dickey *OSU* discussed the reduction of the observed data to obtain the true spectrum in those cases where the slit-function of the spectrometer is known. Morgan remarked that it is almost impossible to suppress maser action at some infrared wavelengths, particularly in xenon, and he surmised that maser action in the infrared has always occurred in xenon discharge tubes.

Another interesting development in instrumentation was described by A. Girard *ONERA:* briefly this is an extension of the multislit spectrometer design[2] but the entrance and exit slits are replaced by patterned grids. The increase in light-gathering power over a conventional slit system is so great that Girard was able to obtain, under quite high resolution, an emission spectrum of methane at 300°. Certain difficulties do, however, obtain with this design; the pattern of the exit grid must correspond to that of the entrance grid imaged through the system, several exit grids are necessary to cover a reasonable angular range of the grating and their alignment, especially in the vertical direction, is quite critical.*

Several contributors described microwave measurements and their reduction to rotational constants, molecular geometry, quadrupole coupling constants and barriers to internal rotation. In particular, barrier heights were reported for methyl isocyanate, *cis*-2-butene and 1-chloro propylene. In the general area of research into the hindered rotation problem the work of B. Kirtman *Berkeley* appears particularly significant. Kirtman has extended Howard's work[3] on ethane-type molecules. In a molecule with a low barrier one must take into account configurations in between the symmetrical staggered and eclipsed ones. When this is done, it is found that the rotational fine structure of the perpendicular bands associated with the nearly degenerate vibrations depends on the difference in vibrational frequency, on the Coriolis coupling between the ordinary internal angular momentum and the vibrational angular momentum, and on the barrier height. Kirtman has considered the case of dimethyl acetylene and has calculated the positions of the rotational fine structure for the perpendicular bands due to the methyl-group bending modes for various assumed values of the barrier height. He found that the observed spectrum is consistent with a barrier height between 0 and 100 cal/mole. It appears that this analysis is capable of yielding considerably more accurate estimates if the details of the fine structure can be resolved.

The interpretation of barrier-height results was taken up by E. B. Wilson *Harvard* in a provocative discussion of nonbonded forces in which he criticized the use of the Urey-Bradley force field as a representation of the intramolecular potential energy. His criticism can be summarized as follows: if we accept the nonbonded forces determined by fitting a Urey-Bradley field to the vibrational frequencies, then we should expect significant contributions from these same forces to the barriers to internal rotation, to the equilibrium configurations of the molecules and to the relative stability of *cis* and *trans* isomers. The fact that such contributions do not appear significant leads Wilson to believe that the Urey-Bradley field is not a particularly good potential function. However, from the evidence he cited, it seems that some nonbonded interactions do occur and are probably responsible for certain structural effects. Wilson drew attention to the equilibrium configurations of methyl alcohol and $CH_2$:NOH; in each case it appears that the contiguous proton is attracted by the lone pairs on the oxygen and nitrogen, respectively.

Other speakers addressed themselves to the important problem of intramolecular force constants, from both theoretical and experimental viewpoints. P. Phillipson *Michigan* discussed the derivation of force constants from exact and approximate wave functions, and R. N. Porter *Columbia* and M. Karplus *Arkansas* a new semi-empirical treatment of the potential energy of $H_3$. An interesting report of experimental force constants was given by G. C. Pimentel *Berkeley* and C. B. Moore *Berkeley* who advanced a revised assignment for diazomethane based on data taken with the matrix-isolation technique. The band at 852 $cm^{-1}$, previously assigned[4] to the out-of-plane CH deformation mode $\nu_9$ was reassigned as $2\nu_9$ and a band at 406 $cm^{-1}$ in the gas phase, which persists at 20°K is assigned to $\nu_9$. With this revision, the force constant for the out-of-plane deformation coordinate is found to be very much lower than those found for

* *Editor's note*—Girard has described his grills in Appl. Opt. **2**, 79 (1963.)

*continued on page 1060*

# Photorefractometer II. Measurement of *N* and *K*

N. S. Kapany and D. A. Pontarelli

A study of the extension of the rod and cone photorefractometer principle to the measurement of $N$ and $K$, the real and imaginary parts of refractive index of absorbing fluids, is made. Theoretical analysis indicates high sensitivity in the low-absorption-coefficient region of the specimen when the illumination is incident at the interface at an angle close to the critical angle. Experiments are made on various rod configurations and results agree closely with theory.

## I. Introduction

The dielectric rod photorefractometer has been studied by Kapany and Pike,[1] and Kapany and Pontarelli.[2] Previous theoretical and experimental investigations concerning the limitations on refractive index sensitivity imposed by rod geometry, difference in refractive index of rod and specimen liquid, illumination system design, and detector configuration have been confined to spectral regions in which neither the rod nor surrounding medium is absorbing. In the present work absorption and anomalous dispersion occurring in an absorption band is related to fluid photorefractometry, and the possibility of increased refractive index sensitivity is indicated. Calculations of Fresnel reflection in regions of absorption demonstrate the importance of controlled wavelengths and angle of incidence at the glass-to-absorbing medium interface, and a large number of internal reflections in the refractive element. The absorption photorefractometer is shown to be applicable to concentration measurements and ultimately to dispersion effects in weakly and highly absorbing compounds. Experimental results on an absorbing fluid photorefractometer are presented.

## II. Theory

For the rod photorefractometer, expressions have been derived[1] relating refractive index changes of the surround to the transmitted flux. In the extended theory, considerations have been given to include absorption losses in the rod, reflection losses at the rod ends, and internal reflection losses at the cylindrical walls. In the theory developed by Kapany and Pontarelli[2] for the rod and cone photorefractometers, the fractional sensitivity is enhanced and the operational index range extended to lower refractive index values of the surround and to larger index differences of the two media by the use of a spherical entrance rod end, hollow cone illumination, and an immersed detector.

The above-mentioned photorefractometer systems may be designed to operate in absorption regions of the surrounding medium. This redesign involves two modifications of the basic photorefractometer: (1) When the spectral bandwidth of the incident illumination is larger than the absorption bandwidth, partial reflections occur at each reflection. Variation in the transmitted radiation caused by radiation absorption at each reflection is also an indication of the specimen fluid concentration. (2) Illumination of a photorefractometer by narrow-bandwidth radiation contained within the absorption band amplifies the gains realizable in the basic instrument through utilization of the large refractive index changes occurring in the absorption band. These refractive index changes, referred to as anomalous dispersion,[3] are a function of concentration and, therefore, permit the determination of specimen concentration.

A transparent glass-to-absorbing medium interface described by the indices $N$ and $N' = n' - ik$ is shown in Fig. 1. The absorption coefficient $k$ is related to the transmission ratio $I_t/I_0$ and the path length in the absorbing medium $P$ by the equation

$$k = (\lambda/2\pi P) \ln (I_0/I_t), \qquad (1)$$

where $I_0$ is the incident radiation, $I_t$ the transmitted radiation, and $\lambda$ the wavelength.[4] Since $k$ and $N'$ are functions of wavelength and concentration, and $N$ is a function of wavelength, the Fresnel reflection at the glass-to-absorbing medium interface is expressed as:

$$\mathbf{R}\{N(\lambda), N'[n'(\lambda), k(c, \lambda)], \theta'_1\},$$

The authors were both in the Physics Division, Armour Research Foundation, Chicago 16, Illinois. N. S. Kapany is now at Optics Technology, Inc., 248 Harbor Blvd., Belmont, California.

Received 13 January 1962.

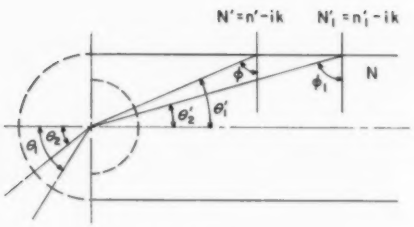


Fig. 1. Cylindrical rod geometry.

where $c$ is the concentration and $\theta'_1$ is the angle between the rod axis and the transmitted ray. Other variables necessary for estimation of the flux transmitted through a rod of length $L$ and diameter $D$ by multiple total reflections $\eta$ are: the solid angle $2\pi \sin\theta'_1 \, d\vartheta'_1$, absorption in the rod $\exp(-\alpha L \sec\vartheta'_1)$, the number of reflections at glass-to-absorbing medium interface given by $(2L/D)\tan\vartheta'_1$, the two reflections at the rod ends, and the entrant flux angular distribution $F(\theta'_1)$.

Combining these factors, the integral expression for the total transmitted flux for a fixed concentration is:

$$\tau = K \int_{\theta'_1}^{\theta'_2} \int_{\lambda}^{\lambda'} F(\theta_1)\{1 - R[1, N(\lambda), \theta_1]\}^2 \cdot \mathbf{R}\{N(\lambda), N'[n'(\lambda), k(c, \lambda)], \theta'_1\}^{\eta} \cdot \exp(-\alpha L \sec\theta'_1) \cdot \sin\theta'_1 \cdot d\theta'_1 \cdot d\lambda, \quad (2)$$

where $K$ is a constant of integration.

To simplify the glass-to-absorbing medium discussion, let $\alpha = 0$ and $R(1, N(\lambda)) = 0$ in the above equation. This gives

$$\tau = K \int_{\theta'_1}^{\theta'_2} \int_{\lambda}^{\lambda'} F(\theta_1) \cdot \mathbf{R}\{N(\lambda), N'[n'(\lambda), k(c, \lambda)], \theta'_1\}^{\eta} \cdot \sin\theta'_1 \cdot d\theta'_1 \cdot d\lambda, \quad (3)$$

where $\mathbf{R}$ contains reflection losses for both planes of polarization. A number of special cases of an absorbing medium surrounding a glass rod may now be discussed.

*Case I.* If we assume that the absorption is proportional to the concentration of the specimen medium, the incident radiation spectral band is centered at the absorption band peak, and the spectral bandwidth is much smaller than the total absorption bandwidth, then integration over $\lambda$ is not necessary (Fig. 2, Region A). Taking $\lambda = \lambda_0$, $F(\theta_1) = F(0) = 1$ for all angles of incidence, and $N' = n_0 - ik$, where $n_0$ is the medium refractive index outside the absorption band, the expression for $\tau$ becomes:

$$\tau = K_1 \int_{\phi_1}^{\phi_2} \{\mathbf{R}[N(\lambda_0), N'_1[n_0(\lambda_0), k(c, \lambda_0)], \phi]\}^{\eta} \cos\phi \, d\phi. \quad (4)$$

The change of angular variable from $\theta'_1$ to $\phi$ simplifies the analysis of $\tau$ with respect to the Fresnel reflection coefficient. Obviously the value of $\tau$ is a function of concentration and angle of incidence.

*Case II.* When the conditions are similar to Case I but with a spectral band width equal to the absorption bandwidth, Fig. 2 (Region C), the integral has the form

$$\tau = \int_{\phi_1}^{\phi_2} \int_{\lambda_2}^{\lambda_3} \{R[N(\lambda_0), N'[n_0(\lambda), k(c, \lambda)], \phi]\}^{\eta} \cos\phi \cdot d\phi \cdot d\lambda \quad (5$$

For a weakly absorbing medium the dispersion curve is symmetrical about $\lambda_0$ and $n' = n_0$ at $\lambda = \lambda_0$. The limits of integration $\phi_1$ to $\phi_2$ are chosen to eliminate the detrimental solid angle increase for $\lambda_2 \leq \lambda \leq \lambda_0$. Also strongly absorbing media have asymmetric dispersion curves which must be taken account of in the $\tau$ integral.

This arrangement can be used when narrow spectral bandwidths are impossible; however, the expected sensitivity is much less than that of Case I or, as will be shown, Case III. In this case the photorefractometer sensitivity is decreased because radiation of wavelength near the absorption band edge is relatively unaffected by absorption.

*Case III.* When the absorption is proportional to concentration ($k = ac$) and the spectral band is centered at $\lambda_1$, the peak of the dispersion curve corresponding to an increase in refractive index, Fig. 2 (Region B) the integral expression can be written in the form:

$$\tau = \int_{\phi_1}^{\phi_2} \{\mathbf{R}[N(\lambda_1), N'[n'(c, \lambda_1), k(c, \lambda_1)], \phi]\}^{\eta} d\phi. \quad (6$$

The equation relating $n'$ to $k$ is given by

$$n' = \frac{k}{n_0 p} + n_0 = \frac{ac}{n_0 p} + n_0,$$

where $p$ is a function of wavelength.

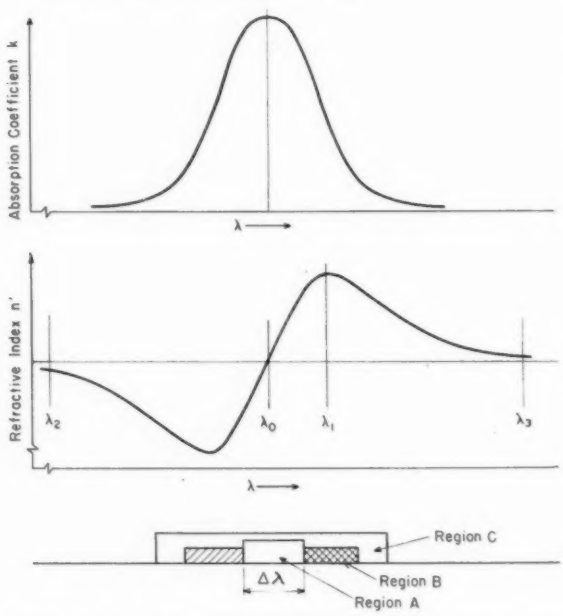


Fig. 2. Illustrating anomalous dispersion and spectral regions of interest.

**Table I. Fresnel Reflection Coefficients for a Glass-Absorbing Medium Interface**

$N = 1.500,000$; $N' = 1.000,000 - ik$; $\phi = 42°$

| $k$ | $\rho_{\parallel}$ (%) | $\rho_{\perp}$ (%) |
|---|---|---|
| 0.100,000 | 10.89 | 36.26 |
| 0.010,000 | 51.81 | 74.36 |
| 0.001,000 | 91.249 | 95.978 |
| 0.000,100 | 99.081 | 99.586 |
| 0.000,010 | 99.990 | 99.996 |

The total transmitted flux is not only influenced by changes in Fresnel reflection but, also, by changes in the total solid angle which is dependent upon the critical angle established by the real part of the refractive index. Because of this, the best properties of the simple photorefractometer are combined with the advantages of the absorption term. An increase of concentration causes a decrease in $\tau$ because of Fresnel reflection losses, likewise an increase in external index causes a decrease in solid angle and a decrease in $\tau$. Thus, the combination of the two effects contributing to a decrease in flux will yield a photorefractometer of greater sensitivity than the ordinary rod photorefractometer. The improved sensitivity will be the product of the spherical ended rod photorefractometer sensitivity, having hollow cone illumination,[2] and the sensitivity of the absorption photorefractometer.

## III. Fresnel Reflection Coefficient at an Absorbing Interface

For a ray incident upon a glass to-absorbing medium interface as shown in Fig. 3, the Fresnel reflection coefficients for a radiation having the electric vector polarized perpendicular to and parallel to the plane of incidence are given by

$$\rho_{\perp} = \left| \frac{[(n' - ik)^2 - N^2 \sin^2\phi]^{1/2} - N\cos\phi}{[(n' - ik)^2 - N^2 \sin^2\phi]^{1/2} + N\cos\phi} \right|^2 \tag{7a}$$

and

$$\rho_{\parallel} = \left| \frac{N[(n' - ik)^2 - N^2 \sin^2\phi]^{1/2} - (n' - ik)^2 \cos\phi}{N[(n' - ik)^2 - N^2 \sin^2\phi]^{1/2} + (n' - ik)^2 \cos\phi} \right|^2. \tag{7b}$$

In performing calculations using these expressions the root of

$$[(n' - ik)^2 - N^2 \sin^2\phi]^{1/2}$$

is taken in the fourth quadrant.

The influence of absorption upon Fresnel reflection at a plane glass-to-absorbing medium interface is illustrated in Fig. 3. These curves are derived from computations performed for monochromatic radiation corresponding to an absorption band peak where $k/n'$ is a maximum and the refractive index $n'$ is approximately unity.[5] The absorption coefficients representative of strong to very weak absorption listed in Table I were used to calculate $\rho_{\parallel}$ and $\rho_{\perp}$ at a glass ($N = 1.500,000$), absorbing medium ($N'_1 = 1.000,000 - ik$) interface for angles of incidence varying from 0 to 90° in 2° intervals. The sensitivity of Fresnel reflection to absorption changes for angles of incidence at, or a few degrees larger than, the critical angle is apparent. This sensitivity of $\rho_{\parallel}$ and $\rho_{\perp}$ to $k$, at an incident angle of 42° corresponding to approximately the critical angle, is shown in Fig. 4. A basic design variable of an absorption photorefractometer is the number of reflections necessary to cause a specified change in the transmitted flux. In Fig. 5 the relationship of the number of reflections to the resultant per cent transmission change is shown for the above data at 42° incident angle.

For absorption coefficients greater than 0.0001, conventional optical elements such as cylinders or slabs will provide the required number of reflections for detectable changes in transmitted flux. As the absorption coefficient decreases and the number of reflections increases, the use of an optical element such as a small-diameter fiber is suggested because a fiber provides the relatively large length-to-diameter ratio necessary for many reflections in a small size.

The optimum conditions necessary to the design of an absorption photorefractometer operating at absorption band peak are now established. As shown in Fig. 3, the Fresnel reflection loss is extremely sensitive to absorption constant for angles of incidence at or slightly greater than the critical angle. This effect, in the case of small $k$, is minor at approximately 4° beyond the critical angle. Thus, an incident beam of small divergence is required and the divergence must not be altered by

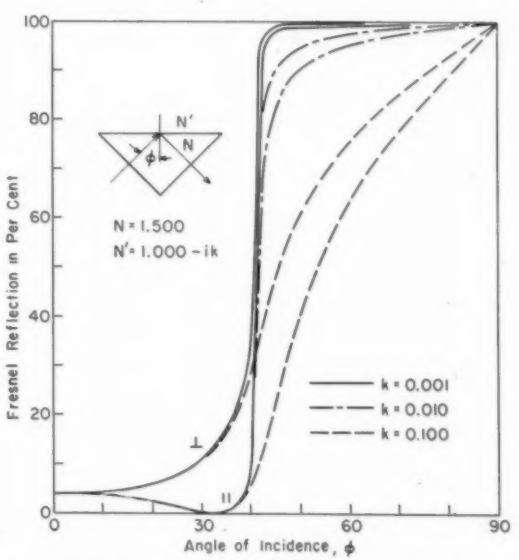


Fig. 3. Fresnel reflection at glass-to-absorbing medium interface for three $k$ values.

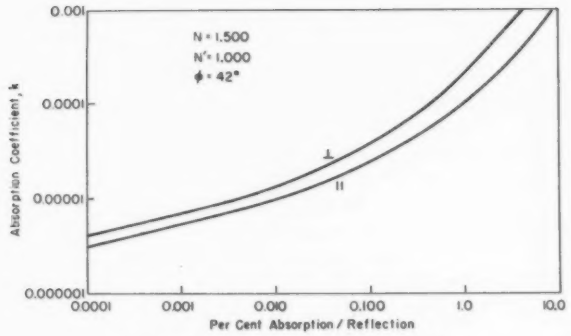


Fig. 4. Percent absorption per reflection.

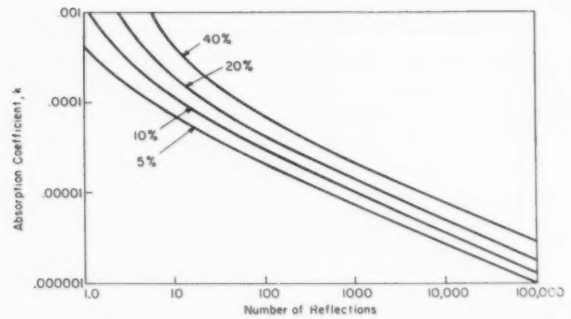


Fig. 5. Number of reflections producing a required percent transmission change—$k$ variable. $\phi = 42°$, $N = 1.5$, $N' = 1.0$-ik, $\|$ polarization.

internal strains or surface scattering. By coiling the rod element a ray incident angle is obtained near the critical angle because the angle of incidence is decreased by bending the rod.[6]

## IV. Experiment

In the theoretical calculations one assumed an idealized physical model having all rays from a nonabsorbing medium incident upon the absorbing medium at the critical angle. A number of experiments designed to achieve this have been performed using optical elements of both cylindrical and rectangular geometry. In the initial experiment a straight cylindrical rod immersed in an absorbing solution was used. The rod was aluminized along a 2.54-cm distance at each end to prevent energy loss at the junction with the absorption chamber walls. An absorbing methylene blue solution in water, having a refractive index of 1.33 surrounding a rod of refractive index 1.52, results in a critical angle of approximately 62°, which requires an oil immersion microscope objective for the illumination system. The experimental arrangement of the straight rod system is shown in Fig. 6(a). In determining the sensitivity of this and other rod configurations, solutions of methylene blue in a buffer solution of pH 5 consisting of a one-to-one mixture of 0.1 $M$ citric acid and 0.2 $M$ disodium phosphate were combined to give a dye concentration range of 200 to 1. The spectral transmission of this dye is shown in Fig. 7 as curve 1, and the transmission of a Type A filter transmitting in the region of absorption is shown as curve 2. This dye and filter combination used with a "Densichron" having a red-sensitive detector provides maximum sensitivity to absorption changes.

The straight rod combined with full cone incident illumination designed for about 30 reflections at the critical angle did not show observable sensitivity to dye concentration changes. This illumination system when converted to a hollow cone illumination system by installing an aperture [Fig. 6(b)] showed sensitivity-to-dye-concentration. The results are plotted as curve 3 in Fig. 8. For this configuration, radiation at or near the critical angle experienced approximately 30 reflections in transversing the absorbing liquid–glass rod region.

Because the angle of incidence at the absorbing medium interface was the most critical variable in the experiment, a slab having right-angle reflecting prisms at the entrance and exit ends, as shown in Fig. 6(c), was constructed. Collimated radiation enters through the slab edge, strikes the tilted slab end, and is internally reflected down the slab at the desired incident angle. The low sensitivity-to-dye-concentration of this optical

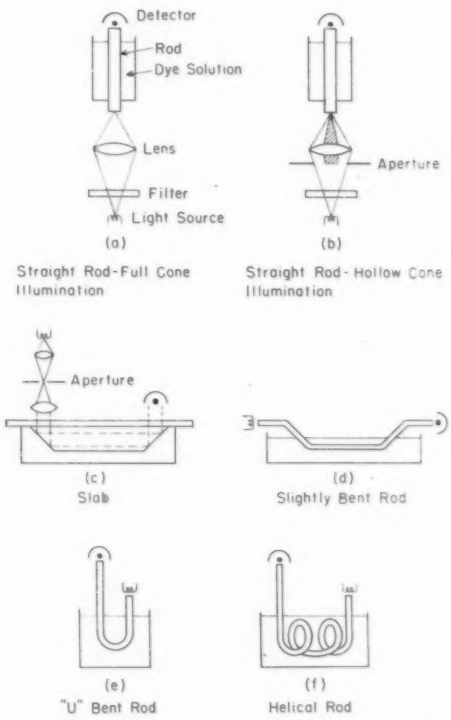


Fig. 6. Experimental absorption photorefractometer arrangements.

**Table II. Transmission through Photorefractometer Geometries Surrounded by an Absorbing Dye Solution**

| Theory (30 reflections) taken from Fig. 5 | | Experiment | | | | | |
|---|---|---|---|---|---|---|---|
| $k$ | % Transmission | Relative dye concentration (dye/$H_2O$) | Straight rod full cone illumination 30 reflections | Straight rod hollow cone illumination 30 reflections | Slab 60 reflections | U Bent rod | Helical rod |
| 0.000,000 | 100 | $H_2O$ | 100 | 100 | 100 | 100 | 100 |
| 0.000,037 | 95 | 1/1000 | 100 | 89 | 89 | 94 | 88 |
| 0.000,057 | 90 | 1/500 | 100 | 86 | 85 | 87 | 76 |
| | | 1/100 | 100 | 79 | 85 | 85 | 44 |
| 0.000,082 | 80 | 1/50 | 100 | 71 | 83 | 79 | 24 |
| 0.000,145 | 60 | 1/10 | 100 | 51 | 74 | 67 | 14 |
| ... | ... | 1/5 | ... | 40 | ... | 62 | 9 |

lement, which produced 30 reflections, as shown in urve 5 of Fig. 8, is attributed to inadequate incident ollimation and farther decollimation due to inhomogeneities in the slab.

It was observed that high sensitivity was achieved when the rod was bent over a steep curve as illustrated in Fig. 6(d). This is primarily because the angle of incidence is decreased by bending the rod over a steep curve. A single bend of 5-mm radius arranged as shown in Fig. 6(e) produced the data shown in curve 4 of Fig. 8. The sensitivity is greater than that observed for the slab but less than that of the straight rod and hollow cone illumination. Extension of the "U" bend to a helix [Fig. 6(f)] of $2^1/_2$ turns resulted in curve 2 of Fig. 8. The slope of the absorption curve observed for the lower dye concentrations indicates high sensitivity. The observed change in sensitivity at high dye concentrations is caused by staining and surface defects created in forming the helix.

The experimental data are summarized in Table II. The data in columns 1 and 2 are obtained graphically from Fig. 5. The high sensitivity of the helix, approaching that expected from theory for thirty reflections (curve 1, Fig. 8) at exactly the critical angle, may be explained by considering the passage of radiation in the curved rod. At any reflection all radiation incident at angles less than the critical angle escapes from the rod, leaving most of the radiation at an angle affected most by the dye absorption. At the next reflection the radiation may escape or experience another absorption loss at an angle closer to the critical angle. All rays reaching the detector will have made numerous reflections at incident angles favorable to absorption losses. This is in contrast to the straight rod and slab geometries in which the angle of incidence for each ray remains constant and only rays initially incident at the critical angle will experience the large absorption losses predicted by theory. Rays incident at angles greater than the critical angle will experience smaller absorption losses per reflection and will produce the lower sensitivity observed for those geometries.

## V. Conclusions

The theoretical analysis of the absorption photorefractometer supplemented by Fresnel reflection coefficient calculations showed a photorefractometer operating in the absorption region to be feasible. Absorption photorefractometry is applicable to liquids, vapor, and gases absorbing in the ultraviolet, visible, and infrared spectral regions. Design variations permit a wide range of absorption coefficients to be accommodated. Weakly absorbing compounds are suitable to the fiber version of the instrument, while geometries resulting in a few controlled reflections have great potential in the analysis of strong absorption bands. In any design configuration, the importance of narrow spectral bandwidth, low angular divergence of radiation within the light transmitting element, and predictable transmitted flux change through controlled number of internal re-

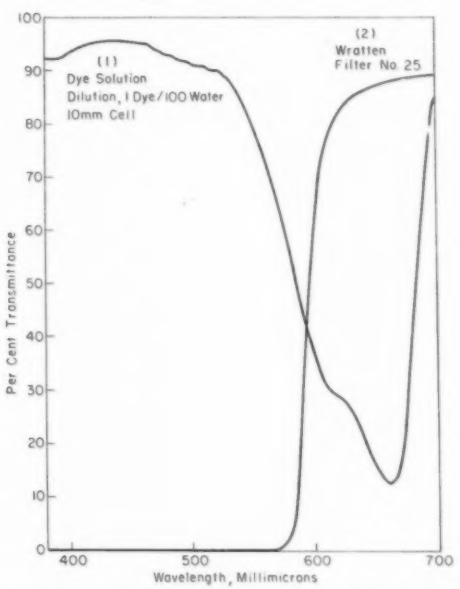


Fig. 7. Percent transmittance of dye and filter.

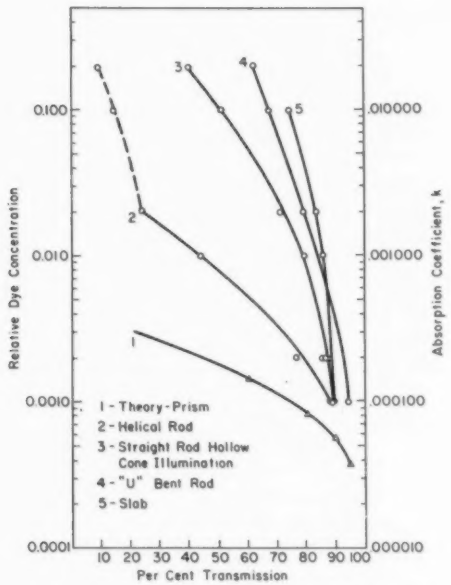


Fig. 8. Absorption photorefractometer experimental results.

flections is established. In scanning a strong absorption band at high spectral resolution the peak of absorption will be shifted to shorter wavelengths owing to refractive index changes resulting from anomalous dispersion.

Experimental verification of the radiation loss at a glass-to-absorbing medium interface has been made using a dye solution surrounding a number of different rod configurations. Sensitivity of the helical rod design approaches that predicted by theory. Rod configurations having a greater number of helical turns made from a glass having a surface of optical quality will in the future extend the sensitivity of the method to a greater range of dye concentrations, thereby making the method applicable to weakly absorbing gases. Finally, dispersion and absorption data of highly opaque fluids or solids in the ultraviolet, visible, and infrared spectral regions would be of great interest and, in industry, would provide an experimental tool not heretofore available.

## References


1. N. S. Kapany and J. N. Pike, J. Opt. Soc. Am. **47**, 1109 (1957).
2. N. S. Kapany and D. A. Pontarelli, Appl. Optics **2**, 425 (1963).
3. R. W. Wood, *Physical Optics*, 3rd ed. (Macmillan, London and New York, 1934), pp. 469–541.
4. O. S. Heavens, *Optical Properties of Thin Solid Films* (Academic Press, New York, 1955), p. 49.
5. W. E. Forsythe, *Smithsonian Physical Tables*, 9th ed. (Smithsonian Institute, Washington, D. C., 1954), p. 533.
6. N. S. Kapany, J. Opt. Soc. Am. **47**, 413 (1957).


# anti-Xi-zero particle

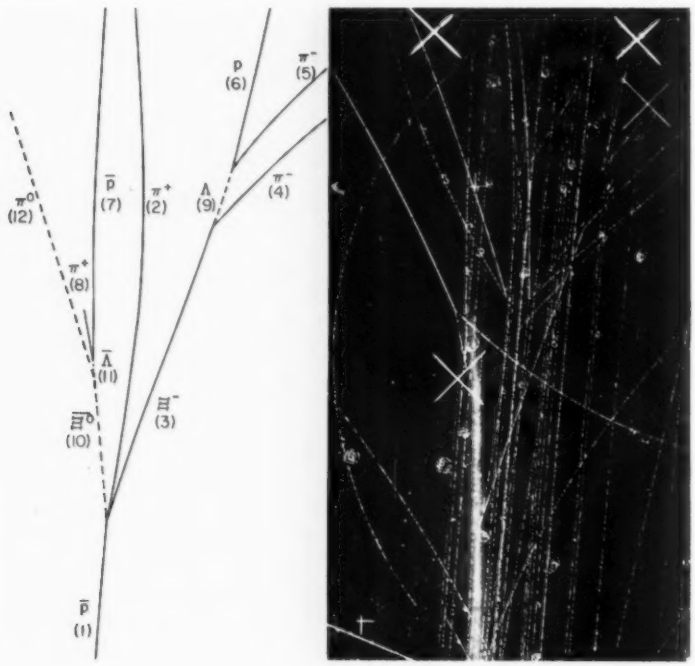


*photo Brookhaven National Laboratory*

Photograph taken in the Brookhaven 20-in. liquid hydrogen bubble chamber, in which the production of an anti-Xi-zero particle is observed for the first time. This has resulted from the collision of an anti-proton (1) from the Alternating Gradient Synchrotron colliding with a stationary proton in the chamber. The path of the anti-Xi-zero (10) is unobservable, since it leaves no track, but subsequent secondary decay products (7) and (8) do leave tracks, and from these the existence of the new particle can be deduced.

# Double Monochromator Systems

Robert L. Christensen and Robert J. Potter

A geometrical analysis of image formation in single monochromators is expanded to include the dual monochromator and the tandem monochromator, a system of two single monochromators used in series. The tandem system is useful in measurements of monochromator transmittance and in providing double dispersion. This analysis leads to expressions for the passbands, radiance in the final slit plane, and transmitted flux, as the widths of the intermediate and final slits are varied.

## I. Introduction

There are a great many applications of commercially available monochromators. The monochromator is often used as a "wavelength tunable" light source, but another significant class of applications includes the spectral analysis of light sources. In order to make certain radiometric measurements, it is necessary to know at least the relative transmittance or, in some cases, the absolute transmittance, of a monochromator as a function of wavelength. A straightforward method for measuring the transmission characteristics of a monochromator has been described by Christensen and Ames.[1] This method involves the use of two monochromators in tandem, and its application to the calibration of a Bausch & Lomb 250-mm monochromator led to this study.

There are other reasons for studying the characteristics of a double monochromator system. It is possible to enhance spectral purity and reduce scattered light with two monochromators. Some of the properties of the double monochromator have been discussed by van Cittert,[2] and this treatment is consistent with and reduces properly to his results. There are a number of double-pass and dual monochromators commercially available, but it is sometimes more convenient and more economical to use a pair of single monochromators in tandem.

For the purpose of this paper, several monochromator types will now be defined: (1) Single monochromator—a monochromator with one dispersing element used only once; (2) double-pass monochromator—a monochromator with one dispersing element which is used twice by appropriate optical design; (3) dual monochromator—a monochromator with two dispersing elements used separately, but where the exit slit of the first half is the entrance of the second half of the monochromator; (4) tandem monochromator—a pair of single monochromators used together. A lens is used to image the exit slit of the first instrument on the entrance slit of the second instrument at 1:1. Types (2)–(4) are "double" monochromators, providing double dispersion under suitable circumstances as described below. Combinations of these types may also be designed or found commercially available, e.g., a dual double-pass instrument.

The purpose of this paper is to describe a simple method for the analysis of a multiple-monochromator system and to elaborate on the details of the monochromator transmittance measurements previously described.[1] We are not attempting to develop a very sophisticated treatment, but rather a useful, phenomenological description of monochromator systems.

## II. The Single Monochromator

The basic parts of a monochromator are the dispersing element, the optical elements to present a parallel beam to the prism or grating, the lens or mirror to focus the dispersed beam on the exit slit, and the entrance and exit slits of the instrument. In practice, the collimating and focusing elements are usually the same mirror or lens, used twice. The properties of a single monochromator have been described by many authors,[3] so it will be assumed that the reader is aware of most of its properties.

It will be useful to recall that the linear (in the direction $x$) dispersion $D$ of a plane grating monochromator at normal incidence is given by:

$$D = dx/d\lambda = (nf/d\cos\theta), \quad (1)$$

The authors are at the International Business Machines Corporation, Thomas J. Watson Research Center, Yorktown Heights, New York.

Received 29 June 1962.

where $n$ is the order in which the grating is used, $f$ is the focal length of the exit mirror or lens, $d$ is the grating space, and $\theta$ is the angle at which the light is diffracted with respect to the normal.

The monochromator action may be considered to be the combined result of two effects, namely *lens action* (inversion of images) and *dispersion effects* (linear displacement from the axis of images corresponding to wavelengths other than that for which the instrument is set, $\lambda_M$). Lens action is, for practical purposes, immaterial in the case of the single monochromator but, as shown below, it is significant for double monochromator systems. There, the fact that $D$ can be either positive or negative (wavelengths greater than $\lambda_M$ displaced to the right or left of the axis) is also important.

The action of a single monochromator is shown in Figs. 1 and 2, and the principles demonstrated there are fundamental to the analysis of more complicated systems. Figure 1 shows images of several representative wavelengths in the entrance slit (S1) plane, which is assumed to be homogeneously illuminated with "white" light and to have a width $s$. The lens action consists in reflecting the arrows shown in Fig. 1 through the $x = 0$ line. In addition, the dispersion effect causes a displacement of the images with slope $1/D$. The result, i.e., images in the exit slit (S2) plane, is shown in Fig. 2.

The shape of the passband is obtained simply by finding the fraction of each image permitted to emerge from the monochromator. Thus, the image for $\lambda_M$ is the only one which comes through the instrument entirely unimpeded by the exit slit if it is equal in width to the entrance slit. The reduction in intensity of the other images is linearly proportional to their distance from the center of the exit slit, i.e., proportional to the difference of their wavelengths from $\lambda_M$ because of the linear dispersion characteristic of the grating monochromator.* Wavelengths at $\lambda_M \pm \Delta\lambda$ are totally prevented from emerging from the monochromator. Hence, the transmission characteristic is the familiar triangle with full width at half maximum equal to $\Delta\lambda$, where

$$\Delta\lambda = s/D. \tag{2}$$

In case the exit slit is set to a width unequal to that of the entrance slit, a similar simple analysis of the portions of the various wavelengths transmitted leads to the passbands shown in Fig. 3 which are, in general, trapezoids. In this figure, the relative transmission,

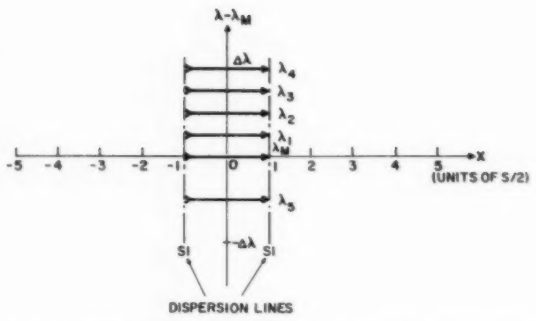


Fig. 1. Schematic diagram of images of several representative wavelengths in the entrance slit (S1) plane of a monochromator set for wavelength $\lambda_M$. The entrance slit-width is $s$, as shown by the position of the S1 lines on the abscissa (distance across slit).

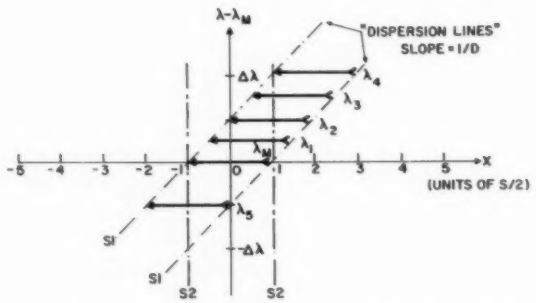


Fig. 2. Images of the same wavelengths in the exit-slit plane (S2) of a single monochromator (or intermediate slit plane of a dual monochromator). This diagram is constructed by reflecting the images of Fig. 1 in the $x = 0$ line (lens action) and then displacing the images with a slope $1/D$ (dispersion effect) as shown. Further along the optical path, portions of images outside the S2 lines are, of course, stopped.

| SLIT WIDTHS (mm) | 1,1 | 1,2 | 1/2,1/2 | 1,1/2 | 1,0 |
|---|---|---|---|---|---|
| $\Delta\lambda$ | 1/D | 2/D | 1/2D | 1/D | 1/D |
| $A_e$ (ARBITRARY UNITS) | 1 | 1 | 1/2 | 1/2 | 0 |

Fig. 3. Passbands for a grating monochromator (linear dispersion $D$ in mm/Å) with various entrance and exit slit-widths. Bandwidth, $\Delta\lambda$, and effective area of source accepted by system, $A_e$, are obtained by consideration of image size relative to exit slit-width as in Fig. 2. $\Delta\lambda$ is proportional to the larger of the two widths, $A_e$ to the smaller.

* Diffraction effects are negligible with the slit-widths usually used. Furthermore, it should be realized that the prism monochromator also exhibits linear dispersion over small wavelength intervals although this paper will be explicitly concerned with the properties of the grating monochromator. This is particularly true if the index of refraction of the prism is not a rapid function of wavelength.

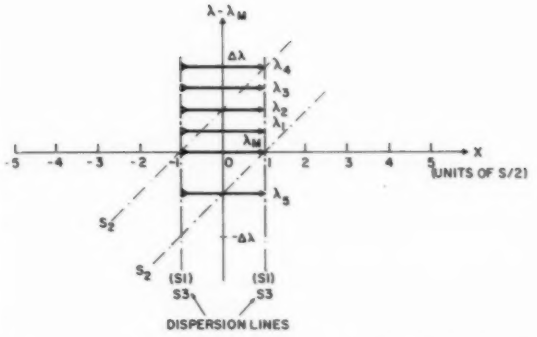


Fig. 4. Images in exit slit (S3) plane of a dual monochromator whose dispersion in both sections is in the "same" direction. These are obtained from Fig. 2 by again reflecting in the $x = 0$ line and displacing to the right the amount corresponding to the dispersion. This diagram is also the mirror image of that for the tandem monochromator system with dispersions in "opposite" directions. It is apparent, from the sizes of the images transmitted, that the passband (for equal slit-widths as shown) is a triangle with half-width $\Delta\lambda$; i.e., identical to the single monochromator case.

$t(\lambda)$, for wavelengths close to the wavelength for which the instrument is set, $\lambda_M$, is plotted. In each case, the maximum value of $t$ is plotted as $T$. This factor is the relative transmittance of the instrument and will itself be a function of wavelength. That is, as the wavelength setting of the monochromator, $\lambda_M$, is changed, $T$ changes due to variations in such factors as reflectance of grating and mirrors and to effects of grating blaze. The value of $T$ as a function of $\lambda$ is usually the objective of monochromator transmission experiments. For strict accuracy (i.e., for adequacy of linear shapes of passbands), the present treatment calls for $\Delta\lambda$ to be

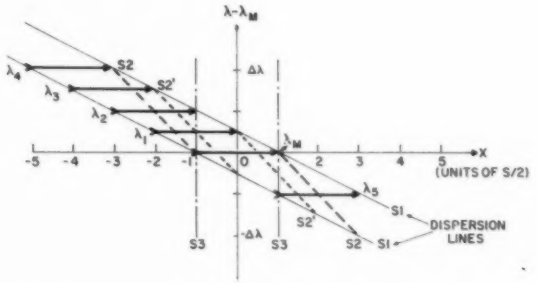


Fig. 5. Distribution of spectral images for the five representative wavelengths in the S3 plane of the dual monochromator whose dispersion is "opposite" in the two sections, obtained in a manner analogous to Fig. 4. This is also the mirror image for the tandem monochromator system with dispersions in the "same" direction (i.e., two identical single monochromators). The dispersion lines (S1) have a slope $-(1/2D)$. The lines S2 represent the intermediate slit with width $s$; S2′ represents the case of half that width. As before, the emitted flux for any wavelength is proportional to the corresponding image length not interrupted by any of the three pairs of limit lines (S) permitting easy determination of passband width, etc.

smaller than an interval over which $T$ would change appreciably, or less than about 100 Å for most applications.

As in Fig. 3, the transmittance, $T$, is always associated with the central wavelength, $\lambda_M$. The actual flux transmitted, $\Phi$, from a continuous source with radiance $W_e$ is easily shown, by integration over the passband, to be:

$$\Phi = W_e(\lambda)\Omega_M T(\lambda)\epsilon\Delta\lambda A_e. \tag{3}$$

Here $A_e$ is the "effective area" of the source, i.e., the area which can be accepted and transmitted by the monochromator. When one slit is narrowed, the transmitted flux decreases because of this factor, not due to a reduction in $T$. As is easily seen from Fig. 3, $\Delta\lambda$ is porportional to the *wider* of the slits. The combination of the foregoing factors indicates that, when slit widths are varied together, the flux varies quadratically.*

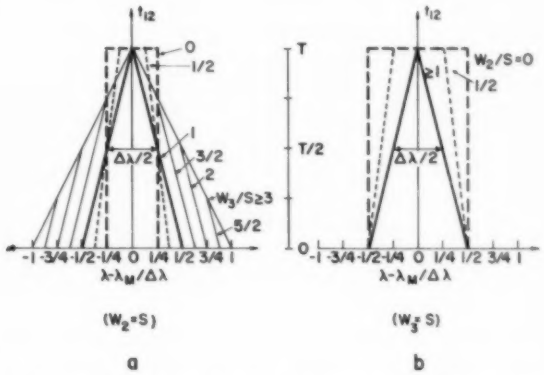


Fig. 6. Calculated passbands of a dual monochromator are shown as the intermediate slit [see (a)] and the exit slit [see (b)] are changed.

In the above equation, $\Omega_M$ is the acceptance solid angle of the instrument, related to $f$-number in the usual way. $\epsilon$ is the absolute efficiency of the instrument so that $\epsilon T(\lambda)$ is the wavelength-dependent absolute transmittance. The fact that this is independent of $\Omega_M$ has been experimentally demonstrated; see Sec. V below.

## III. Double Monochromator Systems

The passband characteristics of systems more complicated than the single monochromator may be determined by extension of the simple imaging techniques used above, combining the lens and dispersion effects.

For example, the dual monochromator is analyzed as follows. The lens action in the second monochromator section reflects the images of Fig. 2 through the $x = 0$ line. The dispersion effect of this section can

* This discussion applies to a continuous source. An equivalent study of the line source is a straightforward extension of the present work.

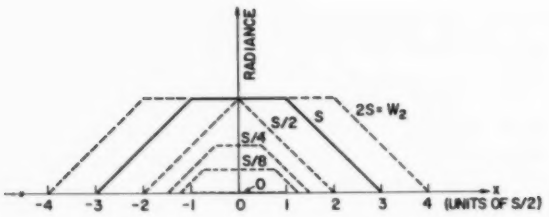


Fig. 7. The calculated radiance in the exit plane of a tandem or dual system is shown for various choices of the intermediate slit-width.

then be the "same" (i.e., again positive) or "opposite" (i.e., negative) as in the previous section, with quite different results. The images in the exit slit (S3) plane for the "same" configuration are shown in Fig. 4. From this it is clear that no double-dispersion effect has occurred; the passband is the same as in the single monochromator case. The combined lens and dispersion action of the second monochromator section, operating on the *ordered* spectrum at the intermediate slit, has only inverted the images.

On the other hand, when the second section has the "opposite" dispersion, the dual monochromator produces double dispersion as shown in Fig. 5. The lens action is the same, but here the second dispersion is to the left, as shown. The effects of this double dispersion are described in the next section.

The tandem monochromator system is very similar to the dual, except that a lens is introduced between the two (constituent) single elements; i.e., S2 may be considered split into two slits, with an intervening lens, operating at 1:1. It is readily apparent that this extra lens serves to cancel the lens action of one of the monochromators; otherwise, the image formation is similar to that in the dual instrument. In fact, we can generalize and obtain the slopes of the dispersion lines at the S3 plane as follows:

$$\text{Slope} = [D_1 + (-1)^L D_2]^{-1},$$

where $L$ is the number of lens actions after the first section and the subscripts refer to the monochromator sections.

Therefore, Fig. 4 also represents the images in the S3 plane of the tandem monochromator with "opposite" dispersions ($D_2 = -D_1$) and Fig. 5, with "same" dispersions ($D_2 = D_1$). (Strictly speaking, the cited figures are mirror images of the true situation.) Thus two identical single monochromators, set up as a dual system, provide a convenient means of attaining double dispersion, the details of which are considered in the next section.

The double-pass monochromator is essentially the same as a single monochromator but with twice the dispersion, which leads to a passband only half as wide as that of the single, as can be seen from Fig. 2.

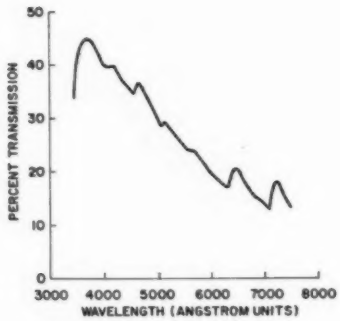


Fig. 8. The absolute transmission is shown as a function o wavelength. These are experimental results.

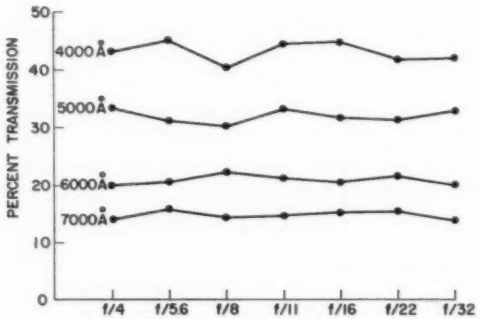


Fig. 9. The absolute transmission for four distinct wavelengths is shown as a function of the *f*-number of the entrance cone of light.

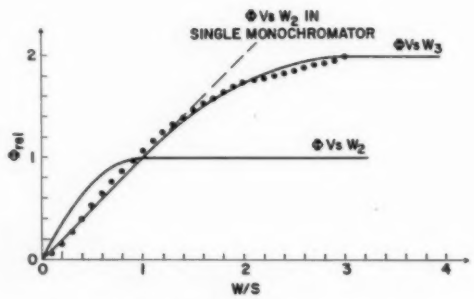


Fig. 10. The total light emerging from a dual (or tandem) monochromator is shown as a function of the slit-widths, $w_2$ and $w_3$, of S2 and S3, respectively. Both curves are calculated and compared with the total light emerging from the single monochromator. Experimental measurements on emergent flux as a function of exit slit ($w_3$) on a tandem monochromator arrangement were made and the results are plotted as solid points. Reasonable agreement with the theoretical curve is shown.

## IV. Double Dispersion Effects

Having established that either the tandem or the dual monochromator can provide double dispersion, we now consider the effects thereby provided. In particular, we are interested in total flux transmitted, shape of the passband, and radiance in the exit slit (S3) plane, all as a function of the widths of slits S2 and S3 (in terms of the width of S1, generally designated as the variable $w_1$ and fixed at a value $s$ ).

These properties can be readily determined by scanning the distribution of images (corresponding to various wavelengths) across the exit slit plane relative to the positions of the slit jaws as shown[4] in Fig. 5. In general, there is an infinite series of images lying between the "dispersion lines"; a few samples are shown. The image of the intermediate slit, S2, cuts off portions of these images, as shown by the dashed, slanting lines. The width of S3, indicated by the vertical broken lines, further restricts the transmission of various wavelengths.

From Fig. 5 the passband for any combination of $w_2$ and $w_3$ can be found. The *intensity* of any wavelength $\lambda_i$ emerging from S3 is given by that length of the image which remains unimpeded by the S2 and S3 construction lines. These intensities are *relative* to that of $\lambda_M$, hence the ordinate of the center of the passband is always taken to be $T$. As in the single monochromator case, this is important when the intensity of $\lambda_M$ is reduced, for $w_3 < s$. In this case, the "effective area", $A_e$, of the source accommodated by the monochromator system is reduced, i.e., by vignetting.

The passbands determined by such an analysis are shown in Fig. 6. In (a), $w_3$ is varied while $w_2$ is held fixed at $s$; and in (b), $w_2$ is varied for $w_3$ fixed at $s$. In the former case, we see that the passband gradually "opens up" from the triangle of half-width $\Delta\lambda/2$ when $w_3 = s$ to the single monochromator situation (triangle of half-width $\Delta\lambda$) for $w_3 = 3s$. It is obvious from Fig. 5 that increasing $w_3$ beyond this has no further effect. For widths narrower than $s$, the triangle becomes a trapezoid and approaches a rectangle in the limit, $w_3 = 0$, with "half-width" constant at $\Delta\lambda/2$. The flux is reduced by the fact that $A_e$ is proportional to $w_3$, as cited above; see Eq. (3).

In case (b), if $w_2 > s$, obviously there is no more light getting through than when $w_2 = s$, so the passband does not change. On the other hand, it is easily seen from Fig. 4 that closing $S_2$ produces a trapezoidal passband (ultimately a rectangle at $w_2 = 0$), but with increasing half-width, up to $\Delta\lambda$ in the limit. Here again, $A_e$ is porportional to $w_2$ because of vignetting.

Figure 5 can also be used to determine the radiance as a function of position, $x$, across S3, for various widths of S2. This quantity, in relative units, is given by the number of images present at any position, i.e., by the vertical height between the dispersion-line or S2-line limits in Fig. 5.

The relative radiance is shown in Fig. 7 for various values of $w_2$, from which several features are apparent: (a) If S2 were absent, the entire exit-plane image would be homogeneously bright; (b) when $w_2 = s$, the exit plane is homogeneously bright over width $s$; (c) in the case (b), there is some radiation at the S3 plane over a total width $3s$; (d) regardless of the size of $w_2$, there is *some* radiation distributed over the full width $s$, going to zero everywhere as $w_2$ is reduced to zero.

## V. Experimental Results

As indicated in the introduction, one of the main motivations for studying the tandem system is to provide a means for measuring the transmittance of one (or both) of the single monochromators. If only the relative (i.e., arbitrarily normalized to unity at its maximum value) transmittance is sought, it is only necessary that all wavelength-dependent factors be taken into account. Thus, for example, geometrical factors leading to vignetting of the beam are inconsequential. This is the approach used in previous work[1] which should be consulted for details of the technique.

On the other hand, it is often desirable to extend the technique to the determination of the absolute transmittance. This consists essentially of introducing a known (i.e., measured) flux at the entrance slit of the second monochromator, $M_2$, and measuring the *total* (i.e., unimpeded by geometrical effects such as stops), flux emerging from its exit slit. The point is, therefore, that the final slit (S4 in the case of the tandem system, S3 in the nomenclature of the dual system) must be wide enough to transmit all the various images present in its plane* and we see from Fig. 7 above, that the minimum width is $3s$. This has been done, and an absolute transmission curve measured in this manner is shown in Fig. 8. These data were taken on a typical 250 mm Bausch & Lomb monochromator with a 600 line/mm grating blazed for 3000 Å. Similar experiments have been done on several other instruments of the same type equipped with similar gratings; the resulting transmission curves are remarkably similar (within $\pm 15\,\%$). The experimental uncertainty on the data shown in Fig. 8 is $\pm 5\,\%$ based on statistical studies of many runs under the same conditions.

It was also of interest to verify that the transmission properties of the monochromator did not depend critically on the numerical aperture of the illumination. The transmission was measured as a function of the size of the cone of light incident on the instrument for several wavelengths. These data are shown in

* We assume, of course, that the detector is homogeneous and wide enough to accept all the incident radiation. Its sensitivity must also be relatively flat over the bandwidth of the emergent beam.

Fig. 9. For all practical purposes, we conclude that the transmission is independent of the numerical aperture of the illumination (up to the $f$/no. of the monochromator, of course). The instrument would obviously vignette if the input beam subtended a solid angle greater than that accepted by the instrument, $f/4$, in this case.

This analysis leads to an inquiry as to how the relative flux emitted from the second monochromator varies with slit-widths; i.e., with $w_2$ and $w_3$, in the terminology of the dual monochromator again. The answer is obtained either from Fig. 7 (by integrating the relative radiance over the available width) or from Fig. 6 and Eq. (3). One experimental verification is shown in Fig. 10 where the total emergent flux $\Phi$ has been plotted as a function of either $w_3$ or $w_2$. Experimental points for variation with $w_3$ are also shown, out to $w_3 = 3s$. The experimental data were averaged over several series of measurements. This result emphasizes the point that the final slit must have width $3s$ to pass all the radiation.

Much of the experimental data quoted in this work is due to the careful work of C. B. Smoyer, W. A. Carlough, and J. Nuñez of this laboratory. In addition, the authors wish to thank C. B. Smoyer for his helpful suggestions and critical reading of this manuscript.

## References

1. R. L. Christensen and I. Ames, J. Opt. Soc. Am. **51**, 22 (1961).
2. P. H. van Cittert, Z. Instrumentenk. **46**, 557 (1926).
3. See, for example, W. E. Forsythe, *Measurement of Radian Energy*, (McGraw-Hill, New York, 1937).
4. See also, van Cittert's work, ref. 2, for a similar figure.

# TOKYO

Lord Todd *Cambridge*, Sir Gordon Sutherland *National Physical Laboratory*, D. M. Dennison *Michigan*, and other participants in Tokyo during the International Symposium on Molecular Structure and Spectroscopy, September 1962.

A. Terenin *Leningrad*, R. R. Brattain *Shell—Emeryville*, and Mrs. Richard C. Lord, wife of the President-Elect of OSA, during the International Symposium on Molecular Structure and Spectroscopy in Tokyo, September 1962.

K. K. Innes *Vanderbilt University*, L. E. Orgel *Cambridge*, and D. A. Ramsay *National Research Council of Canada* during the International Symposium on Molecular Structure and Spectroscopy held in Tokyo, September 1962.

# The Evaporation Rate of Filament Material from Alternating Current Heated Filaments

A. D. Wilson

The operation of an incandescent filament on alternating current of the form, $i = i_0 \sin\omega t$, is reviewed. A model for the ac evaporation rate, in a vacuum of a uniformly heated straight wire, is presented in terms of: (1) The known temperature fluctuations, and (2) The evaporation rate evaluated at the dc and the ac mean filament temperatures. It is shown that the ac evaporation rate can be significantly greater than the dc evaporation rate. A method of evaluating the ac evaporation rate in terms of the spectral modulation is developed.

## Introduction

The rate of evaporation of the filament material for a fixed filament temperature is well known[1] and will, in many instances, determine the "useful life" of an incandescent filament. The net rate of evaporation is a function of both the filament temperature and the partial pressures of gases within the enclosing structure. It has been reported by Johnson[2] that, in an analysis of several thousand "burned out" filaments, investigators discovered that, in a vacuum lamp, 17% of the filament mass had been evaporated while, in gas filled lamps, only 5% had been evaporated.

It is known that the heating of filaments until incandescence with an alternating current causes a small cyclic variation of the filament temperature at a frequency equal to twice that of the heating current. The variation in filament temperature causes a modulation in the radiant energy emitted by the filament. The rate of evaporation is an exponential function of temperature, and thus, intuitively, we conclude that for small temperature variations about a mean value, the net rate of evaporation over one period of the symmetrical temperature variation is greater than that rate of evaporation for the mean temperature. It is this difference which we shall calculate.

Elenbaas[3] has computed the ac rate of evaporation. However, this computation is based upon a mathematical representation for the rate of evaporation of the form $R = A(T)^B$ in which $B$ was considered to be constant over a temperature range $\Delta T$; however, $B$ is not a constant.[4] Furthermore, only the first nonzero term involving the temperature fluctuation has been retained by Elenbaas in the expansion of the ac evaporation rate. The outcome of the present computation is in a closed form and thus is not limited by this restriction. The exponent $B$ can be approximated by the relation $B \approx \nu/T$, where $\nu$ is a constant and $T$ is the thermodynamic temperature of the metal which is being evaporated. A first-order estimate of the error inherent in a computation based upon the assumption $B$ is equal to a constant over a temperature range $\Delta T$ is given in Table I. The error is defined as the difference in the rates of evaporation at a temperature $T_m + \Delta T$ when $B$ is constant, $B_m$, and when $B$ is equal to $\nu/T$, respectively. The difference is normalized with respect to rate of evaporation evaluated with $B$ a constant. The normalized error is approximately equal to $B_m(\Delta T/T_m)^2$. The error has been evaluated (Table I) for $\Delta T/T = 0.10$ and the values of $B_m$ have been taken from the work to follow below.

Nevertheless, Elenbaas' paper is thought by this author to be the only quantitative discussion of the ac rates of evaporation, and it is thus apparent that a very meager amount of attention has been focused on this phenomenon.

**Table I. First-Order Error in the ac Evaporation Rate When $B$ Is Assumed to be a Constant**

| $T_m$(°K) | $B_m$ | Error $\approx B_m\left(\frac{\Delta T_0}{T_m}\right)^2$ (Percent) |
|---|---|---|
| 2000 | 48.3 | 48.3 |
| 2400 | 40.2 | 40.2 |
| 2800 | 34.4 | 34.4 |
| 3200 | 30.1 | 30.1 |

The author is with IBM, General Products Division, Development Laboratory, Endicott, New York.

Received 5 July 1962.

## Analysis

An equation which adequately describes the rate of evaporation of tungsten and other metals, in a vacuum, as a function of temperature has been determined by Langmuir.[5] The approximate form of Langmuir's computation which was found by Reimann[6] to fit experimental data closely is

$$R(T) \approx A' \exp\,[-q_0/KT], \tag{1}$$

where

$A'$ = constant, in units of g cm$^{-2}$ sec$^{-1}$,
$K$ = Boltzmann constant, $1.38 \times 10^{-16}$ erg/°K,
$R(T)$ = rate of evaporation in g/cm$^2$ sec,
$q_0$ = energy of evaporation per atom of metal at $T = 0$, erg, and
$T$ = absolute temperature of the filament, °K.

The physical assumptions which Langmuir made in his original computation are: (i) the third law of thermodynamics is valid in this problem, (ii) the reflection of molecules from the surface of the metal takes place to a negligible degree only; i.e., the "sticking coefficient" is approximately one (1), and (iii) the volume of the metal is very small as compared with the volume of the vapor produced by evaporation. It is probable that Eq. (1) represents the rate of evaporation of tungsten over a temperature range of 2000 to 3500°K with a considerable degree of accuracy when the proper numerical values of $A'$ and $q_0$ are used. Langmuir found for tungsten a value of $1.333 \times 10^{-11}$ ergs for $q_0$, the energy of evaporation at absolute zero per atom of metal. From the experimental data of Reimann, the exponent $q_0$ is found to be numerically equal to the energy of evaporation of Langmuir to three significant figures. The thesis of this paper is not completely dependent upon the interpretation of the exponent $q_0$ being the energy of evaporation at absolute zero or the free energy of the system; however, it is assumed that $q_0$ is constant over a temperature range $\Delta T$, and that $q_0$ has been judiciously chosen so that Eq. (1) adequately describes the temperature dependence of the rate of evaporation over a range in temperature $\Delta T$. The numerical value of $q_0$ used here is that found by Langmuir and also by Reimann.

To obtain an expression for the ac rate of evaporation, one first needs to determine the temperature of the filament as a function of time. The dependence of the filament temperature on time, of an ac-heated filament, has been investigated by Corbino,[7,8] Langmuir,[9] and others. A good approximation of the instantaneous filament temperature, $T$, is given by:

$$T = T_{m1} + \Delta T, \tag{2a}$$

$$\Delta T = \Delta T_0 \sin(2\omega t + \phi), \tag{2b}$$

where $|\Delta T_0| \ll T_{m1}$.
Equation (2) is derived for a straight wire of well-behaved geometrical cross section which is uniformly heated in a vacuum by a current of the form: $i = i_0 \sin\omega t$. It is assumed that the conduction and energy evaporation losses are negligible in comparison with the radiation losses. The magnitude of the peak-to-mean value of the temperature, $\Delta T_0$, is:

$$\Delta T_0 = -\left[\frac{\psi T_{m1}}{4(\psi^2 + 4\omega^2)^{1/2}}\right], \tag{3a}$$

where

$\psi$ = $4T_{m1}{}^3(P\epsilon\sigma/C'\delta A)$,
$\sigma$ = Stefan-Boltzmann constant, $5.67 \times 10^{-5}$ erg cm$^{-2}$ sec$^{-1}$ °K$^{-4}$,
$\epsilon$ = total emissivity,
$\delta$ = density of filament material g/cm$^3$,
$C'$ = specific heat of filament, ergs/(g °K),
$p$ = periphery of filament cross section, cm,
$A$ = area of filament cross section, cm$^2$,
$\omega$ = angular frequency, rad/sec, and
$T_{m1}$ = absolute mean filament temperature, °K.

The phase term $\phi$ in Eq. (2) is: $\phi = \tan^{-1}(\psi/2\omega)$ If it is assumed that $\psi/2\omega \leq 10^{-1/2}$, then Eq. (3a is approximated with an error of less than 5% by the simple expression:

$$\Delta T_0 = -[(\sigma P/\delta A)(\epsilon T_{m1}{}^4/C')(1/2\omega)]. \tag{3b}$$

The validity of the assumption that $\psi/2\omega \leq 10^{-1/2}$ can be established for a practical case by considering for example, a filament operating at a mean thermodynamic temperature of 3000°K which has a periphery-to-cross section ratio ($P/A$) of 4000 cm$^{-1}$. From the accepted values for the physical constants of tungsten at 3000°K, the value of $\psi/2$ is computed: $\psi/2 \approx 101$ rad/sec. Therefore, for Eq. (3b) to be valid, the angular frequency, $\omega$, of the heating current must satisfy the relation $\omega \geq (10^{-1/2})\ 101$ rad/sec. A frequency of 60 cps satisfies this condition. The restriction of $\psi/2\omega \leq 10^{-1/2}$ is equivalent to requiring $(|\Delta T_0|/T_m) \leq (10^{-1/2}/4)$, which is consistent with the derivation of Eqs. (2a), (2b), and (3a).

The negative sign in Eqs. (3a) and (3b) arises because of the choice of the sign of $\Delta T$ in Eq. (2a), and the particular choice of sinusoid in Eq. (2b). The temperature is observed to attain its maximum value, $T_{m1} + |\Delta T_0|$, at a time $t_m + \tau_0$, where $t_m$ is the point in time of maximum current $i_0$ and $\tau_0 = 1/\omega(\pi/4 - \phi)$.

The calculation of the ac rate of evaporation is accomplished by considering Eq. (1) above as the instantaneous rate of evaporation. This implies that the allowed temperature fluctuations are bounded above by a frequency so that the equilibrium between the vapor and solid metal is not disturbed. The substitution of the instantaneous temperature [Eq. (2)], $T = T_{m1} + \Delta T$, into the expression for the instantaneous rate of evaporation [Eq. (1)] yields:

$$R(T_{m1}, \Delta T_0, t) = R(T_{m1}) \exp\left[(q_0/K)\left(\frac{\Delta T_0}{T_{m1}{}^2}\right)\sin(2\omega t + \phi)\right]. \tag{4}$$

The term $R(T_{m1})$ is the evaporation rate at a temperature $T_{m1}$. The temperature $T_{m1}$ is the mean temperature of the ac heated filament. The relation of this temperature ($T_{m1}$) to the mean temperature of the filament attained under the conditions of equal rms current and zero temperature fluctuations (dc or "high" frequency ac current) will be given below. Equation (4) is the instantaneous rate of evaporation as a function of $T_{m1}$, $\Delta T_0$, and time $t$. Of more interest is the rate of evaporation averaged over one time period of the temperature variation. Defining, $\alpha = (q_0/K)(\Delta T_0/T_{m1}^2)$, and then expanding the term exp $[\alpha \sin(2\omega t + \phi)]$ of Eq. (4) in modified Bessel functions, one obtains for the average rate:

$$\langle R(T_{m1}, \Delta T_0, t)\rangle_t = (1/\tau)\int_0^\tau R(T_{m1}, \Delta T_0, t)dt \qquad (5)$$

$$\langle R(T_{m1}, \Delta T_0, t)\rangle_t = [R(T_{m1})/\tau]\int_0^\tau \Big\{I_0(\alpha) + 2\sum_{K=1}^{\infty}(j)^{2K}I_{2K}(\alpha)\cos[2K(2\omega t)] - 2\sum_{K=1}^{\infty}(j)^{2K}I_{2K-1}(\alpha)\sin[(2K-1)(2\omega t)]\Big\}\,dt. \qquad (6)$$

The two infinite series within the braces $\{\ \}$ may be shown to converge uniformly for all $\alpha$; therefore, the operations of integration and summation in Eq. (6) may be interchanged. Performing this interchange and then integrating term by term yields the simple expression below for the time average of the instantaneous rate of evaporation:

$$\langle R(T_{m1}, \Delta T_0)\rangle = R(T_{m1})I_0(\alpha), \qquad (7)$$

where $I_0(\alpha)$ is the modified Bessel function of the first kind of zero order. When there are zero temperature fluctuations, $\alpha = 0$ and $I_0\ (0) = 1$;[10] therefore, $\langle R(T_{m1}, 0)\rangle = R(T_{m1})$, as should be expected. To determine the ac rate of evaporation it is therefore necessary to know only the physical properties of the filament material, the geometrical parameters of the filament, and the rate of evaporation at a temperature $T_{m1}$. The parameter $\alpha$ may be evaluated from the expression

$$\alpha = [(q_0\sigma/K\delta)(P/A)(\epsilon T_m^2/C')(1/2\omega)], \qquad (8)$$

and thus $I_0\ (\alpha)$ determined. $\alpha$ has now been taken to be positive since there is no physical significance in the minus sign of Eq. (3a). $I_0(\alpha)$ is a rapidly increasing function of the parameter $\alpha$; thus, if a filament is selected with either a large ratio of periphery-to-cross section, $P/A$, or a low current frequency, $\omega$, or both of these conditions simultaneously, a rate of evaporation which is considerably greater than the rate evaluated at the filament mean temperature will occur.

To compare the evaporation rate of a filament operated on a "low-frequency" sinusoidal current to the corresponding evaporation rate of a filament first operated on a direct or "high-frequency" current, it is first necessary to determine a relation between the respective mean temperatures. The two mean temperatures are not equal. The difference is a second-order function of the temperature variation, $\Delta T_0$. Elenbaas[11] has shown that, for two filaments operated at voltages so that the rms value of the instantaneous voltage, $v = V_0 \sin \omega t$, is equal to the dc voltage (or an rms ac voltage of a frequency so that $\Delta T_0 \to 0$), the temperature ratio is given by:

$$\left.\frac{T_{m1}}{T_{m2}}\right|_{\substack{\text{effective}\\ \text{voltages equal}}} = 1 - \left(\frac{a+b-1}{4}\right)(\Delta T_0/T_{m1})^2, \qquad (9)$$

where

$T_{m2}$ = mean temperature of dc (or ac such that $\Delta T_0 \to 0$) heated filament,
$a = 4 + \mu$,
$\mu = (T/\epsilon)(d\epsilon/dT)$,
$b = (T/\rho)(d\rho/dT)$, and
$\rho$ = specific resistivity.

Terms involving $(\Delta T_0/T_{m1})^n$ with $n > 2$ have been neglected in arriving at the approximate value for $T_{m1}/T_{m2}$ in Eq. (9). One can also show, following an approach similar to Elenbaas', that from a consideration of the energy balance equation (neglecting conduction and evaporation losses) a similar approximate relation for the ratios of the *mean* temperatures is obtained when the rms value of the current $i = i_0 \sin \omega t$ is made equal (for purposes of comparison) to the filament direct current (or an rms alternating current of a frequency so that $\Delta T_0 \to 0$). The ratio of the mean temperature $T_{m1}$ of a filament with a temperature fluctuation $\Delta T_0$ to the mean temperature of the same filament with no temperature fluctuations, $T_{m2}$, under the constraint of equal rms current is given by the approximate equation:

$$\left.\frac{T_{m1}}{T_{m2}}\right|_{\substack{\text{effective}\\ \text{currents equal}}} \approx 1 - \gamma\left(\frac{\Delta T_0}{T_{m1}}\right)^2, \qquad (10)$$

where

$$\gamma = \left(\frac{a+b-1}{4} - \frac{2b}{a-b}\right).$$

To demonstrate the difference in the rates of evaporation between a filament with temperature fluctuations and one without, when operated at an equivalent effective current, consider a tungsten filament in a vacuum with a periphery to cross section ratio $(P/A)$. From Eqs. (3b) and (8), the quantities $\Delta T_0[f(P/A)]$ and $\alpha[f(P/A)]$, respectively, have been computed for tungsten at several temperatures and tabulated in Table II. To make these calculations, the specific heat $C'$ was obtained from the relation $C' = (4H'/\delta\pi)$ where $H'$ is from the data of Jones and Langmuir.[12] The total emissivity was obtained from the data of

**Table II. Normalized Temperature Fluctuations $\Delta T_0$ and $\alpha$ and Corresponding $I_0(\alpha)$ as a Function of Temperature for Tungsten**

| $T_{m1}$ (°K) | $B \approx \frac{\nu}{T_{m1}} = \frac{q_0}{KT_{m1}}$ | $\epsilon$ | $H^1 \times 10^7$ (ergs/cm³ −°K) | $R(T_{m1})$ (g cm$^{-2}$ sec$^{-1}$) | $\Delta T_0\left(\frac{f}{P/A}\right)$ (°K-cm-cps) | $\alpha\left(\frac{f}{P/A}\right) \times 10^2$ (cm-cps) | $\psi(P/A) \times 10^2$ (cm rad/sec) | $\frac{f_{min}}{(P/A) \times 10^2}$ (cm-cps) |
|---|---|---|---|---|---|---|---|---|
| 2000 | 48.3 | 0.259 | 2.66 | $7.48 \times 10^{-14}$ | 0.552 | 1.33 | 1.40 | 3.51 |
| 2400 | 40.2 | 0.294 | 2.87 | $2.32 \times 10^{-10}$ | 1.22 | 2.02 | 2.54 | 6.37 |
| 2800 | 34.4 | 0.321 | 3.07 | $7.20 \times 10^{-8}$ | 2.28 | 2.80 | 4.12 | 10.32 |
| 3000 | 32.2 | 0.334 | 3.18 | $7.14 \times 10^{-7}$ | 3.02 | 3.23 | 5.07 | 12.75 |
| 3200 | 30.1 | 0.341 | 3.22 | $5.33 \times 10^{-6}$ | 3.95 | 3.72 | 6.23 | 15.65 |
| 3400 | 28.4 | 0.348 | 3.38 | $3.14 \times 10^{-5}$ | 4.88 | 4.06 | 7.25 | 18.20 |

Forsythe and Watson[13] and the evaporation rate from the data of Reimann.[14] No corrections for possible differences in the experimental temperature scales have been made (i.e., the data of Table II are as found in the literature). Table II includes computed values of $\psi/(P/A)$ from Eq. (3a) and $f_{min}/(P/A)$ where $f_{min}$ satisfies the condition $\omega_{min} = (10^{-1/2}/2)\psi$ and $f_{min} = 2\pi\omega_{min}$. Constructed in Table III are numerical values of $\Delta T_0$, $\alpha$, and $I_0$ ($\alpha$) for several filament temperatures as a function of multiples of $f_{min}/(P/A)$. If it is desired to know the ac evaporation rate for frequencies below $f_{min}$, keeping $(P/A)$ a constant, then it is necessary to use Eq. (3a) rather than Table III since Table III is derived assuming Eq. (3b) to be valid. As an example in the use of Tables II and III, consider a ribbon filament at 3000°K heated by 60 cps current whose width is very much greater than the thickness, thus $P/A \approx 2$ thickness. Let the thickness be chosen so that $f/(P/A) = f_{min}/(P/A)$, that is, thickness $= 4.25 \times 10^{-3}$ cm which follows from Table II. From Table III, one finds that at 3000°K and 60 cps ($f_{min}$) $\Delta T_0 = 237$°K, $\alpha = 2.54$ and $I_0(\alpha) = 3.39$. One can thus conclude that the rate of evaporation of the filament with the temperature fluctuation of 237°K (peak) is 3.39 times as large as a filament with no fluctuations, both operating at the *same mean temperature* of 3000°K; that is, $\langle R(T_{m1}, \Delta T_0)\rangle = I_0(2.54)\, R(T_{m1}) = 3.39\, R(T_{m1})$. Since we are interested in comparing the evaporation rates of the filament heated by the same effective current, it is thus necessary to determine $R(T_{m2})$ in terms of $T_{m1}$ making use of Eq. (10). Hence,

$$R(T_{m2}) = R(T_{m1}) \exp\left[\left(\frac{\gamma K T_{m1}}{q_0}\right)\alpha^2\right] \tag{11}$$

An expression similar to Eq. (11) can be computed for the condition of equal effective voltage by making use of Eq. (9), and thus, in general,

$$\frac{\langle R(T_{m1}, \Delta T_0)\rangle}{R(T_{m2})} = I_0(\alpha) \exp\left[\left(\frac{-\gamma K T_{m1}}{q_0}\right)\alpha^2\right], \tag{12}$$

where the correct value of $\gamma$ has been chosen depending upon the type of comparison: equal effective voltage or current.

For the above examples, one therefore finds for the ratio, $\langle R(T_{m1}, \Delta T_0)\rangle / R(T_{m2})$, a value $\approx 3.39\, e^{-0.138} \approx 2.78$. It has thus been shown that the evaporation rate of the example filament experiencing symmetrical temperature variations is 2.78 times greater than the evaporation rate of the filament when it is experiencing no temperature variations, yet heated with the *same effective current*.

The ratio of the rates of evaporation evaluated for equal effective (1) current and (2) voltage is greater than or equal to one (1). We can show from Eqs. (9), (10), and (12) that this ratio is given by the equation

$$\frac{\langle R(T_{m1}, \Delta T_0)\rangle|R(T_{m2})|_I}{\langle R(T_{m1}, \Delta T_0)\rangle|R(T_{m2})|_V} = \exp\left\{\left(\frac{2b}{a-b}\right)\left(\frac{KT_{m1}}{q_0}\right)\alpha^2\right\}. \tag{13}$$

Recently, two quantitative papers discussing the modulation of radiant energy have appeared in the literature.[15,16] There is an interesting relation for $\alpha$ which can be derived from this modulation and used experimentally to assist in evaluating the ac rate of evaporation. The spectral modulation defined as

**Table III. $\Delta T_0$, $\alpha$, and $I_0(\alpha)$ as Functions of Frequency, $f_{min}$, and Temperature for a Fixed $P/A$**

| | $\Delta T_0$ (°K) | | | $\alpha$ | | | $I_0(\alpha)$ | | |
|---|---|---|---|---|---|---|---|---|---|
| $T_{m1}$ (°K) | $f_{min}$ | $2f_{min}$ | $3f_{min}$ | $f_{min}$ | $2f_{min}$ | $3f_{min}$ | $f_{min}$ | $2f_{min}$ | $3f_{min}$ |
| 2000 | 157 | 78.5 | 51 | 3.80 | 1.90 | 1.27 | 9.53 | 2.13 | 1.45 |
| 2400 | 191 | 95.5 | 63.5 | 3.17 | 1.59 | 1.06 | 5.56 | 1.72 | 1.29 |
| 2800 | 221 | 110 | 73.6 | 2.71 | 1.36 | 0.91 | 3.84 | 1.52 | 1.22 |
| 3000 | 237 | 118 | 79 | 2.54 | 1.27 | 0.85 | 3.39 | 1.45 | 1.17 |
| 3200 | 252 | 126 | 84 | 2.38 | 1.19 | 0.78 | 2.94 | 1.40 | 1.15 |
| 3400 | 268 | 134 | 89.5 | 2.23 | 1.12 | 0.75 | 2.66 | 1.32 | 1.14 |

$$M_\lambda = \frac{\text{Energy emitted at } T - \text{Energy emitted at } T_m}{\text{Energy emitted at } T_m}$$

was computed from Planck's radiation equation by Tolles and Ihrig. Their approximation is

$$M_\lambda \approx \left|\frac{c_2}{\lambda}\left(\frac{\Delta T_0}{T_m{}^2}\right)\right|, \tag{14}$$

where

$\lambda$ = wavelength of the radiant energy, cm,
$c_2$ = second radiation constant, 1.4388 cm °K.

From Eq. (14) $\alpha$ is computed in terms of the modulation $M_\lambda$:

$$\alpha = (q_0/kc_2)(\lambda M_\lambda). \tag{15}$$

The product $(\lambda M_\lambda)$ is easily determined experimentally for a given filament and operating conditions. Therefore, $\alpha$ may be evaluated without use of Eq. (8) by using Eq. (15) and experimental data $(\lambda M_\lambda)$ instead. The ac rate of evaporation can then be computed from Eq. (7).

## Conclusions

The average rate of evaporation of filament material from an ac heated filament has been computed in terms of the temperature fluctuations and in terms of (1) the rate evaluated at the filaments mean temperature, and (2) the rate evaluated at the mean temperature a filament would attain if no temperature fluctuations were present and the respective effective currents were made equal. A relation has been presented to determine the parameter $\alpha$, which is a function of the temperature fluctuations in terms of an experimentally measurable quantity, the spectral modulation. The ac evaporation rate has been found to be greater than the dc evaporation rate under the constraint of either equal effective current or voltage. Furthermore, the ac rate of evaporation, under the constraint of equal effective current is greater than the ac rate of evaporation under the constraint of equal effective voltage.

The author wishes to thank H. B. Ulsh of this laboratory for several helpful discussions.

## References

1. H. A. Jones, I. Langmuir, and G. M. J. Mackay, Phys. Rev. **30,** 201 (1927).
2. R. P. Johnson, Phys. Rev. **54,** 459 (1938).
3. W. Elenbaas, Physica **5,** 929 (1938).
4. W. E. Forsythe and A. G. Worthing, J. Astrophys. **61,** 153 (1925).
5. Ref. 1, p. 206.
6. A. L. Reimann, Phil. Mag. **25,** 834 (1938).
7. O. M. Corbino, Physik Z. **11,** 413 (1910).
8. O. M. Corbino, Physik Z. **12,** 292 (1911).
9. I. Langmuir, Gen. Elec. Rev. **17,** 294 (1914).
10. For tabulated values of $I_0(\alpha)$ see E. Jahnke and F. Emde, *Tables of Functions* (Dover, New York, 1945), p. 226.
11. W. Elenbaas, Physica **5,** 932 (1938).
12. H. A. Jones and I. Langmuir, Gen. Elec. Rev. **30,** 313 (1927).
13. W. E. Forsythe and E. M. Watson, J. Opt. Soc. Am. **24,** 117 (1934).
14. A. L. Reimann, Phil. Mag. **25,** 842 (1938).
15. W. E. Tolles and L. C. Ihrig, J. Opt. Soc. Am. **47,** 101 (1957).
16. W. J. Condell and F. T. Byrne, J. Opt. Soc. Am. **47,** 1135 (1957).


# November is the Coblentz Commemorative Issue

# The Publications of W. W. Coblentz on Infrared Spectroscopy

The principal work of the late W. W. Coblentz on infrared spectroscopy originally appeared in three Publications of the Carnegie Institution of Washington. Publication No. 35, issued in 1905, dealt with his investigations at Cornell University of the infrared absorption spectra of some 135 organic compounds, with shorter supplementary sections on transmission and reflection spectra. Publication No. 65 (1906) and Publication No. 97 (1908) are concerned with later work on the transmission and reflection spectra of minerals and other inorganic compounds carried out at the U.S. Bureau of Standards.

These classical investigations form the basis of most modern work on analytical infrared spectroscopy. The journals have long been out of print, but, with the kind permission of the Carnegie Institution, they have recently been reprinted in a single volume under the joint sponsorship of the Coblentz Society and the Perkin-Elmer Corporation.

All concerned with modern applications of infrared spectroscopy to problems of chemical structure and analysis should be conversant with this early work, which provides the basis for much of the modern technique. To maintain a properly balanced outlook on the subject, this volume should accompany the standard modern texts on the library shelf of the spectroscopy laboratory.

A limited number of copies of the first reprinting are still available at $3.50 per copy on application to Dr. H. B. Kessler, The Secretary, c/o The Perkin-Elmer Corporation, Norwalk, Connecticut.

*continued from page 1042*

the corresponding coordinate in related molecules (e.g., ethylene and its derivatives). Pimentel and Moore explain this result in terms of a molecular structure based on two resonating forms, $H_2C{=}N{=}N$ and $H_2C{-}\overset{+}{N}{\equiv}N$, the former having trigonal and the latter tetrahedral bonding at the carbon atom. They also suggest that this model might account for the extraordinary high intensity of the overtone.

There was considerable interest expressed in vibrational anharmonicity and the higher terms in the potential energy. Under the chairmanship of E. B. Wilson *Harvard*, V. W. Laurie *Stanford* and L. S. Bartell *Iowa State* entered a spirited debate on the relative merits of spectroscopic and electron-diffraction methods for the determination of molecular geometry. Each speaker stressed, in his individual way, the importance of including corrections based on anharmonic constants to the apparent geometrical parameters in order to obtain the most precise results from experimental data.

Recent developments in infrared intensities came up for discussion: G. Thyagarajan and P. Schatz *University of Virginia* pointed out that, in making direct measurements of absorption intensities of thin solid films deposited on optically dense plates, a correction, often as large as 10%, must be applied for reflection effects. Further, these effects can lead to marked distortion of the true band shape, especially with intense narrow bands. Of the many other intensity papers, one by J. C. Breeze and C. C. Ferriso *General Dynamics/Astronautics* appeared particularly interesting. These authors have used shock-tube techniques to heat $CO_2$ gas and have measured the total emission from the 2.7 $\mu$ resonance doublet at temperatures in the range 1000° to 3000°K. They find the total intensity to be moderately temperature dependent and their experimental points fall almost exactly on a curve calculated on the assumption that all the intensity is attributable to the transition $\nu_1 + \nu_3$ and none to $2\nu_2 + \nu_3$. This looks like a promising approach to the problem of unscrambling the intensity contributions of the several components in resonance multiplets. More shock-tube work was reported by R. C. Millikan *GE-Schenectady* who described some of his recent work on carbon monoxide. In his experiments, the carbon monoxide was translationally heated in the shock, and by observing the total emission in the fundamental region, Millikan was able to detect the vibrationally excited molecules. He found that, after the shock front passed, there was an initial lag followed by a rise in the population of the vibrationally excited state as equilibrium was established. The experimental curve fits the Decius rate equation suggesting that a stair-climbing process is involved. He also described some vibrational fluorescence studies in which carbon monoxide was irradiated by an infrared beam and its emission spectrum observed at right angles to the direction of illumination. From the intensity distribution in the spectrum the vibrational and rotational temperatures were found to be respectively, 1000°K and 300°K. Millikan also reported some preliminary quenching studies which indicate that, in general polyatomic molecules are efficient quenchers of this vibrational fluorescence.

A great deal of interest was expressed in the question of molecular rotation in condensed phases—a question which is worrying many practitioners of the matrix isolation technique. A. Cabana and D. F. Hornig (*Princeton University*) presented some interesting results on methane and methane-$d_1$ in rare gas crystals. Their results appear consistent with a hindered-rotation model but details remain to be worked out.

Although this report is incomplete and biased in the direction of molecular vibrations, the reporter hopes it covers some high points of the meeting and indicates some current trends in spectroscopic research. As always, apology must be offered for any misrepresentations and emissions—these are the responsibility of the reporter. Columbus has become a tradition in spectroscopy; it is heartening to find the attendance growing and we look forward to another successful meeting in 1964.

## References


1. G. Eckhardt, R. W. Hellwarth, F. J. McClung, S. E. Swartz, and D. Weiner, Phys. Rev. Letters **9**, 455 (1962).
2. M. J. Golay, J. Opt. Soc. Am. **39**, 437 (1949).
3. J. B. Howard, J. Chem. Phys. **5**, 451 (1937).
4. B. L. Crawford, W. H. Fletcher, and D. A. Ramsay, J. Chem. Phys. **19**, 406 (1951).


## Applied Optics BOOKS

*Books for review should be submitted to the Managing Editor. APPLIED OPTICS, 1155 16th St., N.W., Washington 6, D.C.*

**A Photographic History of Mars, 1905 to 1961.** By E. C. Slipher. Lowell Observatory, in conjunction with Sky Publishing Corporation, Cambridge, Massachusetts, and Northland Press, Flagstaff, Arizona. 162 pp. $8.50.

This monograph presents the results of a lifetime devoted to the observation of Mars: its author has studied the planet intensively, both visually and photographically, for over half a century. In this time he has obtained nearly two-hundred thousand photographic images of the planet, a few thousand of which are represented by the hundreds of composite images reproduced in this book. The official Air Force edition, reviewed here, is substantially identical with the civil edition distributed by Sky Publishing Corporation, except for cover color and title page (the civil edition is called *The Photographic Story of Mars*).

The volume begins with 70 pages of text, divided into seven chapters. For the most part these are introductory or only semi-technical, although Chapter III contains quantitative data on the melting of the South Polar Cap which impressively demonstrate the regularity of seasonal phenomena.

Chapter V is an excellent discussion of the violet layer and the controversial "blue clearing" on Mars, and is strengthened by a wealth of previously unpublished statistical data on the subject. There is a strong dependence of clearing on central meridian, with a preponderance of clearings near the longitude of Syrtis Major. It is not certain whether this is simply an observational effect resulting from the prominence of this and other nearby dark markings, or whether the atmosphere is really clearer on this side of the planet. Since the *median* value of clearing is practically the same near opposition as it is sixty or more days from opposition, the well-known high frequency of clearings very near to opposition must be largely an observational selection effect; most observations are concentrated near opposition, so that a clearing at this time is most likely to be detected. But in spite of the importance of selection effects, the blue photographs clearly show that large variations in the visibility of the surface markings occur, sometimes within a few hours.

The second half of the book consists of some fifty plates, each of which contains several composite images of Mars. Each plate is accompanied by a page of text which describes in detail the phenomena shown in the pictures. In addition, a few maps and drawings are included for comparison, and one plate shows the results of terrestrial photographic experiments which assist the

*continued on page 1087*

# Interferometric Measurement of Vibration Amplitudes

Glenn E. Bowie

As part of an investigation of contact-stress problems, it became necessary to build an interferometer to calibrate certain strain transducers. The strain under investigation was produced by simple harmonic stresses with loads consisting of internal energy dissipation. The calibration was performed under unloaded conditions. The results of this calibration gave confidence in the validity of the method used. The disappearing Fizeau fringe technique was used in the interferometric measurement of vibration amplitudes.

An interferometer has been constructed specificially for calibrating electrical measures of displacements from devices that sense motion produced by piezoelectric driving elements. However, the mechanical design of the instrument anticipates future use as a laboratory standard for calibrating a wide range of both displacement- and strain-measuring transducers. This interferometer is pictured in Fig. 1. The discussion is restricted to consideration of Fizeau-type interferometers in which beams of light interfere after encountering a wedge-shaped air gap between two closely spaced optical surfaces. It is now fairly common for instruments of this type to be applied to the problem of measuring small displacements of an object undergoing cyclic linear motion. In the present case, a front-surface mirror is attached to the free end of a driving transducer, and a transparent surface is brought close to the former. In one technique that has two variations, one of which was used here, monochromatic light directed onto the air gap between the two optical surfaces consists of stroboscopic flashes at a repetition rate that is a rational fraction of the frequency of mechanical motion. In one variation, interference fringes move slowly across a field of view when a phase shifter in a circuit producing the stroboscopic flashes is caused to vary slowly the phase of the flashes. The positions of the phase-shifter controls corresponding to the maximum and minimum amplitudes of motion are found, and an observer counts the number of fringes passing a fixed reference point in the field of view when the phase of the flashes is changed from one position to the other. This procedure was discussed by Smith *et al.*[1] However, in the present study, phase shifting was accomplished in the electrical circuit causing the mechanical motion being observed. This variation of the technique was chosen because it had been decided to perform experiments at a driving frequency of 60 cps, and suitable phase-shifting equipment was available from earlier work.

In a second technique, called the fringe-disappearance method, a steady beam of light is used in an interferometer. The method is based on the observation, reported by Thomas and Warren[2] in 1928, that, as the amplitude of motion of one optical surface with respect to another is increased from zero, interference fringes can be seen to become indistinct, disappear, reappear, and alternatively disappear and reappear as the amplitude is increased. The name of the method attests to the fact that amplitudes for fringe disappearances can be found with greater precision than amplitudes for which the fringe intensities are maxima. A somewhat loosely defined requirement of the method is that the frequency of motion observed should be greater than the critical flashing rate below which the eye can detect alternations in brightness. According to Monk,[3] this rate is about 30 times/sec. In the past, the utility of the fringe-disappearance method has been based on the fact that for two-beam interferometers (defined below) a discrete set of ratios of amplitude of motion to wavelength of light at which the disappearances take place can be theoretically predicted. Some care was required in applying the method with the interferometer discussed here because it belongs to the class of multiple-beam interferometers for which a detailed discussion of fringe disappearances has not been published.

The author is with the University of Minnesota, Minneapolis, Minnesota.

Received 7 August 1962.

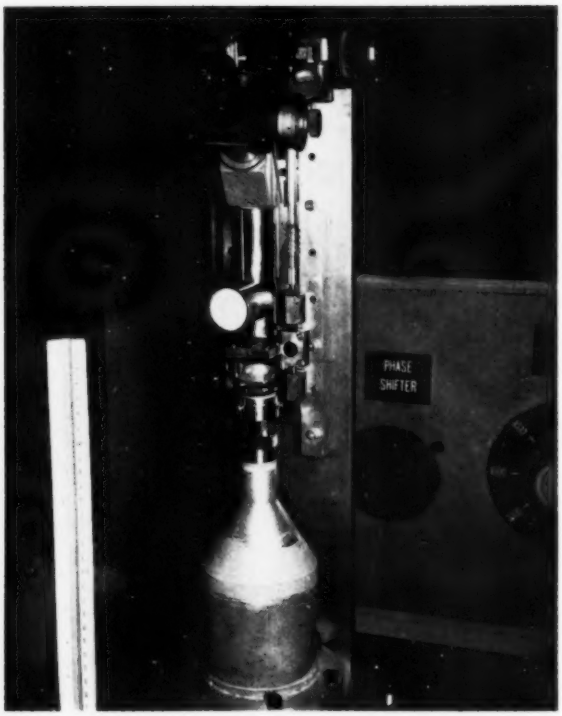


Fig. 1. Interferometer for calibrating piezoelectric driving transducer.

## Construction of the Interferometer

In a two-beam interferometer a beam of light is divided by reflection into two beams of approximately the same intensity in such a way that the divided beams travel different optical paths and then are recombined to form an interference pattern. The reflecting surfaces commonly are uncoated glass, for which a reflection coefficient of 0.04 is often quoted. The resolution of such an instrument is limited by the fact that the intensity of light within the fringe follows a $\cos^2$ distribution in which the light and dark regions are of similar area. In a multiple-beam interferometer, a single beam is divided multiply by reflection into many beams, which upon recombination under proper conditions produce narrow interference fringes sharply defined in a uniform background. Fringes are dark lines in a bright background when viewed in back-reflected light or bright lines in a dark background in transmitted light. The geometry of the object whose motion is to be measured often dictates that back-reflection techniques be used. Such was the case, for example, with an instrument described by Edelman *et al.*[4] in 1955. Their interferometer was of the two-beam Fizeau type in which Newton's rings were observed between a glass flat placed on a moving object and a planoconvex lens placed at the focus of a 2× microscope objective. (In a Fizeau-type interferometer, fringes are localized in an air gap and thus can be viewed in a microscope.) Light was introduced into their interferometer by directing it on a diagonal placed between the objective lens and a microscope ocular.

In the present case, fringes are formed in an air gap between two flat optical surfaces on 25.4-mm diam by 12.7-mm thick fused-quartz disks. One of the disks is a front-surface mirror with a polished coating of aluminum. The makers of the flats, at E and W Optical Company, Minneapolis, stated that the front-surface mirror has a reflection coefficient of approximately 0.9 for incident light having a wavelength of the order of 0.5 $\mu$. The flat surfaces of the second disk were optically polished, and a transparent coating of titanium dioxide was deposited on one of the flat surfaces. The second flat has a reflection coefficient of 0.37 for green light of mercury incident at 15°. The flat is a type commonly used in machine-shop metrology for examination of surface irregularities and has a titanium-dioxide coating of a thickness optimal for this purpose. Much sharper fringes are obtained than with an uncoated flat. In Figs. 3 and 4 and in the following discussion, the disk having a front-surface mirror is identified as mirror B, and the disk with a transparent coating as mirror A.

There are incorporated in the interferometer means of holding the two mirrors, of introducing parallel rays of light, and of viewing interference fringes. Before the mirrors are placed in their respective holders, their cylindrical surfaces are each wrapped with a protective strip of Mylar. Mirror B is placed in a closely fitted holder shown in cross section in Fig. 5 and is held firmly in position by three screws, which are equally spaced about the circumference of the holder and located at midheight of the mirror. The arrangement for holding mirror A is more complicated. The mirror is mounted on a slide mechanism that can be translated in a direction perpendicular to the mirror surfaces when a two-pitch screw, identified in Fig. 5, is driven through a worm-gear reducer. One initiates translation by turning a knob attached to the input shaft of the reducer. A complete turn of the knob causes mirror A to move approximately 2.5 $\mu$. This feature allows one to make fine adjustments in the thickness of the air gap between mirrors A and B and makes the instrument applicable as a laboratory standard for calibrating transducers, such as Statham gauges, that sense small changes in the distance between two gauge points. The wedge angle between mirrors A and B also can be adjusted. Mirror A is held by three screws in a ring that is separated from an upright portion of the slide mechanism by a rubber cushion. Four screws pass through body-size holes in the upright and the rubber and enter tapped holes in the ring. The wedge angle is changed by rotating any one of these four screws. Incident light is directed on a diagonal placed between an objective lens and the

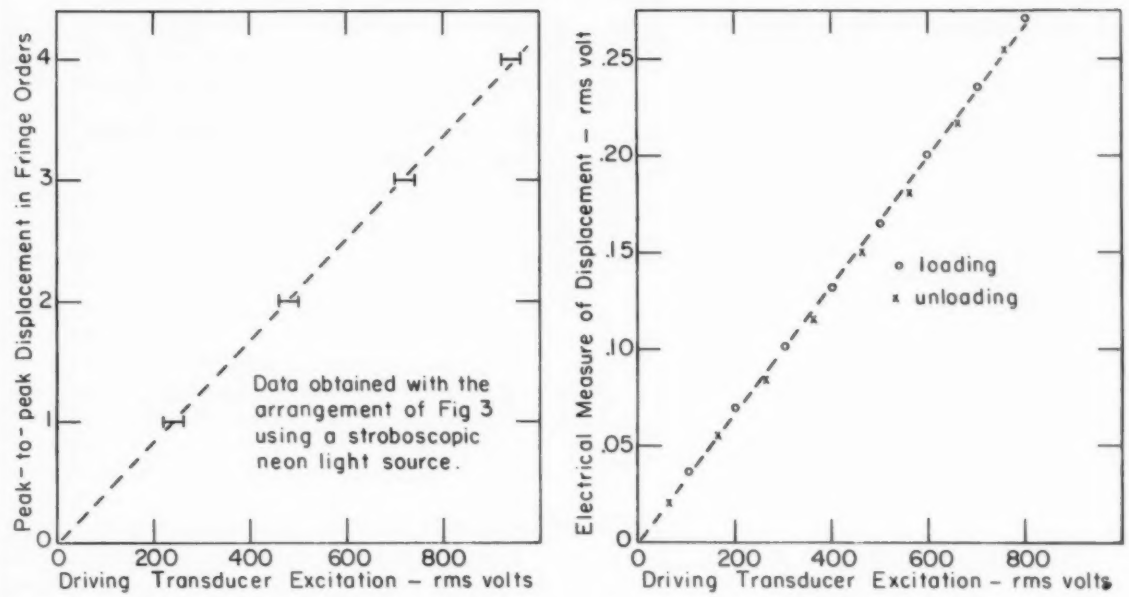


Fig. 2. Graphs of peak-to-peak displacement of the unloaded end of a piezoelectric driving transducer versus voltage on the driver.

interferometer mirrors. The diagonal was made from a carefully selected microscope slide and was coated with a transparent film of aluminum. The objective lens has a focal length of 4 cm. A prism and filar micrometer ocular used with the microscope are identified in Fig. 3. Focusing of the microscope on the air gap between mirrors A and B is accomplished with the aid of a conventional rack-and-pinion on the microscope tube.

## Displacement Calibration Using a Stroboscopic Light Source

In the variation of the interferometric-stroboscopic technique used here, a 60-cps voltage of continuously variable phase is impressed on the driving transducer. In the voltage source, three wye-delta connected transformers supply from three three-phase line terminals the three stator coils of a selsyn motor. A clamping arrangement allows one to position the rotor at any desired angular position defined on a fixed, graduated circle by a pointer attached to the shaft of the rotor. A single-phase voltage taken from the rotor varies in phase when the shaft is rotated. A fraction of this voltage is placed on the input of a McIntosh model MC60 power amplifier whose output is connected to the low-voltage winding of an illuminating-tube transformer. The transformer's high-voltage winding provides the excitation voltage for the driving transducer. A driving voltage of desired magnitude is obtained by adjusting the gain control on the power amplifier. A General Radio Company Strobotac serves as a light source. It is operated at the line frequency position of a selector switch so that the flashing rate coincides with the frequency of motion of the driving transducer. The Strobotac is modified by removing the type 631-P1 strobotron tube from its socket, mounting the tube with its longitudinal axis vertical, and electrically connecting the tube to its normal socket by means of an extension cord. Light from the tube is focused by condensing lenses on a pinhole. The pinhole provides access for light entering the interferometer through a pair of collimating lenses.

The following procedure was used in obtaining the data for the calibration curve on the left in Fig. 2. Mirrors A and B were spaced approximately 254 $\mu$ apart with a wedge angle selected so that approximately 10 fringes could be seen in the field of view of the microscope. The dark bands were not distinct enough to warrant using a smaller wedge angle. The gain setting of the power amplifier was adjusted to place an arbitrary driving voltage on the driving transducer; an assistant rotated the shaft of the selsyn slowly while the writer observed the fringe pattern. The position of the shaft corresponding to a stationary position of the fringes was noted, and a dust particle that was situated close to or on a dark band in the field of view was selected as a reference. The phase was then changed by 180° to determine whether or not the peak-to-peak displacement corresponded to an integral number of fringe orders. If not, a new driving voltage (unknown to the writer) was selected, and the process was repeated. With practice, an average value of driving voltage for a given number of whole-fringe orders could be obtained with a standard deviation of 20 V. The average driving voltages for the first four fringe orders were 240, 480, 720,

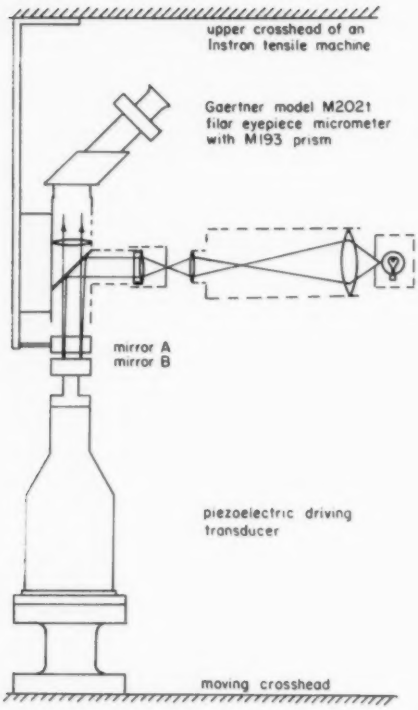
upper crosshead of an Instron tensile machine
Gaertner model M2021 filar eyepiece micrometer with M193 prism
mirror A
mirror B
piezoelectric driving transducer
moving crosshead

Fig. 3. Schematic of optical system used for displacement calibration.

and 940 rms V. The writer cannot suppress a feeling of dissatisfaction for these results. One should be able to make a setting of a fringe with respect to a reference with a precision of the order of a tenth of the fringe half-width. With a two-beam interferometer, this precision would be 1/20 of a fringe order, and since two settings are required to obtain a measure of fringe displacement, an over-all accuracy of 1/10 order would be expected. An upper limit on the precision, with which one might expect to measure by direct observation peak-to-peak displacement with a multiple-beam interferometer employing highly reflecting mirrors, is 1/250 of a fringe order. The uncertainty in measuring a peak-to-peak displacement of one fringe order in the present case was 20/240 = 1/12 fringe order indicating that considerable improvement might be obtained by making appropriate modifications of the apparatus.

## Displacement Calibration by the Fringe-Disappearance Method

Two different light sources are used to replace the strobotron tube in the arrangement discussed in the previous section. One is a 10-mm helium U-tube, which was made by a neon-sign maker, with a tube length (exclusive of electrodes) of 150 mm. Output of a 7500-V illuminating-tube transformer causes the tube to discharge. The second is a General Electric H4AB mercury lamp, the light of which is intercepted by a Kodak No. 74 Wratten filter, which transmits the mercury green line having a wavelength of 0.546 $\mu$. The procedure followed in one calibration series is given below.

The 60-cps voltage for the driving transducer was obtained from a transformer whose primary voltage was controlled by a Variac. Mirrors A and B were spaced approximately 254 $\mu$ apart, and a wedge angle was selected so that about 20 fringes could be seen in the microscope field. With either the helium or the mercury light source present, the driving voltage was increased gradually by turning the Variac control knob until fringes appeared to vanish in a uniform background. In cursory examination, six fringe disappearances were seen as the driving voltage was increased to a maximum value that could safely be placed on the driving transducer. For the purposes of the contact-stress investigation, calibrations were limited to the first four disappearances. Root mean square driving voltages were read on the 1200-V scale of a Triplet model 630-NA volt-ohmmeter. Voltages were recorded to three significant figures. The possible error in making a single reading of the scale was of the order of $\pm 2$ V. Ten readings were obtained for each fringe disappearance. The writer observed the fringe pattern while slowly oscillating the Variac knob with decreasing amplitude about a position corresponding to a disappearance and finally set the knob midway between fringe appearances. The last motion of the knob was made as many times to the right as to the left, and after each

**Table I. Amplitude Ratios for Different Orders of Disappearance**

| | Mercury light source | | Helium light source | | | Two-beam interferometer | | Eleven-beam interferometer | |
|---|---|---|---|---|---|---|---|---|---|
| | 1 | 2 | 3 | 4 | 5 | 6 | 7 | 8 | 9 |
| Order of disappearance | Rms driving volts | Driving voltage ratios | Rms driving volts | Driving voltage ratios | Averages of cols. 2 and 4 | $\xi_0 = 4\pi x_0/\lambda$ | Amplitude ratios | $\xi_0 = 4\pi x_0/\lambda$ | Amplitude ratios |
| 1 | 176 ± 1 | 1.00 | 157 ± 0.5 | 1.00 | 1.00 | 2.405 | 1.00 | 1.87 | 1.00 |
| 2 | 404 ± 1 | 2.30 | 387 ± 0.5 | 2.46 | 2.38 | 5.520 | 2.30 | 5.93 | 3.17 |
| 3 | 604 ± 5 | 3.43 | 603 ± 0.7 | 3.84 | 3.63 | 8.654 | 3.60 | 7.89 | 4.22 |
| 4 | 801 ± 5 | 4.55 | 824 ± 0.8 | 5.25 | 4.90 | 11.79 | 4.90 | — | — |

**NEW SUBSCRIPTION ORDER**

# APPLIED OPTICS

Please enter my/our subscription* and continue until countermanded:

- ☐ OSA member rate $6.00 per year
- ☐ Other AIP Societies' rate $8.00 per year
- ☐ Regular rate $10.00 per year
- ☐ Please send OSA membership information
- ☐ check enclosed ☐ bill me
- ☐ Single copy of issue ..... $2.00

Name ..... Membership No. .....

Address .....

.....

*Subscriptions entered for calendar year only.

Please allow eight weeks for order processing.

**NEW SUBSCRIPTION ORDER**

# APPLIED OPTICS

Please enter my/our subscription* and continue until countermanded:

- ☐ OSA member rate $6.00 per year
- ☐ Other AIP Societies' rate $8.00 per year
- ☐ Regular rate $10.00 per year
- ☐ Please send OSA membership information
- ☐ check enclosed ☐ bill me
- ☐ Single copy of issue ..... $2.00

Name ..... Membership No. .....

Address .....

.....

*Subscriptions entered for calendar year only.

Please allow eight weeks for order processing.

**FIRST CLASS**
Permit No. 18297
New York, N. Y.

**BUSINESS REPLY MAIL**
No postage stamp necessary if mailed in the U. S. A.

POSTAGE WILL BE PAID BY

**APPLIED OPTICS**
American Institute of Physics
335 E. 45th Street
New York 17, N. Y.

**FIRST CLASS**
Permit No. 18297
New York, N. Y.

**BUSINESS REPLY MAIL**
No postage stamp necessary if mailed in the U. S. A.

POSTAGE WILL BE PAID BY

**APPLIED OPTICS**
American Institute of Physics
335 E. 45th Street
New York 17, N. Y.

reading the knob was returned either to zero or to a position corresponding to the disappearance of next lowest order. The voltmeter was observed only after the knob had been set. The results are given in Table I. The scale on the Variac is numbered to 110, and the highest driving voltages (for the fourth disappearance )were obtained at a Variac setting of 15. It is therefore interesting that one could, especially in the tests with the helium source, obtain sets of readings with such small deviations because a change of several volts took place with a motion of the Variac knob that was almost imperceptible to the touch.

A particular observational detail on the behavior of fringes during the tests with the helium source must be recorded because it remains to be explained. The interferometer was arranged so that light and dark bands were of approximately equal area. As the driving voltage was increased from zero, the dark bands became narrower until they were of a quality that one would expect to see in a multiple-beam interferometer with highly reflecting mirrors. At this stage a second set of fine fringes appeared with each fringe of the new set midway between two fine fringes of the old set. One could find a critical driving voltage at which a uniform set of very fine fringes twice as numerous as usual could be seen. A slight increase in driving voltage caused the old set of fringes to disappear and the new set to broaden slightly. A further increase of driving voltage produced light and dark bands of equal area. The driving voltage recorded as one for a fringe disappearance would more accurately be described as the critical voltage at which both sets of fine fringes could be seen.

## Theoretical Prediction of Fringe Disappearances

The object of the present section is to try to predict fringe disappearances for a Fizeau-type interferometer using two plane mirrors with reflection coefficients of 0.37 and 0.90. The simplest model will be considered, in which mirror A is a nonabsorbing film bounded on either side by air. A plane wave whose electric vector is of unit amplitude and which is polarized parallel to A strikes A at normal incidence. A fraction of the incident light having intensity $T$ enters a parallel air gap between A and B, and a fraction with intensity $R = 1 - T$ is reflected from A. The reflectance of mirror B is denoted by $r$. Figure 4 indicates the intensities of the first few interfering rays. One must examine the variations in intensity of the vector sum of the waves, which emerge from A and are collected at a point in the focal plane of a lens. When mirror B is stationary and is separated from A by a distance $x$, each successive wave collected by the lens lags behind the preceding one by a distance $2x$. If B undergoes a motion $x_0 \sin\omega t$ in the direction perpendicular to the mirrors, the path difference between successive waves at any instant $t$ is $2(x + x_0 \sin\omega t)$. The phase difference between successive waves is $\delta = (4\pi/\lambda)(x + x_0 \sin\omega t)$, where $\lambda$ is the wavelength of light used. If $E = e^{ipt}$ represents, in complex form, the amplitude of the wave incident on A, then the amplitudes of the waves up to the $n$th that are emergent from A may be expressed as follows:

$$\begin{aligned} E_0 &= R^{1/2}e^{ipt} \\ E_1 &= r^{1/2}Te^{i(pt-\delta)} \\ E_2 &= rR^{1/2}Te^{i(pt-2\delta)} \\ &\cdot \\ &\cdot \\ &\cdot \\ E_n &= R^{-1/2}T(rR)^{n/2}e^{i(pt-n\delta)}. \end{aligned}$$

The instantaneous amplitude of the vector sum of all the waves collected may be expressed as $\mathcal{E}e^{i(pt-\Delta)}$. The intensity of the resultant wave is given by the real part of

$$\mathcal{E}^2 = \sum_{i=0}^{n} E_iE_i^* + \sum_{\substack{i=0 \\ i\neq j}}^{n}\sum_{j=0}^{n} E_iE_j^*.$$

If the motion of mirror B is too fast for the eye to follow, the eye will record an average intensity, which is represented by the real part of

$$I = \frac{2\pi}{\omega}\int_0^{\frac{2\pi}{\omega}} \mathcal{E}^2 dt.$$

One finds that when $n$ beams interfere,

$$\begin{aligned} ReI = {} & R + rT^2\sum_{m=0}^{n-2}(rR)^m \\ & + 2T\sum_{j=1}^{n-1}(rR)^{j/2}\cos(4\pi jx/\lambda)J_0(4\gamma jx_0/\lambda) \\ & + r^{1/2}R^{-1/2}T^2\sum_{j=2}^{n-1}(rR)^{j/2}\cos(4\pi jx/\lambda)J_0(4\pi jx_0/\lambda) \\ & + \sum_{m=2}^{n-2}\left[2R^{-1}T^2(rR)^{m/2}\sum_{j=m+1}^{n-1}(rR)^{j/2}\cos(4\pi jx/\lambda)J_0(4\pi jx_0/\lambda)\right]. \end{aligned}$$

It is convenient to assume that $x$ is an integral multiple of $\lambda$, in which case $\cos(4\pi jx/\lambda) = 1$ for all $j$, and to ignore terms independent of $x_0$. Let $\xi_0 = 4\pi x_0/\lambda$, and write

$$\begin{aligned} I = {} & 2T\sum_{j=1}^{n-1}(rR)^{j/2}J_0(j\xi_0) \\ & + 2r^{1/2}R^{-1/2}T^2\sum_{j=2}^{n-1}(rR)^{j/2}J_0(j\xi_0) \\ & + \sum_{m=2}^{n-2}\left[2R^{-1}T^2(rR)^{m/2}\sum_{j=m+1}^{n-1}(rR)^{j/2}J_0(j\xi_0)\right]. \end{aligned}$$

One would expect that fringes would disappear with respect to a uniform background whenever $\xi_0$ takes on values which make $\bar{I} = 0$. Figure 6 displays graphs of $|\bar{I}|$ computed at increments of $\xi_0$ equal to 0.25 for different numbers of interfering waves. Very little additional information would be gained by considering a model in which more than 11 waves interfere.

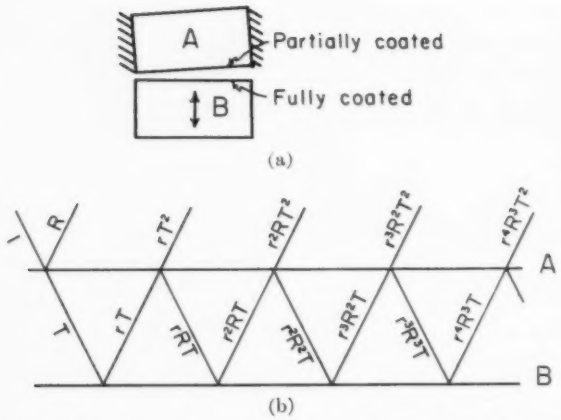


Fig. 4. Description of optical flats and mathematical model. (a) A and B are cylindrical fused-quartz flats, each 25.4-mm diam and 12.7-mm thick. The lower surface of A is partially coated with titanium dioxide, the upper surface of B is fully coated with aluminum. A is stationary; B is moving. (b) An idealization showing intensities of transmitted and reflected rays resulting from incidence of a ray of unit intensity on the lower surface of flat A.

## Discussion of the Fringe-Disappearance Method

Table I lists driving voltages for the first four fringe disappearances obtained with both helium- and mercury-light sources. Since it is known from the tests made with the capacitance-type displacement pickup that the driving voltage/displacement relation of the driving transducer is linear, the ratio of driving voltage for a disappearance other than the first to the driving voltage for the first disappearance should be predictable. Accordingly, there are also given in Table I ratios of amplitude of motion for disappearances other than the first to amplitude for the first disappearance when the interferometer used is of the two-beam type or one in which 11 beams interfere. Note that the driving-voltage ratios in cols. 2 and 4 correspond much more closely with the amplitude ratios in col. 7 than with those in col. 8. This means that the interferometer used in the present study behaves much more like a two-beam interferometer than like the model of an 11-beam interferometer discussed in the previous section. Col. 5 lists driving-voltage ratios obtained by averaging the results for the two different light sources. These average values agree very closely with the amplitude ratios for a two-beam interferometer.

At the present time, it is best to assign a numerical value to only the wavelength of the mercury light and not the helium light, because the former is filtered and the latter is not. For the purposes of the contact-stress investigations, a displacement-calibration factor for the driving transducer under no-load conditions is obtained from the data for the second disappearance when the wavelength of light is 0.546 $\mu$, the wavelength of the mercury green line. It is assumed that the ratio of the amplitude of motion to the wavelength of light has the value 0.439, as would be the case with a two-beam in

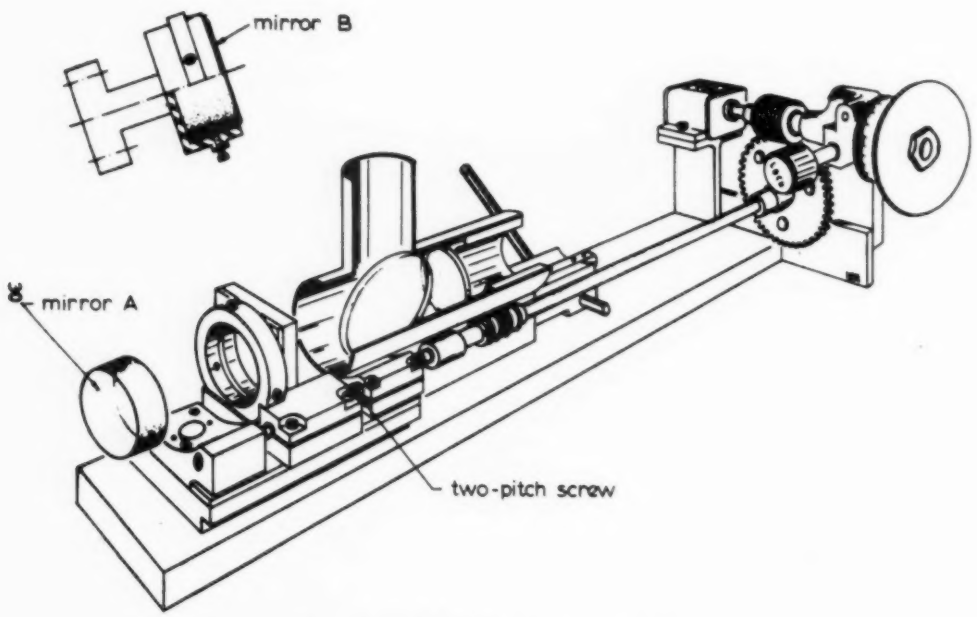


Fig. 5. Interferometer and drive mechanism.

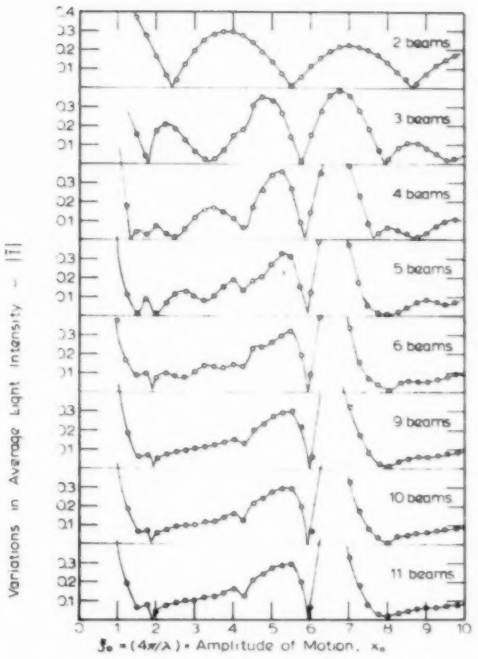


Fig. 6. Variations in average light intensity with changes in amplitude of motion of mirror B when different numbers of waves interere.

terferometer. The pertinent calibration factor is thus

$$\frac{404 \text{ rms V}}{0.439 \times 0.546\,\mu} = \frac{1685 \text{ rms V}}{\mu}.$$

## Conclusions

It has been established that the piezoelectric driving transducer can be calibrated with the interferometer described. The stroboscopic-interferometric technique could be improved by using two mirrors of high reflectivity and by changing the light source and filtering so that fringes of the quality reported in ref. 1 could be obtained. It is still not known whether fringe disappearances can be accurately predicted in an interferometer employing highly reflecting mirrors. It is likely that a more complicated model than the one described would be required in a theoretical analysis. One approach would be to extend the analysis of Holden[5] to include sinusoidal motion of one of the mirrors.

## References

1. E. R. Smith, S. Edelman, E. Jones, and V. A Schmidt, J. Acoust. Soc. Am. **30**, 867 (1958).
2. H. A. Thomas and G. W. Warren, Phil. Mag. **5**, 1125 (1928).
3. G. S. Monk, *Light Principles and Experiments*, 1st ed. (McGraw-Hill, New York, 1937), p. 328.
4. S. Edelman, E. Jones, and E. R. Smith, J. Acoust. Soc. Am. **27**, 728 (1955).
5. J. Holden, Proc. Phys. Soc. (London) **B62**, 27 (1949).


# THE SCIENCE OF COLOR

**THIS DEFINITIVE BOOK ON COLOR,** prepared by OSA's Colorimetry Committee and setting forth the history, physics, physiology, psychology, and technology of color vision and color measurement, will be reprinted later this year by OSA.

**LIMITED EDITION.** Twenty-five color plates make this book uniquely beautiful, and when the original supply of color sheets is exhausted, they cannot be reproduced. Therefore, this edition is limited.

**AUTHORITATIVE DATA,** mostly unavailable in other books, 39 tables, 102 figures, 340 pages of text, 22 pages of bibliography, and 23 pages of glossary-index have all been critically re-examined and corrected. The new **SCIENCE OF COLOR** is therefore the most up-to-date as well as the most complete source book for color science.

**ORDER NOW** **SEND CASH WITH ORDER** **PRICE $10.00; OSA MEMBERS $8.50**

Optical Society of America
Room 101, 1155 16th Street N.W., Washington, D.C. 20036

**Order Form**

Please send one ..... copy of SCIENCE OF COLOR.

☐ Cash/check herewith ☐ $10.00 ☐ $8.50 (OSA Member price)

Name ..... OSA Membership # .....

Address .....

**The following selected titles are for publications which have appeared in *Radio Propagation*, Section D, *Journal of Research of the National Bureau of Standards*, and may be of interest to some of the readers of *Applied Optics*.***

D. M. Gates, "Preliminary results of the National Bureau of Standards radio and ionospheric observations during the International Geophysical Year", J. Res. NBS 63D (Radio Prop.), No. 1, 1–14 (1959).

F. E. Roach, J. W. McCaulley, and E. Marovich, "Origin of [OI] 5577 in the airglow and the aurora", J. Res. NBS 63D (Radio Prop.), No. 1, 15–18 (1959).

F. E. Roach, J. W. McCaulley, and C. M. Purdy, "Comparison of absolute intensities of [OI] 5577 in the auroral and subauroral zones", J. Res. NBS 63D (Radio Prop.), No. 1, 19–20 (1959).

J. R. Wait and A. M. Conda, "Diffraction of electromagnetic waves by smooth obstacles for grazing angles", J. Res. NBS 63D (Radio Prop.), No. 2, 181–197 (1959).

A. D. Wheelon, "Radio-wave scattering by tropospheric irregularities", J. Res. NBS 63D (Radio Prop.), No. 2, 205–233 (1959).

R. E. McGavin and L. J. Maloney, "Study at 1046 megacycles per second of the reflection coefficient of irregular terrain at grazing angles", J. Res. NBS 63D (Radio Prop.), No. 2, 235–248 (1959).

F. E. Roach and E. Marovich, "A monochromatic low-latitude aurora", J. Res. NBS 63D (Radio Prop.), No 2, 297–301 (1959).

E. Tandberg-Hanssen and F. E. Roach, "Excitation mechanisms of the oxygen 5577 emission in the upper atmosphere", J. Res. NBS 63D (Radio Prop.), No. 2, 319–324 (1959).

M. B. Kraichman, "Basic experimental studies of the magnetic field from electromagnetic sources immersed in a semi-infinite conducting medium", J. Res. NBS 64D (Radio Prop.), No. 1, 21–25 (1960).

B. Y.-C. Koo and M. Katzin, "An exact earth-flattening procedure in propagation around a sphere", J. Res. NBS 64D (Radio Prop.), No. 1, 61–64 (1960).

F. E. Roach and E. Marovich, "Aurora of October 22/23, 1958, at Rapid City, South Dakota", J. Res. NBS 64D (Radio Prop.), No. 2, 205–216 (1960).

T. B. A. Senior and K. M. Siegel, "A theory of radar scattering by the moon", J. Res. NBS 64D (Radio Prop.), No. 3, 217–229 (1960).

M. P. Bachynski, "Propagation at oblique incidence over cylindrical obstacles", J. Res. NBS 64D (Radio Prop.), No. 4, 311–315 (1960).

H. E. J. Neugebauer and M. P. Bachynski, "Diffraction by smooth conical obstacles", J. Res. NBS 64D (Radio Prop.), No. 4, 317–329 (1960).

H. Bremmer, "On the theory of wave propagation through a concentrically stratified troposphere with a smooth profile", J. Res. NBS 64D (Radio Prop.), No. 5, 467–482 (1960).

G. A. M. King and F. E. Roach, "Relationship between red auroral arcs and ionospheric recombination", J. Res. NBS 65D (Radio Prop.), No. 2, 129–135 (1961).

Ming-Kuei Hu, "Fresnel region fields of circular aperture antennas", J. Res. NBS 65D (Radio Prop.), No. 2, 137–147 (1961).

S. A. Bowhill, "Statistics of a radio wave diffracted by a random ionosphere", J. Res. NBS 65D (Radio Prop.), No. 3, 275–292 (1961).

V. A. Bailey, "Power density requirements for airglow excitation by gyrowaves", J. Res. NBS 65D (Radio Prop.), No. 4, 321–32[illegible] (1961).

L. E. Vogler, "Smooth earth diffraction calculations for horizontal polarization", J. Res. NBS 65D (Radio Prop.), No. 4, 397–39[illegible] (1961).

H. S. Hayre and R. K. Moore, "Theoretical scattering coefficient for near vertical incidence from contour maps", J. Res. NBS 65[illegible] (Radio Prop.), No. 5, 427–432 (1961).

A. P. Barsis and R. S. Kirby, "VHF and UHF signal characteristics observed on a long knife-edge diffraction path", J. Res. NB[illegible] 65D (Radio Prop.), No. 5, 437–448 (1961).

R. K. Moore and W. E. Blair, "Dipole radiation in a conducting half space", J. Res. NBS 65D (Radio Prop.), No. 6, 547–56[illegible] (1961).

H. Bremmer, "On the theory of wave propagation through a concentrically stratified troposphere with a smooth profile. Part II. Expansions of the rigorous solution", J. Res. NBS 66D (Radio Prop.), No. 1, 31–52 (1962).

F. H. Northover, "Reflection of electromagnetic waves from thin ionized gaseous layers", J. Res. NBS 66D (Radio Prop.), No. 1, 73–80 (1962).

J. R. Johler and J. D. Harper, Jr., "Reflection and transmission of radio waves at a continuously stratified plasma with arbitrary magnetic induction", J. Res. NBS 66D (Radio Prop.), No. 1, 81–99 (1962).

L. C. Walters and J. R. Johler, "On the diffraction of spherical radio waves by a finitely conducting spherical earth", J. Res. NBS 66D (Radio Prop.), No. 1, 101–106 (1962).

J. R. Winckler, "Atmospheric phenomena, energetic electrons, and the geomagnetic field", J. Res. NBS 66D (Radio Prop.), No. 2, 127–143 (1962).

D. Barbier, F. E. Roach, and W. R. Steiger, "The summer intensity variations of [OI] 6300 A in the tropics", J. Res. NBS 66D (Radio Prop.), No. 2, 145–152 (1962).

M. M. Siddiqui, "Some problems connected with Rayleigh distributions", J. Res. NBS 66D (Radio Prop.), No. 2, 167–174 (1962).

D. F. Winter, "A theory of radar reflections from a rough moon", J. Res. NBS 66D (Radio Prop.), No. 3, 215–226 (1962).

K. M. Siegel and T. B. A. Senior, "A lunar theory reasserted", J. Res. NBS 66D (Radio Prop.), No. 3, 227–229 (1962).

P. Beckmann, "Statistical distribution of the amplitude and phase of a multiply scattered field", J. Res. NBS 66D (Radio Prop.), No. 3, 231–240 (1962).

A. D. Wheelon, "Amplitude distribution for radio signals reflected by meteor trails, II", J. Res. NBS 66D (Radio Prop.), No. 3, 241–247 (1962).

F. du Castel, P. Misme, A. Spizzichino, and J. Voge, "On the role of the process of reflection in radio wave propagation", J. Res. NBS 66D (Radio Prop.), No. 3, 273–284 (1962).

T. Hagfors, "On the forward scattering of radio waves in the lower ionosphere", J. Res. NBS 66D (Radio Prop.), No. 4, 409–418 (1962).

* Compiled by David M. Gates.

*continued on page 107*

# Optics in the German Democratic Republic

Paul Görlich

## Introduction

Several cities in the German Democratic Republic claim to be birthplaces of optical industry and research, and today, after many decades of progress and development, they can look back upon a long and famous tradition. Jena, however, has been and still is the center of the optical industries in the Republic. It was in this town that Carl Zeiss, the official mechanic of the University of Jena more than 110 years ago, started a small shop for the production of optical instruments. Nearly a century ago he was joined by Ernst Abbe, a mathematician who could solve scientific problems the master mechanic was unable to tackle, and thereby initiated the fruitful cooperation between science and industry which helped to establish the world-wide reputation of the Jena Works. This cooperation also laid the foundation for the VEB Carl Zeiss, with its 18,000 workers, one of the greatest optomechanical undertakings in the world. Industry and research in the field of optics is, however, domiciled not only in Jena but also in other places, e.g., Rathenow, Gorlitz. Dresden, Berlin, Potsdam, Leipzig, and Ilmenau.

## Optical Industry

The wide variety of the products of the GDR optomechanical industry—those turned out by the VEB Carl Zeiss Jena alone amounted to more than 4000 listed items—makes it impossible to give here more than a brief survey of the subject matter.

## Raw Materials for Optics

Want of raw glass, which computations indicated to be necessary for powerful optics, induced Abbe in the 1880's to persuade Otto Schott to come to Jena to establish the Jenaer Glaswerk Schott & Genossen. The pioneer work of both investigators, which was directed at creating a large number of optical glasses, has been continued in the VEB Jenaer Glaswerk Schott & Genossen, which now supplies lanthanum-containing glasses of the latest type. In 1919, the Jena Glass Works became a part of the Carl Ziess Foundation.

In addition to the production of optical glasses, VEB Carl Zeiss is also engaged in the growth of crystals from solution and from the melt for optical and other purposes ($CaF_2$, quartz, and others).

## Microscope Optics

The more than 110-year-old tradition of the Zeiss Works laid the foundations for the latest developments of microscopes. By equipping the microscopes with supplementary devices, all classical as well as modern investigative methods, ranging from observations in transmitted or incident light to investigations with variable phase-contrast, polarized, or fluorescent light, can be carried out. Auxiliary apparatus include photomicrographic equipment and automatic-exposure devices as well as drawing equipment. The optics used in these instruments are far superior to the apochromats developed by Abbe, and use is now made not only of plane-field achromats developed by Roegehold, a past master of computational optics, but recently also of plano-apochromats which, being computed for infinite focal intercept, are also employed in incident-light microscopes. Particular attention has been paid to catoptric lens systems for microscopy.

A special development in the area of microscopy resulted in the construction of the nuclear track measuring microscope, giving scientists the possibility to measure very precisely the tracks of highly energetic nuclei in photographic emulsions. Microscopic equipment is built not only by Zeiss in Jena but also by VEB Rathenower Optische Werks, which builds, for example, polarization microscopes (for transmitted and incident light), units with built-in special 35-mm cameras, as well as auxiliary electrical-integrator equipment.

## Photo and Cine Optics

The second field in which the Zeiss workshops gained a world-wide reputation is that of photolenses, the best known of which is the Tessar, the pioneering invention of Rudolph, which, following the expiration of the

The author, who is from Jena, is a director of the Institute for Optics and Spectroscopy in Berlin-Adlershof.

Received 20 April 1962.

original patent has for decades been copied all over the world. It is still manufactured in the Jena Works as a 2.8/50 lens, with its quality considerably improved. Since 1945, several outstanding novel designs have been introduced, e.g., the Flektogons 4/25 and 2.8/35 lenses for 35-mm film, the 4/50 and 2.8/65 lenses for 60 × 60-mm² film, catoptric-lens systems 4/500 for 35-mm film, and 5.6/1000 for the medium format 60 × 60 mm². Thus, the lens series now at our disposal are complete for focal lengths from 25 to 1000 mm for 35-mm films and from 50 to 1000 mm for medium format.

Further Zeiss developments are these: for aerial cameras, the Pinatar 4/210 for 180 × 180 mm² image size; the recently designed Apo-Germinars in addition to the Apo-Tessars for reproduction purposes; the 0.85/100 and 0.85/55 lenses, which are used on the Zeiss x-ray screen image cameras for radiophotography; and the Dokumars as photographing and reproduction lenses for the Zeiss Dokumator system, which consists of the Dokumator photo recorder, film reader, and other accessories.

In the field of vario-optics, the Pontovar 2.8 . . . 32, developed by the Kamera und Kinowerke, Dresden, is manufactured by the Zeiss optical works in Jena for 8-mm film cameras.

In addition to lenses of normal focal length $f/50$, with the relative aperture 1:2 (Domigon as Gauss type) and with the relative aperture 1:2.8 both as Domiplan (Triplet) and as Primotar (Tessar type), the VEB Fein-Optisches Werk, Gorlitz, also manufactures short-focus lenses, e.g., Domigon 3.5/30 and Primagon 4.5/35, as well as long-focus lenses, e.g., the Tele-Meger up to 4.5/3000 (as telelens).

Cineprojection lenses for 35-mm film have been produced in Jena for decades. About 10 years ago, the Kipronars were replaced by Prokinars, while these have been replaced recently by the Visionars with relative aperture 1:1.6, achieving for the first time an excellent image quality throughout the whole field with such relative apertures. Today, these lenses as well as the anamorphic cylindrical lens attachment for expanding squeezed pictures in projection and the spherical and aspherical concave mirrors for cineprojectors are supplied by VEB Rathenower Optische Werkes.

The metropolis of camera production in the GDR is Dresden; well known are the 35-mm single-lens reflex cameras Exakta Varex, Praktina, Praktica, Pentacon, and Pentina; the 35-mm Prakti camera; Penti for 18 × 24-mm² film; and the single-lens reflex camera Praktisix for 60 × 60-mm² format; to name but a few. In addition to these, a completely newly designed camera has been turned out by VEB Carl Zeiss Jena—the Werra-Camera, which is available in five different models, with the automatic cameras Werramat and Werra V being the latest of this series.

## Opto-Physical Measuring Instruments

In the early 1890's, the Zeiss optical works expanded their manufacturing program to include optophysical measuring instruments, which made it possible to carry through chemicoanalytical examinations more quickly by optical methods. Especially rapid advances are being made today in this field toward the use of large electronic recording and controlling instruments. Originally, only those instruments were manufactured which have become the "classical" instruments for the determination of the refractive index, e.g., the Abbe and Pulfrich refractrometers and later the Rayleigh-Löwer-Haber interferometers. Today's program covers emission and absorption spectral analysis with the wavelength region being constantly extended at both ends. In this connection, mention must be made of the quartz spectrograph Q24, the three-prism spectrograph with four interchangeable camera equipments (particularly intended for Raman analysis), and the plane grating 2-m spectrograph, which has stood the test of time in analyzing pure substances and in solving special research tasks. It was not until a heavy-duty linear dividing machine was developed that the construction of this spectrograph was made possible. Rapid visual analysis is afforded by the industrial spectroscope, having a dispersion corresponding to four 60° glass prisms. Flame emission and absorption analyses are also employed as investigation methods, and Feussnar spark generators, intermittent and permanent arc-producers, serve as excitation instruments. For evaluation of spectra, a spectrum projector is available as are the Abbe-comparator and the rapid photometer, the latter now being equipped with a compensation recorder. Extraordinarily high fidelity of records is warranted by a new photoelectric recording photometer. Employment of filter photometers (Pulfrich photometer used in conjunction with photoelectric auxiliary equipment, Leukometer, UV-photometer, and others) opened a way to absorption-spectrum analysis, with its border fields of fluorescence and turbidity measurements, emission, and reflection measurements. Outstanding in recent developments is the all-automatic infrared-spectrophotometer UR 10, with a spectral region from 2 to 25 $\mu$ covered by lithium fluoride, rocksalt, and potassium-bromide prisms that can be automatically interchanged. By means of a program selector, any wavelength region may be picked out and recorded. The applicability of the instrument is considerably increased by numerous accessories: as a unit assembly, the nonrecording universal spectrophotometer can be adapted to routine and research tasks that may occur in a spectral region covering the range from the ultraviolet to the near infrared. The heavy-duty mirror monochromator combines convenience in

operation with a large field of application (0.2 to 50 $\mu$) and provides a choice of prisms or diffraction gratings.

A few remarks should perhaps be added on the Konimeter as well as on the Schlieren apparatus. The Konimeter is used to measure the dust content of the air in industrial centers and works as well as in large cities, while the Schlieren apparatus uses the Toepler Schlieren method for investigations of, for example, high-molecular substances.

## Astronomical Instruments

Toward the end of the nineteenth century, Zeiss started producing astronomical instruments, which were made to special order. Recent instruments are the Astrograph 400/1600 and the Double Astrograph 400/2000. Coudé Refractors 150/2250 and 200/3000 have been developed for use in smaller observatories or universities. Besides these refractors, in recent years it was primarily the reflector telescopes (based on the Schmidt-mirror system) that met with favorable reception, such as the Schmidt reflector telescope 600/900/1800. Perhaps the best known among the Zeiss telescopes is the Schmidt reflector telescope 800/1200/2400 supplied to the Hamburg-Bergedorf Observatory. Zeiss also built the largest reflector telescope in Europe, the 2-m Schmidt mirror complete with all accessories, which was erected in Tautenburg near Jena in the Karl Schwarzschild Observatory of the German Academy of Sciences and made available to all German astronomers for individual and joint research work.

## Photogrammetric Instruments

At the turn of the century, the photogrammetric department grew as a special branch out of the measuring-instruments department of the Zeiss Works; in the more than 60 years of its existence, this field has become one of the most important in Jena instrument manufacture. In addition to the Stereoplanigraph used for decades, an advanced design of the Stereoautograph has been brought out in recent years. Terrestrial photographs plotted in the Stereoautograph may be produced by the Phototheodolite 19/1318. The aerial survey camera MRB 21/1818 fitted with the above-mentioned Pinatar 4/210 is a fully automatic film camera for aerophotogrammetric survey work. The plotting of photographs reduced in reduction printers can be carried out in the Multiplex, a stereomapping equipment of second order that is now supplied as ultra-wide-angle equipment in addition to the former models of the normal and wide-angle Multiplex instruments. The Stereometrograph, which operates by the well-established "classical" method of strict spatial reproduction of the exposure process, represents the latest design of second-order stereoplotters. The corresponding measuring rays from the model point to the image point are produced by means of mechanical precision guides. For evaluation, Zeiss supplies a newly developed instrument, the Coordimeter, which not only permits the automatic recording of machine coordinates of photogrammetric evaluating instruments but also carries out program-controlled calculations.

## Surveying Instruments

Scarcely a decade had passed after photogrammetric instruments were included in their production program when Zeiss started manufacturing surveying instruments. The production program, covering a wide range of instruments, includes the reducing tacheometers, as well as a small-type theodolite. Special mention should also be made of the seconds theodolite with an elongated mirror-lens telescope (Cassegrain), having a free-objective aperture of 53-mm diameter and a magnification of 31× [mean-square directional error in one set of measurements $\pm 1.3''$ $(\pm 4)^{\infty}$]. It is especially suited for triangulation work up to the second order and, with Invar base subtense staff and target-signal equipment, for precision traversing. Another tacheometer theodolite without a micrometer and with a telescope magnification of 25× permits direct reading of the values with the mean-square directional error not exceeding $\pm 5''$ $(15^{\infty})$. It is equipped with a device for repetition measurements and an automatically leveled vertical index.

Other specialized levels include one for leveling work of first and second order, with a mean-square error per km double leveling amounting to ± 0.4 mm and a level with an automatically leveled sighting line, which is optionally usable for ordinary leveling work by estimating staff intervals (±2 . . . 3 mm for 1-km double leveling) or for precision leveling by using a parallel-plate micrometer (±0.5 . . . 0.8).

## Opto-Ophthalmological Instruments

Approximately 50 years ago, Zeiss extended their manufacturing program to include spectacle lenses, multifocal lenses, and ophthalmological instruments, e.g., the coincidence refractionometer, the electrical hand ophthalmoscope and the retinal camera Retinophot. The optical elements of the latter as well as the light source (high-pressure xenon lamp) are so adjusted that a diameter of the pupil of only 5.5 mm proves to be sufficient for perfect exposures. The Schiotz standard tonometer, though not an optical device, is a new and important ophthalmological instrument for the mechanical measurement of the interocular pressure of the eye.*

* Editor's Note: There is an interesting article on the "Golden Jubilee of Works on Aids to Vision" by August Sonnefeld of the Zeiss Works in Nature **194,** 825 (1962). It should also be noted that the June 1962 number of the Jena Review contains special articles concerning the 50-year history of Jena aids to vision and ophthalmological instruments.

## Institutes

The great traditions of the optical industries in the German Democratic Republic are the background for the intensive research activities in the institutes of the academies and universities.

The Institute of Optics and Spectroscopy is affiliated with the Society for Scientific Research of the German Academy of Sciences in Berlin. It was founded in 1948 by E. Lau as a small laboratory, from which developed the two large domains of science with more than 100 cooperators (including 32 scientists) doing research work in 18 special laboratories, now led by R. Ritschl and P. Görlich, who direct complex research projects in theoretical, interference, geometrical, atmospheric, and physiological optics, microscopy, contrast-transmission theory, scientific photography, spectroscopy of atoms and molecules, and optical media.

An interesting modification of the conventional light microscope whose resolving power cannot be extended beyond a certain limit is the so-called double microscope, developed by Lau. By means of a rotating ground-glass disk mounted in the plane of the intermediate image, an effective enlargement of the exit pupil of the microscope is obtained. In this way, entoptic phenomena in the eye and similar phenomena in the optics of the instrument are practically eliminated, while the exploitation and utilization of the optimum theoretical efficiency of the objectives is highly facilitated. Higher magnification combined with a noticeable gain in information are practicably possible.

Fundamental investigations into double and multibeam interference in the field of interference optics resulted in a new theory of double-beam interference (visibility and position of fringes, aperture ratios, etc). Comparative studies on interference microscopes led to new suggestions for interference microscopes in transmitted and incident light that allowed exact quantitative measurements to be carried through; outstanding in this series of microscopes is an incident light interference microscope without depiction of the usual reference surface.

Special attention has been given by the institute to two-dimensional photometry. In the case of photographic pictures, curves of equal density (equidensities) corresponding to the isophots on the object are obtained in different ways: photographic, photochemical, and electronic automatic techniques have been developed that may be used with advantage to enhance the measuring accuracy of physical and technical working procedures. Equidensity curves have gained importance in measurements both of displacements of interference fringes and deflections within the spectral lines, in photometric and sensitometric investigations, in dosimetry, in obtaining isophots, in photoelasticity, and in solving many other problems. On the basis of the screen technique, a new method could be developed for a complete two-dimensional photometry of photographic pictures. A novel type of photometry already used with advantage for spectra of stars was introduced by the interference microscopical evaluation of the density relief of the photographic plate.

In the field of raster optics (moiré fringes), Institute research workers developed the technique of dupligrammetry which, for example, facilitates the evaluation of interference patterns of objective testers.

In the province of scientific photography, new techniques have been developed concerning the increase in sensitivity, desensibility, and contrast control. Here use is made of colored masks and emulsions without toe and switch.

Atmospheric-optics investigations are being made on the effect aerosols have on the degree of polarization of celestial radiation as well as of studies on the infrared transmittance of the atmosphere.

Other Institute research work includes studies on accommodation, near-astigmatism, binocular vision and its disturbances, vision in traffic, chromatic aberration of the eye, color perception, as well as on the development of instruments and tests for the examination of the eye and quick and routine examinations in factories.

In connection with studies on the correction of eye defects by means of optical aids, Lau-Jaeckel-Riekher developed and tested a spectacle lens with a continuously changing refractive effect over a range of 1.5, 2, and 3 D. This glass is a multifocal lens with continuously increasing refractive power, a valuable visual aid for presbyopes, which proved its efficiency in extensive series of tests.

The Institute has been particularly active in the province of spectroscopy: the wide range of investigation covers not only scientific spectroscopy but also studies on the application of spectroscopy of all wavelengths for routine examinations, especially industrial applications. Spectroscopic investigations into energy states of atoms are being carried through. Research objectives are the transfer of energy through collisions of the second kind, metastable excitation states and their lifetimes, self-absorption, isotope effects as well as hyperfine structure. Moreover, research work is being conducted in the fields of vacuum and molecular spectroscopy: e.g., investigations of infrared spectra of organic molecules; assignment of bands; intensity measurements of infrared bands; and isotope effects produced by substitution of hydrogen, nitrogen, and other isotopes. The work of the Institute also includes spectroscopical studies on the behavior of absorbed-pigment molecules (photographic sensitizers and desensitizers) as well as analyses of luminescence spectra of pigment molecules. The Institute investigates light

sources, excitation modes for the emission-spectrum analysis, time-resolved spectra, and effect of buffers, and conducts statistical studies on the accuracy of emission analysis. Moreover, attention is given to the development of methods and instruments employing Raman spectroscopy of liquids and gases as well as to the construction of Raman burners. Due to the great importance attached to optical media, spectroscopic examinations and experiments are also carried out with the aim of producing such materials with as high a degree of purity as possible.

R. Ritschl, in cooperation with both the First Physical Institute of the Humboldt University, Berlin, and the Institute of Optics and Spectroscopy, studied several spectroscopy problems. Spectroscopy in the far infrared and the examination of organophosphors may be regarded as specialties of the Physical Institute.

Of the vast number of publications issued by the Institute, mention should be made of a comprehensive reference book, *ABC der Optik*, which in about 1000 pages contains 10,000 contributions by a great number of distinguished scientists; the text is illustrated by 1600 figures and by black and white and colored plates.*

Part of the complex task of the Institute of Instrument Manufacture, under the directorship of H. Jancks, which is likewise affiliated with the Society for Scientific Research of the German Academy of Sciences in Berlin, is to develop special instruments for the application of optical methods in analysis techniques.

## Universities

The Institute of Applied Optics (M. Kühne, director) of the Friedrich Schiller University of Jena is concerned with the problems of interferometric testing of objectives, interferometric measurement of lengths, and molecular-optical investigations of glasses. At the Institute of Mathematics of the Karl Marx University, Leipzig, J. Focke lectures on geometrical optics (theory of image errors). Other research activities, dealing with physiological optics and ophthalmological optics, are affiliated with the ophthalmic hospitals of the Medical Academies in Magdeburg, Erfurt, and Dresden. Spectroscopic teams are doing research work at the Physical Institute of the Friedrich Schiller University in Jena (W. Schuetz, director) in the area of molecular Raman spectroscopy and at the Physico-Chemical Institute of the same university (H. Dunken, director) in the field of molecular spectroscopy, especially in the infrared.

## Technical and High Schools

Research in optics receives the strong support of the Institute of Theoretical Physics of the Potsdam Pedagogic High School (H. Picht, director), whose main fields of investigation are diffraction theory and theory of total reflection. Thorough investigations in infrared and Raman spectroscopy are carried out by a spectroscopic group under the direction of A. Simon at the Technical University, Dresden.

Jena is the home of a technical school specializing in ophthalmic optics.

## Scientific Conferences and Commissions

Conferences on optics usually are held by the GDR Physical Society at Jena every few years. In 1954, the conference topic was "Optics"; in 1958, the subject was "Optics of all Wavelengths"; while in 1960, it was called more precisely "Optics and Spectroscopy of All Wavelengths". The next conference is scheduled to take place in 1963. Scientists from many countries attended these conferences and gave them an international flavor (see the proceedings of the conferences). In addition to these large-scale meetings, courses, which are also attended by an international audience, are being held regularly on the application of microscope equipment, measuring instruments, and photogrammetric and fine-limit measuring instruments. The spectroscopy sections of the GDR Physical Society, under the leadership of R. Ritschl, plays an important part not only insofar as whole industries employing spectroscopy for routine work are concerned (e.g., Elektrochemisches Kombinat Bitterfeld, Farbwerke Wolfen, Gummikombinat Kowalit, Buna-Werke Schkopau, and others) but also insofar as institutes working on individual problems of scientific spectroscopy are concerned and, accordingly, in an exchange of scientific results and experiences (e.g., Institut für Reinststoffe Dresden, Zentralinstitut für Kernforschung Rossendorf, Institut für Physikalische Stofftrennung Leipzig, and others).

The Commission for Spectroscopy of the German Academy of Sciences, under the leadership of P. Görlich, grew out of the Infrared Commission constituted in 1955. It is the aim of this Commission to stimulate and coordinate research in the field of molecular structure and molecular properties as well as research in the province of spectrum analyses by physical methods. In addition, it is incumbent on the Commission to establish and foster relations with scientists abroad and to maintain a rapid information service in the fields of infrared, Raman, and high-frequency spectroscopy.

It gives the author great pleasure to acknowledge the help and cooperation of W. Krug, R. Ritschl, and R. Tiedeken during the preparation of this article.

* A review of this volume appears in Appl. Opt. 1, 302 (1962).

# RUSSIAN MASERS

## Typical examples of Russian masers papers published in recent issues of OPTICS AND SPECTROSCOPY, OSA's monthly translation journal:

**Transmission and Reflection of a Plane-Parallel Layer in the Conditions of Amplification and Generation** Stepanov and Khapalyuk

**Detection of the Isotope $K^{40}$ by Means of Optical Pumping** Alexandrov and Chodovoy

**Deformation Splitting of Lines in the Spectra of Alkali Fluoride Crystals Activated by Sm and Eu Divalent Ions** Kaplyanskii and Przhevuskii

**Zeeman Effect in the Absorption and Luminescence Spectrum of $CaF_2$-$Sm^{++}$ and $SrF_2$-$Sm^{++}$** Zakharchenya and Ryskin

**Microwave Spectrum of the HDNCN and $D_2NCN$ Molecules** Shipulo

**Spectroscopic Sum Rules Taking into Account the Induced Emission** Rebane and Sild

**Determination of the Mean Lifetime of Excited States by a Polarimetric Method** Agarbiceanu, Kukurezianu, Popesku, and Vasilu

**Some Problems of the Nonlinear Theory of the Optical Properties of Plane-Parallel Layers** Samson and Stepanov

**Calculation of the Maser Power of a System of Particles with Three Energy Levels** Stepanov and Samson

**Amplification Properties of a Dielectric Filament** Prokhurov

**Emission Pulsations from a Ruby Laser** Galanin, Leontovich, Sviridenkov, Smorchkov, and Chizhikova

**Absorption, Luminescence and Stimulated Emission of Neodymium in $SrF_2$ Crystals** Kariss and Feofilov

## Order your subscription to the 1963 issues now (August '63 issue published in English translation in November)

---

**OPTICS AND SPECTROSCOPY**
**ROOM 101, OSA**
**1155 16th St. N.W.**
**Washington, D.C. 20036**

**ORDER FORM**

Please enter my/our subscription to the 1963 issues of OPTICS AND SPECTROSCOPY (Vols. XIV and XV):

- ☐ OSA member rate — $7.50 for twelve issues
- ☐ OiS club member rate — $11.00 for twelve issues
- ☐ Nonmember rate — $15.00 for twelve issues

Name _____ OSA Membership No. _____

OiS Club Cooperating Society _____

Address _____

_____

_____

_____ **cash with order preferred**

# Optical Physics Research in a Small Liberal Arts College

J. H. Taylor

To encourage more activity in the field of optical physics in the small colleges the program at Southwestern is described. It is believed that the Southwestern program has been effective in motivating many undergraduate physics majors to pursue optical physics as a career in graduate school. The undergraduate is directly involved in the program. The small size of the staff has not been a handicap since the department is concerned only with this one research program.

## I. Introduction

In 1956 when the author joined the Physics Department at Southwestern it was a one-man department. The college had previously undergone a succession of turnovers in this department, and when it was unable to obtain a man in physics it asked the writer, an alumnus, to return. Prior to coming to Southwestern the author was working with L. F. Drummeter, Jr., and H. W. Yates in J. A. Sanderson's Optics Division at the Naval Research Laboratory. The situation that was inherited at Southwestern was typical of most small liberal arts colleges in the pre-Sputnik era. The efforts of the department previously had been purely pedagogical. No attempt at research had ever been made; there was no equipment for research and no money in the budget for it. With a teaching load of six 3-hr courses per semester plus three different laboratory courses, the prospects for launching a research program were not only exceedingly dim but ridiculous to contemplate.

## II. Effect of Research Activity on our Undergraduate Physics Program

We believe that the program described below has had a positive influence on our physics majors. There is definite evidence that it has been effective in motivating many of them toward the pursuit of optics as a career. In the past 6 years there have been 21 students graduating with a B.S. degree, and all but two have gone to graduate school, including Vanderbilt University, University of Florida, Ohio State University, Louisiana State University, University of North Carolina, Harvard University, Virginia Polytechnic Institute, Rensselaer Polytechnic Institute. Six of them are now at The Johns Hopkins University in various stages of graduate work. This is doubly gratifying in view of the shortage of undergraduate physics majors who now enter the field of optics.

It is felt that the research program being pursued, in which the undergraduate physics major is directly involved, is important regardless of the significance of the results in that it provides an excellent proving ground, so-to-speak, for physics majors. In a large university it is likely that such participation would be reserved for graduate students.

The author is in the Department of Physics, Southwestern College, Memphis, Tennessee.

Received 31 May 1963.

Southwestern has for many years had an Honors program. In the Physics Department those physics majors who qualify for this program can do work beyond that normally required for the B.S. degree. The program consists of two semesters of a theoretical physics course plus a project, usually experimental. Staff research provides excellent material for Honors research projects, and, in general, a student will work on a problem in some phase of optics of current interest to the staff. Although our experimental research activities are solely in the field of optical physics we try for a balanced physics curriculum. Our majors begin their work in the freshman year and, by the time of graduation, will have completed at least seven physics courses (each of two semesters' duration). In order for the majors to participate in the research program as early as possible the optics course (two semesters) taken in the sophomore year, was changed to Optics and Radiometry, and a senior-level course on Infrared Spectroscopy was added.

Since no research could be started the first year it was felt that the least that one could do would be to begin to develop the "right arm" of any experimental program; namely, machine-shop support facilities. The full-time services of an instrument maker were obtained a few months later. The room which he inherited as a shop was equipped with, at most, a few hand-tools and nothing in the way of metal stock. The limited budget mentioned previously made it impossible to purchase any new machinery whatsoever for the shop. Realizing this, the acquisition of government surplus machine-shop equipment was pursued. Government surplus is made available through the Department of Health, Education and Welfare for a fraction of its original cost. Before too long a facility was assembled that one was not ashamed to call a machine shop. Currently included in the shop are three lathes varying in sizes from 25.4-cm swing to 38.1-cm swing; two Number 2 milling machines, one horizontal and one vertical; one 91.4-cm DoAll metal cutting saw; one 40.6-cm drill press and one 17.8-cm shaper. This equipment, excluding the shaper, was government-surplus obtained for an average cost of $175 each. It should also be mentioned that various metal stock has been obtained from the above source.

At the end of the second year, and with the machine shop in competent hands, it was obvious that additional teaching staff would have to be secured if one was going to have any time for research. Shortly thereafter a second man at the Master's level was added to the staff.

Most likely in almost everyone's life a memorable experience

Fig. 1. Apparatus assembled to study near infrared radiation from the sun's atmosphere during a total solar eclipse. The apparatus consists of a 25.4-cm diam ($f$/4.5) reflecting telescope feeding a Perkin-Elmer "hasty scan" spectrometer.

Fig. 2. Completed mobile infrared observatory. This observatory consists of three sections. The section on the left slides over the center section and the section on the right slides out on the tracks.

stands out where a kind word by a friend, or that break, when one really needed it, leaves a lasting impression. Such was the author's experience with the Air Force Cambridge Research Laboratories. The writer will always feel a deep debt of gratitude to John N. Howard of AFCRL for having given the initial contract for work in the field of infrared physics and to his colleague, John Garing, for his continued support in this respect. With this initial contract a Perkin-Elmer Model 112 spectrometer (having "hasty scan" capabilities) and associated equipment were made available. Equipment of this kind would never have been possible for us otherwise. Since that time (1958) much additional infrared equipment has been obtained.

About two years later the department added another staff member (a molecular spectroscopist) at the Ph.D. level, who is doing work under contract with the AFCRL and, shortly thereafter, a full-time electronic technician.

The department now has a modest optics shop. Due to the generosity of a former undergraduate classmate of the writer, the Physics Department gained a modified Draper polishing-machine, a rough-grinding machine, and a diamond saw. Our electronics technician, who for many years has been interested in amateur astronomy, took a concentrated summer course in optical

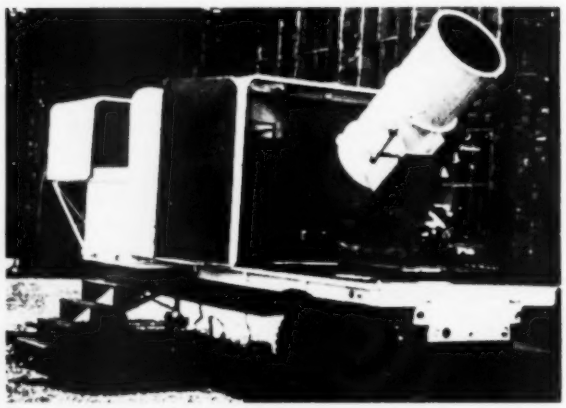

Fig. 3. Photograph of mobile observatory with the end sections open. The 78.7-cm diam radiometer ($f$/2) is mounted on a government surplus 40-mm antiaircraft gun mount.

production and testing techniques at the Institute of Optics at Rochester in 1962 and he is now in charge of this phase of our work. Mirrors up to 20.3-cm diam can be aluminized using thermal evaporation apparatus built here. This evaporation apparatus has also been of much pedagogical value in the optics laboratory course.

## III. Research Program

The nature of the program is such that this laboratory is often engaged in field expeditions. It has made a trip to the Canary Islands to participate in the total solar eclipse of 2 October 1959, to Santa Rosa Island (Florida) in July-August 1960 to participate in Project Firefly and to Climax, Colorado (High Altitude Observatory) in December 1962 for near-infrared solar studies using a coronagraph. It is now preparing for a trip to Gulkana, Alaska, to make infrared studies of the corona during the total solar eclipse of 20 July 1963. The research activities are described below.

### Total Solar Eclipse of 2 October 1959

Figure 1 shows the apparatus that was assembled in our laboratory to study the near infrared radiation from the sun's

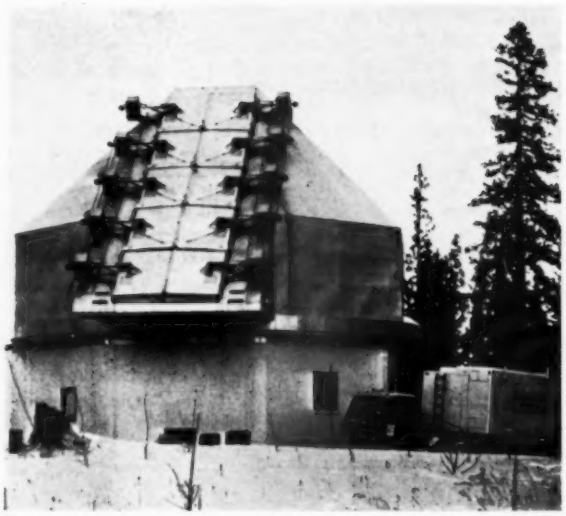

Fig. 4. Photograph of the Physics Department's small trailer located outside the large dome at the Climax Observing Station. This trailer was obtained from government surplus and was used to transport equipment on this expedition.

atmosphere during a total solar eclipse. The apparatus consists of a 25.4-cm diam ($f$/4.5) reflecting telescope of the Newtonian type feeding a Perkin-Elmer "hasty scan" spectrometer. This apparatus was mounted on a sturdy camera-panning head obtained from government surplus for $5.00. This equipment was carried to the island of Fuerteventura, but, unfortunately, clouds at the time of totality prevented the acquisition of data.

## Project Firefly (July-August) 1960

This work was concerned primarily with studying the infrared radiation (in the PbS region) from high-altitude chemical releases. To prepare for this expedition a government-surplus trailer (see Fig. 2) was obtained for $100.00. It was decided to build on this flat-bed trailer a mobile infrared observatory that could be carried to any part of the world. The finished mobile observatory in three sections is shown in Fig. 2, built entirely by the physics department. Figure 3 shows the observatory in the open position. On the larger end will be seen a 78.8-cm diam radiometer ($f$/2), mounted on a government-surplus 40-mm anti-aircraft gun mount. Four of our physics majors accompanied us on this expedition, under the NSF Undergraduate Research Participation Program.

Fig. 5. Photograph showing some of the spectroscopic equipment that was set up in the spectrometer room of the large dome at the Climax Observing Station.

## High Altitude Observatory (December 1962)

Our next efforts to study infrared radiation from the sun's atmosphere were made in December 1962, where John Firor, Director of the High Altitude Observatory, invited this laboratory to use the Observatory's 40.6-cm diam coronagraph. Their coronagraph (located at the Climax Observing Station) was successfully used to study the infrared radiation from the solar atmosphere in the PbS region.[1] The equipment was carried to Climax in a trailer obtained for $65 from government surplus (Fig. 4). Some of the spectroscopic equipment that was set up in the spectrometer room of the large dome at Climax is shown in Fig. 5.

## Total Solar Eclipse of 20 July 1963

For the past several months this laboratory has been preparing to participate in the total solar eclipse of 20 July 1963. The expedition (consisting of 12 persons, 4 of whom will be undergraduate students majoring in physics) will go to Gulkana, Alaska, in an attempt to study infrared radiation from the sun's atmosphere in the 1–15 $\mu$ region. These students will be participating under the NSF program to encourage research on the part of undergraduates. Figure 6 is a photograph of the mobile observatory and small trailer set up as they will be in Alaska. (It was necessary to increase the length of the observatory for this expedition.) The tracks on which the new section slides are dismantled and stored under the observatory when it is in transit.

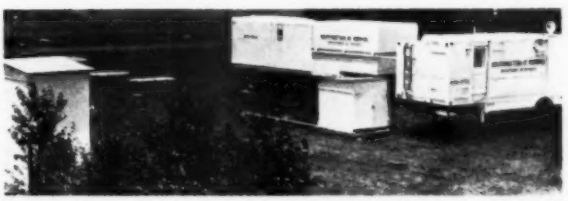

Fig. 6. Photograph of mobile infrared observatory and small trailer set up as they will be in Alaska. The right end of the observatory has been lengthened and the roof section of this end redesigned (see Fig. 3). The small white house covers 76.2-cm diam coelostat and the large white house covers a 76.2-cm secondary mirror.

Two scanning infrared spectrometers (Perkin-Elmer), each fed by a 35.6-cm diam ($f$/4.5) parabola, are located in the new section. Mounted under each of these spectrometers is a 12.7-cm diam (63.5-cm focal length) camera that is boresighted with the spectrometer. Each of these two systems (namely, camera, spectrometer, and associated mirrors) is mounted on a Mark 51 gun director (see Fig. 7). These Mark 51 gun directors were obtained without cost from the Naval Air Technical Training Center (Millington, Tennessee). On the other end of the observatory are mounted two radiometers (see Fig. 7). In addition, there is also mounted alongside the large radiometer a 12.7-cm diam (152-cm focal length) camera (see Fig. 8). All of these cameras were built in our laboratory using government surplus aerial camera parts.

The small trailer (see Fig. 6) houses an infrared spectrometer (Perkin-Elmer) and associated optics to measure the temperature of the ozone layer during totality. Under the small white

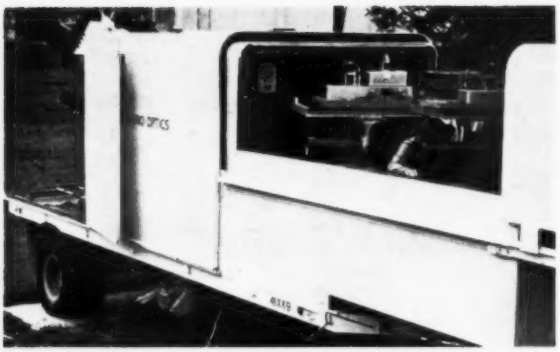

Fig. 7. Photograph showing the mobile observatory in the open position. On the right end can be seen two infrared spectrometers (Perkin-Elmer) mounted on Mk51 gun directors. On the left end of the observatory are mounted two radiometers and a long focal length camera.

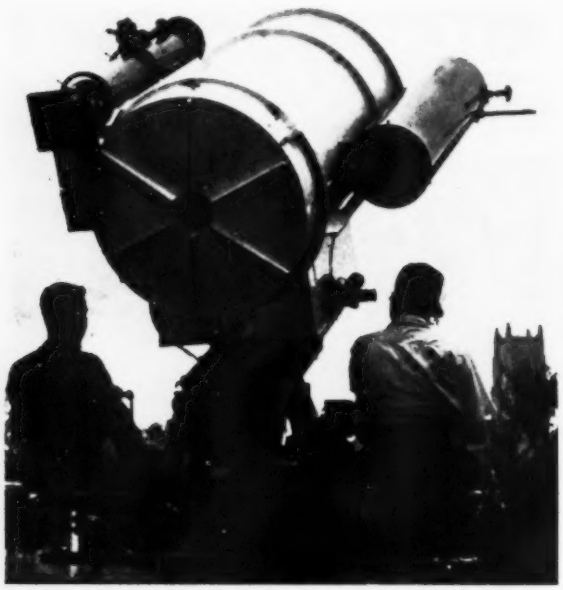

Fig. 8. Photograph of radiometer section of the mobile observatory. Mounted on the upper left of the large radiometer is a 12.7-cm diam (152-cm focal length) camera.

house is a 76.2-cm diam coelostat (built in our machine shop) and under the large white house is a 76.2-cm diam secondary pick-off mirror. Radiation from the sun is directed into the small trailer.

As pointed out above, this work is done under contract with AFCRL but the magnitude of this particular expedition is more than the contract can cover financially. In view of the opportunity such an expedition affords for the training of young physicists in the field of infrared, additional funds were sought to help defray the expense. Even though every attempt has been made to keep the cost to a minimum it can be readily appreciated that considerable expense is involved. It should be pointed out that the expedition will sleep in tents and will cook its own food! A local wholesale distributor of groceries assisted us by giving the food; another local firm gave all the tents, cooking utensils, etc.; finally, we were given four new tires which were needed on the mobile observatory. The Research Corporation, in particular Alfred Kelleher, made it possible by means of a grant for us to take on the expedition a former student of ours who is now in his third year of graduate work.

## Laboratory Activities

In addition to field trips, the staff maintains a continuing laboratory program. The laboratory has an infrared grating-spectrometer (Perkin-Elmer) equipped with a fore-prism monochromator that is to be used to study near infrared radiation from plasma arcs. The plasma arc being used was recently constructed and used by one of our students as part of his Honors work.

Figure 9 shows a Fabry-Perot interferometer of the pressure-scanning type being built in our laboratory. It consists of 10.2-cm diam fused-quartz plates (flat to $^1/_{20}$ wavelength) and is being designed primarily for auroral studies. Mention should also be made of work being done to measure quantum vibrational lifetimes in the infrared using a technique suggested by John Strong. Another activity is the construction of a radiometer to measure infrared radiation from planets. Designed primarily as a pedagogical instrument to be used by our students, the collimator for

Fig. 9. Photograph of Fabry-Perot interferometer (10.2-cm diam fused quartz plates) of the pressure scanning type that is being built by the Physics Department for auroral studies.

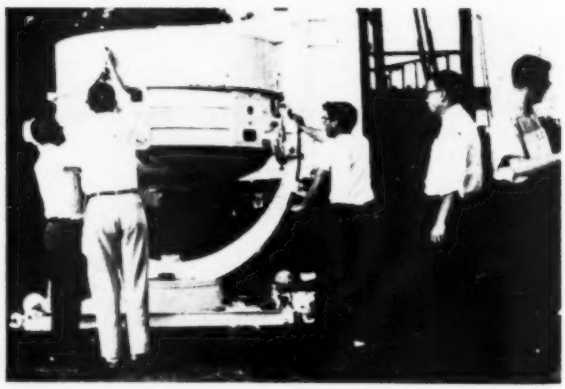

Fig. 10. Planetary radiometer (153-cm diam) being assembled by the Physics Department.

the radiometer is a 153-cm diam anti-aircraft searchlight mirror. Figure 10 shows this instrument located on our campus.

## IV. Conclusions

The author believes that the research program described here has been of value both to the undergraduate program in physics and to the physics staff. Such a program helps to motivate a student during what is probably the most sensitive period of his career, at a time when it is possible to really "fire him up". Because of a limited staff we have had to direct our efforts into one field of activity, and even the Honors program is designed so that it can assist staff research. It is felt that with a "one for all and all for one" attitude, a modest amount of headway in this particular field of endeavor can be made.

When discussing research in small colleges it should be pointed out that the ratio of staff members/field of research is probably comparable to that in many large universities, particularly if the large universities are concerned with many different research programs and if the small colleges confine their activities to one or two fields of endeavor.

In addition to the various people already mentioned by name in this paper the writer would like to express appreciation to John Strong and V. Z. Williams for their continuing encouragement, and to thank Harvey T. Marshall, Director, State Educational Agency for Surplus Property (Nashville, Tennessee) for his assistance in obtaining many specialized pieces of equipment from government surplus.

## Reference

1. J. H. Taylor and R. M. MacQueen, "Near Infrared Observations of the Solar Atmosphere," Appl. Opt. (in press).

*Editor's note:* John Howard remembers the letter he received in 1957 from Jack Taylor at Southwestern asking for research support. Taylor was alone in the Department with many teaching duties, no graduate students, no equipment; just a splendid background from Johns Hopkins and NRL and an impressive list of previous publications. He had sent the same letter seeking support to several possible sponsors, but this was the time period immediately preceding the first Sputnik when research funding was unusually austere. It so happened that AFCRL had just acquired an infrared spectrometer that had been specially constructed to work with a large cloud-chamber, and that particular effort had just collapsed. Howard sent Taylor this instrument plus an infinitesimal amount of funding—all that AFCRL could scrape up at that moment. In practically no time Taylor had students working out advanced problems on this instrument, he had matched it with a home-made Newtonian telescope to do sky studies, and was making plans to study solar eclipses. His success in turning out students eager to continue in optics research testifies to the capability of a dedicated teacher to inspire.

CHANGES OF ADDRESS

Changes of address should be sent to APPLIED OPTICS SUBSCRIPTION HANDLING, American Institute of Physics, 335 East 45th Street, New York, New York *as far in advance as possible.* Eight weeks should be allowed to effect such changes.

*continued from page 1068*

K. H. B. Wilhelmsson, "Interaction between an obliquely incident plane electromagnetic wave and an electron beam in the presence of a static magnetic field of arbitrary strength", J. Res. NBS 66D (Radio Prop.), No. 4, 439–451 (1962).

J. Galejs, "Scattering from a conducting sphere embedded in a semi-infinite dissipative medium", J. Res. NBS 66D (Radio Prop.), No. 5, 607–612 (1962).

V. H. Weston and R. Hemenger, "High-frequency scattering from a coated sphere", J. Res. NBS 66D (Radio Prop.), No. 5, 613–619 (1962).

K. C. Yeh, "Propagation of spherical waves through an ionosphere containing anisotropic irregularities", J. Res. NBS 66D (Radio Prop.), No. 5, 621–636 (1962).

C. J. Marcinkowski and L. B. Felsen, "On the geometrical optics of curved surfaces with periodic impedance properties", J. Res. NBS 66D (Radio Prop.), No. 6, 699–705 (1962).

C. J. Marcinkowski and L. B. Felsen, "On the limitations of geometrical optics solutions for curved surfaces with variable impedance properties", J. Res. NBS 66D (Radio Prop.), No. 6, 707–712 (1962).

J. V. Evans, "A lunar theory reasserted—a rebuttal", J. Res. NBS 67D (Radio Prop.), No. 1, 1–4, (1963).

K. Furutsu, "On the theory of radio wave propagation over inhomogeneous earth", J. Res. NBS 67D (Radio Prop.), No. 1, 39–62 (1963).

R. L. Smith-Rose, "The protection of frequencies for radio astronomy", J. Res. NBS 67D (Radio Prop.), No. 2, 99–105 (1963).

G. H. Millman and F. L. Rose, "Radar reflections from the moon at 425 Mc/s", J. Res. NBS 67D (Radio Prop.), No. 2, 107–117 (1963).

J. R. Roach, "Effects of radio wave propagation through mid-latitude 6300 A arcs", J. Res. NBS 67D (Radio Prop.), No. 3, 263–271 (1963).

K. Furutsu, "On the statistical theory of electromagnetic waves in a fluctuating medium (1)", J. Res. NBS 67D (Radio Prop.), No. 3, 303–323 (1963).

# Conference on Interference and Coherence Sydney, Australia, 24–25 August 1964

**Provisional Subjects** to be covered at a short ICO-AAS Conference on Interference and Coherence to be held preceding the conference in Tokyo and Kyoto (1–8 September 1964) include applications of interferometry to length standards and measurements, testing of optical systems, studies of the properties of materials, and to radio astronomy; new techniques in interferometry and new types of interferometers; and coherence and correlations. Both invited lectures and short papers on these topics are planned.

**Provisional Timetable:** Reunions at private homes on 23 August; conference sessions in Sydney University on 24 and 25 August; visits to National Standards and Radiophysics Laboratories, Sydney University, and University of New South Wales on 26 August; visits to scientific installations outside Sydney 27–29 August either as tours or by private arrangement made at the conference. OSA's Around-the-World Group Flight provides transport to this and the Tokyo meeting.

**Scientific Tours** could include visits to Narrabri, a country town 565 km north of Sydney, where there is an intensity interferometer for measuring stellar diameters and a radioheliograph for mapping the sun; Parkes, a country town 400 km west of Sydney and the site of a large radio telescope; Canberra, the national capital, 320 km south of Sydney (enroute to Melbourne) and the home of the Australian National University and Mount Stromlo Observatory; and Melbourne, capital of State of Victoria, the location of CSIRO Division of Physical Chemistry, the University of Melbourne, and Monash University.

**Accommodations** can be arranged at one of the University Colleges either for the conference only or for the full week at £A2.12.6 ($7.00) a day including meals.

**Registration** fee will be £A4 ($9.00) including the conference dinner. Students may register for the meeting only for £A1 ($2.20). Tours will be extra.

**Additional Information** can be obtained from the Australian National Committee for Optics, W. H. Steel, Convenor, CSIRO Division of Physics, City Road, Chippendale, N.S.W., Australia.

## International Commission for Optics

## CONFERENCE ON PHOTOGRAPHIC AND SPECTROSCOPIC OPTICS

### Tokyo and Kyoto 1–8 September 1964

### arranged by

### SCIENCE COUNCIL OF JAPAN and JAPANESE SOCIETY OF APPLIED PHYSICS

A Conference on Photographic and Spectroscopic Optics, arranged on an international level by the Science Council of Japan and the Japanese Society of Applied Physics under the auspices of the International Commission for Optics, will be held in Tokyo and Kyoto, Japan, 1–8 September 1964. The Conference will be composed of some 10 sessions, and each session will include one or two invited papers (30–40 min presentation time) and some contributed papers (15 min each). The subjects to be dealt with at the Conference will be:

**Design and Evaluation of Photographic and Spectroscopic Optical Systems**
**Recent Instrumentation in the Far Infrared and the Extreme Ultraviolet**
**Optical Materials for Use in Photographic and Spectroscopic Optics**

Offers of papers should be made no later than 31 January 1964, by sending an abstract to the Organizing Committee. This abstract must be adequate for the Committee to decide on the suitability of the paper: the scope of the paper should be indicated, and principal new results included. The working languages of the Conference will be English, French, and German. However, in view of the fact that English will be the only language comprehensible to the majority of participants, speakers are strongly recommended to read their papers in English.

Visits to research institutes, universities, and optical companies are being planned. More detailed information will be circulated in due course.

**All inquiries concerning the Conference should be addressed to: Prof. H. Kubota, Secretary, Organizing Committee, ICO-Tokyo & Kyoto, Science Council of Japan, Ueno Park, Tokyo. For planning purposes the Japanese Committee is very eager to estimate the number of people who will attend; If you are interested in this meeting please write immediately to Prof. Kubota for further information.**

# A New Family of Flat-Field Cameras

Rubin Gelles

A family of flat-field catadioptric objectives is discussed. These are aplanatic and anastigmatic with small amounts of distortion. One distortion-free case is also discussed. The objectives represent a development of the flat-field Schmidt camera. An afocal doublet lens is used in place of the conventional aspheric corrector plates. The resulting system is more easily fabricated, although there is no sacrifice in performance.

The excellent optical image characteristics of the Baker flat-field Schmidt system are well known.[1] In common with all Schmidt systems it is limited in practice by the difficult aspheric plates which are required. Hence, the system is usually used only where the necessity for highest optical performance overrides considerations of manufacturing difficulty. The problem is heightened if control of chromatic aberration is necessary, for a pair of color correcting plates then becomes necessary. Consequently, it would be useful if a substitute for the aspheric correcting plates were available, provided that optical performance could be maintained.

It is clear that any modification of the flat-field Schmidt system must retain at least an equal number of degrees of freedom in the design if there is to be no degradation in the optical performance. In the systems under discussion it has been found feasible, in place of the aspheric plates, to substitute a doublet lens whose net power is zero. The doublet is composed of closely spaced positive and negative lenses of low power. The individual bending of each component enables the designer to achieve correction of the aberrations. In the following discussion, systems involving only spherical surfaces, one aspheric surface, and finally two aspheric surfaces will be discussed.

The substitution of afocal lens combinations for the aspheric plates was described in a patent issued to Houghton[2] who used two or more thin lenses in contact forming an afocal system at the center of curvature of the mirror. Hawkins and Linfoot[3] describe an afocal cemented doublet at the center of curvature of a concentric catadioptric system. The refractive indices in $d$-light of the two glasses used in the doublet are similar. But the dispersions are chosen so as to correct the longitudinal chromatic aberration of the concentric corrector.

The starting point of the design proceeds from the assumption that the central radii of the concave primary mirror and the convex secondary mirror are equal, resulting in zero Petzval curvature. Initially, the components of the front doublet are assumed to be thin lenses in contact, with the aperture stop in this position, and the optical system is laid out to conform with the requirements of focal length, position of the focal plane, etc. The third-order aberrations of the primary and secondary mirrors are calculated and use is made of the stop shift equations in a form similar to that given by Conrady[4]:

$$\begin{aligned} S^* &= S, \\ C^* &= C + SQ, \\ A^* &= A + 2CQ + SQ^2, \\ P^* &= P, \\ D^* &= D + (I^2P + 3A)Q + 3CQ^2 + SQ^3. \end{aligned} \tag{1}$$

In these equations, $S$, $C$, $A$, $P$, $D$ are spherical aberration, coma, astigmatism, Petzval curvature, and distortion, respectively, before shifting the stop. The starred quantities are the aberration contributions after stop shifting and $Q$ is the ratio of the height of the "new" principal ray in the entrance pupil plane to the height of the marginal ray. The optical invariant $I$ is given by $I = n'(yu_p' - y_pu')$, where $y$ and $y_p$ are the heights of the marginal and principal rays, respectively, and $u'$ and $u_p'$ are the angles of the marginal and principal rays, respectively.

In the case of the system utilizing only spherical surfaces, the aperture stop is assumed to be at the primary mirror, and the aberration contributions of the primary and secondary mirrors are computed. In order to

The author is at the Kollsman Instrument Corporation, Elmhurst, New York.

Received 13 December 1962.

EFL = 20
f/3

| $R$ | $d$ | |
|---|---|---|
| −25.279 | .500 | BK7 (517/645) |
| −17.092 | .500 | air |
| −11.637 | .328 | BK7 (517/645) |
| −15.122 | 21.718 | air |
| −23.000 | 6.553 | air |
| −23.000 | | |

Fig. 1. Constructional data for the all-spherical optical system.

correct the system the aberrations of the front doublet must be equal and opposite to the aberrations of the rest of the system. Therefore, making use of Eqs. (1), we write:

$$S_1 = -(S_2 + S_3), \tag{2}$$

$$C_1^* = C_1 + S_1Q_1 = -(C_2 + C_3^*), \tag{3}$$

$$A_1^* = 2C_1Q + S_1Q_1^2 = -(A_2 + A_3^*). \tag{4}$$

In these equations the subscripts 1, 2, 3 refer to the front doublet, the primary mirror, and the secondary mirror, respectively. After substituting $S_1$ from Eq. (2) into Eqs. (3) and (4), these are solved simultaneously for $C_1$ and $Q_1$. The solution for $C_1$ is the coma of the front doublet with the stop at the lens. From the calculated values of spherical aberration and coma, the shapes of the positive and negative components are determined from the usual thin lens equations. The equations for thin lens aberrations discussed by Wynne[5] have been found to be very useful. The curvatures calculated in this way are of course only approximations

EFL = 24
f/4

| $R$ | $d$ | |
|---|---|---|
| 25.85 | 0.500 | BK7 (517/645) |
| Plano | 0.300 | air |
| −31.99 | 0.350 | BK7 (517/645) |
| 126.13 | 18.766 | air |
| −28.57* | 8.620 | air |
| −28.57 | | |

$$\text{* Aspheric } X = \frac{-\ 0.03500W^2}{1 + \sqrt{1 - 9.35977 \times 10^{-4}W^2}}$$

Fig. 2. Schematic of the optical system incorporating one aspheric surface.

and will be modified when thicknesses are added to the lenses.

An optical system of this type with a 2-m focal length and aperture ratio $F/3$ is shown in Fig. 1. The third-order aberrations with the exception of distortion are zero.

It will observed that the relatively large amount of spherical correction required of the front doublet has resulted in rather deep meniscus forms for the lenses. This is undesirable both from the point of view of manufacture and the introduction of large amounts of higher order aberrations. This seems to indicate that the all-spherical system is more suited to systems of only moderate aperture.

It is possible to reduce the curvatures of the front lenses by employing an aspheric surface in the system. In one form, illustrated in Fig. 2, the front doublet only partially corrects the spherical aberration, and aspheric figuring of the primary mirror controls the remaining

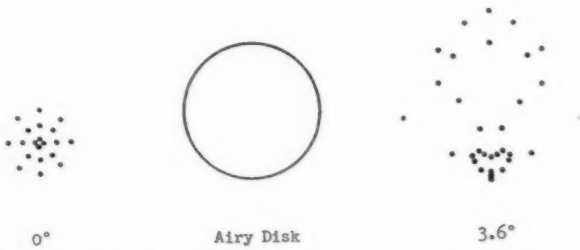


Fig. 3. Spot diagrams of the optical system of Fig. 2. The Airy disk is shown for comparison.

spherical aberration. The aperture stop is taken to be at the primary mirror and using Eqs. (1) we write:

$$C_1^* = C_1 + S_1Q_1 = -(C_2 + C_3^*), \tag{5}$$

$$A_1^* = 2C_1Q_1 + S_1Q_1^2 = -(A_2 + A_3^*), \tag{6}$$

$$\bar{S}_2 = -(S_1 + S_2 + S_3). \tag{7}$$

Here the barred quantities refer to the aberration contributions of an aspheric surface. It will be recalled that the extra-axial aberrations of an aspheric surface at the aperture stop are zero. With an arbitrary choice of the value of $S_1$, Eqs. (5) and (6) yield simultaneous solutions for $C_1$ and $Q_1$. The resulting required value of $\bar{S}_2$ determines the aspheric figuring necessary for spherical correction.

Spot diagrams for the axial bundle and a bundle 3.6° off-axis are plotted in Fig. 3. These give an indication of the capabilities of the system, although the optical system is not completely corrected. Nevertheless a comparison with the diameter of the Airy disk indicates an approach to diffraction-limited performance over the entire field. The asphericity of the primary mirror is quite mild, amounting to about 4.25 wavelengths of sodium light at the edge of the primary mirror.

Since the value of $S_1$ is arbitrary, it can be selected to give favorable shapes to the components of the front doublet. In Fig. 4, a system designed by Rosin[6] is illustrated. In this system the rear surfaces of the lenses were kept plano. The curvatures of the front surfaces were varied to achieve coma correction, at the same time maintaining a net power of zero for the combination. This procedure left undercorrected spherical aberration which was corrected by a mild asphericity on the first surface of the front doublet. This system has great utility from the standpoint of manufacture, since plano lenses are easier to make than any other form.

In none of the systems discussed so far has there been any specific attempt to correct distortion. However, the distortion in these systems appears to be quite small. The optical system of Fig. 2, for example, has only about 10 $\mu$ of distortion at the edge of the field.

It is instructive to consider the approach to the design of a system in which distortion as well as the other aberrations are corrected. To do this, we will suppose that we have, as an additional degree of freedom, a second asphericity which will be placed on the secondary mirror. If, for convenience, the aperture stop is assumed to beat the front doublet, the stop shift equations are as follows:

$$\bar{A}_2 + \bar{A}_3 = \bar{S}_2 Q_2^2 + \bar{S}_3 Q_3^2 = -(A_2^* + A_3^*), \quad (8)$$

$$\bar{D}_2 + \bar{D}_3 = \bar{S}_2 Q_2^3 + \bar{S}_3 Q_3^3 = -(D_2^* + D_3^*), \quad (9)$$

$$S_1 = -(S_2 + \bar{S}_2 + S_3 + \bar{S}_3), \quad (10)$$

$$C_1 = -(C_2^* + \bar{C}_2 + C_3^* + \bar{C}_3). \quad (11)$$

Simultaneous solution of Eqs. (8) and (9) yield the required $\bar{S}_2$ and $\bar{S}_3$ and consequently the asphericities of the primary and secondary mirrors. Equations (10) and (11) then give the spherical and coma contributions for the front doublet, from which the required bendings are readily calculated.

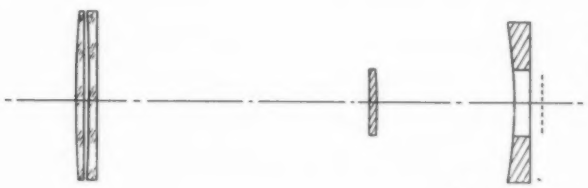

EFL = 78.74
f/3

| $R$ | $d$ | |
|---|---|---|
| 172.41* | | |
| Plano | 1.500 | K3 (518/590) |
| −169.16 | .750 | air |
| Plano | 1.500 | K7 (511/605) |
| −92.788 | 83.0 | air |
| −92.788 | 27.335 | air |

* Aspheric $X = 2.9000 \times 10^{-2} W^2 - 2.765 \times 10^{-7} W^4$

Fig. 4. Schematic of optical system incorporating one aspheric surface.

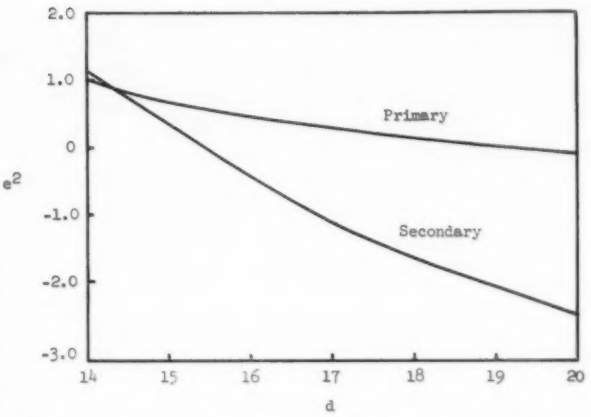


Fig. 5. The squared eccentricities of the primary and secondary mirrors plotted as a function of the distance between the front doublet and the primary mirror.

Superficially it would appear that such a system would have little attraction, provided that distortion could be tolerated, because of the difficulty of testing an aspheric convex secondary. But an inspection of Eqs. (8) and (9) shows that there may be solutions in which the asphericity of either the primary or the secondary mirror is zero, since no restrictions have been placed on the value of $S_2$ and $S_3$. If the distance between the front doublet and the primary mirror is varied, while the separation between primary and secondary is held constant, it will be found that the surface figures change from hyperboloidal through spherical to oblate spheroidal. This is shown in Fig. 5 where the squares of the eccentricity of both the primary and secondary have been plotted as a function of the distance between the front doublet and the primary mirror. These results were obtained from calculations on an optical system in which the paraxial radius of the primary and secondary mirrors was 28.57. The separation between the primary and secondary was held at 8.503, and the focal length was 24.0. It will be recalled that the following holds:

$e > 1$ for a hyperboloid,
$e = 1$ for a paraboloid,
$e < 1$ for an ellipsoid,
$e = 0$ for a sphere,
$e$ is imaginary for an oblate spheroid.

Thus, from Fig. 5, when the secondary is spherical, the primary is ellipsoidal, and when the primary is spherical, the secondary is an oblate spheroid. An interesting feature of the graph is seen at the point where the primary and secondary have the same eccentricity. If the primary has been accurately figured, the secondary could then be tested against it with a simple Newton's ring test.

If the front doublet were actually composed of thin

lens elements in contact, the combination would be color-corrected if both the positive and negative lens were made of the same glass. In reality, however, the lenses have a finite thickness and separation, with resultant chromatic aberration which must be corrected. In the system of Fig. 2, the same glass has been used for both components with a consequent small amount of undercorrected longitudinal and lateral chromatic aberration. For example, lateral chromatic aberration is approximately 12 $\mu$ at the edge of the field. It has been calculated that this aberration would be corrected if the glasses used had a difference of 2.4 in Abbe $\nu$ numbers. Alternatively, it is possible to correct the small amount of chromatic aberration by departing slightly from the requirement that the front doublet have zero power.

Provided that systems of small aperture are desired, it seems likely that the all-spherical system will be very useful. The simplicity of construction combined with good optical imagery facilitates the construction of long focal length objectives. On the other hand, despite the increased complexity, the additional degree of freedom afforded by the aspheric surface lends itself to the design of systems with larger aperture and excellent correction. It might be supposed that the goal of eliminating Schmidt plates has been reached at the price of an equally difficult aspheric surface. But it must be considered that the testing of a concave aspheric reflecting surface is very much easier than the refracting aspheric Schmidt plates.

## References


1. J. G. Baker, Proc. Am. Phil. Soc. **82**, 339 (1940).
2. J. L. Houghton, British Patent 546, 307.
3. D. G. Hawkins and E. H. Linfoot, Monthly Notices Roy. Astron. Soc. **105**, 334 (1945).
4. A. E. Conrady, *Applied Optics and Optical Design* (Dover, New York, 1957), Vol. 1.
5. C. G. Wynne, Opt. Acta **8**, 255 (1961).
6. S. Rosin, private communication.



**FUTURE MEETINGS**

**OPTICAL SOCIETY OF AMERICA**

**1963 23–25 October, 48th Annual Meeting, Sherman House, Chicago, Ill.**

**1964 1–3 April, Spring Meeting, Sheraton Park Hotel, Washington, D.C.**

**7–9 October, 49th Annual Meeting, Statler-Hilton Hotel, New York, N.Y.**

**1965 31 March, 1 and 2 April, Spring Meeting, Statler-Hilton Hotel, Dallas, Tex.**

Executive Office
1155 16th Street, N.W. Washington, D.C. 20036



**Applied Optics** January 1962

featuring **OPTICAL PUMPING AND MASERS**
editor B. H. Billings

**Magnetic Resonance in Radiating or Absorbing Atoms**—Francis Bitter

**Composite Rod Optical Masers**—G. E. Devlin, J. McKenna, A. D. May, and A. L. Schawlow

**Atomes à l'Intérieur d'un Interféromètre Perot-Fabry**—A. Kastler

**Synthetic Maser Ruby**—Robert D. Olt

**Proposal for an Electron Accelerator Using an Optical Maser**—Koichi Shimoda

**Recent Developments in Maser Devices and Materials**—Hendrik J. Gerritsen

**The Interference between Beams from the Opposite Ends of a Ruby Optical Maser**—P. Kisliuk and D. J. Walsh

**Photomixing Experiments with a Ruby Optical Maser and a Traveling-Wave Microwave Phototube**—B. J. McMurtry and A. E. Siegman

**Properties of the Hydrogen Maser**—Daniel Kleppner, H. Mark Goldenberg, and Norman F. Ramsey

**Principles of Operation of the Rubidium Vapor Magnetometer**—Arnold L. Bloom

**$2.00 a copy** cash with order preferred

**See order card facing page 852**
**Order from APPLIED OPTICS Back Numbers**
AIP Attn. Mr. Uszak, 335 E. 45th St., New York, 17, N.Y.

Applied Optics

# Letters to the Editor

*Letters to the Editor should be addressed to the Editor, APPLIED OPTICS, 1155 16th St., N.W., Washington 36, D.C.*

## Illumination of the Slit Source of the Hough-Powell Digitizer

Seymour Rosin

Brookhaven National Laboratory, Upton, Long Island, New York.

Received 6 May 1963.

Work performed under the auspices of the United States Atomic Energy Commission.

There are in general two means of illuminating a subject for projection. The first of these is to form an image of the source directly on the subject, and the angular subtense (numerical aperture) of the beam must be equal to or preferably greater than that of the projection lens to follow. With this method all of the inhomogeneities of the source are projected. The second method is to image the source into the projection lens by means of condensers close to the subject, such as in the projection of lantern slides, film transparencies, and the like. The requirement here is that the source image at the projection lens must be equal to or preferably larger than the aperture of the projection lens. Following terminology used in microscopy, we can call the first method "critical illumination" and the second "Koehler illumination".

In the Hough-Powell Flying Spot Digitizer, the available source is a General Electric BH6 mercury arc lamp 1.5 mm in diameter and 25 mm long. The slit to be illuminated is a few microns wide and 75 mm long. The projection lens aperture is situated 425 mm beyond the slit.

Originally, a condenser was employed between the source and the slit which magnified the source by a factor of 3× so as to cover the slit length. A field lens adjacent to the slit imaged this condenser into the projection aperture. While, according to Gaussian optics, the projection lens was filled, the optical demands on the condenser lens as to numerical aperture were so severe that the 3× magnification delivered a beam afflicted with a considerable amount of both spherical and chromatic aberration.

The system described below was superior in all respects to the more conventional one described in the preceding paragraph and actually increased the illumination of the slit by a factor of three in the instrument in use at Brookhaven National Laboratory. It is a hybrid of the two methods, critical illumination being employed across the source and slit-widths and Koehler illumination along their lengths. The optical arrangement is shown in Fig. 1.

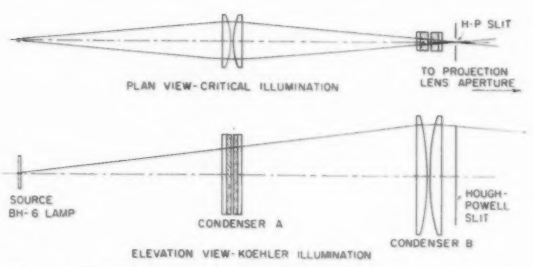


Fig. 1 Hybrid illumination system using cylindrical lenses.

Referring to the plan view the source is imaged directly on the slit by a pair of cylindrical condensers A at unit magnification. In this view condensers B have no power and act as a pair of plane parallel plates. However, in elevation, cylindrical condensers B serve to image the length of the source in the projection lens aperture. Again in this latter view condensers A have no power.

Besides the increase in illumination, the fact that any point of the slit receives rays from all points along the source length results in even illumination along the slit.

## Note on Hole Burning Model of Oscillation For Ruby Lasers

A. J. DeMaria

United Aircraft Research Laboratories, East Hartford, Connecticut.

Received 12 July 1963.

In a recent paper,[1] the occurrence of an ensemble of micropulses emitted from a ruby laser with relatively large separation between the optical feedback reflectors was reported and explained as due to a "hole burning" process as suggested by Hughes.[2] Tang *et al.*[3,4] have recently proposed a "spatial hole burning" model of operation for ruby lasers which avoids the problem of explaining "hole burning" in the temperature broadened ruby line as encountered in the previous model. Spatial hole burning is proposed to take place because of the spatial variation in the field intensity of the optical standing wave of the feedback cavity which results in a nonuniform distribution of the inverted population of $Cr^{3+}$ ions along the length of the ruby rod. The purpose of this letter is to acknowledge that the micropulse ensemble and the simultaneous oscillation at two optical frequencies corresponding to eigenwavelengths of the Fabry-Perot cavity reported in ref. 1 may be explained by the Tang, Statz, and deMars model.

### References

1. A. J. DeMaria and R. Gagosz, Appl. Opt. **2**, 807 (1963).
2. T. P. Hughes, Nature **195**, 325 (1962).
3. H. Statz, C. Tang, and G. deMars, Bull. Am. Phys. Soc. **8**, 87 (1963).
4. C. Tang, H. Statz, and G. deMars, Appl. Phys. Letters **2**, 222 (1963).

# British National Hydrogen Bubble Chamber

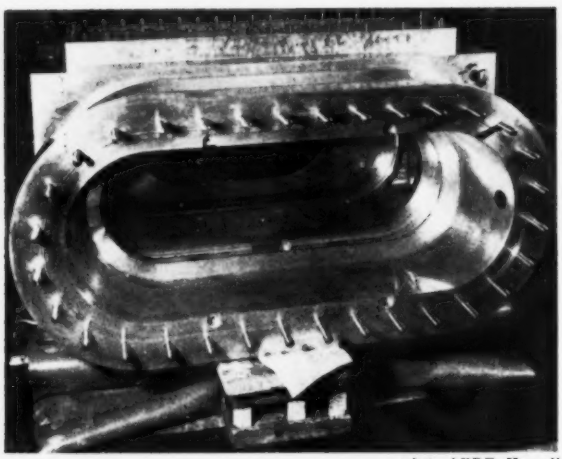

*photo AERE, Harwell*

The chamber body of the British national hydrogen bubble chamber with the window retaining flanges attached. These items were made from a single forging of an aluminum alloy containing 3% magnesium and weighing 13½ tons. The chamber top plate can also be seen.

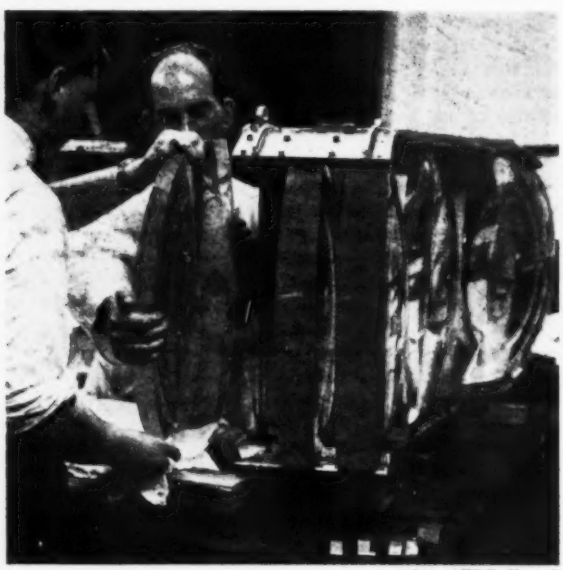

*photo AERE, Harwell*

The assembly of three triplet condensers for dark-ground illumination of the British national hydrogen bubble chamber.

*photo AERE, Harwell*

The magnet yoke of the British national hydrogen bubble chamber during assembly. This is made from a low carbon steel and as indicated weighs 240 tons.

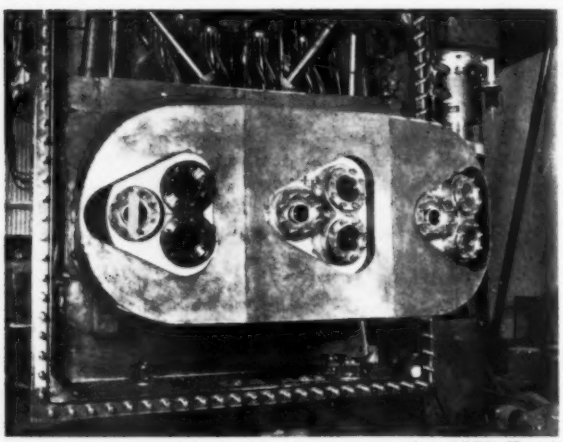

*photo AERE, Harwell*

The British national hydrogen bubble chamber with thermal radiation shield in position. This shield, which is cooled by pumping liquid nitrogen (temperature 78°K) around pipes attached to it, is fabricated from stainless steel sheets electroplated with copper to reduce the emissivity.

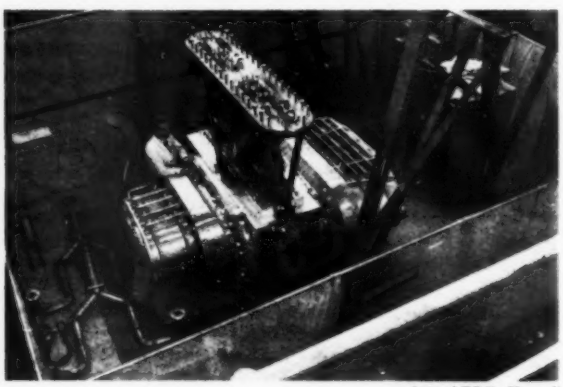

*photo AERE, Harwell*

View of the assembled British national hydrogen bubble chamber. The forty-eight pipes of the expansion system, the chamber suspension, and the top plate of the vacuum tank, through which all pipelines and electrical services are taken, can be seen.

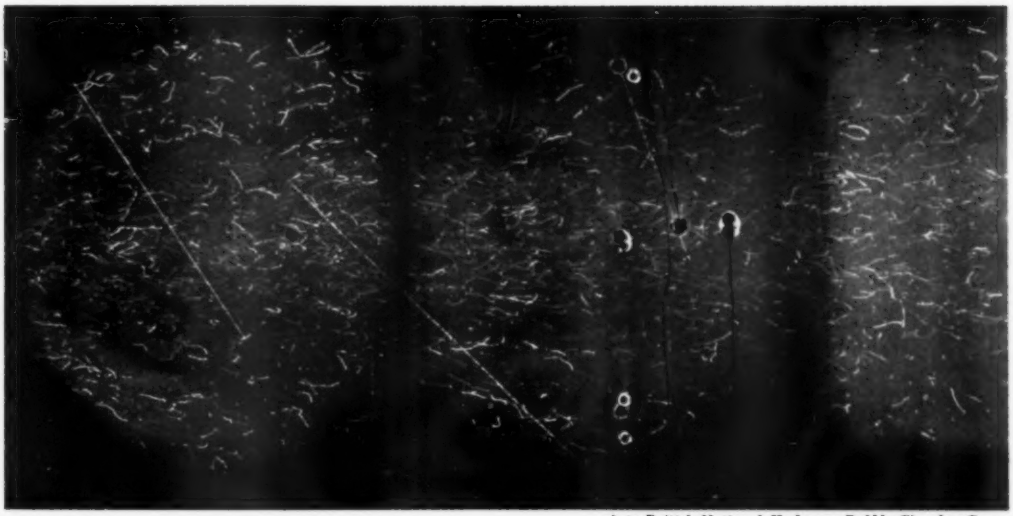

*photo British National Hydrogen Bubble Chamber Group*

A photograph taken during the test run of the British national hydrogen bubble chamber in January 1963. The liquid hydrogen was made sensitive to charged particles at 26.8°K by lowering the pressure by about 3 atm. The short tracks are low-energy electrons produced by a pulsed beam of $\gamma$ rays originating from a $Co^{60}$ source. The longer straight tracks were produced by cosmic rays (probably muons). The black disks and wires are copper-constantan thermocouples used to measure the temperatures of the windows during cooldown. Heavy background is due to chalk dust on optics collected during vacuum leak testing and to air frost due to failure of differential pump in $H_2$ shield.

**Books** *continued from page 1060*

reader in interpreting the planetary images. Most of the Mars photographs are from the Lowell Observatory collection, but a number of very good photographs from other observatories are included as well.

Finally, a map of the planet is included inside the back cover so that it can be unfolded and viewed directly beside each plate in order to identify named features.

The plates are the real heart of the book. They show in detail the regular seasonal changes, blue and yellow clouds, and both short- and long-term alterations in the surface markings. All the major phenomena of the Martian surface and atmosphere are illustrated distinctly and described clearly. Here we have a permanent record of great value, showing the principal periodic, sporadic, and secular changes that take place on Mars. It is truly a photographic history of the planet, and deserves the careful scrutiny of every serious planetary worker.

Several of the plates deserve special comment. Plates VII, VIII, and XXXV show the remarkable changes in the northern hemisphere between longitudes of 220° and 280° over the past sixty years. This area has changed so strongly that one wonders whether any surface feature is truly permanent. Plates X, XI, and XVI show an almost clocklike regularity in the seasonal changes at different oppositions. A series of six plates, beginning with number XXVIII, displays the complexity of the "blue clearing" phenomenon.

Plates XXXVII and XXXVIII compare several visual observers' drawings with photographs taken at or near the same time, and expose the unreliability of visual observations. Slipher says that "The visual observations have been of great help in the representation of the fine structure, such as sharpness, width and regularity of boundary lines or canals. On the other hand many markings are quite satisfactorily shown by the photographs which were not noticed in the visual observations . . . Whatever visual observations disclose concerning existence or nonexistence of the more difficult canals and oases is obviously of little value." (pp. 142–144). Considering the gross distortion of easily photographed features in the drawings—which show a strong tendency to simplify the complexity of the surface, and to straighten or smooth out irregularities—one wonders whether any weight at all should be given to visual descriptions of still finer and more difficult detail.

Plate XLVII is an actual photographic print, entitled "Photo Evidence of Lines (Canals) on Mars". The smallest resolvable spots on the photographs are about 3 degrees in diameter, while the "canals" on Slipher's map are about 1° wide. Thus, while one can see from the photographs that "something is there" where Slipher draws his major canals, the photographs do not disprove the idea that the "canals" can be resolved into a series of disconnected spots, and are not truly line-like in character: the necessary information (i.e., the high-frequency Fourier components of the brightness distribution) is missing. (At the best oppositions, 1° on Mars corresponds to 0.2 sec of arc, which is about at the diffraction limit of a 50-cm aperture.) It appears that the canal controversy is still undecided on the basis of impersonal observations, but the problem now concerns the detailed nature of these markings rather than their existence.

There are a fair number of misprints, but most are no more serious than the frequent substitution of "Lucus" for "Lacus". Two important errors are the reference to Plate VI instead of VIII in the text accompanying Plate XXI, and the apparent omission of "not" from the end of line 26, p. 162. But such errors do not diminish the importance of this definitive summary of the photographic study of Mars. The reader may disagree with the author's conclusions, but he will find that the pictures speak for themselves, and that a careful study of the photographs is more instructive than any text could be.

ANDREW T. YOUNG

# Applied Optics — Optical Activities in Industry

*reported by FRANK COOKE, 66 Summer Street, North Brookfield, Mass.*
*Mr. Cooke welcomes news and comments for this column which should be sent to him at the above address*

In place of Mr. Cooke's column this month, we are reproducing, by permission of the Editor of *The Boston Globe*, the following editorial by Peter B. Greenough which appeared on 17 May 1963 under the heading "Russians Do Better—Optics Neglected in U.S.A."

To develop the Zeiss Tessar lens for cameras, it required the mathematical calculations of one man working 25 years.

By computer, the same job takes less than an hour. Not only that, the computer will also tell you what kind of grinding ratios have to be used for a specific lens job. It also dictates what type of glass must be used.

From the foregoing, you might believe that automation now completely dominates lens making, and that old-time skills no longer are needed.

Then think again.

In a brochure describing the capabilities of a small new company in Bedford—Diffraction Limited, Inc.—there is the following notation:

> In an age in which the measure of progress appears to be the reduction of craft to automation, there is something reassuring about the fact that in optics the master craftsman still reigns supreme . . . Quality walks in the door every morning on two legs.

Rare is this quality, too—to the extent that the strategic capabilities of the United States in optics may be much too thin. You can count on the fingers of both hands the number of companies with high proficiency in the field.

The importance of optics—in tracking the capsule of Maj. Gordon Cooper, for example—hardly needs amplification here. Our reconnaissance capabilities, either via satellite or high-altitude plane, absolutely depend on how good the resolution is from new-type lenses.

Diffraction Limited (on the Middlesex Turnpike around the corner from Mitre Corp.) is a good spot to learn what is going on in this field. Some of it is good, even great. Some is not.

Sophistication of what is coming out of United States lens companies ranks tops in the world. We're doing dandy with systems. In quantity, it is quite another tale.

According to Dr. Willem Brouwer, president of Diffraction, the University of Rochester, N.Y., is the "only school training people in lens designing and grinding today".

Two prime Rochester industries, Eastman Kodak and Bausch & Lomb, are the beneficiaries.

Neither M.I.T. nor Harvard have, says Brouwer, any courses specifically based on optics (although it comes under training as physicists).

"Government schools aren't interested in creating sources in optics," Brouwer says.

Which is odd. Our skilled base in this field exists around Rochester, at American Optical in Southbridge, Mass., in Perkin-Elmer down in Connecticut, and finally at Itek Corp. and Diffraction Limited here.

Holland is heavy in optical work. You'll find a small corner of Holland out at Diffraction, because so many of its employees came from around Delft, where Brouwer was trained, at the Technical University.

The West and East Germans still excel at it although, says Brouwer, there are "no more good young ones". Japan, too, and Russia, especially.

Brouwer has talked with Russian lens designers at trade shows in New York. "They are very capable there. They have optical institutes at both Leningrad and Moscow. The government itself takes great interest in it."

Why do we ignore this field?

Because, Brouwer thinks, the "Russians don't throw away their old fields when a new one comes along. They're still training men to run a lathe. Here we consider optics an old and ancient art, with no progress".

Another restrictive factor is that American-produced glass simply isn't good enough for the jobs needed. All Diffraction's glass is imported from Germany.

"Not that glass men over here aren't aware of it," Brouwer says. "But they just don't know how."

Quite aside from military applications, Brouwer foresees a great growth of optics applications in aerial surveying and mapping. Surveying by aerial photography is now legal in Europe; it will be here soon, Brouwer thinks.

In alignment problems and control situations where there has to be accuracy up to one-millionth of an inch, there is a great opportunity for fine optical equipment, according to Brouwer. He also is interested in the "information explosion", not to make entire systems but where lenses are needed to reduce things to micro measurements.

Eventually Brouwer expects refined lenses to be used in forestry and agriculture, to determine "how much wood there is in an acre and how far crops are toward harvesting".

A closed corporation, Diffraction now does about $750,000 worth of business annually. It grows only as fast as it can get trained people.

Thus people who live—or work—in glass houses don't have to worry much about throwing stones. There are too few of their kind for them to hit anybody else.


## ANNUAL SUBSCRIPTIONS

| | |
|---|---|
| OSA members | $ 6.00 |
| Other AIP societies' members | $ 8.00 |
| Non-members and libraries | $10.00 |
| Single copies | $ 2.00 |

Subscriptions should be addressed to APPLIED OPTICS Subscription Handling, American Institute of Physics, 335 East Forty-Fifth Street, New York 17, New York. **Eight weeks should be allowed for order processing.**



## ADVERTISING

**Advertising inquiries, orders, plates, and correspondence should be addressed to the APPLIED OPTICS Advertising Office, 1155 Sixteenth Street, N.W., Washington, D.C. 20036 • 202-DI 7-4131 • Mrs. Boraks**

# SCHOTT

## BUBBLE CHAMBER WINDOWS

### Made to combine excellent mechanical stability and optical quality

Examining a 5½" thick bubble chamber window in the Optical Laboratory of the JENAER GLASWERK SCHOTT & GEN., Mainz.

Schott Bubble Chamber Windows are being used all over the world by laboratories, institutes and science centers specializing in nuclear research.

FORMS AVAILABLE: Round or oval. Tempered if operated under high pressure. Largest sizes can be made.

•

SCHOTT&GEN MAINZ

JENA GLASS

**SCHOTT OPTICAL GLASS AND SCHOTT FILTER GLASS FOR OPTIMUM OPTICAL PERFORMANCE**

Used in precision and massive optics, satellite tracking and aerial reconnaissance cameras, missile guiding systems, fiber optics, Cerenkov counters, etc.

**FISH-SCHURMAN CORPORATION, New Rochelle, N. Y.**

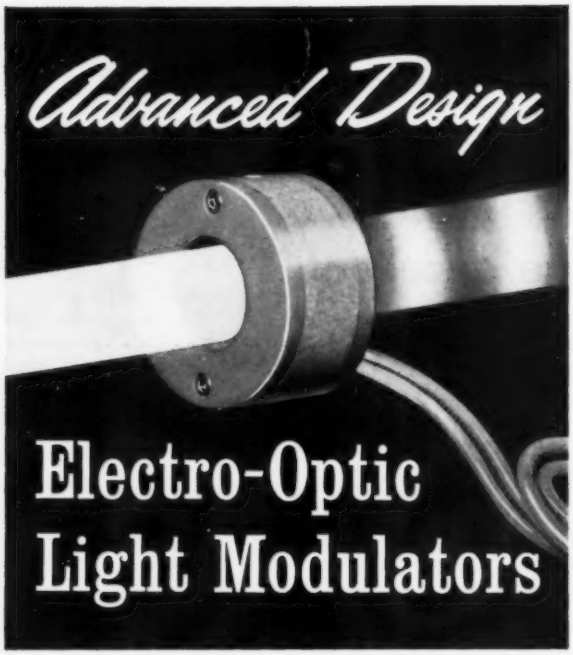


# Electro-Optic Light Modulators

**for**
**Laser Modulation**
**Communications**
**High Speed Photography**
**Photometry**
**Metrology**

The ISOMET Electro-Optic Light Modulators are solid state analogs of the Kerr cell offering the advantages of

**Smaller Size • Shorter Path Length**
**Less Power Consumption • Longer Life**

In addition to a complete line of modulators using ammonium dihydrogen phosphate (ADP) and potassium dihydrogen phosphate (KDP), ISOMET features several models using potassium dideuterium phosphate (KD*P), requiring only 50% of the voltage needed to drive KDP. New models allow up to 90% transmission and require less than 1300 volts (rms) for half wave retardation at 5641 angstrons.

**Ten standard models,** covering a wide range of applications, are currently available. Special models, allowing response to several thousand megacycles, are available on a custom basis.

*Write or phone for New technical bulletin AO 1200.*

**ISOMET**
CORPORATION
PALISADES PARK, NEW JERSEY
Area Code 201 Windsor 4-4100

## OPPORTUNITY FOR INDIVIDUAL CONTRIBUTION

Our clients are seeking both theoretical and experimental physicists who are capable of making significant individual contributions in the field of modern optics. If your interest and experience encompass any of the following areas, you are invited to investigate growth opportunities offering remuneration up to $25,000.

Electro-optical imaging systems. . .interferometric techniques. . .spatial filtering. . . diffraction theory. . .modern image theory . . .geometric lens design . . .laser research and investigation.

For further information, you are invited to direct your resume to:

Mr. Vincent A. Nickerson
Department B-10

ABBOTT'S of Boston
"EMPLOYMENT SPECIALISTS"
150 Tremont Street
Boston 11, Massachusetts
HAncock 6-8400

**APPLIED OPTICS**

**Subscription Order**

☐ 1 year, at OSA member rate of $6.00

☐ 1 year, at special rate, to other AIP Societies members, of $8.00

☐ 1 year, at non-member rate of $10.00

☐ Please send OSA membership information

Membership No.....

Name.....

Address.....

.....

.....

CEROX

BARNESITE

Super-C

AND THE NEW

MARK V

PASTE

*from the* **HOUSE OF RHODES**

. . . the most complete line of cerium polishing materials for all types of optical work

produced by

LINDSAY

FOR OVER HALF A CENTURY THE HALLMARK OF DEPENDABILITY

Rhodes has been serving all facets of the optical industry for more than fifty years.

You can depend on the Rhodes organization, anywhere from coast to coast, for helpful technical service.

Your Rhodesman always has available for service to you the comprehensive facilities of the LINDSAY research laboratory which is staffed by a technical group with many years of practical experience in optical polishing materials and processes.

How can we serve you today?

COLOSSUS BRAND™ *Since 1898*

*®Registered trademarks of Rare Earth (Lindsay) Division, American Potash & Chemical Corporation*

**THE HOUSE OF RHODES** / JAMES H. RHODES & COMPANY

General Offices: 1028 West Jackson Blvd., Chicago 7, Illinois • Regional Offices: Long Island City, N. Y. and San Marino, Calif.



## Physical Chemist

Our Central Research Division currently has an attractive position for a Ph.D. Physical Chemist with background in photochemistry or electronic spectroscopy and experience in quantum yield, or other optical measurements. The successful candidate will conduct research in liquid phase luminescence and energy transfer processes.

This is a challenging assignment with excellent opportunity for professional growth in Cyanamid's large Research Laboratory, located in Stamford, Connecticut.

Please address a complete resume in confidence to:

Mr. C. Benton

**AMERICAN CYANAMID COMPANY**
**Stamford Research Laboratories**
**1937 WEST MAIN STREET**
**STAMFORD, CONNECTICUT**

*An Equal Opportunity Employer*

CYANAMID



*New Catalog . . .*

**OPTICAL BENCHES**

- ☐ triangular benches
- ☐ lathe bed benches
- ☐ massive research benches
- ☐ non-magnetic and student-teaching benches

*Free catalog . . . just ask*

THE **Ealing** CORPORATION

2239 Massachusetts Avenue
Cambridge, Massachusetts 02140

# TWO INDIVIDUAL CONTRIBUTOR OPENINGS IN ELECTRO OPTICAL FIELD

with

## GENERAL ELECTRIC

**Require advanced thinking on wide range of Optical Systems for Space and Defense Programs**

Both openings are with the Scranton Operation of G.E. which is the headquarters for all major electro optical work of General Electric's Ordnance Dept. This Operation moved to Scranton just a year ago because of a major expansion of its efforts in electro optical devices and equipment. Its laboratory facilities have been recognized as one of the country's most modern and best equipped in electro optics.

If qualified, you will be joining a nucleus of engineers and scientists who are recognized in the electro optical field; and it is anticipated that your background will indicate similar professional stature.

### ELECTRO OPTICAL PHYSICIST

An opening for a senior contributor to lead activities in the continuing development of a wide range of laser spectrometric and other advanced electro optical equipment for application to space and defense projects. The newness of the field and advanced nature of the work require a man who has the technical imagination to explore the unconventional, and who is ingenious and creative in his approach to problems. BS, MS in Physics, with a minimum of 4 to 6 years in electro optical spectroscopic instrument development or related work is required.

### ELECTRO OPTICAL DESIGN ENGINEER

An individual contributor to plan, direct and execute design efforts on a wide variety of optical systems for space and defense programs. Must have a background of proven competence through actual experience in lens and optical systems design using advanced computer programs. Required: BS in Optical Engineering or equivalent, and 6 to 8 years' optical design experience.

*Please send full details to: Mr. H. B. Ebbets, Room 154-1, Ordnance Department, General Electric Co., Scranton Operation, 600 Sanders Street, Scranton, Pennsylvania.*

GENERAL ELECTRIC

*An equal opportunity employer*



# THE SCIENCE OF COLOR

**THIS DEFINITIVE BOOK ON COLOR,** prepared by OSA's Colorimetry Committee and setting forth the history, physics, physiology, psychology, and technology of color vision and color measurement, will be reprinted later this year by OSA.

**LIMITED EDITION.** Twenty-five color plates make this book uniquely beautiful, and, when the original supply of color sheets is exhausted, they cannot be reproduced. Therefore, this edition is limited.

**AUTHORITATIVE DATA,** mostly unavailable in other books, 39 tables, 102 figures, 340 pages of text, 22 pages of bibliography, and 23 pages of glossary-index have all been critically re-examined and corrected. The new **SCIENCE OF COLOR** is therefore the most up-to-date as well as the most complete source book for color science.

**ORDER NOW**

**SEND CASH WITH ORDER**

**PRICE $10.00; OSA MEMBERS $8.50**

Order Form

Optical Society of America
Room 101, 1155 16th Street N.W.
Washington, D.C. 20036

Please send one ..... copy of SCIENCE OF COLOR.

- ☐ Cash/check herewith
- ☐ $10.00
- ☐ $8.50 (OSA Member price)

Name .....

OSA Membership # .....

Address .....

.....

.....

# NO GUESSWORK HERE

■ Peak image sharpness—without guesswork or estimates—is insured in the new Statimatic* reprographer by calibrating the optical system with LogEtronic's Model C Focatron** Meter. According to Arnold Wheelock of The Plastic Coating Corp., "High quality in offset duplicating masters produced in the reprographer depends critically on sharpest possible focus—we just cannot count on the human eye in unit after unit. The positive, unambiguous indication we get on the Focatron meter does the job far more accurately and quickly."

■ The inspector simply places the target in the copy position, spots the Focatron probe in the projected image on the glass platen, and adjusts the optical system until he gets a peak reading on the meter. That's all.

■ **If you can't afford guesstimates in focusing either, the Focatron Image Sharpness Meter may help you, too. Drop us a line, and we'll send you a Focatron technical bulletin which will tell you the whole story.**

*Reg. Trade Mark **Reg. Trade Mark

LogE Focatron® BY LogEtronics Inc.

500 E. Monroe Ave., Alexandria, Va. TE 6-5180

# HIGH QUALITY STANDARDS

## . . . in Optical Crystal Blanks

| | |
|---|---|
| Calcium Fluoride | Sodium Chloride |
| Barium Fluoride | Potassium Chloride |
| Lithium Fluoride | Potassium Bromide |

• *Prompt Delivery* • *Large Size Availability*
• *Precision Cutting* • *Scattering Free*
• *Impurity Absorption Free* • *Strain Free*

## . . . in Optical Maser Crystals

| | | |
|---|---|---|
| $U^{+3} \cdot CaF_2$ | $Dy^{+2} \cdot CaF_2$ | $Nd^{+3} \cdot CaF_2$ |
| $U^{+3} \cdot BaF_2$ | $Sm^{+2} \cdot CaF_2$ | $Nd^{+3} \cdot BaF_2$ |
| $U^{+3} \cdot SrF_2$ | $Sm^{+2} \cdot SrF_2$ | $Nd^{+3} \cdot SrF_2$ |
| $Tm^{+3} \cdot SrF_2$ | $Tm^{+2} \cdot CaF_2$ | $Ho^{+3} \cdot CaF_2$ |

Also, all other trivalent rare earths in $CaF_2$, $BaF_2$ and $SrF_2$.

Indicative of our quality, most of the above were first mased in Optovac grown crystals.

OPTOVAC

OPTOVAC, INC.

NORTH BROOKFIELD, MASSACHUSETTS

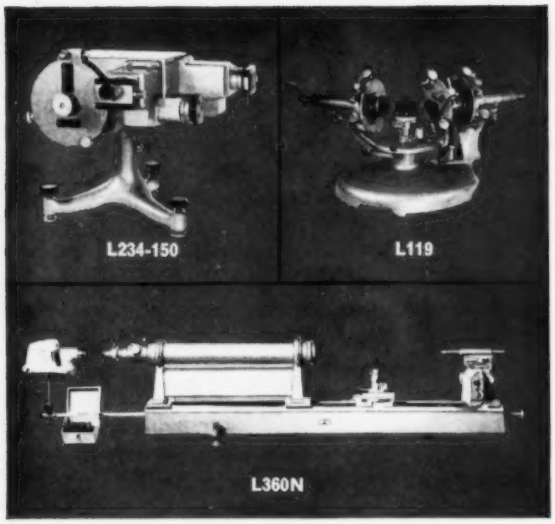


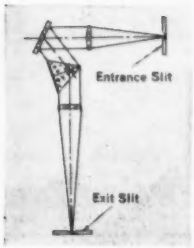


Optical Diagram of
L234-150 Monochromator

**DEPENDABLE ACCURACY**

*Gaertner Scientific thrives on solving difficult measuring problems . . . with precision unexcelled—reputation unsurpassed. Instruments shown represent a few of the many optical measuring systems available that can be applied or modified to your requirements.*

**L234-150 QUARTZ MONOCHROMATOR**—High speed enables studies of absorption spectra, photosensitive materials, phosphorescence, and energy distribution. With camera attachment, unit converts to high aperature spectrograph. **Request Bulletin 158-61**

**L119 ELLIPSOMETER**—Accurate measurement of extremely thin film down to 2 or 3 Angstroms. Also adaptable to birefringence and surface studies with elliptically polarized light. **Request Bulletin 203-61**

**L360N OPTICAL-INSTRUMENT BENCH**—For checking optics, experimental and mock-up arrangements requiring alignment, unique positioning, linear or rotational movement of test pieces or components. **Request Bulletin 156-59**

Your inquiry for existing or proposed instrumentations will be answered immediately. GSC-3-219

**Gaertner**
SCIENTIFIC CORPORATION
1294 Wrightwood Ave., Chicago 14, Ill.
Area Code 312, BUckingham 1-5335

**Use THIN FILM (8μ) BEAM SPLITTERS**

**NO GHOSTS!**

**NO REFRACTIVE ERRORS!**

- Flatness to 1/8" wave and parallelism to less than 1 fringe per inch; on special order.
- Sizes: Up to 24" (and still growing).
- Large coating selection, including dichroics.

**SEND FOR FREE BOOKLET**

"Application and Specification of Pellicles"

Important reading for manufacturers, designers and users of glass beam splitters, mirrors, filters and prisms.

**NPC National Photocolor Corp.**
225 East 44th Street, New York 17, N. Y.
MU 7-0267-8

**BUBBLE CHAMBER OBJECTIVE**

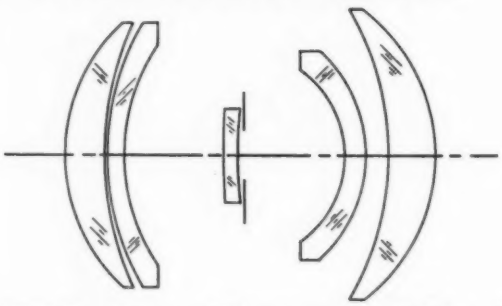

FIELD—60°, or 192 mm. with E.F.L. of 154 mm
DISTORTION—2½ Microns or Less
IMAGE QUALITY—Diffraction Limited at *f*/16
SPECTRAL REGION—4300 to 5500 Angstroms
MAGNIFICATION—1:13.6

This photographic objective for the 80-inch Brookhaven Bubble Chamber was designed & produced by TROPEL. It is typical of the specialized optical design & fabrication tasks that our firm is organized & equipped to perform. Optical designs & prototype optical systems of superior quality have been our main line of business since 1953. Brochure on "PROGRESS IN DESIGN OF OPTICAL SYSTEMS" available upon request.

**TROPEL, INC., 52 West Ave., Fairport, N.Y.**

ISOMET
CORPORATION

a technically-oriented company in northern New Jersey, is expanding its program of research and development in optical detection instruments and systems and advance laser applications.

# Challenging opportunities

in

## Electro-Optics

We need an **OUTSTANDING ENGINEER or PHYSICIST** with a mature background in optical, mechanical and electro-optic systems with emphasis on design and hardware followthrough.

in

## Semi-Conductor materials/devices

We need a **PHYSICIST or ENGINEER** with experience in one or more of the following: Semi-conductor studies; Crystal Growth; Device fabrication and measurement; Diffusion in films and epitaxial layers.

***Opportunity for stock option***

Write in complete confidence to
Dr. Warren Ruderman, *President*

ISOMET
CORPORATION

433 COMMERCIAL AVENUE
PALISADES PARK, NEW JERSEY

*An Equal Opportunity Employer*



# GOT A DICHROIC COATING PROBLEM?

$$T = \frac{4nn_a n_g}{(nn_a + n_g)^2 - (n^2 - n_g^2)(n_g^2 - 1)}$$

T = transmission
n = index of coating material
$n_a$ = index of air
$n_g$ = index of glass

This might give you the answer. It's a simple transmission formula to arrive at the specific coating that will produce the desired results.

If this formula doesn't solve your particular set of problems, Liberty Mirror engineers will welcome the challenge to develop one that does. They've done it for many specialized applications of dichroic reflectors that are not met by Liberty Mirror's standard line of Hi-Efficiency coatings. These reflect 90% or more of incident light in wave lengths as low as 350 millimicrons up to 1,000 millimicrons.

Our vacuum-deposited coatings of various metals are used to make front-surface mirrors, neutral filters, transparent mirrors, high-efficiency beam splitters, beam-splitting dichroic mirrors and filters. Metallic and transparent electrically conducting coatings are available for resistance heating. Static-dissipating and high-frequency shielding coatings are also available.

Applied to all types of glass, metal or plastic, the coatings are used in such varied products as scientific and optical instruments, cameras, toys, pin setters, wheel-aligning equipment, aircraft and missiles. Free data sheets are available on all coatings.

Write L·O·F, Liberty Mirror Division, 55103 Libbey·Owens·Ford Building, Toledo 2, Ohio.

LIBERTY
MIRROR DIVISION
LIBBEY·OWENS·FORD

MADE IN U.S.A.
LOF GLASS

# INJECTION LASERS

NOW AVAILABLE ON
RAPID DELIVERY SCHEDULES

GaAs Injection Lasers . . . 8400 Å

GaAsP Injection Lasers . . . 6200 Å-8400 Å

GaP Injection Sub-Lasers . . . 6400 Å

GaAs Injection Sub-Lasers . . . 9100 Å

GaAsP Injection Sub-Lasers . . . 6600 Å-9100 Å

GaSb Injection Sub-Lasers . . . 16000 Å

Tiny p-n junction diodes emit coherent radiation by direct application of electric current. Standard configurations now available. Consultation and design services on custom configurations offered.

Diodes operated beneath the laser threshold emit non-coherent light retaining the general spectral characteristic and fast time-constant of the Injection Laser. Sub-Lasers listed above are available, in standard configurations, on rapid delivery schedules. Other III-V sources available on special order.

For illustrated brochure, write to:

**ELECTRO-NUCLEAR LABORATORIES, INC.**

2437 LEGHORN STREET, MOUNTAIN VIEW, CALIFORNIA

# The Optical Society of America

## Officers of the Society

*President* STANLEY S. BALLARD, Department of Physics, University of Florida, Gainesville, Fla.
*President-Elect* RICHARD C. LORD, Spectroscopy Laboratory, MIT, Cambridge 39, Mass.
*Past President* DAVID L. MACADAM, Research Laboratories, Eastman Kodak Company, Rochester 4, N.Y.
*Executive Secretary* MARY E. WARGA, OSA, 1155 16th Street N.W., Washington 6, D.C.
*Treasurer* ARCHIE I. MAHAN, Applied Physics Laboratory, 8621 Georgia Avenue, Silver Spring, Md.
*Editor of the Journal of the Optical Society of America* DEANE B. JUDD, National Bureau of Standards, Washington 25, D.C.
*Editor of Applied Optics* JOHN N. HOWARD, AFCRL, Bedford, Mass.

## Directors-at-Large

* *Term expires December 31 of the indicated year.*

RUDOLF KINGSLAKE (63)* Eastman Kodak Company, Rochester 4, N.Y.
EARLE K. PLYLER (63)* Department of Chemistry, Florida State University, Tallahassee, Fla.
DAVID RICHARDSON (63)* Bausch & Lomb, Inc., Rochester 2, N.Y.
GEORG H. HASS (64)* ERDL, Fort Belvoir, Va.
R. CLARK JONES (64)* Polaroid Corp., Cambridge, Mass.
E. D. MCALISTER (64)* Scripps Institution of Oceanography, La Jolla, Calif.
W. LEWIS HYDE (65)* University of Rochester, Rochester 20, N.Y.
JOHN A. SANDERSON (65)* Naval Research Laboratory, Washington 25, D.C.
GEORGE WALD (65)* Biological Laboratories, Harvard University, Cambridge 38, Mass.

## Local Sections

*Rochester*
JOSEPH L. ROOD *President*
ROBERT M. BLAKNEY *President-Elect*
JOSEPH H. ALTMAN *Secretary*
Research Laboratories
Eastman Kodak Co.
Rochester 4, N.Y.
VERNON L. PARKS *Treasurer*

*Detroit*
RICHARD MAJKOWSKI *President*
CARL LEISTNER *President-Elect*
DANIEL L. HARMON *Secretary*
16152 Parkside, Detroit 21, Mich.
SAMUEL COHEN *Treasurer*

*Niagara Frontier*
E. SCHUSTIK *President*
THOMAS FROST *President-Elect*
CALVIN W. YOUNG *Secretary*
Carborundum Metals Co.
Box 32, Akron, N.Y.
RAY ANNINO *Treasurer*

*New England*
DAVID S. GRAY *President*
CHARLES KOESTER *Vice-President*
GEOFFREY HARVEY *Secretary*
Itek Corporation
10 Maguire Rd.
Lexington, Mass.
WILLIAM J. DAVIS *Treasurer*

*Texas*
P. O'B. MONTGOMERY *President*
HARRY J. AUVERMANN *President-Elect*
NORMAN C. ALLEN *Secretary-Treasurer*
Texas Instruments, Inc.
Box 6015
Dallas 22, Tex.

*Delaware Valley*
F. J. WARZAK *President*
J. E. TUDOR *Secretary*
General Electric Company MSVD
3316 Spring Garden Street
Philadelphia, Pa.
M. CONSHERRY *Treasurer*

*Pittsburgh*
THOMAS P. VOGL *President*
JEROME J. WOLKEN *President-Elect*
GEORGE L. BUC *Secretary*
Fisher Scientific Company
717 Forbes Street
Pittsburgh 19, Pennsylvania
IRVING S. STAPSY *Treasurer*

*Chicago*
HAROLD BENNETT *President*
HOWARD PADGITT *Vice-President*
CARL R. LAMBRECHT *Secretary*
7729 N. Ashland Avenue
Chicago 31, Ill.
EDWARD L. SOMERVILLE *Treasurer*

*Southwestern Connecticut*
LEONARD EISNER *President*
ROBERT C. GORE *Vice-President*
MARTIN ROME *Secretary*
Machlett Laboratories, Inc.
1063 Hope Street
Springdale, Connecticut
EDWARD SPEYER *Treasurer*

*Southern California*
ERNEST DAVIDSON *President*
WM. S. GALLAWAY *Vice-President*
MILTON LAIKIN *Secretary*
1913 Preuss Road
Los Angeles 34, Calif.
JEROME J. ROSENBLATT *Treasurer*

*Northern California*
ANDREW L. JORGENSEN *President*
CLYDE C. SHAW *Vice-President*
HARVEY MORTON *Secretary-Treasurer*
Tinsley Laboratories
2448 Sixth Street
Berkeley, Calif.

*National Capital*
MATTHEW P. THEKAEKARA *President*
FREDERICK W. PAUL *First Vice-President*
HARRY K. HAMMOND, III, *Secretary*
National Bureau of Standards
Washington 25, D.C.
RICHARD S. HUNTER *Treasurer*

*San Diego*
JOHN E. TYLER *President*
JOHN H. TAYLOR *Vice-President*
JOHN M. HOOD *Secretary-Treasurer*
Bldg. 4, U.S. Navy Electronics Laboratory
San Diego 52, Calif.

*Detroit*
CARL J. LEISTNER *Chairman*
W. K. LESNICK *Chairman-Elect*
D. L. HARMON *Secretary*
University of Detroit
Detroit, Mich.
SAMUEL COHEN *Treasurer*

**The Optical Society of America** was organized in 1916 **"to increase and diffuse the knowledge of optics in all its branches, pure and applied, to promote the mutual interests of investigators of optical problems, of designers, manufacturers and users of optical instruments and apparatus of all kinds and to encourage cooperation among them."** The Society invites to membership all who are interested in any branch of optics, either in research, in instruction, in optical or illuminating engineering, in the manufacture and distribution of optical goods of all kinds, or in physiological and medical optics. Further information may be obtained from the Executive Secretary of the Society. **Annual Dues:** Regular members and Fellows, $17.00; Associate members, $13.00; Corporate members, $125.00. These dues include subscription to the Society's official journal, the **Journal of the Optical Society of America,** but not to its other publications.

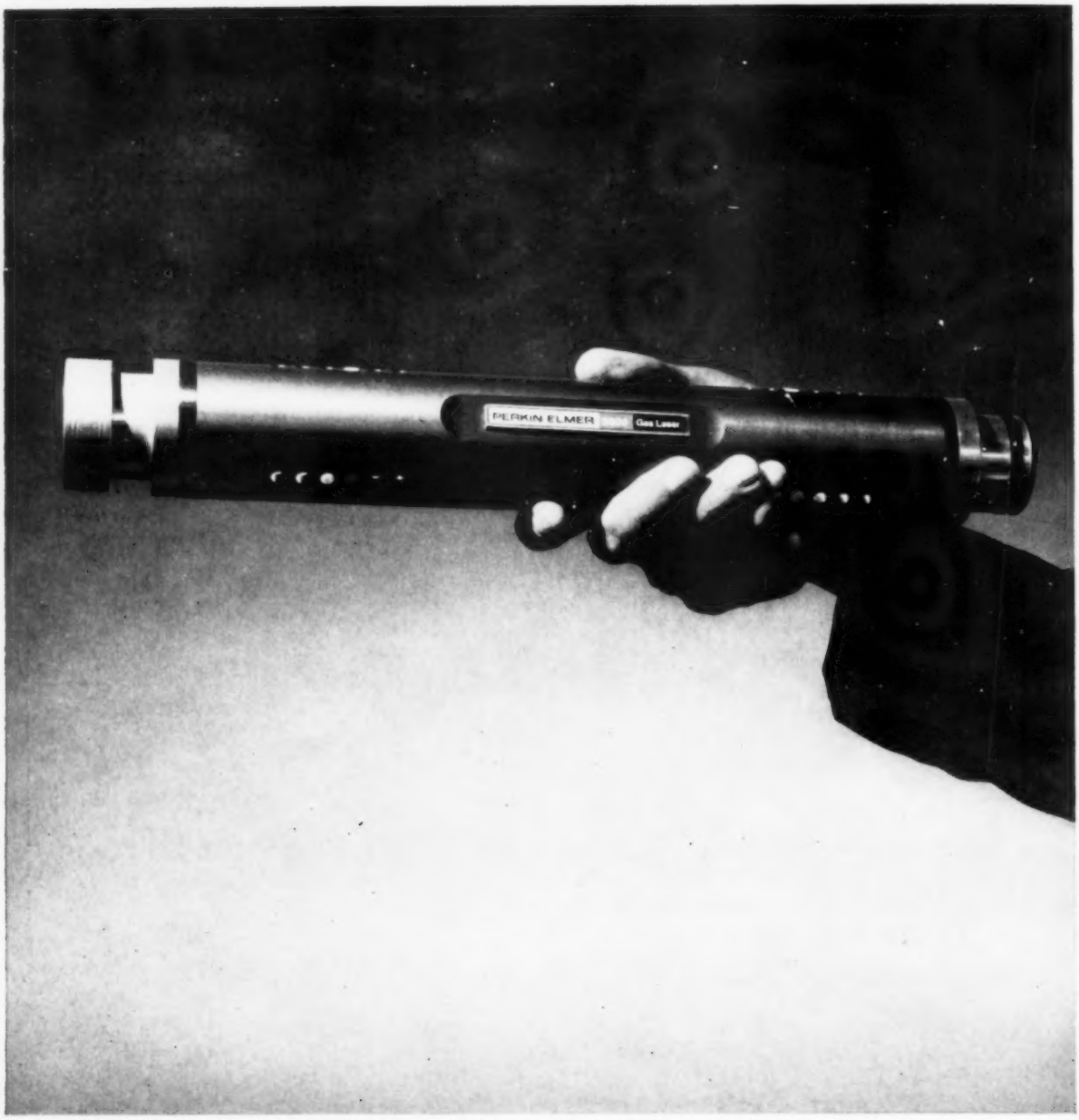


Until now the gas laser has been tied to the laboratory — too big, too complicated, too fragile for practical uses. The new Perkin-Elmer Model 5200 Laser removes these limitations and sets new standards of technical performance.

The Model 5200 helium-neon laser features a newly-developed, double-walled, compact, gas discharge tube only 10" long. The plasma is generated inside a capillary by a small, direct-current discharge between an internal anode and heated cathode. The discharge tube is mounted inside a rugged, coaxial, cylindrical resonator with adjustable mirror holders and camera-type optical accessory mounts at each end. The result is a highly stable and useful configuration.

PERKIN-ELMER ANNOUNCES

# THE LIBERATION OF THE LASER

The superb quality of the Perkin-Elmer optics permits operation in the pure fundamental mode for diffraction-limited optical performance.

The separate electronically regulated Model 5201 power supply provides the necessary power to achieve a highly stable, noise-free light output from the discharge tube. Connection to an external jack on the 5201 permits direct modulation of the laser beam up to frequencies of 500 KC.

For detailed information on the new Model 5200 Laser and complete Perkin-Elmer Optical Maser Product Services contact Optical Maser Marketing, Perkin-Elmer Corporation, XXX Danbury Road, Norwalk, Connecticut. Telephone (203) 847-0411.

PERKIN-ELMER